

สารยับยั้งไทโรซิเนสจากละมุด *Manilkara zapota* L.



นางสาวสุทธิเดือน ชุมหกันต์

บทคัดย่อและแฟ้มข้อมูลฉบับเต็มของวิทยานิพนธ์ตั้งแต่ปีการศึกษา 2554 ที่ให้บริการในคลังปัญญาจุฬาฯ (CUIR)
เป็นแฟ้มข้อมูลของนิสิตเจ้าของวิทยานิพนธ์ ที่ส่งผ่านทางบัณฑิตวิทยาลัย

The abstract and full text of theses from the academic year 2011 in Chulalongkorn University Intellectual Repository (CUIR)
are the thesis authors' files submitted through the University Graduate School.

วิทยานิพนธ์นี้เป็นส่วนหนึ่งของการศึกษาตามหลักสูตรปริญญาวิทยาศาสตรดุษฎีบัณฑิต

สาขาวิชาเทคโนโลยีชีวภาพ

คณะวิทยาศาสตร์ จุฬาลงกรณ์มหาวิทยาลัย

ปีการศึกษา 2560

ลิขสิทธิ์ของจุฬาลงกรณ์มหาวิทยาลัย

TYROSINASE INHIBITORS FROM SAPODILLA PLUM *Manilkara zapota* L.

Miss Sutthiduean Chuhakant



A Dissertation Submitted in Partial Fulfillment of the Requirements
for the Degree of Doctor of Philosophy Program in Biotechnology
Faculty of Science
Chulalongkorn University
Academic Year 2017
Copyright of Chulalongkorn University

Thesis Title TYROSINASE INHIBITORS FROM
SAPODILLA PLUM *Manilkara zapota* L.
By Miss Sutthiduean Chunchakant
Field of Study Biotechnology
Thesis Advisor Assistant Professor Chanya Chaicharoenpong,
Ph.D.

Accepted by the Faculty of Science, Chulalongkorn University in Partial
Fulfillment of the Requirements for the Doctoral Degree

..... Dean of the Faculty of Science
(Associate Professor Polkit Sangvanich, Ph.D.)

THESIS COMMITTEE

..... Chairman
(Associate Professor Nattaya Ngamrojanavanich, Ph.D.)

..... Thesis Advisor
(Assistant Professor Chanya Chaicharoenpong, Ph.D.)

..... Examiner
(Professor Supason Wanichwecharungruang, Ph.D.)

..... Examiner
(Assistant Professor Kanoktip Packdibamrung)

..... External Examiner
(Damrong Sommit, Ph.D.)

จุฬาลงกรณ์มหาวิทยาลัย
CHULALONGKORN UNIVERSITY

สุทธิเดือน ชุมหวานต์ : สารยับยั้งไทโรซิเนสจากละมุด *Manilkara zapota* L. (TYROSINASE INHIBITORS FROM SAPODILLA PLUM *Manilkara zapota* L.) อ.ที่ปริกษาวิทยานิพนธ์หลัก: ผศ. ดร. จรรยา ชัยเจริญพงศ์, 185 หน้า.

ส่วนต่าง ๆ ของละมุด 6 ส่วนประกอบด้วยเปลือก ดอก ผล ใบ ราก และเมล็ดถูกนำมาตรวจสอบหาปริมาณสารประกอบฟีนอลิกทั้งหมด ปริมาณสารประกอบฟลาโวนอยด์ทั้งหมดฤทธิ์ต้านอนุมูลอิสระและฤทธิ์ยับยั้งไทโรซิเนส ส่วนสกัดหยาบเมทานอลของดอกแสดงปริมาณสารประกอบฟีนอลิกทั้งหมดสูงสุด (368.73 ± 0.65 mg GAE/g) ขณะที่ ส่วนสกัดหยาบเมทานอลของเมล็ดและรากแสดงปริมาณสารประกอบฟลาโวนอยด์ทั้งหมดสูง (90.21 ± 0.57 และ 89.03 ± 1.00 mg QE/g, ตามลำดับ) ส่วนสกัดหยาบเมทานอลของเมล็ดแสดงฤทธิ์ต้านอนุมูลอิสระ DPPH (IC_{50} 282.05 ± 0.60 μ g/mL) และ ABTS (IC_{50} 205.11 ± 0.89 μ g/mL) สูงสุดและแสดงความสามารถในการรีดิวซ์ FRAP สูงสุดด้วยค่า 296.46 ± 0.08 mg TEAC/mg ส่วนสกัดหยาบเมทานอลของรากแสดงฤทธิ์ยับยั้งไทโรซิเนสสูงที่สุดทั้งการยับยั้งมอโนฟีโนเลส (IC_{50} 0.81 ± 0.92 mg/mL) และ ไดฟีโนเลส (IC_{50} 0.55 ± 0.50 mg/mL) ปริมาณสารประกอบฟีนอลิกทั้งหมดและฤทธิ์ต้านอนุมูลอิสระ แสดงความสัมพันธ์สูงโดยวิธี ABTS, DPPH และ FRAP ความสัมพันธ์ระหว่างปริมาณฟีนอลิกทั้งหมดกับฤทธิ์ยับยั้งไทโรซิเนสกับปริมาณสารประกอบฟลาโวนอยด์ทั้งหมดมีค่าต่ำมาก สารประกอบฟลาโวนอยด์ทั้งหมดกับฤทธิ์ต้านอนุมูลอิสระ โดยวิธี DPPH, ABTS และ FRAP มีความสัมพันธ์ต่ำ สารประกอบฟลาโวนอยด์ทั้งหมดกับฤทธิ์ยับยั้งไทโรซิเนส และฤทธิ์ต้านอนุมูลอิสระและฤทธิ์ยับยั้งไทโรซิเนสไม่มีความสัมพันธ์กัน นอกจากนี้การติดตามฤทธิ์ยับยั้งไทโรซิเนสถูกใช้ในการแยกสารยับยั้งไทโรซิเนสจากเปลือกต้นละมุด การแยกของส่วนสกัดหยาบออร์มัลเฮกเซนและเอทิลแอลกอฮอล์ของเปลือกต้นละมุดได้สาร 7 ชนิด คือ taraxerol methyl ether (I), 6-hydroxyflavanone (II), (+)-dihydrokaempferol (III), 3,4-dihydroxybenzoic acid (IV), taraxerol (V), taraxerone (VI) และ lupeol acetate (VII) (+)-dihydrokaempferol (III) (IC_{50} 32.17 ± 0.32 μ M) แสดงการยับยั้งไทโรซิเนสอย่างมีนัยสำคัญต่อฤทธิ์ยับยั้งมอโนฟีโนเลสได้ดีกว่า kojic acid (IC_{50} 40.21 ± 0.63 μ M) ยิ่งกว่านั้น (+)-dihydrokaempferol (III) (IC_{50} 31.60 ± 0.73 μ M) แสดงฤทธิ์ยับยั้งไทโรซิเนสแบบไดฟีโนเลสเทียบเท่ากับ kojic acid (IC_{50} 30.07 ± 0.32 μ M) ยิ่งกว่านั้นสารที่แยกได้ I-VII ถูกทดสอบหาฤทธิ์ต้านอนุมูลอิสระและความเป็นพิษต่อเซลล์มะเร็ง (+)-dihydrokaempferol (III) แสดงฤทธิ์ต้านอนุมูลอิสระ DPPH (IC_{50} 2.21 ± 0.77 μ M) และ ABTS (IC_{50} 214.83 ± 0.51 μ M) สูงที่สุดและแสดงความสามารถในการรีดิวซ์ FRAP สูงที่สุดด้วยค่า 6.23 ± 0.10 μ M สารนี้แสดงความเป็นพิษต่อเซลล์มะเร็ง BT474, ChaGo-K-1, HepG2, KATO-III และ SW620 ด้วยค่า IC_{50} เท่ากับ 11.66 ± 0.42 , 12.32 ± 0.73 , 13.67 ± 0.38 , 39.79 ± 0.38 และ 41.11 ± 1.08 μ M, ตามลำดับ การศึกษานี้แสดงให้เห็นว่าละมุดอาจเป็นแหล่งที่มีปริมาณฟีนอลิกทั้งหมดสูงและแหล่งของสารต้านอนุมูลอิสระจากธรรมชาติ นอกจากนี้ (+)-dihydrokaempferol (III) สามารถพัฒนาเป็นสารยับยั้งไทโรซิเนสจากธรรมชาติได้

5472908523 : MAJOR BIOTECHNOLOGY

KEYWORDS: ANTITYROSINASE ACTIVITY / ANTIOXIDANT ACTIVITY / TYROSINASE INHIBITOR

SUTTHIDUEAN CHUNHAKANT: TYROSINASE INHIBITORS FROM SAPODILLA PLUM
Manilkara zapota L.. ADVISOR: ASST. PROF. CHANYA CHAICHAROENPONG, Ph.D., 185 pp.

Six different parts of *Manilkara zapota* which consisted of barks, flowers, fruits, leaves, roots and seeds were investigated for total phenolic content, total flavonoid content, antioxidant and antityrosinase activities. Methanol crude extract of flowers showed the highest total phenolic content (368.73 ± 0.65 mg GAE/g), while methanol crude extracts of seeds and roots showed high total flavonoid content (90.21 ± 0.57 and 89.03 ± 1.00 mg QE/g, respectively). Methanol crude extract of seeds showed the strongest DPPH ($IC_{50} 282.05 \pm 0.60$ μ g/mL) and ABTS ($IC_{50} 205.11 \pm 0.89$ μ g/mL) radical scavenging activities and showed the highest FRAP value of 296.46 ± 0.08 mg TEAC/mg. Methanol crude extract of roots showed the highest tyrosinase inhibitory activities on both monophenolase ($IC_{50} 0.81 \pm 0.92$ mg/mL) and diphenolase inhibitory activities ($IC_{50} 0.55 \pm 0.50$ mg/mL). Total phenolic content and antioxidant radical activities showed high correlation by ABTS, DPPH and FRAP assays. Correlations between total phenolic content with antityrosinase activities and with total flavonoid content were very low. A low correlation was found between total total flavonoid content and antioxidant activities by DPPH, ABTS and FRAP assays. There were no correlation between total flavonoid content with antityrosinase activities and no correlation between antioxidant and antityrosinase activities. Moreover, bioassay-guided fractionation on tyrosinase inhibitory activity was used to isolate tyrosinase inhibitors from *M. zapota* barks. Separation of *n*-hexane and ethyl acetate crude extracts of *M. zapota* barks afforded seven isolated compounds; taraxerol methyl ether (I), 6-hydroxyflavanone (II), (+)-dihydrokaempferol (III), 3,4-dihydroxybenzoic acid (IV), taraxerol (V), taraxerone (VI) and lupeol acetate (VII). (+)-Dihydrokaempferol (III) displayed significant tyrosinase inhibition ($IC_{50} 32.17 \pm 0.32$ μ M) against monophenolase activity which was more potent than kojic acid ($IC_{50} 40.21 \pm 0.63$ μ M). Furthermore, (+)-dihydrokaempferol (III) ($IC_{50} 31.60 \pm 0.73$ μ M) showed similar activity on diphenolase inhibitory activity when compared with kojic acid ($IC_{50} 30.07 \pm 0.32$ μ M). Furthermore, isolated compounds I-VII were evaluated antioxidant and cytotoxic activities. (+)-Dihydrokaempferol (III) exhibited the strongest scavenging activities on DPPH ($IC_{50} 2.21 \pm 0.77$ μ M) and ABTS ($IC_{50} 214.83 \pm 0.51$ μ M) and showed the highest FRAP value of 6.23 ± 0.10 μ M. It displayed strong cytotoxic activity against human cancer cell lines; BT474, ChaGo-K-1, HepG₂, KATO-III and SW620 with IC_{50} values of 11.66 ± 0.42 , 12.32 ± 0.73 , 13.67 ± 0.38 , 39.79 ± 0.38 and 41.11 ± 1.08 μ M, respectively. This study indicated that *M. zapota* might constitute a rich source of total phenolic contents and natural antioxidants. Moreover, (+)-dihydrokaempferol (III) could be developed as a natural tyrosinase inhibitor.

Field of Study: Biotechnology

Academic Year: 2017

Student's Signature

Advisor's Signature

ACKNOWLEDGEMENTS

I wish to express my sincere gratitude to my advisor Assistant Professor Dr.Chanya Chaicharoenpong for supervising this study, suggesting the research project, and special supports in correcting and criticizing all of this study.

I wish to express sincere thanks to Associate Professor Dr.Surachai Pornpakakul for guidance on elucidating chemical structure and Mrs. Songchan Puthong for cytotoxicity assay.

I am gratitude to Associate Professor Dr.Nattaya Ngamrojanavanich, Professor Dr.Supason Wanichwecharungruang, Assistant Professor Dr.Kanoktip Packdibamrung and Dr.Damrong Sommit for useful advice and for serving as thesis committe.

In addition, I would like to thank Graduate School, Chulalongkorn University and National Research Council of Thailand (NRCT) in 2017 for the financial support on my research. I would like to thank Pranakorn Rajabhat University for the financial support on my study.

Moreover, I would like to thank the Institute of Biotechnology and Genetic Engineering (IBGE) for supporting, encouragement and remarkable experiences during my thesis work. I extend my sincere thanks to all members of room no. 604 for their friendship and help during the course of my graduate. Finally, I would like to express my appreciation to my parents and my family for their moral support and great encouragement.

CONTENTS

	Page
THAI ABSTRACT	iv
ENGLISH ABSTRACT.....	v
ACKNOWLEDGEMENTS	vi
CONTENTS.....	vii
LIST OF TABLE	ix
LIST OF FIGURE.....	xii
CHAPTER I INTRODUCTION.....	1
CHAPTER II THEORETICAL	3
2.1 Melanin	3
2.2 Tyrosinase enzyme	5
2.3 Tyrosinase inhibitor	6
2.4 Mechanism of enzyme inhibition	7
2.5 Literature reviews	12
2.6 <i>Manilkara zapota</i> Linn.	39
CHAPTER III MATERIALS AND METHODS	48
3.1 Materials	48
3.2 General techniques and procedures	48
CHAPTER IV RESULTS AND DISCUSSIONS	60
4.1 Extraction of different parts of <i>M. zapota</i>	60
4.2 Determination of total phenolic and total flavonoid contents of different parts of <i>M. zapota</i>	61
4.3 Determination of antioxidant and antityrosinase activities of different parts of <i>M. zapota</i>	63
4.4 Correlations.....	66
4.5 Extraction of <i>M. zapota</i> barks.....	69
4.6 Isolation of crude extracts of <i>M. zapota</i> barks.....	70
4.7 Elucidation of isolated compounds I-VII	85
4.8 Antityrosinase activities of isolated compounds I-VII	102

	Page
4.9 Determination of antioxidant activities of isolated compounds I-VII.....	103
4.10 Determination of cytotoxicity of isolated compounds I-VII	105
CHAPTER V CONCLUSION.....	107
REFERENCES	109
APPENDIX.....	124
VITA.....	185



LIST OF TABLE

	Page
Table 1 Antityrosinase activity of crude extracts of plants	14
Table 2 Antityrosinase activity of phytochemicals of plants	18
Table 3 Antityrosinase activity of synthetic compounds	33
Table 4 Phytochemical and biological activities of genus <i>Manilkara</i>	41
Table 5 Extraction yield of crude extracts of different parts of <i>M. zapota</i>	60
Table 6 Total phenolic and total flavonoid contents of crude extracts of different parts.....	62
Table 7 Antioxidant activities of crude extracts of different parts of <i>M. zapota</i>	64
Table 8 Antityrosinase activities of crude extracts of different parts of <i>M. zapota</i>	65
Table 9 Correlation values of total phenolic content and antioxidant activities of.....	66
Table 10 Correlation values of total phenolic content and antityrosinase activities of crude extracts of different parts of <i>M. zapota</i>	67
Table 11 Correlation values of total flavonoid content and antioxidant activities of	68
Table 12 Correlation values of total flavonoid content and antityrosinase activities of crude extracts of different parts of <i>M. zapota</i>	68
Table 13 Correlation values of antityrosinase and antioxidant activities of crude of crude extracts of different parts of <i>M. zapota</i>	69
Table 14 Extraction yield and tyrosinase inhibitory activity of crude extracts of	70
Table 15 Tyrosinase inhibitory activity of fractions A-D of n-hexane crude extract	71
Table 16 Tyrosinase inhibitory activity of subfractions A1-A4 of fraction A.....	71
Table 17 Tyrosinase inhibitory activity of subfractions A11-A14 of subfraction A1	72
Table 18 Tyrosinase inhibitory activity of subfractions C1-C3 of fraction C	72
Table 19 Tyrosinase inhibitory activity of subfractions C31-C34 of subfraction C3	73
Table 20 Tyrosinase inhibitory activity of fractions E-H of ethyl acetate crude extract	73
Table 21 Tyrosinase inhibitory activity of subfractions E1-E9 of fraction E.....	74
Table 22 Tyrosinase inhibitory activity of subfractions F1-F6 of fraction F.....	74

Table 23 Tyrosinase inhibitory activity of subfractions F11-F16 of subfraction F1 ..	75
Table 24 Tyrosinase inhibitory activity of subfractions F111-F116 of subfraction F11 ..	75
Table 25 Tyrosinase inhibitory activity of subfractions F1131-F1135 of subfraction F113 ..	76
Table 26 Tyrosinase inhibitory activity of subfractions F11311-F11315 of subfraction F1131 ..	76
Table 27 Tyrosinase inhibitory activity of subfractions F21-F23 of subfraction F2 ..	77
Table 28 Tyrosinase inhibitory activity of subfractions F31-F34 of subfraction F3 ..	77
Table 29 Tyrosinase inhibitory activity of subfractions F41-F46 of subfraction F4 ..	78
Table 30 Tyrosinase inhibitory activity of subfractions F431-F435 of subfraction F43 ..	78
Table 31 Tyrosinase inhibitory activity of subfractions F4331-F4336 of subfraction F433 ..	79
Table 32 Tyrosinase inhibitory activity of subfractions F43321-F43322 of subfraction F4332 ..	79
Table 33 Tyrosinase inhibitory activity of subfractions F43351-F43353 of ..	80
Table 34 Tyrosinase inhibitory activity of all subfractions F51-F59 of subfraction ..	80
Table 35 Isolation of subfractions F531-F532 of subfraction F53 ..	81
Table 36 Tyrosinase inhibitory activity of subfractions F591-F5910 of subfraction ..	81
Table 37 Tyrosinase inhibitory activity of subfractions F61-F63 of subfraction F6 ..	82
Table 38 Isolation of subfractions F621-F626 of subfraction F62 ..	82
Table 39 Tyrosinase inhibitory activity of subfractions G1-G5 of fraction G ..	82
Table 40 Tyrosinase inhibitory activity of subfractions G31-G34 of subfraction ..	83
Table 41 Tyrosinase inhibitory activity of subfractions G331-G333 of subfraction ..	83
Table 42 Tyrosinase inhibitory activity of subfractions G3321-G3322 of ..	84
Table 43 Tyrosinase inhibitory activity of subfractions G51-G52 of subfraction G5 ..	84
Table 44 Tyrosinase inhibitory activity of subfractions G511-G512 of subfraction ..	84
Table 45 Comparison of NMR data of compound I and taraxerol methyl ether ..	86
Table 46 Comparison of NMR data of compound II and 6-hydroxyflavanone ..	88

Table 47 Comparison of NMR data of compound III and dihydrokaempferol.....	90
Table 48 Comparison of NMR data of compound IV and 3,4-dihydroxybenzoic acid	92
Table 49 Comparison of NMR data of compound V and taraxerol	94
Table 50 Comparison of NMR data of compound VI and taraxerone.....	97
Table 51 Comparison of NMR data of compound VII and lupeol acetate	100
Table 52 The IC ₅₀ values of compounds I-VII for antityrosinase activities.....	103
Table 53 Antioxidant activities of isolated compounds I-VII	104
Table 54 Cytotoxic activities of compounds I-VII	106



LIST OF FIGURE

	Page
Figure 1 Cross-section of skin structure	4
Figure 2 Melanin biosynthesis pathway.....	5
Figure 3 Structure of tyrosinase	6
Figure 4 Michaelis-Menten plot.....	8
Figure 5 Michaelis-Menten plot of competitive inhibition	9
Figure 6 Lineweaver-Burk plots of competitive inhibition	9
Figure 7 Michaelis-Menten plot of noncompetitive inhibition.....	10
Figure 8 Lineweaver-Burk plots of noncompetitive inhibition	10
Figure 9 Lineweaver-Burk plots of mixed inhibition	11
Figure 10 Michaelis-Menten plot of uncompetitive inhibition.....	11
Figure 11 Lineweaver-Burk plots of uncompetitive inhibition	12
Figure 12 Phytochemical structures of tyrosinase inhibitors	22
Figure 13 Structure of synthetic compounds of tyrosinase inhibitors	35
Figure 14 Phytochemical structure of genus Manilkara	43
Figure 15 Extraction procedure of six different parts of <i>M. zapota</i>	50
Figure 16 Extraction procedure of <i>M. zapota</i> barks.....	51
Figure 17 HMBC correlations of compound I	87
Figure 18 The structure of compound I	87
Figure 19 HMBC correlations of compound II	89
Figure 20 The structure of compound II	89
Figure 21 HMBC correlations of compound III	91
Figure 22 The structure of compound III	91
Figure 23 HMBC correlations of compound IV	92
Figure 24 The structure of compound IV	93
Figure 25 HMBC correlations of compound V	95
Figure 26 The structure of compound V	95

Figure 27 HMBC correlations of compound VI	98
Figure 28 The structure of compound VI	98
Figure 29 HMBC correlations of compound VII	101
Figure 30 The structure of compound VII	101
Figure 31 Calibration curve of gallic acid for total phenolic content of crude extracts of different parts of <i>M. zapota</i>	110
Figure 32 Calibration curve of quercetin for total flavonoid content of crude extracts of different parts of <i>M. zapota</i>	110
Figure 33 Calibration curve of ferrous sulphate of crude extracts of different parts of <i>M. zapota</i>	111
Figure 34 Correlation between total phenolic content and DPPH radical scavenging activity of crude extracts of different parts of <i>M. zapota</i>	111
Figure 35 Correlation between total phenolic content and ABTS radical scavenging activity of crude extracts of different parts of <i>M. zapota</i>	112
Figure 36 Correlation between total phenolic content and FRAP activity of crude extracts of different parts of <i>M. zapota</i>	112
Figure 37 Correlation between total phenolic content and monophenolase inhibitory activity of crude extracts of different parts of <i>M. zapota</i>	113
Figure 38 Correlation between total phenolic content and diphenolase inhibitory activity of crude extracts of different parts of <i>M. zapota</i>	114
Figure 39 Correlation between total phenolic content and total flavonoid content of crude extracts of different parts of <i>M. zapota</i>	115
Figure 40 Correlation between total flavonoid content and DPPH radical scavenging activity of crude extracts of different parts of <i>M. zapota</i>	115
Figure 41 Correlation between total flavonoid content and ABTS radical scavenging activity of crude extracts of different parts of <i>M. zapot</i>	116
Figure 42 Correlation between total flavonoid content and FRAP activity of crude extracts of different parts of <i>M. zapota</i>	116
Figure 43 Correlation between total flavonoid content and monophenolase Inhibitory activity of crude extracts of different parts of <i>M. zapota</i>	117

	Page
Figure 44 Correlation between total flavonoid content and diphenolase inhibitory activity of crude extracts of different parts of <i>M. zapota</i>	117
Figure 45 Correlation between monophenolase inhibitory activity and DPPH radical scavenging activity of different parts of <i>M. zapota</i>	118
Figure 46 Correlation between monophenolase inhibitory activity and ABTS radical scavenging activity of crude extracts of different parts of <i>M. zapota</i> ...	118
Figure 47 Correlation between monophenolase inhibitory activity and FRAP activity of different parts of <i>M. zapota</i>	119
Figure 48 Correlation between diphenolase inhibitory activity and DPPH radical scavenging activity of different parts of <i>M. zapota</i>	119
Figure 49 Correlation between monophenolase inhibitory activity and ABTS radical scavenging activity of crude extracts of different parts of <i>M. zapota</i>	119
Figure 50 Correlation between monophenolase inhibitory activity and FRAP activity of different parts of <i>M. zapota</i>	119
Figure 51 The ¹ H-NMR spectrum of taraxerol methyl ether (I).....	120
Figure 52 The ¹³ C-NMR spectrum of taraxerol methyl ether (I)	121
Figure 53 The DEPT90 spectrum of taraxerol methyl ether (I)	122
Figure 54 The DEPT135 spectrum of taraxerol methyl ether (I).....	123
Figure 55 The HSQC spectrum of taraxerol methyl ether (I).....	124
Figure 56 The HMBC spectrum of taraxerol methyl ether (I).....	125
Figure 57 The COSY spectrum of taraxerol methyl ether (I).....	126
Figure 58 The HR-EI-MS spectrum of taraxerol methyl ether (I).....	127
Figure 59 The ¹ H-NMR spectrum of 6-hydroxyflavanone (II)	128
Figure 60 The ¹³ C-NMR spectrum of 6-hydroxyflavanone (II).....	129
Figure 61 The HSQC spectrum of 6-hydroxyflavanone (II).....	130
Figure 62 The HMBC spectrum of 6-hydroxyflavanone (II).....	131
Figure 63 The COSY spectrum of 6-hydroxyflavanone (II).....	132
Figure 64 The HR-EI-MS spectrum of 6-hydroxyflavanone (II).....	133
Figure 65 The ¹ H-NMR spectrum of (+)-dihydrokaempferol (III).....	134

	Page
Figure 66 The ^{13}C -NMR spectrum of (+)-dihydrokaempferol (III).....	135
Figure 67 The HSQC spectrum of (+)-dihydrokaempferol (III).....	136
Figure 68 The HMBC spectrum of (+)-dihydrokaempferol (III).....	137
Figure 69 The COSY spectrum of (+)-dihydrokaempferol (III).....	138
Figure 70 The HR-EI-MS spectrum of (+)-dihydrokaempferol (III).....	139
Figure 71 The ^1H -NMR spectrum of 3,4-dihydroxybenzoic acid (IV).....	140
Figure 72 The ^{13}C -NMR spectrum of 3,4-dihydroxybenzoic acid (IV).....	141
Figure 73 The HSQC spectrum of 3,4-dihydroxybenzoic acid (IV).....	142
Figure 74 The HMBC spectrum of 3,4-dihydroxybenzoic acid (IV).....	143
Figure 75 The COSY spectrum of 3,4-dihydroxybenzoic acid (IV).....	144
Figure 76 The HR-EI-MS spectrum of 3,4-dihydroxybenzoic acid (IV).....	145
Figure 77 The ^1H -NMR spectrum of taraxerol (V).....	146
Figure 78 The ^{13}C -NMR spectrum of taraxerol (V).....	147
Figure 79 The DEPT90 spectrum of taraxerol (V).....	148
Figure 80 The DEPT135 spectrum of taraxerol (V).....	149
Figure 81 The HSQC spectrum of taraxerol (V).....	150
Figure 82 The HMBC spectrum of taraxerol (V).....	151
Figure 83 The COSY spectrum of taraxerol (V).....	152
Figure 84 The HR-EI-MS spectrum of taraxerol (V).....	153
Figure 85 The ^1H -NMR spectrum of taraxerone (VI).....	154
Figure 86 The ^{13}C -NMR spectrum of taraxerone (VI).....	155
Figure 87 The DEPT90 spectrum of taraxerone (VI).....	156
Figure 88 The DEPT135 spectrum of taraxerone (VI)	157
Figure 89 The HSQC spectrum of taraxerone (VI)	158
Figure 90 The HMBC spectrum of taraxerone (VI)	159
Figure 91 The COSY spectrum of taraxerone (VI)	160
Figure 92 The HR-EI-MS spectrum of taraxerone (VI)	161
Figure 93 The ^1H -NMR spectrum of lupeol acetate (VII)	162
Figure 94 The ^{13}C -NMR spectrum of lupeol acetate (VII)	163

	Page
Figure 95 The DEPT90 spectrum of lupeol acetate (VII)	164
Figure 96 The DEPT135 spectrum of lupeol acetate (VII)	165
Figure 97 The HSQC spectrum of lupeol acetate (VII)	166
Figure 98 The HMBC spectrum of lupeol acetate (VII)	167
Figure 99 The COSY spectrum of lupeol acetate (VII)	168
Figure 100 The HR-EI-MS spectrum of lupeol acetate (VII)	169



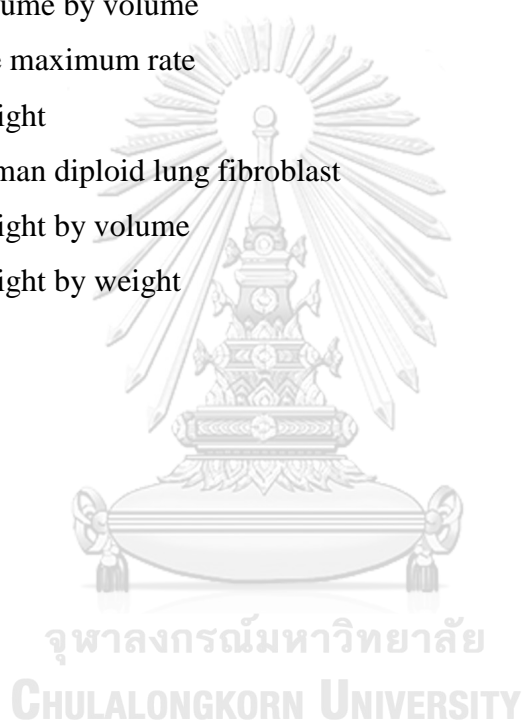
LIST OF ABBREVIATIONS

$^1\text{H-NMR}$	Proton nuclear magnetic resonance spectroscopy
$^{13}\text{C-NMR}$	Carbon nuclear magnetic resonance spectroscopy
δ	Chemicals shift
$^{\circ}\text{C}$	Celsius
%	Percentage
μg	Microgram
μL	Microliter
μm	Micrometre
μM	Micromolar
Abs	Absorbance
ABTS	2,2-Azino-bis(3-ethylbenthiiazoline-6-sulphonic acid)
ATCC	The American type culture collection
BT474	Human breast carcinoma cell line
CC	Column chromatography
CDCl_3	Deuterated chloroform
CD_3OD	Deuterated methanol
ChaGo-K-1	Human lung bronchus carcinoma cell line
cm	Centimetre
cm^{-1}	Reciprocal centimetre
COSY	Correlation spectroscopy
CC	Column chromatography
d	Doublet (for NMR spectra)
dd	Doublet of doublet (for NMR spectra)
DEPT	Distortionless enhancement by polarization transfer
DHI	5,6-Dihydroxyindole
DHICA	5,6-Dihydroxyindole-2-carboxylic acid
DI water	Deionized water
DDI water	Distilled deionized water
DMSO	Dimethyl sulfoxide
DPPH	2,2-Diphenyl-1-picrylhydrazyl
e.g.	Exempli gratia

E	Enzyme
EAC	<i>Ehrlich ascites carcinoma</i>
EC	Enzyme commission
EC ₅₀	Half maximal effective concentration
ES	Enzyme-substrate complex
EI	Electron impact ionization
<i>et al.</i>	<i>et alii</i>
EtOH	Ethanol
F ₂₅₄	Fluorescent indicator 254 nm
Fast Blue BB	<i>N</i> -(4-amino-2,5-diethoxy phenyl) benzamide
FRAP	The ferric reducing antioxidant power
g	Gram
h	Hour
HepG ₂	Human liver carcinoma cell line
HL-60	Human promyelocytic leukemia
HMBC	Heteronuclear multiple bond correlation
HMQC	Heteronuclear multiple quantum correlation
HPLC	High performance liquid chromatography
HREIMS	High resolution electron impact ionization mass spectrometry
HSQC	Heteronuclear single quantum correlation
HT-29	Human colon adenocarcinoma cell line
Hz	Hertz
I	Inhibitor
IC ₅₀	Half maximal inhibitory concentration
In	Inch
Inches ²	Square of inches
<i>J</i>	Coupling constant
KATO-III	Human gastric carcinoma cell line
kg	Kilogram
<i>K</i> _{cat}	The turnover number
<i>K</i> _i	Dissociation constant
<i>K</i> _m	Michaelis constant

L	Litre
L-DOPA	L-3,4-Dihydroxyphenylalanine
m	Multiple (for NMR spectra)
M	Molar
m/z	Mass-to-charge ratio
m ²	Square of metre
mg	Milligram
mg GAE	Milligram of gallic acid equivalent
mg QE	Milligram of quercetin equivalent
mg TEAC	Milligram of trolox equivalent antioxidant capacity
min	Minute
mL	Millilitre
mm	Millimetre
mM	Millmolar
MIC	Minimum inhibitory concentrations
MMP	Matrix metalloproteinases
MTT	3-(4,5-dimethylthiazol-2-yl)-2,5-diphenyltetrazolium bromide
NA	No activity
ND	No detection
nm	Nanometre
NMR	Nuclear magnetic resonance spectroscopy
P	Product
pH	A logarithmic measure of hydrogen ion concentration
ppm	Part per million
PTLC	Preparative thin layer chromatography
ROS	Reactive oxygen
RPMI	Roswell park memorial institute
s	Siglet (for NMR spectra)
S	Substrate
SD	Standard deviation
SPSS	Statistical package for the social sciences
SW620	Human colon carcinoma cell line

t	Triplet (for NMR spectra)
TLC	Thin layer chromatography
TMS	Tetramethylsilane
TYR	Tyrosine
TYRP1	Tyrosinase-related protein 1
TYRP2	Tyrosinase-related protein 2
UV	Ultraviolet
v	The initial rate of reaction
v/v	Volume by volume
V_{\max}	The maximum rate
w	Weight
Wi-38	Human diploid lung fibroblast
w/v	Weight by volume
w/w	Weight by weight



CHAPTER I

INTRODUCTION

Skin whitening assigns to the process of using chemical ingredients for lightening skin tone [1, 2]. One property of skin whitening cosmetics treats an overproduction of melanin. Melanin is the pigment that blocks ultraviolet (UV) radiation for protecting human skin [3]. The outer layer of skin is epidermis and consists of two cell types; keratinocytes and melanocytes. Melanocytes produce and keep melanin in melanosomes [4]. The two type of melanin calls eumelanin and pheomelanin. Both types are produced from biosynthesis pathway of melanin which tyrosinase is a key enzyme [5]. Tyrosinase (EC 1.14.18.1) contains two copper ions and catalyzes reaction in melanin synthesis. The reaction of tyrosinase involves in the initial step of the hydroxylation of *L*-tyrosine to *L*-3,4-dihydroxyphenylalanine (*L*-DOPA). Then, *L*-DOPA is oxidized to *L*-dopaquinone. Finally, a family of non-enzymatic reactions is converted to make either eumelanin or pheomelanin [6, 7]. Hyperpigmentation disorders produce abnormal melanin such as freckles, melasma, senile lentigo and spot on the body surface area [8, 9].

Tyrosinase inhibitors inhibit the increasing of skin color and reduce the activity of tyrosinase. Depigmentation mechanisms include pre-melanin synthesis, during melanin synthesis and after melanin synthesis [10]. Type of tyrosinase inhibitors is classified into three groups including competitive inhibitor, mixed type (competitive/uncompetitive) inhibitor and uncompetitive inhibitor [5]. Mechanism of depigmentation agents depends on the movement of melanin from melanocytes. Arbutin, kojic acid and vitamin C are commercially ingredients in cosmetic and pharmaceutical products and show slow-binding on diphenolase inhibitory activity [11].

Previously researches, tyrosinase inhibitors have been investigated from both natural and synthetic sources [12]. A small number of tyrosinase inhibitors have been used in cosmetic products because most of tyrosinase inhibitors showed harmful side effects on skin. Side effect of arbutin and kojic acid is a contact dermatitis and an allergic dermatitis, when a concentration of arbutin and kojic acid in cosmetic above

1% [13, 14]. From our preliminary study, ethanol and aqueous extracts of flowers of *Clitoria ternatea*, seeds of *Abrus precatorius*, barks of *Dalbergia oliveri*, barks of *Millettia brandisiana*, barks of *Smilax corbularia*, barks, twigs and roots of *Mimusops elengi*, barks, leaves and roots of *Manikara zapota* were evaluated for tyrosinase inhibitory activity using *L*-DOPA as a substrate. The results showed that ethanol extract of barks of *M. zapota* exhibited the highest antityrosinase activity with percentage inhibition value of $96.49 \pm 0.10\%$ at the concentration of 1.0 mg/mL.

Sapodilla plum (*M. zapota* L.) is a tree in family Sapotaceae. In Thailand, it is called Lamut or Lamutfarang. Its fruits are shape like eggs and ripe fruits are edible and sweet with rich fine flavor [15]. This plant has been shown many bioactivities such as antidiabetic, anti-inflammatory, antilipidemic, antimicrobial, antioxidant, anti-pyretic and antityrosinase activities [16-18]. However, the literatures were reported a few effective of the isolated compounds from *M. zapota* on tyrosinase inhibitory activity. Thus, the current study is undertaken to isolate chemical constituents of *M. zapota* barks and evaluate their tyrosinase inhibitory activity.

Objectives

To investigate the tyrosinase inhibitors from *M. zapota* L.

CHAPTER II

THEORETICAL

2.1 Melanin

Skin is the site of various complex, helps to regulate temperature and protects structure from the external environment [19]. Skin is a living organism and consists of three main parts as epidermis, dermis and subcutaneous fat layers (Figure 1). The epidermal barrier prevents the skin from chemicals, microbes, physical injury and dehydration of epidermis. The epidermal barrier produces by differentiation of keratinocytes. They migrate from the basal cell layer into the stratum corneum. The keratinocytes of the epidermis are created and renewed by stem cells in the basal layer [20]. It produces every 28 days for replacement of epidermis. The basal layer takes 14 days to reach stratum corneum and scrubs for another 14 days. Keratinocytes build keratins. Keratins are structural proteins and make up the keratinocyte cytoskeleton. In stratum spinosum, keratin filaments emit from the nucleus and link with desmosomes. Then, they move into the stratum granulosum. Keratohyalin granules form keratin and profilaggrin. Profilaggrin transforms into filaggrin. It flows and aligns keratin filaments into fully compressed parallel when the cell of stratum corneum are formed the matrix. The mutation of filaggrin genes connects with ichthyosis vulgaris and atopic dermatitis. Keratinocyte moves and develops a flat hexagon model into the stratum corneum [21].

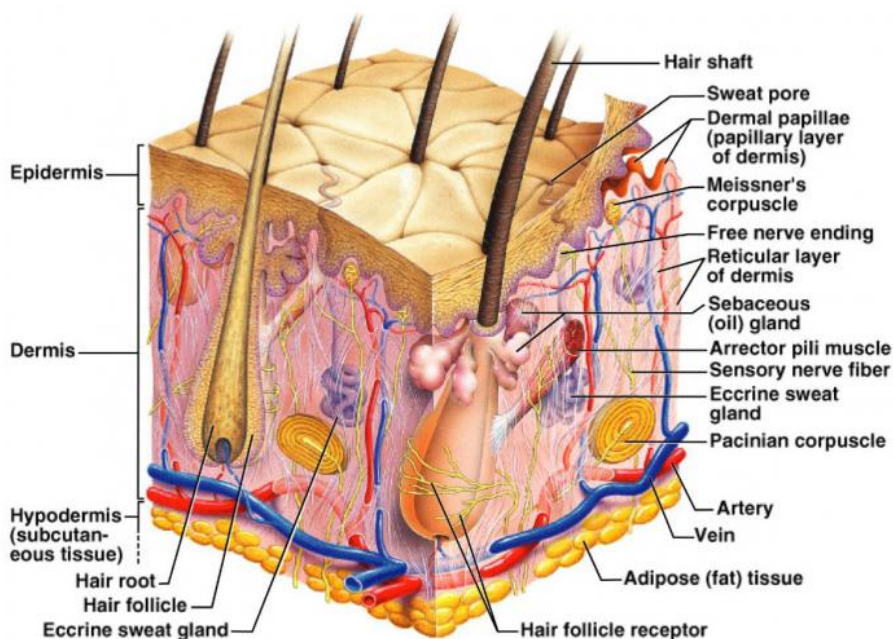


Figure 1 Cross-section of skin structure

Melanins are widely dispersed pigments in animals, plants, fungi and bacteria. Melanins are divided into two types as eumelanin and pheomelanin [22]. Melanin structure is a heterogeneous polymer with complex pigments. Melanin pigments are synthesized by melanocyte cells. Melanocyte cells contain a specific enzyme as tyrosinase in the stratum basale of dermis. Tyrosinase controls the produce of melanins. Synthesis of melanins occurs in melanosomes. It carries out from the melanocyte cells to keratinocyte cells. The function of melanin is protection of UV to damage the skin and discarded reactive oxygen species (ROS) in organisms [23-25]. The initial step of melanogenesis is the hydroxylation of *L*-tyrosine into *L*-DOPA. Then, *L*-DOPA is oxidized to *L*-dopaquinone. Both two steps are catalyzed by tyrosinase. After that, the reaction *L*-dopaquinone is cyclized into leukodopachrome at 1,4-addition position and rapidly oxidized to dopachrome. The dopachrome is brought to produce eumelanin into two difference reactions. The first reaction, dopachrome is decarboxylated into 5,6-dihydroxyindole (DHI). Then, it is oxidized to indole-5,6-quinone. Finally, indole-5,6-quinone is polymerized to eumelanin. The second reaction, dopachrome is transformed into 5,6-dihydroxyindole-2-carboxylic acid (DHICA) by tautomerase. Then, DHICA is oxidized into indole-5,6-quinone carboxylic acid. Then, indole-5,6-quinone carboxylic acid is polymerized to eumelanin. For synthesis of pheomelanin, *L*-dopaquinone is reacted with glutathione or cysteine to form glutathionyl-dopa or cysteinyl-dopa. The

glutathionyl-dopa or cysteinyl-dopa is then cyclized into 1,4-benzothiazinylalanine. Finally, 1,4-benzothiazinylalanine is polymerized to pheomelanin (Figure 2) [7, 26].

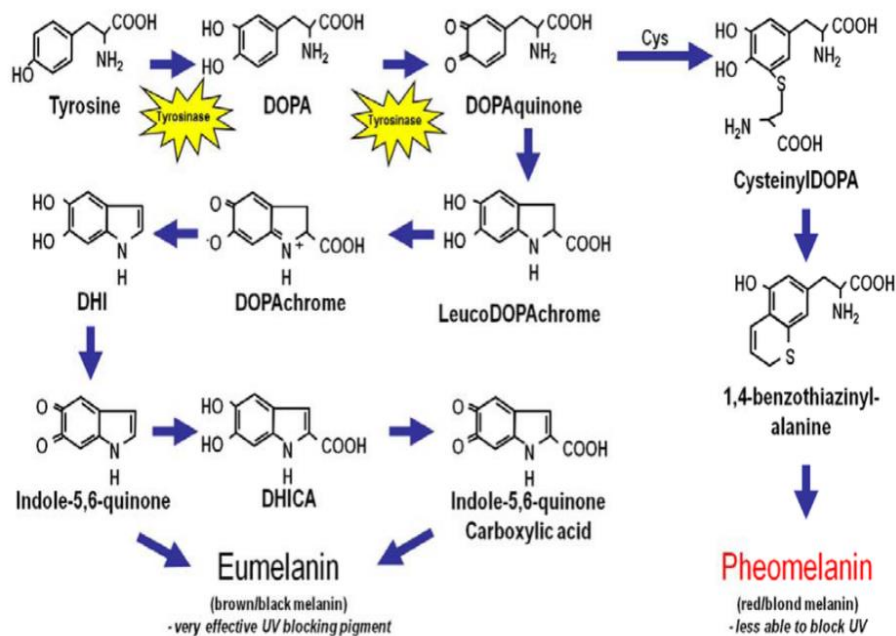
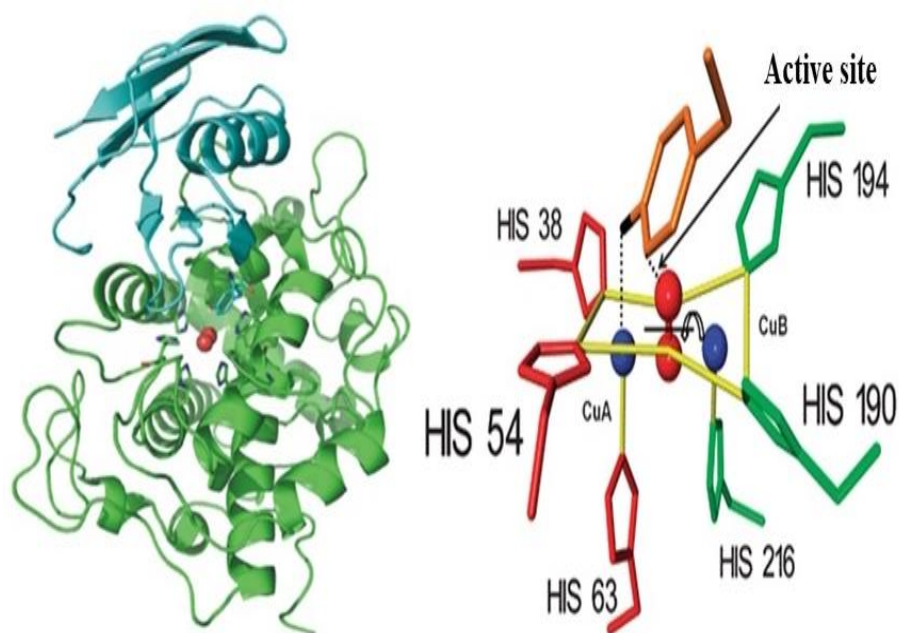


Figure 2 Melanin biosynthesis pathway

Hyperpigmentation appears when melanin is overproduced on the skin. Many hyperpigmentation disorders such as acne scars, age spots, freckles, melisma and senile lentigo are attributed by the darkness of the human skin. The factors of hyperpigmentation are age, hormones, pregnancy, UV radiation [27] and others.

2.2 Tyrosinase enzyme

A family of tyrosinase as tyrosinase (TYR), tyrosinase-related protein 1 (TYRP1) and tyrosinase-related protein 2 (TYRP2) is related in human melanogenesis. Tyrosinase (EC 1.14.18.1) is a polyphenol oxidase. It contains binuclear copper on molecular oxygen (Figure 3). Tyrosinase catalyzes two initial steps in melanin biosynthesis pathway. The hydroxylation of *L*-tyrosine into *L*-DOPA is called monophenolase activity and the oxidation of *L*-DOPA into *L*-dopaquinone is called diphenolase activity [28]. TYRP1 and TYRP2 catalyze other step to control the type of melanin synthesis. However, if one reaction of melanin synthesis fails, melanins are not found on the skin [29].



A= Tertiary structure of tyrosinase

1. B = Coordination sphere of binuclear copper center and location of tyrosinase substrate

Figure 3 Structure of tyrosinase

2.3 Tyrosinase inhibitor

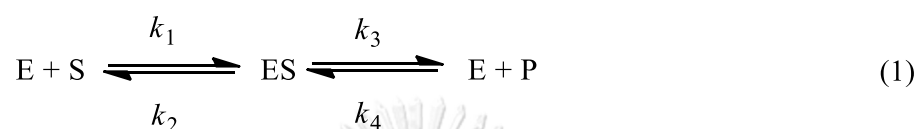
Various tyrosinase inhibitors were identified from both synthetic and natural sources. They were investigated using *L*-tyrosine or *L*-DOPA as substrates. The inhibitory activity of tyrosinase inhibitors are exhibited in the formation of dopachrome [6]. Monophenolase and diphenolase inhibitory activities of tyrosinase inhibitor can be described by one of the following:

- (1) *L*-Dopaquinone is reduced by reducing agents. Reducing agents are used as melanogenesis inhibitors such as ascorbic acid.
- (2) *L*-Dopaquinone is reacted with *L*-dopaquinone scavenger for the colorless of product. Then, the melanogenesis process is slowed. The *L*-dopaquinone scavenger was used as thio-containing compounds and the reaction is overturned to original rates.
- (3) Dopachrome formation is protected by alternative enzyme substrate such as phenolic compounds.
- (4) Nonspecific enzyme in-activators denature the enzyme as acids or bases.
- (5) Specific tyrosinase in-activators inhibit tyrosinase activity using suicide substrate such as kojic acid.

(6) Specific tyrosinase inhibitors reduce tyrosinase.

2.4 Mechanism of enzyme inhibition

Enzyme displays an essential role in biochemical processes. Enzyme is a specific function in few conditions. Enzyme (E) binds to the substrate (S) to form enzyme-substrate complex (ES). Then, it changes to enzyme and product (P). The reaction was described in equation 1 [30, 31].



From theoretical, reactions are reversible reactions. Enzyme reactions are studied by using steady-state conditions. In steady-state conditions, ES is the rate constant, P is increasing and S is reducing. The conditions were described in equation 2.

$$k_1[E][S] = (k_2 + k_3)[ES] \quad (2)$$

When equation 2 was rearrange to

$$[E][S]/[ES] = (k_2 + k_3) / k_1 \quad (3)$$

$$K_m = (k_2 + k_3)/k_1 \quad (4)$$

Where K_m is the Michaelis constant, it gives the enzyme-substrate binding constant under steady-state conditions and measures the rate in the initial milliseconds of the reaction.

$$[ES] = [E][S]/K_m \quad (5)$$

$$[E] = [E_{total}] - [ES] \quad (6)$$

$$[ES] = [E_{total}] - [E] \quad (7)$$

Instead from equations 3 and 4 and solve for ES

$$[ES] = [E_{total}][S]/[S] + K_m \quad (8)$$

The initial rate of reaction (v) is proportional to $[ES]$ when $[S]$ is small and the maximum rate (V_{max}) is proportional to $[E_{total}]$ when $[S]$ is saturating. The Michaelis-Menten equation can be described in term of the reaction rate.

$$v = V_{max}[S]/[S] + K_m \quad (9)$$

K_m is determined by measuring the reaction rate at various $[S]$ and $[E_{total}]$ is constant and v is represented to $[S]$ when $[S]$ is low and $K_m = [S]$ when $v = V_{max}/2$

(Figure 4). Determination of kinetic parameters uses plotting of the reciprocals of the Michaelis-Menten equation (9). It is called a Lineweaver-Burk plot.

$$1/v = 1/V_{\max} + [K_m/V_{\max}][1/[S]]$$

(10)

At V_{\max} , $[ES]$ is equal to $[E_{\text{total}}]$ and the rate of the reaction is proportional to k_3 which represented to the turnover number (k_{cat}). The equation can be determined, if $[E_{\text{total}}]$ is known. k_{cat}/K_m is called catalytic efficiency.

$$k_3 = V_{\max}/[E_{\text{total}}] \quad (11)$$

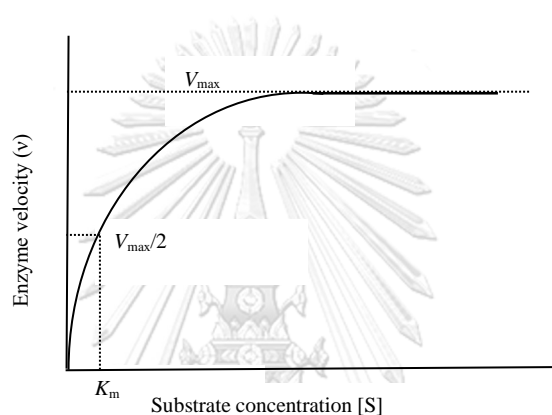
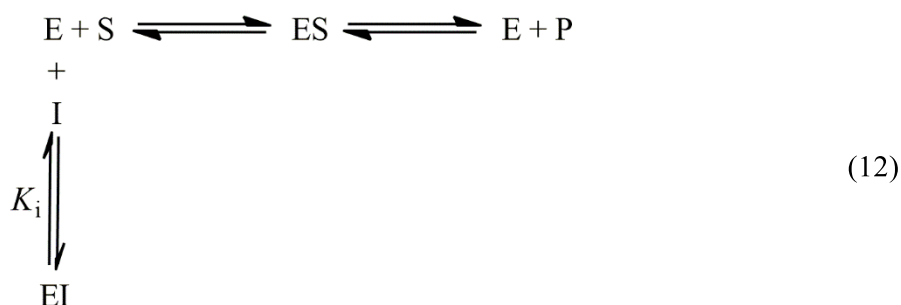


Figure 4 Michaelis-Menten plot

2.4.1 Competitive inhibition

The enzyme inhibitor (I) binds to the enzyme at the active site as same as the substrate binds to the enzyme.



From Michaelis-Menten plot, K_m is increased but V_{\max} is unchanged when the substrate concentration is increased (Figure 5). Dissociation constant (K_i) can be calculated from Michaelis-Menten equation or a reciprocal plot versus $[I]$ in plotting

the slopes of the lines. In Lineweaver-Burk plot, the slopes of inhibitor and without inhibitor lines cross the y-axis at the same point (Figure 6).

$$K_i = [I]/[(K_{m, \text{obs}}/K_m)-1] \quad (13)$$

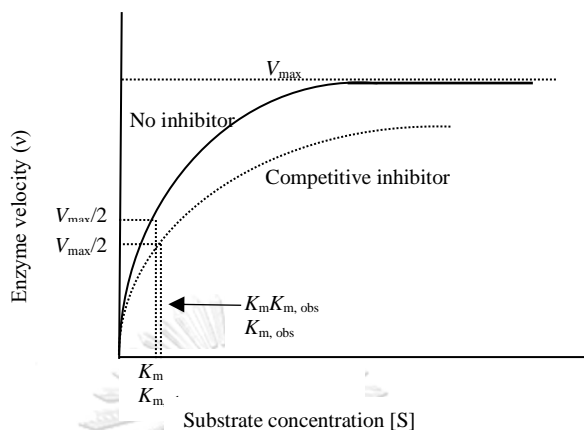


Figure 5 Michaelis-Menten plot of competitive inhibition

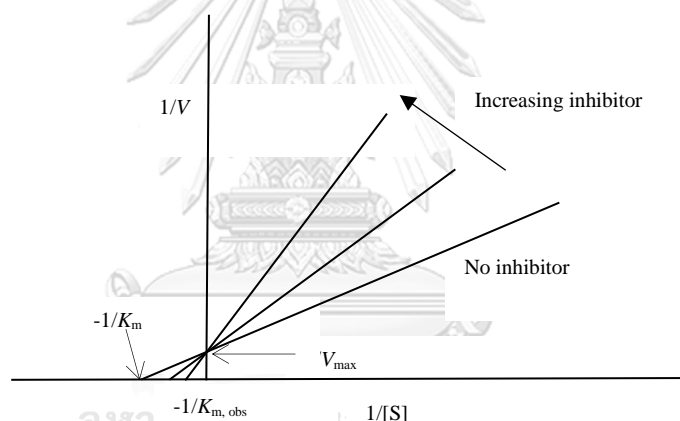
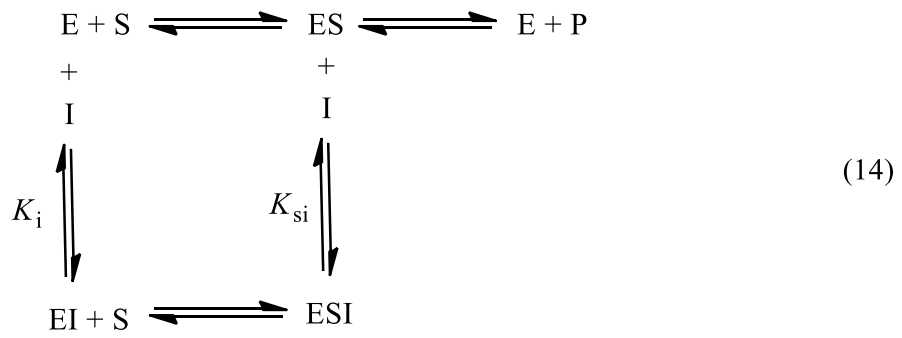


Figure 6 Lineweaver-Burk plots of competitive inhibition

2.4.2 Mixed inhibition

The inhibitor binds to a site other than the active site of the enzyme to change form an inactive complex. Inhibitor binds to either the enzyme or the enzyme-substrate complex. From Michaelis-Menten equation, K_m of inhibitor and without inhibitor is the same value. V_{max} of inhibitor is lower than V_{max} of without inhibitor (Figure 7) and K_i can be calculated from Michaelis-Menten equation or plotting $1/v$ versus $[I]$ in plotting the slopes of the lines. In a Lineweaver-Burk plot, the slopes of inhibitor and without inhibitor lines converge on the X-axis at $-1/K_m$ (Figure 8). It is called noncompetitive inhibition. In mixed inhibition, K_i and K_{si} are equivalent. The slopes of inhibitor and without inhibitor lines cross at the same point in the quadrant (Figure 9).



3

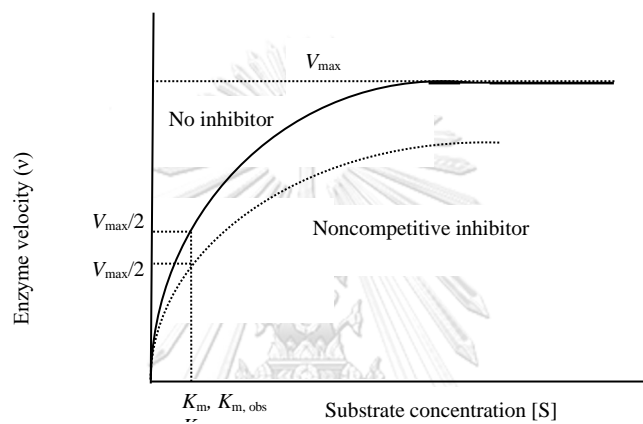


Figure 7 Michaelis-Menten plot of noncompetitive inhibition

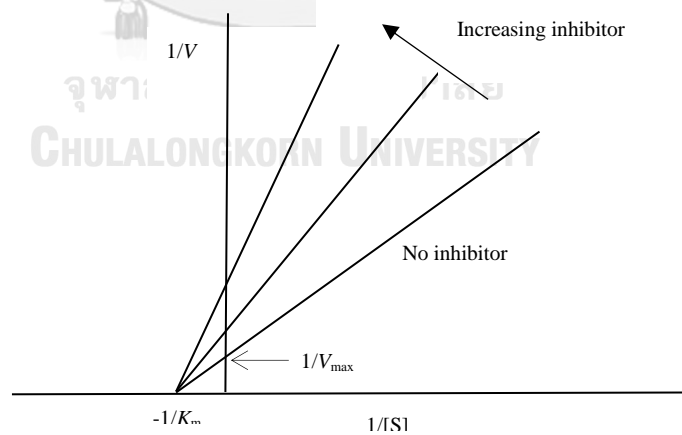


Figure 8 Lineweaver-Burk plots of noncompetitive inhibition

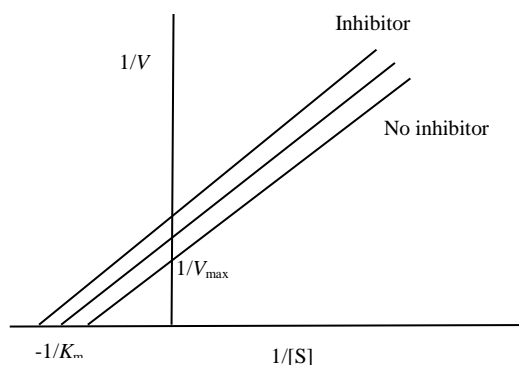


Figure 11 Lineweaver-Burk plots of uncompetitive inhibition

2.5 Literature reviews

2.5.1 Tyrosinase inhibitory activity of medicinal plants

The various plants extracts and ethanol crude extract of medicine formulation of herbs were investigated for tyrosinase inhibitory activity. Antityrosinase assays were tested by either *in vitro* or *in vivo* methods on monophenolase and diphenolase inhibitory activities. For monophenolase inhibitory activity, ethyl acetate fraction of *Acanthopanax koreanum* leaves exhibited antityrosinase activity (IC_{50} 186.20 ± 11.70 $\mu\text{g/mL}$) and triterpenoid compounds were isolated from this plant. $3\alpha,20\alpha,29$ -Trihydroxylupane-23,28-dioic acid (IC_{50} 8.61 ± 1.09 μM) showed tyrosinase inhibitory activity and compared with kojic acid (IC_{50} 36.36 ± 2.83 μM) [32]. (2S)-2',4',4'-Dihydroxy-5'-(1''',1'''-dimethylallyl)-8-prenyl pinocembrin which was isolated from *Dalea elegans* exhibited antityrosinase activity with IC_{50} value of 2.32 ± 0.01 μM and compared with kojic acid with IC_{50} value of 4.90 ± 0.01 μM [33]. Ethanol extract of fruit pericarps of *Dimocarpus longan* showed antityrosinase activity with percentage inhibition value of 23.60 ± 1.20 at a concentration of 100 $\mu\text{g/mL}$ [34]. 2',4',6'-Trihydroxydihydrochalcone was isolated from *Greyia flanaganii* leaves and exhibited tyrosinase inhibitory activity with IC_{50} value of 69.1 μM [35]. Dihydrokeampferol, naringenin and rhoiptelol which were isolated from *Juglans mandshurica* barks showed more potent antityrosinase activity than arbutin (IC_{50} 22.40 ± 4.70 mM) [36]. Ethanol crude extracts of *Litchi sinensis* seeds showed antityrosinase activity in a concentration-dependent manner [37]. Methanol crude extract of *Mimusops elengi* flowers showed strong antityrosinase activity [38]. Essential oil of *Rubus pungens* var. *oldhamii* (IC_{50} 0.92 mg/mL) showed strong tyrosinase inhibitory activity and compared with arbutin (IC_{50} 0.66 mg/mL) [39]. Acetone and methanol crude extracts of

Sideroxylon inerme barks showed antityrosinase activity and compared with arbutin and kojic acid (IC_{50} 63.00 ± 2.10 , 82.10 ± 2.70 , 149.00 ± 1.20 and 1.14 ± 0.05 $\mu\text{g/mL}$, respectively) [40].

For diphenolase inhibitory activity, dichloromethane fraction of *Acmella oleracea* showed antityrosinase activity (IC_{50} 0.50 mM) and compared with kojic acid (IC_{50} 0.13 mM) [41]. Artocaepein E, artocarpanone, liquiritigenin and steppogenin were isolated from *Artocarpus heterophyllous* woods showed more potent tyrosinase inhibitory activity than kojic acid (IC_{50} 6.70 ± 0.80 , 2.00 ± 0.10 , 22.00 ± 2.5 , 7.50 ± 0.5 and 44.60 ± 0.40 μM , respectively) [42]. Aqueous crude extract of *Asparagus officinalis* showed tyrosinase inhibitory activity with IC_{50} value of 1.21 mg/mL and exhibited mixed-type of kinetic inhibition [43]. Essential oils which were extracted from *Cinnamomum zeylanicum*, *Citrus grandis* and *Citrus hystrix* showed potent tyrosinase inhibitory activity when compared with kojic acid (IC_{50} 2.05 ± 0.07 , 2.07 ± 0.15 , 2.08 ± 0.25 and 44.60 ± 0.40 2.28 ± 0.05 $\mu\text{g/mL}$) [44]. Nobiletin which was isolated from *Citrus unshiu* peels showed stronger inhibition against tyrosinase than arbutin (IC_{50} 1.49 and 27.31 mM, respectively) [45]. Ethanol extracts of root barks and twigs of *Morus alba* showed tyrosinase inhibitory activity with percentage inhibition values of 78.00 and 62.00 at a concentration of 60 $\mu\text{g/mL}$, respectively [46]. Moreover, methanol crude extract of *Podocarpus* species showed antityrosinase activity in a dose-dependent manner [47]. Purpurin which was isolated from roots of *Rubia cordifolia* showed antityrosinase activity and compared with kojic acid (IC_{50} 0.29 ± 0.09 and 0.0019 mg/mL) [48]. Moracin M which was isolated from ethanol crude extract of woods of *Streblus ilicifolius* exhibited antityrosinase activity and compared with kojic acid (IC_{50} 67.69 and 38.67 $\mu\text{g/mL}$) [49]. In addition, herbal formulations were studied on tyrosinase inhibitory activity. Qian-wang-hong-bai-san composed of fruits of *Benincasa hispida*, pericarps of *Punica granatum*, tubers of *Bletilla striata* and tubers of *Typhonium giganteum* (1:1:1:1). Ethanol crude extract of Qian-wang-hong-bai-san showed mushroom tyrosinase inhibitory activity (IC_{50} 1.21 mg/mL) and *in vivo* antityrosinase activity on mouse B16 cells (IC_{50} 177.90 $\mu\text{g/mL}$). Qi-bai-gao consisted of rhizomes of *Atractylodes macrocephala*, rhizomes of *Smilax glabra*, roots of *Ampelopsis japonica*, roots of *Angelica dahurica*, root and rhizomes of *Asarum heterotropoides*, tubers of *B. striata* and tubers of *T. giganteum* (10:3:3:10:3:3:10).

Ethanol crude extract of Qi-bai-gao showed percentage of tyrosinase inhibition as $60.30 \pm 0.90\%$ at concentration of 1 mg/mL and percentage of tyrosinase inhibition on mouse B16 cells as $44.10 \pm 8.60\%$ at concentration of 1 mg/mL. Qiong-yu-gao consisted of root of *Rehmannia glutinosa*, roots and rhizomes of *Panax ginseng* and rhizomes of *S. glabra* (1:1:1). Qiong-yu-gao ($IC_{50} > 1000 \mu\text{g/mL}$) showed less *in vitro* tyrosinase inhibitory activity than *in vivo* assay on mouse B16 cells ($IC_{50} 531.20 \mu\text{g/mL}$) [50]. The literature reviews of antityrosinase activity for crude extracts of plants are shown in Table 1. The literature reviews of antityrosinase activity for phytochemicals of plants are shown in Table 2 and Figure 12.

Table 1 Antityrosinase activity of crude extracts of plants

Scientific name	Plant part	Crude extract	Reference
<i>Acanthopanax koreanum</i>	Leaves	Ethyl acetate fraction of methanol extract ($IC_{50} = 186.20 \pm 11.70 \mu\text{g/mL}$ on monophenolase inhibitory activity)	[32]
<i>Acmella oleracea</i>	Leaves Stems	Dichloromethane fraction of methanol extract ($IC_{50} = 0.50 \text{ mM}$ on diphenolase inhibitory activity)	[41]
<i>Anacardium occidentale</i>	Fresh leaves	Methanol extract by blanching (% diphenolase inhibition = $44 \pm 3.5\%$ at 0.25 mg/mL) Methanol extract by maceration (% diphenolase inhibition = $40 \pm 2.2\%$ at 0.25 mg/mL) Methanol extract by microwave (% diphenolase inhibition = $49 \pm 4.0\%$ at 0.25 mg/mL)	[51]
<i>Ampelopsis japonica</i>	Roots	Ethanol extract (<i>in vitro</i> , $IC_{50} = 152.1 \mu\text{g/mL}$ on diphenolase inhibitory activity) (<i>in vivo</i> , $IC_{50} = 117.3 \mu\text{g/mL}$ on diphenolase inhibitory activity)	[50]
<i>Asparagus officinalis</i>	Whole plant	Aqueous extract (Mixed inhibitor, $IC_{50} = 1.21 \text{ mg/mL}$ on diphenolase inhibitory activity) Aqueous extract inhibited melanin production (% diphenolase inhibition = $18.6 \pm 1.7\%$ at 0.05 mg/mL) (% diphenolase inhibition = $18.4 \pm 2.2\%$ at 0.20 mg/mL) (% diphenolase inhibition = $20.4 \pm 2.3\%$ at 1.00 mg/mL)	[43]
<i>Asphodelus microcarpus</i>	Flowers Leaves Tubers	Aqueous extract (% diphenolase inhibition = $6.55 \pm 0.21\%$ at 0.2 mg/mL) Ethanol extract (% diphenolase inhibition = $40.25 \pm 4.4\%$ at 0.2 mg/mL) Methanol extract (% diphenolase inhibition = $13.9 \pm 2.4\%$ at 0.2 mg/mL) Aqueous extract (% diphenolase inhibition = $9.85 \pm 0.21\%$ at 0.2 mg/mL) Ethanol extract (% diphenolase inhibition = $29.9 \pm 0.14\%$ at 0.2 mg/mL) Methanol extract (% diphenolase inhibition = $20.4 \pm 1.4\%$ at 0.2 mg/mL) Aqueous extract (% diphenolase inhibition = $10.65 \pm 1.34\%$ at 0.2 mg/mL) Ethanol extract (% diphenolase inhibition = $8.4 \pm 1.3\%$ at 0.2 mg/mL) Methanol extract (% diphenolase inhibition = $2.25 \pm 1.0\%$ at 0.2 mg/mL)	[52]
<i>Beilschmiedia pulverulenta</i>	Aerial parts	Essential oil (% diphenolase inhibition = $67.6 \pm 0.40\%$ at 1 mg/mL)	[53]
<i>Berberis aristata</i>	Stem barks and woods	Aqueous extract (% monophenolase inhibition = 97% at 110 $\mu\text{g/mL}$) Aqueous extract ($IC_{50} = 412.01 \mu\text{g/mL}$ on diphenolase inhibitory activity) Methanol extract (Mixed inhibitor, % monophenolase inhibition = 78% at 110 $\mu\text{g/mL}$)	[54]

Table 1 Antityrosinase activity of crude extracts of plants (continue)

Scientific name	Plant part	Crude extract	Reference
<i>Bryophyllum pinnatum</i>	Leaves	Methanol extract (IC ₅₀ = 431.11 µg/mL on diphenolase inhibitory activity)	[55]
		Aqueous extract (IC ₅₀ = 8.12 mg/mL on diphenolase inhibitory activity)	
		50% Methanol extract (IC ₅₀ = 0.56 mg/mL on diphenolase inhibitory activity)	
<i>Cinnamomum cassia</i>	Stem barks	Methanol extract (IC ₅₀ = 9.78 mg/mL on diphenolase inhibitory activity)	[44]
		Essential oil (Mixed inhibitor, IC ₅₀ = 6.16 ± 0.04 µg/mL on monophenolase inhibitory activity)	
<i>Cinnamomum zeylanicum</i>	Leaves	Essential oil (Uncompetitive inhibitor, IC ₅₀ = 2.05 ± 0.07 µg/mL on monophenolase inhibitory activity)	[44]
<i>Citrus grandis</i>	Fruit peels	Essential oil (Competitive inhibitor, IC ₅₀ = 2.07 ± 0.15 µg/mL on monophenolase inhibitory activity)	[44]
	Leaves	Essential oil (IC ₅₀ = 6.82 ± 0.16 µg/mL on monophenolase inhibitory activity)	
<i>Citrus hystrix</i>	Fruits	Essential oil (Uncompetitive inhibitor, IC ₅₀ = 2.08 ± 0.25 µg/mL on monophenolase inhibitory activity)	[44]
<i>Citrus reticulata</i>	Leaves	Essential oil (IC ₅₀ = 19.75 ± 1.75 µg/mL on monophenolase inhibitory activity)	[44]
<i>Cupressus macrocarpa</i>	Leaves	Essential oil (IC ₅₀ = 70.98 ± 0.23 µg/mL on monophenolase inhibitory activity)	[44]
<i>Cynanchum atratum</i>	Roots	30% Ethanol extract (<i>in vitro</i> , % diphenolase inhibition = 51.8 ± 1.1% at 2 mg/mL) (<i>in vivo</i> , % diphenolase inhibition = -7.4 ± 1.2% at 2 mg/mL)	[50]
<i>Cymbopogon citratus</i>	Leaves	Essential oil (IC ₅₀ = 132.16 ± 2.54 µg/mL on monophenolase inhibitory activity)	[44]
<i>Dimocarpus longan</i>	Fruit pericarps	50% Ethanol extract (% monophenolase inhibition = 23.6 ± 1.2% at 100 µg/mL)	[34]
		50% Ethanol extract by ultra-high-pressure-assisted (% monophenolase inhibition = 19.5 ± 0.6% at 100 µg/mL)	
<i>Eucalyptus camaldulensis</i>	Leaves	Methanol extract (IC ₅₀ = 2258 µg/mL on monophenolase inhibitory activity)	[56]
<i>Euphoria longana</i>	Dried seeds	Hot water extract (IC ₅₀ = 3.20 mg/mL on diphenolase inhibitory activity)	[57]
	Fresh seeds	Hot water extract (IC ₅₀ = 2.90 mg/mL on diphenolase inhibitory activity)	
<i>Ginkgo biloba</i>	Leaves	30% Ethanol extract (<i>in vitro</i> , % diphenolase inhibition = 70.0 ± 1.3% at 2 mg/mL) (<i>in vivo</i> , % diphenolase inhibition = 45.5 ± 2.8% at 2 mg/mL)	[50]
<i>Intsia palembanica</i>	Seeds	Aqueous fraction of methanol extract (IC ₅₀ = 4.34 µg/mL on diphenolase inhibitory activity)	[58]
		Ethyl acetate fraction of methanol extract (IC ₅₀ = 3.97 µg/mL on diphenolase inhibitory activity)	
<i>Juglans regia</i>	Leaves	30% Ethanol extract (IC ₅₀ = 505 mg/mL on diphenolase inhibitory activity)	[50]
<i>Laurus nobilis</i>	Leaves	Essential oil (IC ₅₀ = 127.66 ± 2.73 µg/mL on monophenolase inhibitory activity)	[44]
<i>Lavandula x intermedia</i> <i>var. Grosso</i>	Leaves	Essential oil (IC ₅₀ = 19.36 ± 0.20 µg/mL on monophenolase inhibitory activity)	[44]
<i>Lindera aggregate</i>	Leaves	30% Ethanol extract (<i>in vitro</i> , IC ₅₀ = 276.3 µg/mL on diphenolase inhibitory activity) (<i>in vivo</i> , IC ₅₀ = 115.1 µg/mL on diphenolase inhibitory activity)	[50]
<i>Litchi chinensis</i>	Seed coats	Ethyl acetate extract (<i>in vivo</i> , IC ₅₀ = 197.80 ± 1.23 µg/mL on diphenolase inhibitory activity)	[59]
<i>Litchi sinensis</i>	Seeds	Ethanol extract (% monophenolase inhibition = 8.8 ± 0.8% at 100 µg/mL)	[37]

Table 1 Antityrosinase activity of crude extracts of plants (continue)

Scientific name	Plant part	Crude extract	Reference
<i>Melaleuca quinquenervia</i>	Leaves	Essential oil (IC ₅₀ = 150.28 ± 0.29 µg/mL on monophenolase inhibitory activity)	[44]
<i>Mentha pulegium</i>	Leaves	Ethanol extract (IC ₅₀ = 286 ± 45 µg/mL on monophenolase inhibitory activity)	[60]
<i>Mentha rotundifolia</i>	Leaves	Ethanol extract (IC ₅₀ = 108 ± 20 µg/mL on monophenolase inhibitory activity)	[60]
<i>Mentha spicata</i>	Leaves	Ethanol extract (IC ₅₀ = 223 ± 41 µg/mL on monophenolase inhibitory activity)	[60]
<i>Mimosa elengi</i>	Flowers	Methanol extract (IC ₅₀ = 401 µg/mL on monophenolase inhibitory activity)	[38]
<i>Morus alba</i>	Root barks	Ethanol extract (% diphenolase inhibition = 0 - 62% at 0 - 60 µg/mL)	[46]
	Twigs	Ethanol extract (% diphenolase inhibition = 0 - 78% at 0 - 60 µg/mL)	
<i>Peucedanum knappii</i>	Aerial parts	Ethyl acetate fraction of methanol extract (IC ₅₀ = 517 µg/mL on diphenolase inhibitory activity)	[61]
<i>Pimenta dioica</i>	Leaves	Essential oil (IC ₅₀ = 21.33 ± 0.127 µg/mL on monophenolase inhibitory activity)	[44]
<i>Piper betel</i>	Leaves	Essential oil (IC ₅₀ = 87.97 ± 1.052 µg/mL on monophenolase inhibitory activity)	[44]
	Leaves	Methanol extract by maceration (% diphenolase inhibition = -20 ± 5.5% at 0.25 mg/mL)	[51]
		Methanol extract by blanching (% diphenolase inhibition = -13 ± 3.8% at 0.25 mg/mL)	
Methanol extract by microwave (% diphenolase inhibition = -23 ± 7.3% at 0.25 mg/mL)			
<i>Piper magnibaccum</i>	Leaves	Essential oil (% diphenolase inhibition = 49.50 ± 0.6%)	[62]
	Stems	Essential oil (% diphenolase inhibition = 57.01 ± 0.8%) Fraction IV of ethanol extract (Uncompetitive inhibitor, IC ₅₀ = 5.81 ± 0.08 µg/mL on diphenolase inhibitory activity)	
<i>Podocarpus elongatus</i>	Leaves	50% Methanol extract (EC ₅₀ = 0.47 ± 0.001 mg/mL)	[47]
	Stems	50% Methanol extract (E ₅₀ = 0.14 ± 0.001 mg/mL)	
<i>Podocarpus falcatus</i>	Leaves	50% Methanol extract (EC ₅₀ = 0.29 ± 0.002 mg/mL on diphenolase inhibitory activity)	[47]
	Stems	50% Methanol extract (EC ₅₀ = 0.35 ± 0.002 mg/mL on diphenolase inhibitory activity)	
<i>Podocarpus henkelii</i>	Leaves	50% Methanol extract (EC ₅₀ = 0.37 ± 0.003 mg/mL on diphenolase inhibitory activity)	[47]
	Stems	50% Methanol extract (EC ₅₀ = 0.40 ± 0.003 mg/mL on diphenolase inhibitory activity)	
<i>Podocarpus latifolius</i>	Leaves	50% Methanol extract (EC ₅₀ = 0.41 ± 0.005 mg/mL on diphenolase inhibitory activity)	[47]
	Stems	50% Methanol extract (EC ₅₀ = 0.36 ± 0.001 mg/mL on diphenolase inhibitory activity)	
<i>Polygonatum odoratum</i>	Rhizomes	30% Ethanol extract (<i>in vitro</i> , IC ₅₀ = 98.4 µg/mL on diphenolase inhibitory activity) (<i>in vivo</i> , IC ₅₀ = 830.1 µg/mL on diphenolase inhibitory activity)	[50]
<i>Polygonum cuspidatum</i>	Fruits	Extract by supercritical carbon dioxide fluid (% monophenolase inhibition = 14.8 ± 1.23% at 100 µg/mL) (% monophenolase inhibition = 22.6 ± 1.64% at 250 µg/mL)	[26]
<i>Populus nigra</i>	Buds	Ethanol extract (Competitive inhibitor, <i>in vitro</i> , IC ₅₀ = 77 ± 8 ppm on monophenolase inhibitory activity) (<i>in vivo</i> , IC ₅₀ = 27 ± 1 ppm on monophenolase inhibitory activity) (Reducing melanin content in B16 cells, IC ₅₀ = 39 ± 9 µg/mL)	[63]
<i>Prunus davidiana</i>	Seeds	30% Ethanol extract (<i>in vitro</i> , IC ₅₀ > 1,000 µg/mL on diphenolase inhibitory activity) (<i>in vivo</i> , IC ₅₀ > 1,000 µg/mL on diphenolase inhibitory activity)	[50]

Table 1 Antityrosinase activity of crude extracts of plants (continue)

Scientific name	Plant part	Crude extract	Reference
<i>Psiadia arguta</i>	Leaves	Essential oil (IC ₅₀ = 20.03 ± 1.542 µg/mL on monophenolase inhibitory activity)	[44]
<i>Psiadia terebinthina</i>	Leaves	Essential oil (IC ₅₀ = 135.13 ± 0.117 µg/mL on monophenolase inhibitory activity)	[44]
<i>Psidium guajava</i>	Leaves	Essential oil (IC ₅₀ = 76.34 ± 0.854 µg/mL on monophenolase inhibitory activity)	[44]
<i>Rhodiola rosea</i>	Roots	Ethanol extract (% monophenolase inhibition = 53.3 ± 1.5% at 4 mg/mL) Ethyl acetate extract (% monophenolase inhibition = 77.1 ± 0.5% at 4 mg/mL)	[64]
<i>Rosa damascena</i>	Flowers	Rose oil distillation water (Uncompetitive inhibitor, IC ₅₀ = 0.41 ± 0.03 µg/mL on monophenolase inhibitory activity) Fraction III of rose oil distillation water (Noncompetitive inhibitor, IC ₅₀ = 89.09 ± 0.16 µg/mL on monophenolase inhibitory activity)	[65]
<i>Rubus pungens</i>	Leaves	Essential oil (IC ₅₀ = 0.92 mg/mL on diphenolase inhibitory activity)	[39]
<i>Salvia officinalis</i>	Leaves	Essential oil (IC ₅₀ = 99.76 ± 1.750 µg/mL on monophenolase inhibitory activity)	[44]
<i>Schinus terebinthifolius</i>	Leaves	Essential oil (IC ₅₀ = 105.03 ± 2.485 µg/mL on monophenolase inhibitory activity)	[44]
<i>Sideroxylon inerme</i>	Stem barks	Acetone extract (IC ₅₀ = 63 ± 2.1 µg/mL on monophenolase inhibitory activity) Acetone extract (IC ₅₀ > 400 µg/mL on diphenolase inhibitory activity) Dichloromethane extract (IC ₅₀ > 400 µg/mL on monophenolase inhibitory activity)	[40]
<i>Sideroxylon inerme</i>	Stem barks	Methanol extract (IC ₅₀ = 82.1 ± 2.7 µg/mL on monophenolase inhibitory activity)	[40]
<i>Sideroxylon inerme</i>	Stem barks	Methanol extract (IC ₅₀ = 82.1 ± 2.7 µg/mL on monophenolase inhibitory activity) Methanol extract (IC ₅₀ > 400 µg/mL on diphenolase inhibitory activity) Ethyl acetate fraction (% diphenolase inhibition = 40% at 25 µg/mL) Ethyl acetate fraction inhibited melanin production in melanocyte at 50 µg/mL	[40]
<i>Solanum ovalifolium</i>	Fruits	Methanol extract (% monophenolase inhibition = 93.6 ± 0.5%)	[66]
<i>Sophora japonica</i>	Flowers	50% Ethanol extract (IC ₅₀ = 0.56 µg/mL on monophenolase inhibitory activity)	[67]
<i>Streblus ilicifolius</i>	Woods	Aqueous extract (% diphenolase inhibition = 3.17 ± 5.24% at 20 µg/mL) Ethanol extract (% diphenolase inhibition = 75.52 ± 5.42% at 20 µg/mL) Ethyl acetate extract (% diphenolase inhibition = 24.38 ± 1.04% at 20 µg/mL) Petroleum ether extract (% diphenolase inhibition = 2.45 ± 5.90% at 20 µg/mL)	[49]
<i>Tamarindus indica</i>		Ethyl acetate extract (IC ₅₀ = 96.15 ± 0.62 µg/mL on diphenolase inhibitory activity)	[59]
<i>Triphasia trifolia</i>	Leaves	Essential oil (IC ₅₀ = 19.87 ± 0.892 µg/mL on monophenolase inhibitory activity)	[44]

Table 2 Antityrosinase activity of phytochemicals of plants

Scientific name	Plant part	Phytochemical	Reference
<i>Acanthopanax koreanum</i>	Leaves	3 α -Hydroxy-lup-20(29)-en-23-al-28-oic acid (1) (IC ₅₀ = 25.81 \pm 1.40 μ M on monophenolase inhibitory activity) (4S)- α -Terpinyl 8-O- β -D-glucopyranoside (2) (IC ₅₀ = 16.90 \pm 0.62 μ M on monophenolase inhibitory activity) 3 α ,11 α ,30-Trihydroxylup-23-al-20(29)-en-28-oic acid (3) (IC ₅₀ = 63.50 \pm 3.43 μ M on monophenolase inhibitory activity) 3 α ,20 α ,29-Trihydroxylupane-23,28-dioic acid (4) (IC ₅₀ = 8.61 \pm 1.09 μ M on monophenolase inhibitory activity)	[32]
<i>Artocarpus heterophyllus</i>	Heart woods	Artocarpin (5) (IC ₅₀ = 0.90 \pm 1.63 μ g/mL on diphenolase inhibitory activity) Brosimon I (6) (IC ₅₀ = 1.78 \pm 0.94 μ g/mL on diphenolase inhibitory activity) Cudraflavon B (7) (IC ₅₀ = 1.03 \pm 0.65 μ g/mL on diphenolase inhibitory activity) Morachalcon A (8) (IC ₅₀ = 0.18 \pm 0.10 μ g/mL on diphenolase inhibitory activity)	[42]
	Roots	(E)-4-[(1E)-3-methyl-1-buten-1-yl]-3,5,2',4'-tetrahydroxylstilbene (9) (IC ₅₀ = 0.20 μ g/mL on diphenolase inhibitory activity)	[68]
	Woods	Artocarpanone (10) (IC ₅₀ = 2.0 \pm 0.1 μ M on diphenolase inhibitory activity) Artocaeplin E (11) (IC ₅₀ = 6.7 \pm 0.8 μ M on diphenolase inhibitory activity) Artocaeplin F (12) (IC ₅₀ > 50 μ M on diphenolase inhibitory activity) Dihydromorin (13) (IC ₅₀ > 50 μ M on diphenolase inhibitory activity) Liquiritigenin (14) (IC ₅₀ = 22.0 \pm 2.5 μ M on diphenolase inhibitory activity) Norartocarpetin (15) (IC ₅₀ > 50 μ M on diphenolase inhibitory activity) Steppogenin (16) (IC ₅₀ = 7.5 \pm 2.5 μ M on diphenolase inhibitory activity)	[42]
<i>Artocarpus integer</i>	Roots	Artocarpanone (10) (IC ₅₀ = 44.56 μ g/mL on diphenolase inhibitory activity) Artocarpin (5) (IC ₅₀ > 200 μ g/mL on diphenolase inhibitory activity) Cudraflavone C (17) (IC ₅₀ > 200 μ g/mL on diphenolase inhibitory activity)	[25]
<i>Blumea balsamifera</i>	Leaves	Blumeatin (18) (IC ₅₀ = 0.624 \pm 0.029 mM on diphenolase inhibitory activity) Dihydroquercetin-7,4'-dimethyl ether (19) (Competitive inhibitor, IC ₅₀ = 0.162 \pm 0.042 mM on diphenolase inhibitory activity) Dihydroquercetin-4'-methyl ether (20) (Competitive inhibitor, IC ₅₀ = 0.115 \pm 0.013 mM on diphenolase inhibitory activity) Luteolin (21) (Noncompetitive inhibitor, IC ₅₀ = 0.258 \pm 0.015 mM on diphenolase inhibitory activity) Luteolin-7-methyl ether (22) (Noncompetitive inhibitor, IC ₅₀ = 0.350 \pm 0.002 mM on diphenolase inhibitory activity) Quercetin (23) (Competitive inhibitor, IC ₅₀ = 0.096 \pm 0.004 mM on diphenolase inhibitory activity) Rhamnetin (24) (Competitive inhibitor, IC ₅₀ = 0.107 \pm 0.017 mM on diphenolase inhibitory activity) Tamarixetin (25) (IC ₅₀ = 0.144 \pm 0.004 mM on diphenolase inhibitory activity) 5,7,3',5'-Tetrahydroxyflavanone (26) (Competitive inhibitor, IC ₅₀ = 0.423 \pm 0.049 mM on diphenolase inhibitory activity)	[69]
<i>Cinnamomum cassia</i>	Stem barks	Cinnamaldehyde (27) (Mixed inhibitor, IC ₅₀ = 4.04 \pm 0.08 mM on diphenolase inhibitory activity)	[70]

Table 2 Antityrosinase activity of phytochemicals of plants (continue)

Scientific name	Plant part	Phytochemical	Reference
<i>Citrus unshiu</i>	Peels	Hesperidin (28) (Noncompetitive inhibitor, IC ₅₀ = 16.08 mM on diphenolase inhibitory activity) Nobiletin (29) (Competitive inhibitor, IC ₅₀ = 1.49 mM on diphenolase inhibitory activity)	[45]
<i>Cleyera japonica</i>	Branches	Aviculin (30) (IC ₅₀ > 200 µg/mL on diphenolase inhibitory activity) 3,3'-Di- <i>O</i> -methylellagic acid (31) (IC ₅₀ > 200 µg/mL on diphenolase inhibitory activity) 3,3'-Di- <i>O</i> -methylellagic acid 4'- <i>O</i> -β- <i>D</i> -xylofuranoside (32) (IC ₅₀ = 0.078 mM on diphenolase inhibitory activity) 3,5,7-Trihydroxychromone 3- <i>O</i> -α- <i>L</i> -arabinofuranoside (33) (IC ₅₀ > 200 µg/mL on diphenolase inhibitory activity)	[71]
<i>Dalea elegans</i>	Aerial parts	Comptonin (34) (% monophenolase inhibition = 22.7 ± 0.6% at 100 µM) Demethoxymatteucinol (35) (IC ₅₀ = 97.60 ± 0.30 µM on monophenolase inhibitory activity) (2 <i>S</i>)-2',4'-Dihydroxy-5'-(1'',1'''-dimethylallyl)-8-prenyl pinocembrin (36) (Competitive inhibitor, IC ₅₀ = 2.32 ± 0.01 µM on monophenolase inhibitory activity) 7-Hydroxy-5-methoxy-6,8-dimethylflavanone (37) (% monophenolase inhibition = 6.97 ± 0.6% at 100 µM) (2 <i>S</i>)-8-Prenylpinocembrin (38) (IC ₅₀ = 80.60 ± 0.30 µM on monophenolase inhibitory activity) Triangularin (39) (Uncompetitive inhibitor, IC ₅₀ = 33.30 ± 0.10 µM on monophenolase inhibitory activity)	[33]
<i>Greyia flanaganii</i>	Leaves	5,7-Dihydroxyflavanone [(2 <i>S</i>)-pinocembrin] (40) (IC ₅₀ > 200 µg/mL on monophenolase inhibitory activity) 2',6'-Dihydroxy-4-methoxydihydrochalcone (41) (IC ₅₀ > 200 µg/mL on monophenolase inhibitory activity) (3 <i>S</i>)-4-Hydroxyphenethyl 3-hydroxy-5-phenylpentanoate (42) (IC ₅₀ > 200 µg/mL on monophenolase inhibitory activity) 2',4',6'-Trihydroxydihydrochalcone (43) (IC ₅₀ = 17.86 µg/mL on monophenolase inhibitory activity) (2 <i>R</i> ,3 <i>R</i>)-3,5,7-Trihydroxy-3- <i>O</i> -acetylflavanone (44) (IC ₅₀ > 200 µg/mL on monophenolase inhibitory activity) 2',6',4'-Trihydroxy-4-methoxydihydrochalcone (45) (IC ₅₀ > 200 µg/mL on monophenolase inhibitory activity)	[35]
<i>Heretheca inuloides</i>	Flowers	Quercetin (23) (Competitive inhibitor, IC ₅₀ = 0.13 mM on diphenolase inhibitory activity)	[72]
<i>Intsia palembanica</i>		4'-Dehydroxyrobidanol (46) (Competitive inhibitor, IC ₅₀ = 15.2 µM on monophenolase inhibitory activity) (Uncompetitive inhibitor, IC ₅₀ = 50.0 µM on diphenolase inhibitory activity) (+)-Epirobidanol (47) (Mixed inhibitor, IC ₅₀ = 20.2 µM on monophenolase inhibitory activity) (Uncompetitive inhibitor, IC ₅₀ = 178.5 µM on diphenolase inhibitory activity) (-)-Robidanol (48) (Competitive inhibitor, IC ₅₀ = 8.7 µM on monophenolase inhibitory activity) (Noncompetitive inhibitor, IC ₅₀ = 26.6 µM on diphenolase inhibitory activity)	[58]
<i>Juglans mandshurica</i>	Barks	Dihydroquercetin (49) (IC ₅₀ = 98.5 ± 17.8 mM on diphenolase inhibitory activity) Dihydrokaempferol (50) (IC ₅₀ = 2.7 ± 0.7 mM on diphenolase inhibitory activity) Kaempferol (51) (IC ₅₀ = 40.8 ± 9.7 mM on diphenolase inhibitory activity) Kaempferol-3- <i>O</i> -α- <i>L</i> -rhamnoside (52) (IC ₅₀ = 117.7 ± 21.6 mM on diphenolase inhibitory activity)	[61]

Table 2 Antityrosinase activity of phytochemicals of plants (continue)

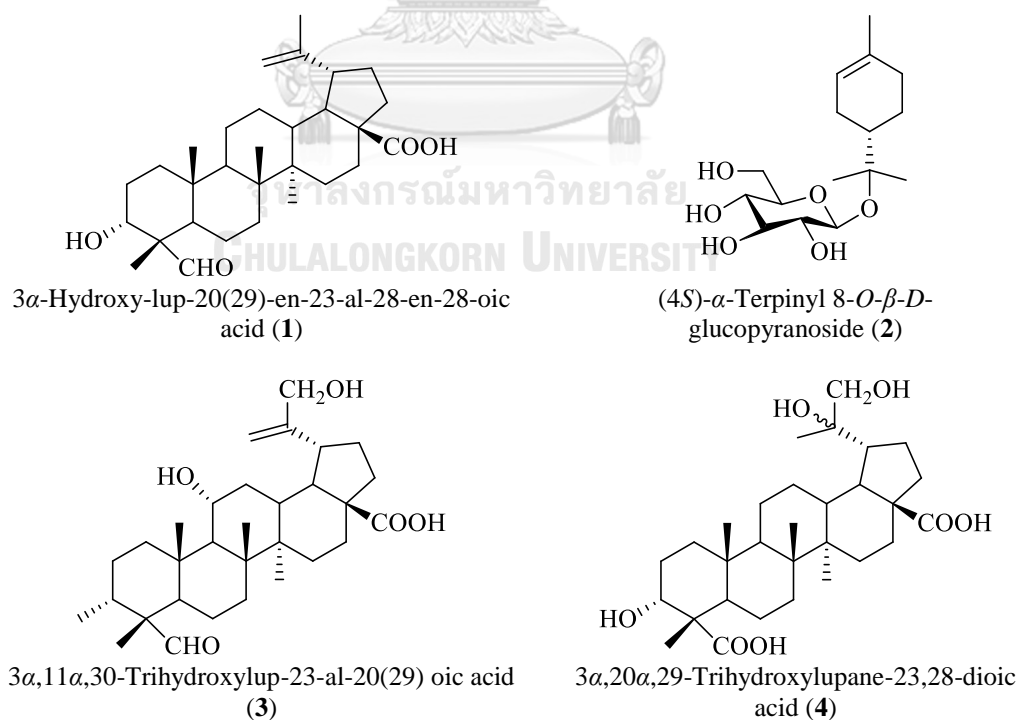
Scientific name	Plant part	Phytochemical	Reference
<i>Juniperus communis</i>	Fruits	Quercetin-3- <i>O</i> - α - <i>L</i> -rhamnoside (53) (IC ₅₀ = 124.9 \pm 20.1 mM on diphenolase inhibitory activity)	[73]
		Rhamnetin-3- <i>O</i> - β - <i>D</i> -glucopyranoside (54) (IC ₅₀ = 27.95 μ g/mL on diphenolase inhibitory activity)	
		Soybean isoflavone (55) (IC ₅₀ = 75.3 \pm 10.1 mM on diphenolase inhibitory activity)	
		Amentoflavone (56) (% diphenolase inhibition = 91.10 \pm 2.78% at 25 μ M) (% diphenolase inhibition = 94.85 \pm 1.80% at 50 μ M)	
		Apigenin (57) (% diphenolase inhibition = 82.96 \pm 1.80% at 25 μ M) (% diphenolase inhibition = 90.06 \pm 6.60% at 50 μ M)	
		Cupressuflavone (58) (% diphenolase inhibition = 83.87 \pm 5.27% at 25 μ M) (% diphenolase inhibition = 88.73 \pm 4.04% at 50 μ M)	
		Hinokiflavone (59) (% diphenolase inhibition = 77.12 \pm 2.25% at 25 μ M) (% diphenolase inhibition = 98.47 \pm 2.09% at 50 μ M)	
		Hypolaetin 7- <i>O</i> - β -xylopyranoside (60) (% diphenolase inhibition = 39.01 \pm 3.36% at 25 μ M) (% diphenolase inhibition = 54.52 \pm 0.67% at 50 μ M)	
		Isoscutellarein 7- <i>O</i> - β -xyloparanoside (61) (% diphenolase inhibition = 88.11 \pm 3.55% at 25 μ M) (% diphenolase inhibition = 93.67 \pm 6.04% at 50 μ M)	
		Podocarpusflavone A (62) (% diphenolase inhibition = 91.38 \pm 1.30% at 25 μ M) (% diphenolase inhibition = 95.76 \pm 2.17% at 50 μ M)	
		Robustaflavone (63) (% diphenolase inhibition = 91.59 \pm 2.92% at 25 μ M) (% diphenolase inhibition = 92.35 \pm 2.69% at 50 μ M)	
		(2' <i>R</i>)-2',3'-Dihydro-2'-(1-hydroxy-1-methylethyl)-2,6'-bibenzofuran-6,4'-diol (64) (Low inhibition, < 50 % diphenolase inhibition at 30 μ M)	
		3,4-Dihydro-7-(6-hydroxy-2-benzofuranyl)-2,2-dimethyl-2 <i>H</i> -1-benzopyran-3,5-diol (65) (Low inhibition, < 50 % diphenolase inhibition at 30 μ M)	
		5,6-Dimethoxy-2-(3-hydroxy-5-methoxyphenyl)benzofuran (66) (Low inhibition, < 50 % diphenolase inhibition at 30 μ M)	
		2-(3-Hydroxy-5-methoxyphenyl)benzofuran-6-ol (67) (Low inhibition, < 50 % diphenolase inhibition at 30 μ M)	
		Moracin B (68) (Low inhibition, < 50 % diphenolase inhibition at 30 μ M)	
		Moracin C (69) (Low inhibition, < 50 % diphenolase inhibition at 30 μ M)	
		Moracin D (70) (Low inhibition, < 50 % diphenolase inhibition at 30 μ M)	
		Moracin O (71) (IC ₅₀ = 6.29 \pm 1.31 μ M on diphenolase inhibitory activity)	
Moracin P (72) (IC ₅₀ = 2.90 \pm 0.17 μ M on diphenolase inhibitory activity)			
Procyanidin B1 (73) (IC ₅₀ = 200 \pm 2.2 μ g/mL, 346 μ M on monophenolase inhibitory activity) (IC ₅₀ > 200 μ g/mL on diphenolase inhibitory activity)			
Sanggenfuran B (74) (Low inhibition, < 50 % diphenolase inhibition at 30 μ M)			
<i>Peucedanum knappii</i>	Aerial part	4'-Dihydrophasic acid (75) (IC ₅₀ = 278.5 \pm 20.4 mM on diphenolase inhibitory activity)	[36]
		3,3'-Dimethoxyellagic acid (76) (IC ₅₀ = 627.5 \pm 23.7 mM on diphenolase inhibitory activity)	
		3,3'-Dimethoxyellagic acid xylopyranoside (77) (IC ₅₀ = 350.2 \pm 28.9 mM on diphenolase inhibitory activity)	
		4,4'-Dimethoxyellagic acid (78) (IC ₅₀ = 310.4 \pm 18.5 mM on diphenolase inhibitory activity)	
		Ellagic acid (79) (IC ₅₀ = 92.0 \pm 13.4 mM on diphenolase inhibitory activity)	

Table 2 Antityrosinase activity of phytochemicals of plants (continue)

Scientific name	Plant part	Phytochemical	Reference			
<i>Polyalthia longifolia</i>	Leaves	(3 <i>R</i>)-3',4''-Epoxy-1-(4-hydroxyphenyl)-7-(3-methoxyphenyl) heptan-3-ol (80) (IC ₅₀ = 59.6 ± 17.2 mM on diphenolase inhibitory activity)	[75]			
		Ethyl gallate (81) (IC ₅₀ = 190.7 ± 18.2 mM on diphenolase inhibitory activity)				
		Gallic acid (82) (IC ₅₀ = 89.1 ± 12.3 mM on diphenolase inhibitory activity)				
		Juglanthrtracenoside A (83) (IC ₅₀ = 39.1 ± 11.1 mM on diphenolase inhibitory activity)				
		Methyl gallate (84) (IC ₅₀ = 187.2 ± 22.1 mM on diphenolase inhibitory activity)				
		Naringenin (85) (IC ₅₀ = 5.1 ± 1.5 mM on diphenolase inhibitory activity)				
		Rhoiptelol (86) (IC ₅₀ = 83.3 ± 19.7 mM on diphenolase inhibitory activity)				
		Rhoiptelol C (87) (IC ₅₀ = 1.5 ± 0.4 mM on diphenolase inhibitory activity)				
		Regiolone (88) (IC ₅₀ = 78.2 ± 15.6 mM on diphenolase inhibitory activity)				
		β-Sitosterol (89) (IC ₅₀ = 395.5 ± 21.2 mM on diphenolase inhibitory activity)				
		Proanthocynidins (90) (IC ₅₀ = 773.09 ± 1.47 µg/mL on diphenolase inhibitory activity)				
		<i>Rhamnus nakaharai</i>		Heart woods	Alaternin (91) (IC ₅₀ = 327.3 µM on diphenolase inhibitory activity)	[76]
					Emodin (92) (IC ₅₀ = 187.5 µM on diphenolase inhibitory activity)	
					6-Methoxysorigenin- 8- <i>O</i> -β-glucopyranoside (93) (IC ₅₀ = 42.2 µM on diphenolase inhibitory activity)	
6-Methoxysorigenin (94) (IC ₅₀ = 97.4 µM on diphenolase inhibitory activity)						
Butin (95) (Competitive inhibitor, IC ₅₀ = 16.00 µM on diphenolase inhibitory activity)						
<i>Rhus verniciflua</i>	Woods	Sulfuretin (96) (Competitive inhibitor, IC ₅₀ = 13.64 µM on diphenolase inhibitory activity)	[77]			
		Ellagic acid (79) (Mixed inhibitor, IC ₅₀ = 1.58 ± 0.09 µg/mL on diphenolase inhibitory activity)				
<i>Rosa damascena</i>	Flowers	Kaempferol (51) (Competitive inhibitor, IC ₅₀ = 1.58 ± 0.18 µg/mL on diphenolase inhibitory activity)	[73]			
		Quercetin (23) (Competitive inhibitor, IC ₅₀ = 1.27 ± 0.06 µg/mL on diphenolase inhibitory activity)				
		Purpurin (97) (Competitive inhibitor, IC ₅₀ = 0.11 ± 0.02 mg/mL on monolase activity) (Competitive inhibitor, IC ₅₀ = 0.29 ± 0.09 mg/mL on diphenolase activity)				
<i>Rubia cordifolia</i>	Roots	Purpurin (97) (Competitive inhibitor, IC ₅₀ = 0.11 ± 0.02 mg/mL on monolase activity) (Competitive inhibitor, IC ₅₀ = 0.29 ± 0.09 mg/mL on diphenolase activity)	[48]			
<i>Sideroxylon inerme</i>	Stem barks	Epigallocatechin gallate (98) (IC ₅₀ = 30 ± 1.9 µg/mL, 65.5 µM on monophenolase inhibitory activity)	[40]			
<i>Stewartia pseudocamellia</i>	Twigs	Stewartianol (99) (IC ₅₀ = 49.33 ± 3.11 µM on melanin production by α-MSH) Stewartianol-3- <i>O</i> -glucoside (100) (IC ₅₀ = 39.23 ± 6.04 µM on melanin production by α-MSH)	[78]			
<i>Streblus ilicifolius</i>	Woods	(<i>E</i>)-2,4-Dihydroxy-3-(3,7-dimethyl -2,6-octadienyl) benzaldehyde (101) (IC ₅₀ > 200 µg/mL on diphenolase inhibitory activity) Flavokawain C (102) (Competitive inhibitor, IC ₅₀ = 60.2 µM on monophenolase inhibitory activity) (Competitive inhibitor, IC ₅₀ = 106.7 µM on diphenolase inhibitory activity)	[49]			

Table 2 Antityrosinase activity of phytochemicals of plants (continue)

Scientific name	Plant part	Phytochemical	Reference
		<i>p</i> -Hydroxybenzoic acid methyl ester (103) (IC ₅₀ > 200 µg/mL on diphenolase inhibitory activity)	
		Isoxanthohumol (104) (Mixed inhibitor, IC ₅₀ = 77.4 µM on monophenolase inhibitory activity)	
		Methylxanthohumol (105) (Competitive inhibitor, IC ₅₀ = 34.3 µM on monophenolase inhibitory activity)	
		(Competitive inhibitor, IC ₅₀ = 70.5 µM on diphenolase inhibitory activity)	
		Moracin M (106) (IC ₅₀ = 67.69 µg/mL on monophenolase inhibitory activity)	
		(Noncompetitive inhibitor, IC ₅₀ = 77.2 µM on diphenolase inhibitory activity)	
		Xanthohumol (107) (Competitive inhibitor, IC ₅₀ = 15.4 µM on monophenolase inhibitory activity)	
		(Competitive inhibitor, IC ₅₀ = 31.1 µM on diphenolase inhibitory activity)	
		Xanthoumol B (108) (Competitive inhibitor, IC ₅₀ = 22.1 µM on monophenolase inhibitory activity)	
		(Competitive inhibitor, IC ₅₀ = 46.7 µM on diphenolase inhibitory activity)	
		Xanthohumol C (109) (Competitive inhibitor, IC ₅₀ = 20.6 µM on monophenolase inhibitory activity)	
		(Competitive inhibitor, IC ₅₀ = 41.3 µM on diphenolase inhibitory activity)	
<i>Zanthoxylum piperitum</i>	Leaves	Quercetin (23) (Competitive inhibitor, IC ₅₀ = 3.8 µg/mL on monophenolase inhibitory activity)	[79]

**Figure 12** Phytochemical structures of tyrosinase inhibitors

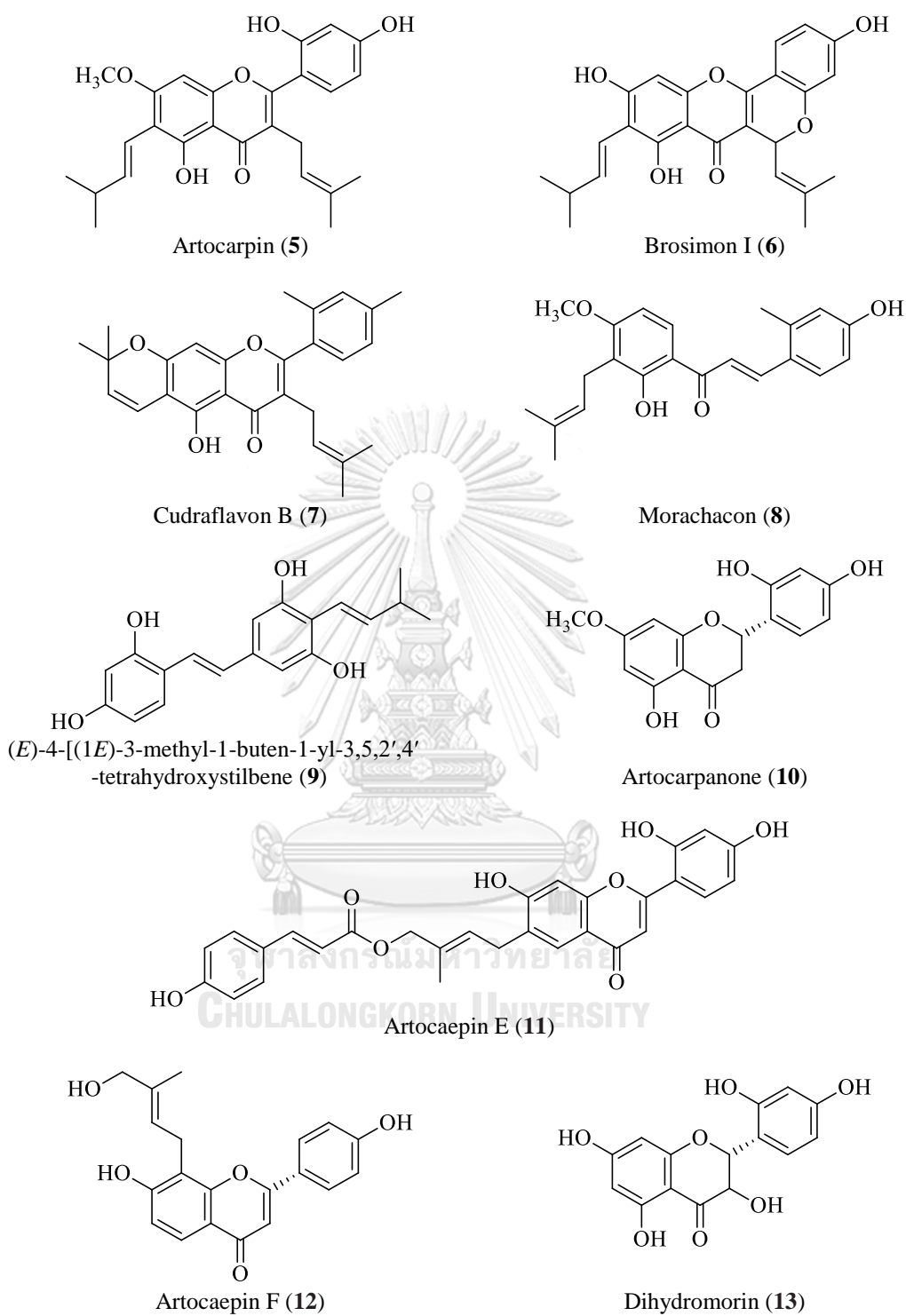


Figure 12 Phytochemical structures of tyrosinase inhibitors (continue)

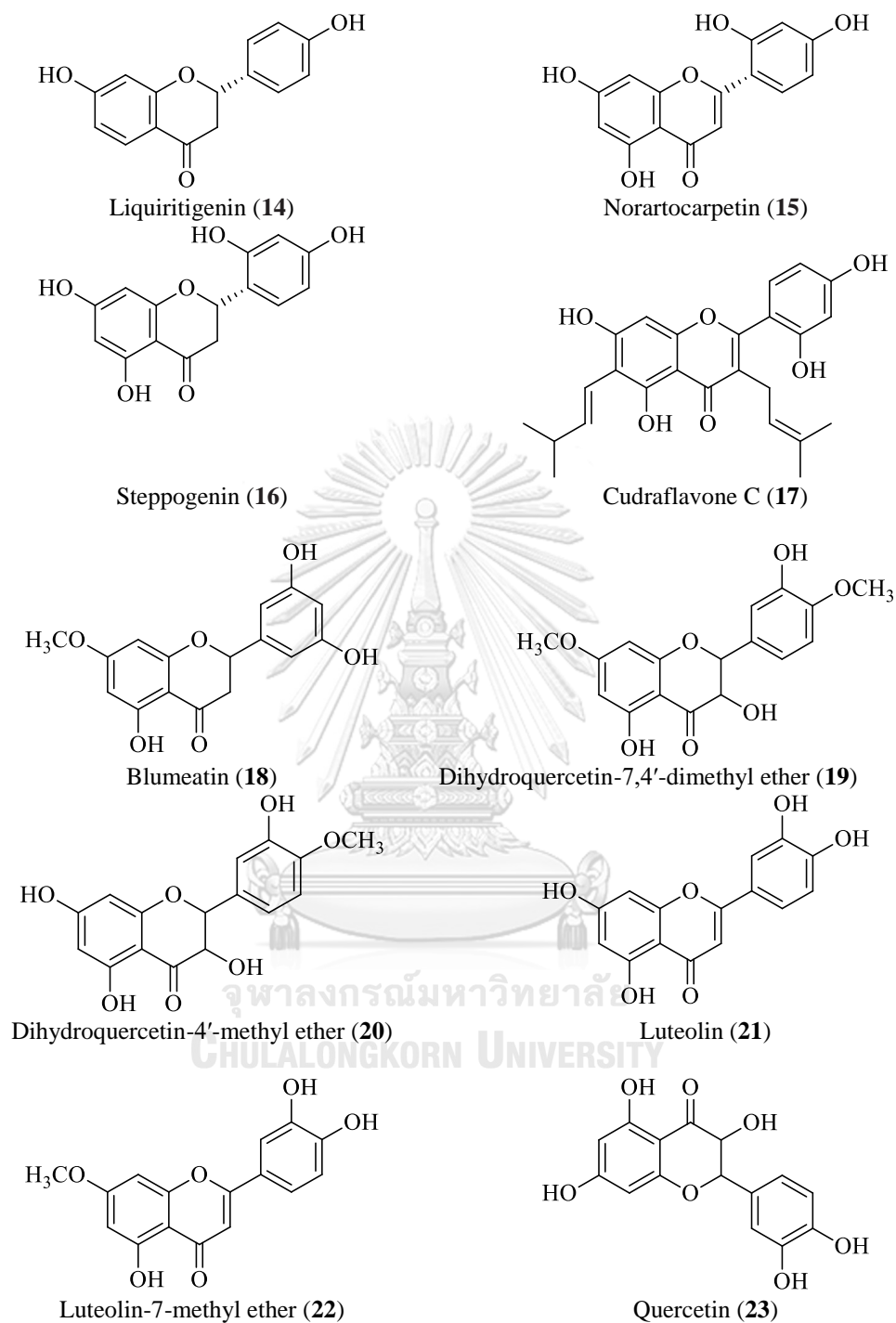


Figure 12 Phytochemical structures of tyrosinase inhibitors (continue)

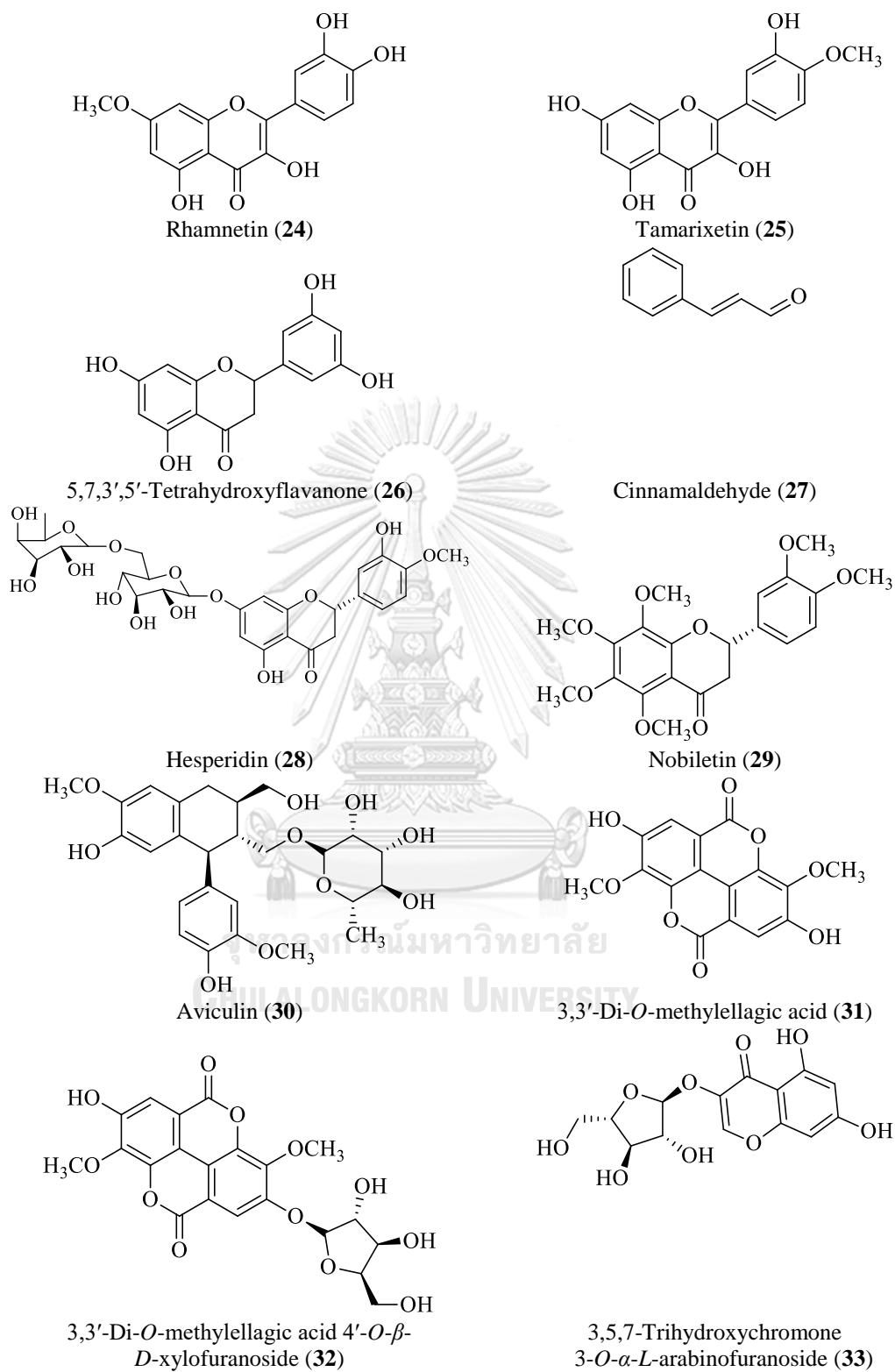


Figure 12 Phytochemical structures of tyrosinase inhibitors (continue)

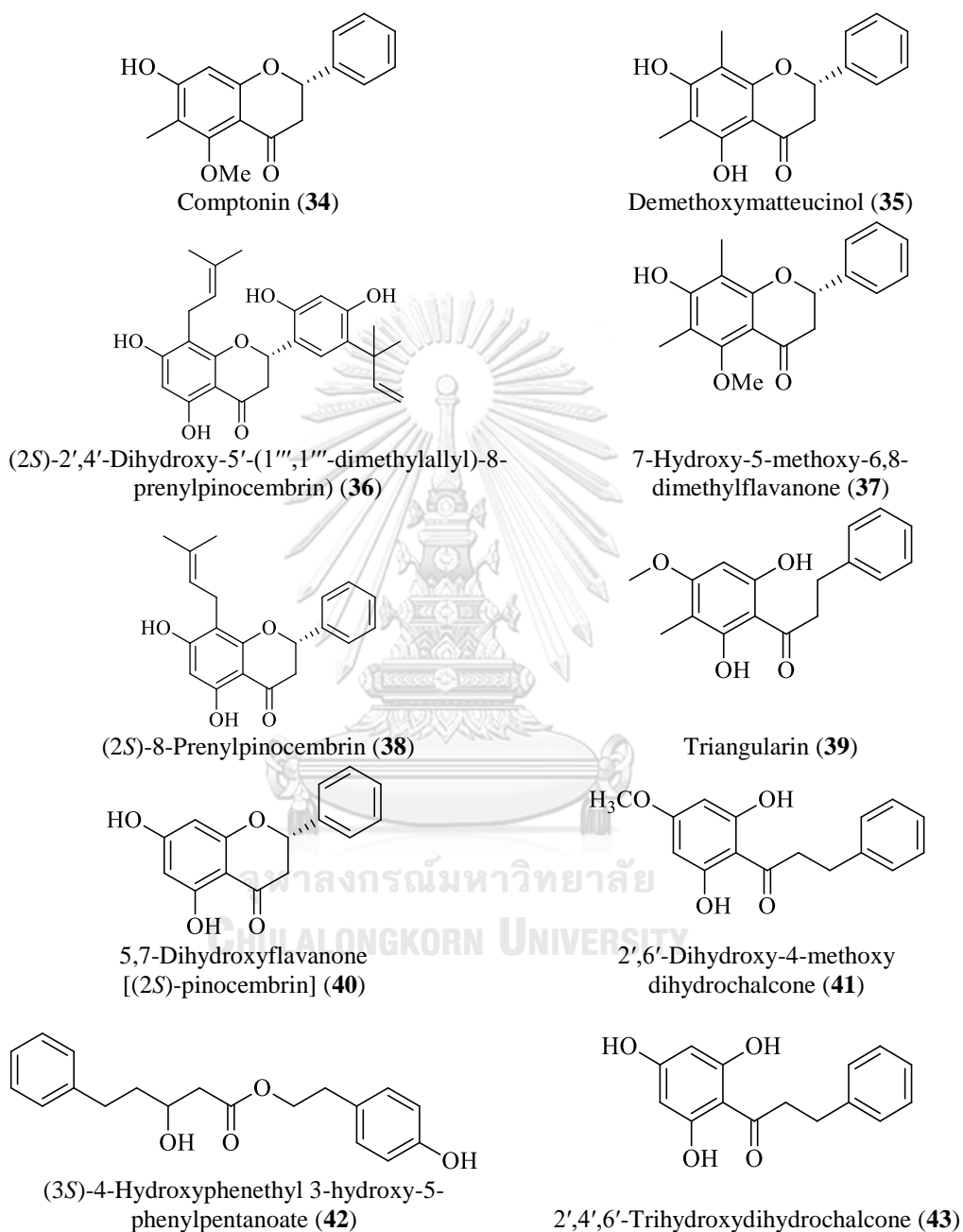


Figure 12 Phytochemical structures of tyrosinase inhibitors (continue)

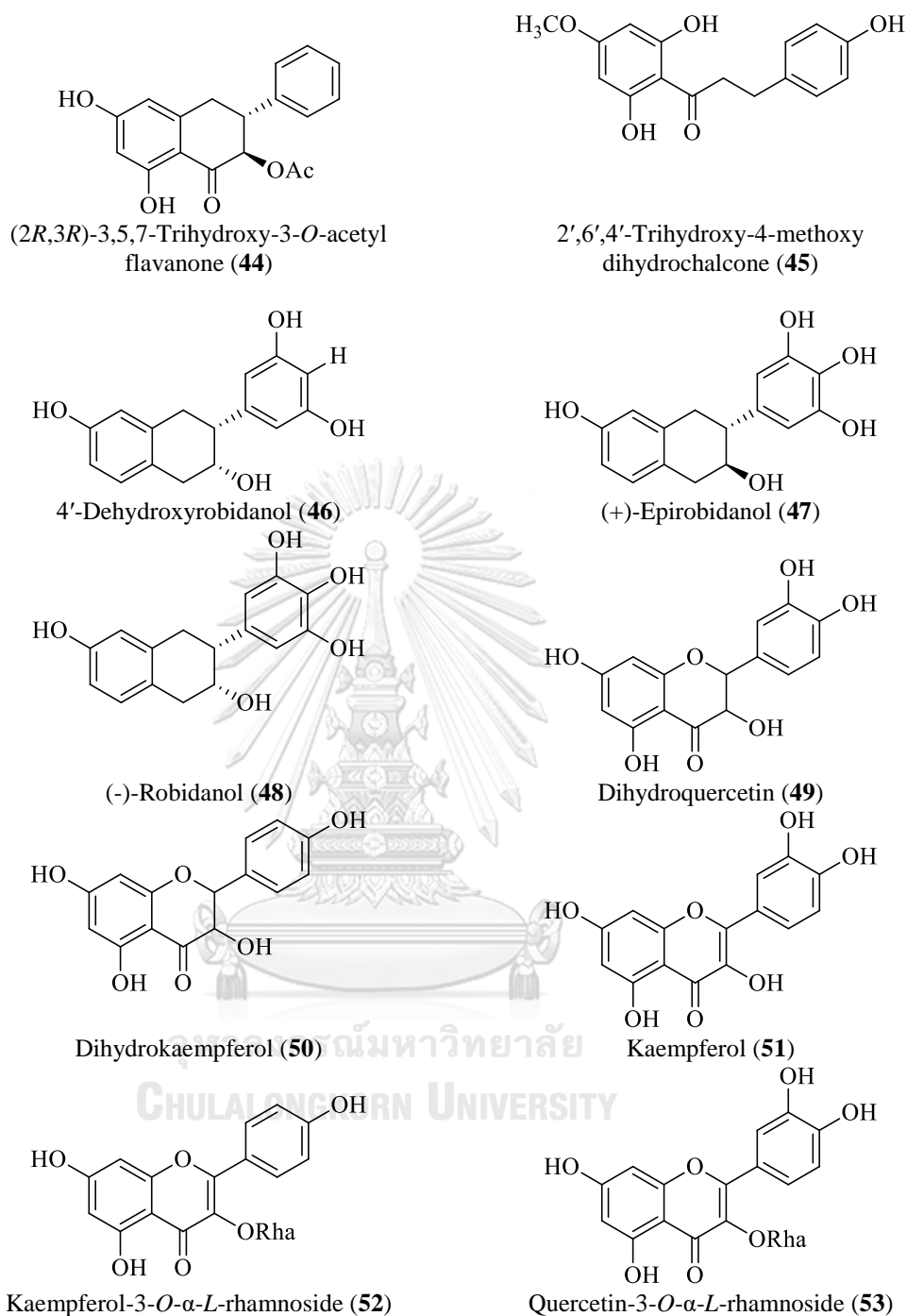


Figure 12 Phytochemical structures of tyrosinase inhibitors (continue)

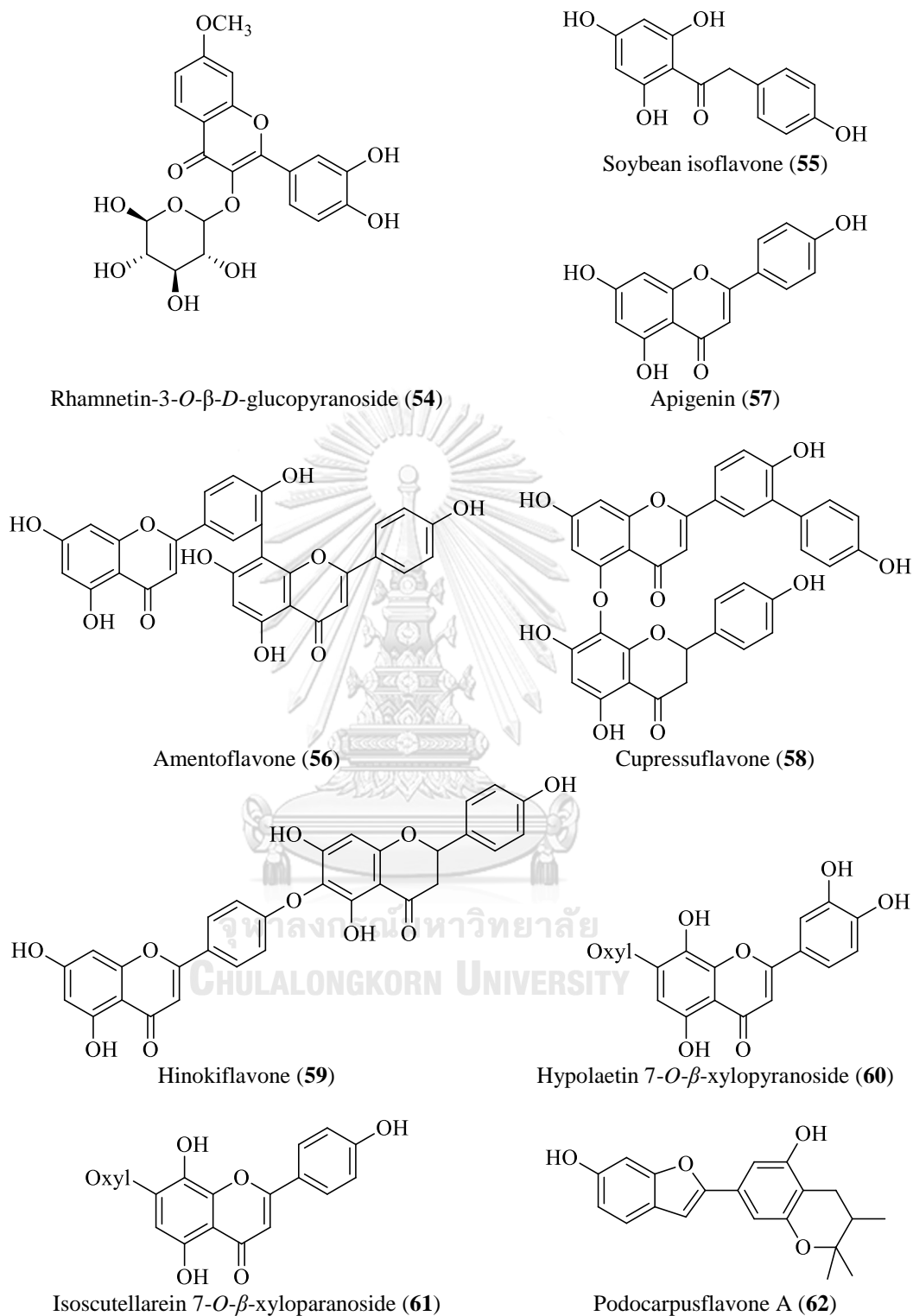


Figure 12 Phytochemical structures of tyrosinase inhibitors (continue)

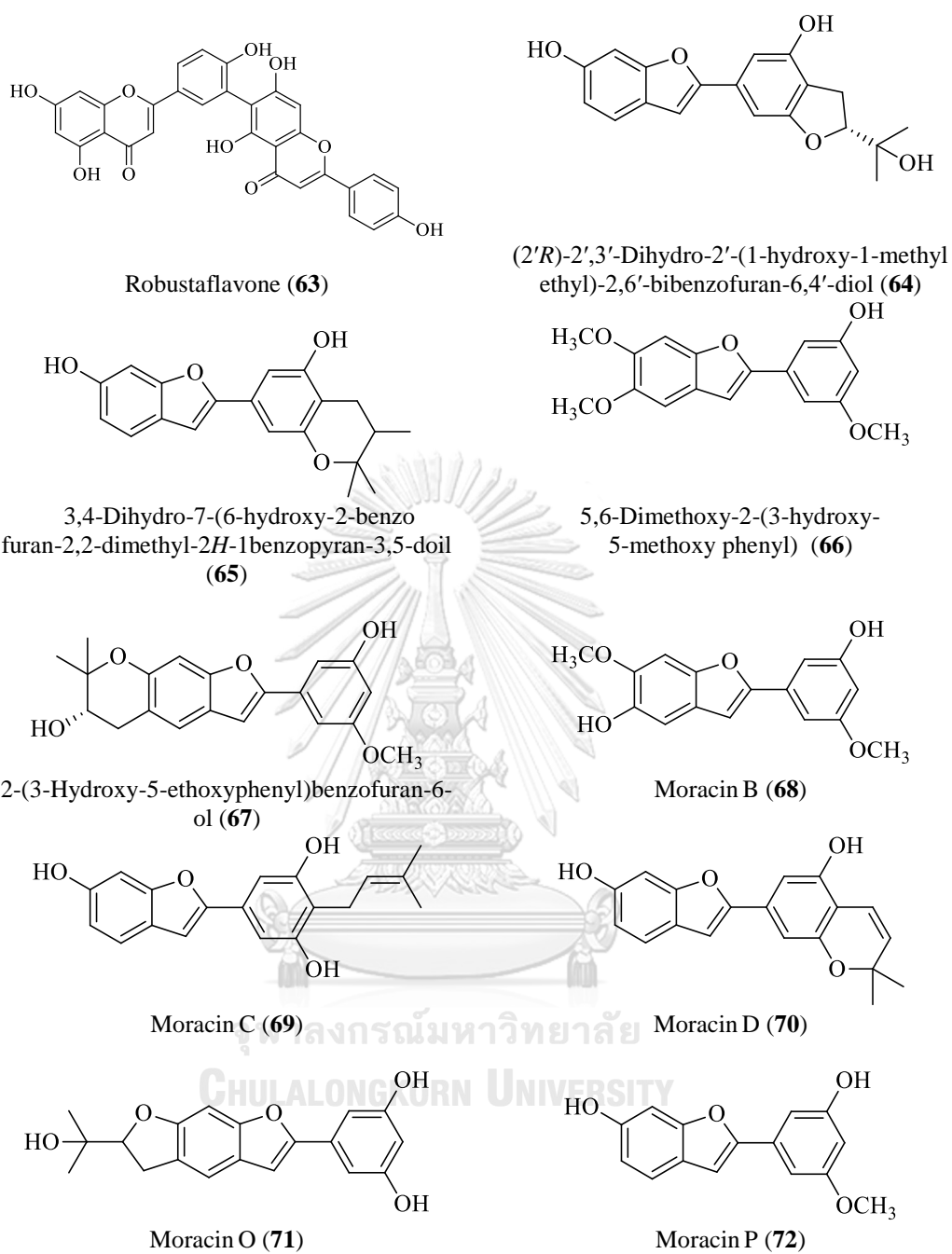
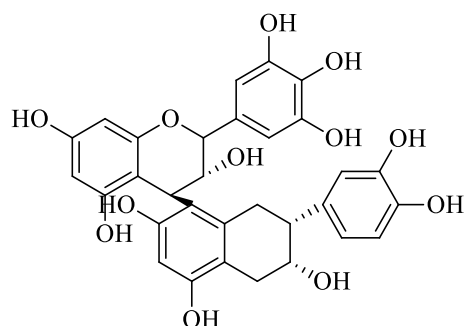
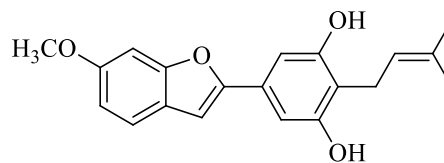


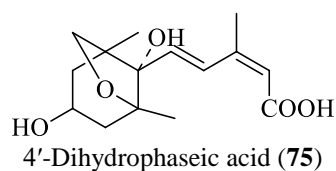
Figure 12 Phytochemical structures of tyrosinase inhibitors (continue)



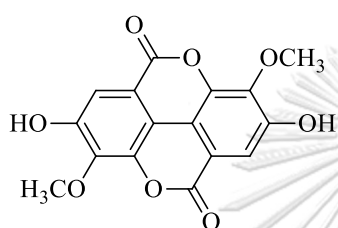
Procyanidin B1 (73)



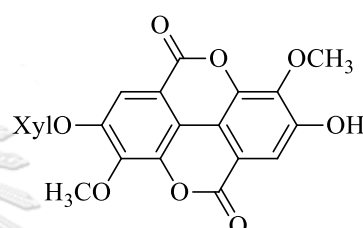
Sanggenfuran B (74)



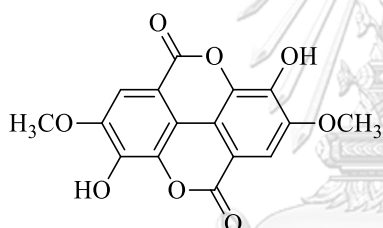
4'-Dihydrophaseic acid (75)



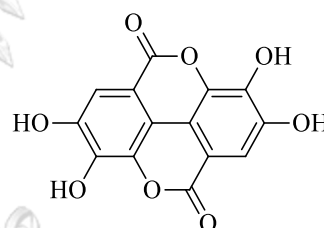
3,3'-Dimethoxyellagic acid (76)



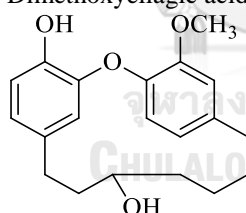
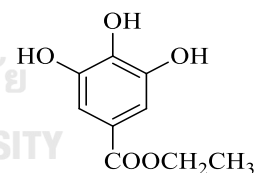
3,3'-Dimethoxyellagic acid xylopyranoside (77)



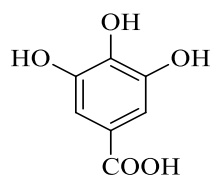
4,4'-Dimethoxyellagic acid (78)



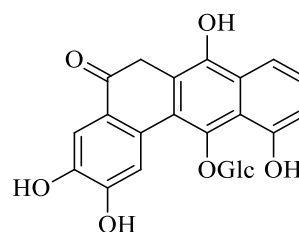
Ellagic acid (79)

*(3R)*-3',4''-epoxy-1-(4-hydroxyphenyl)-7(3-methoxyphenyl) heptan-3-ol (80)

Ethyl gallate (81)



Gallic acid (82)



Juglanthrtracenoside A (83)

Figure 12 Phytochemical structures of tyrosinase inhibitors (continue)

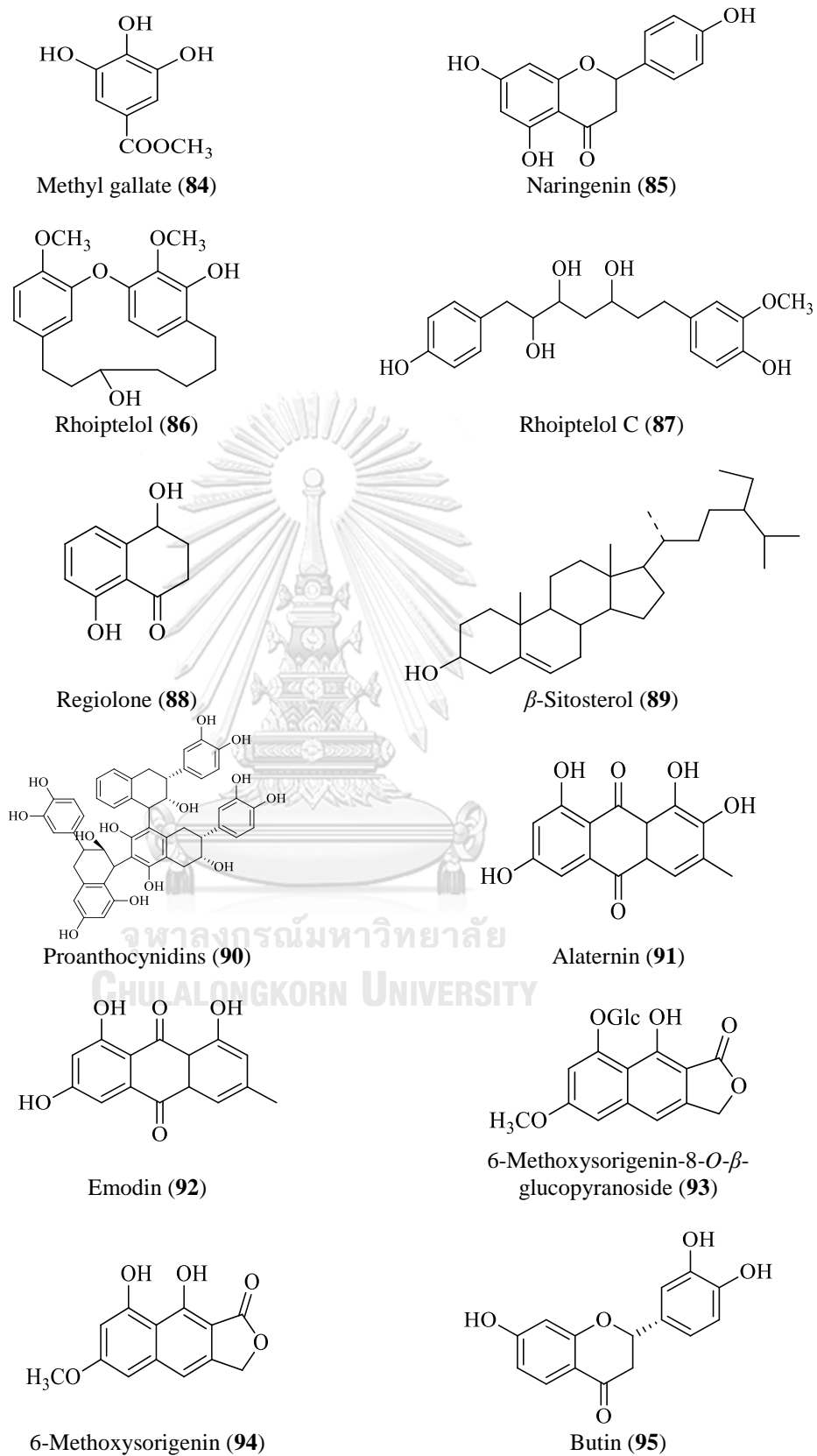


Figure 12 Phytochemical structures of tyrosinase inhibitors (continue)

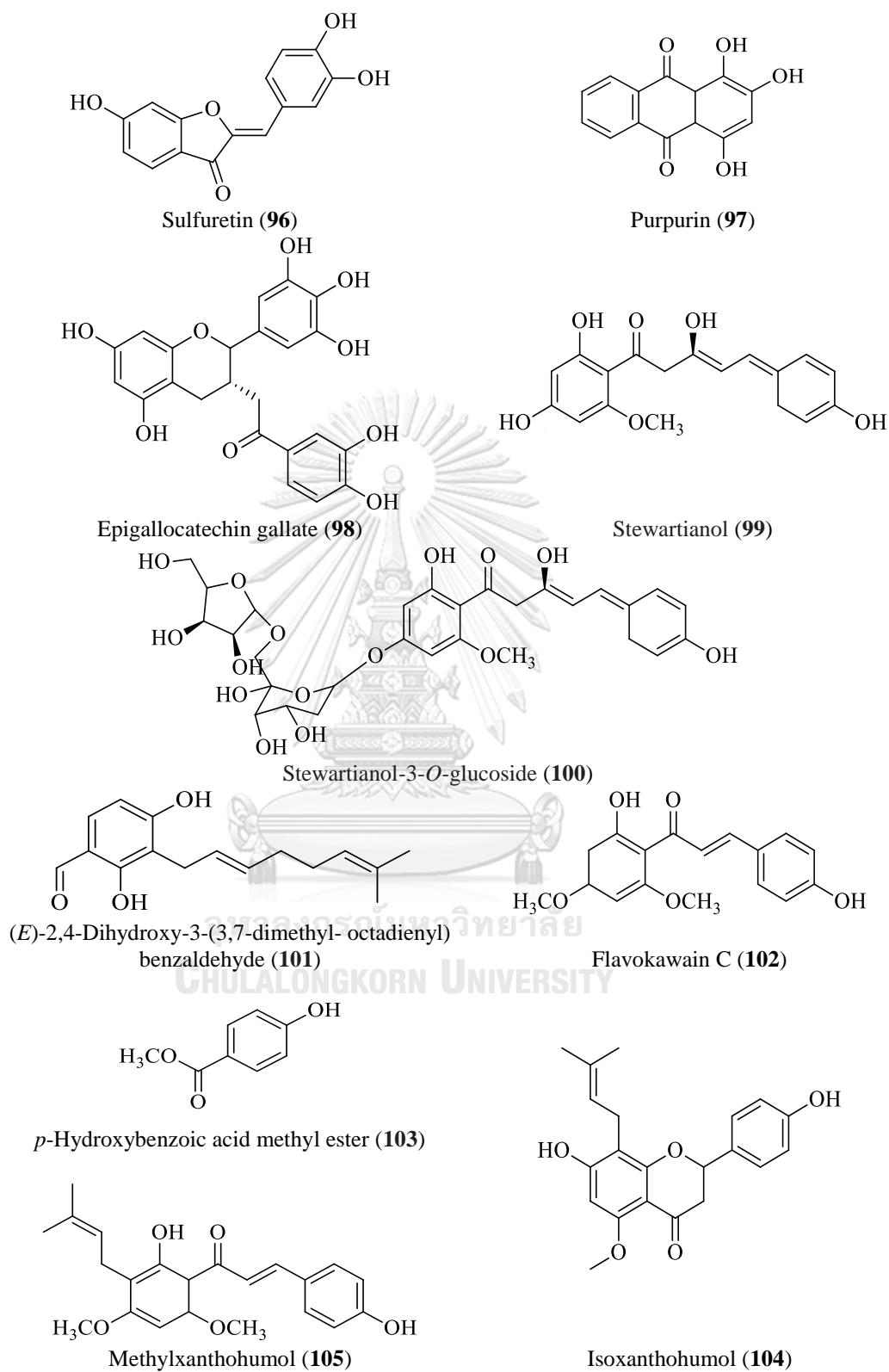


Figure 12 Phytochemical structures of tyrosinase inhibitors (continue)

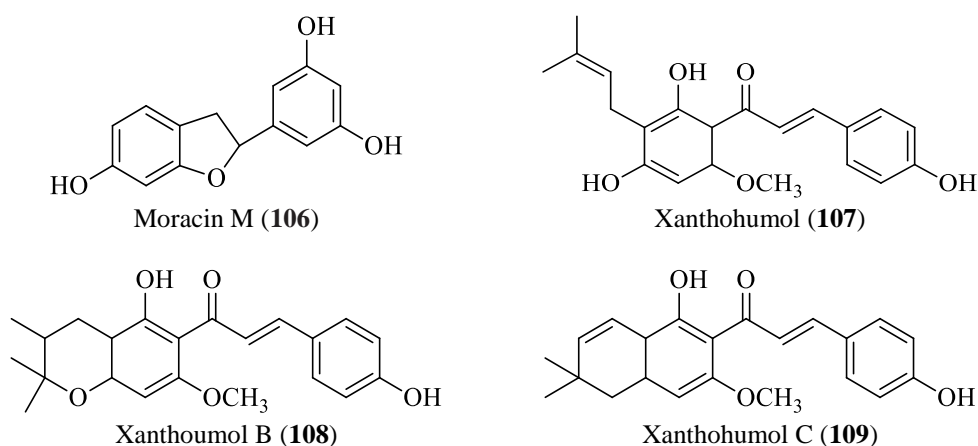


Figure 12 Phytochemical structures of tyrosinase inhibitors (continue)

2.5.2 Tyrosinase inhibitory activity of synthetic chemicals

Many synthetic tyrosinase inhibitors were developed and designed. They were changed action of altered chemical structure but their chemicals cause unacceptable side effect in the body. While, natural tyrosinase inhibitors were able to interact with biological molecules in the body. Natural tyrosinase inhibitors could be less sustainable. Antityrosinase activity depends on classification of synthetic compounds such as the ‘O’ position-1 in pyranone ring was changed to synthesize a conjugate of hydroxypyridinone-amono acid and hydroxypyridinone-dipeptide [80]. Coumarin and flavonoid derivatives were synthesized and evaluated for their tyrosinase inhibitory activity [81]. The literature reviews of antityrosinase activity for synthetic compounds are shown in Table 3 and their structures are shown in Figure 13.

Table 3 Antityrosinase activity of synthetic compounds

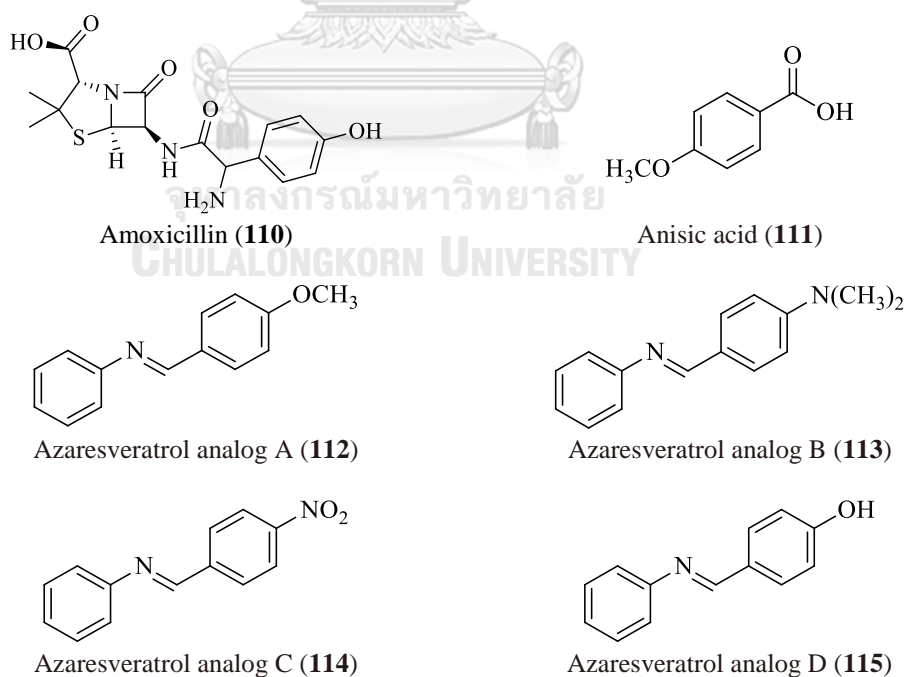
Compound	Tyrosinase inhibitory activity	Reference
Amoxicillin (110)	Mixed inhibitor IC ₅₀ = 9.0 ± 1.8 mM on diphenolase inhibitory activity	[82]
Anisic acid (111)	Noncompetitive inhibitor IC ₅₀ = 0.60 mM on diphenolase inhibitory activity	[80]
Azaresveratrol analogs A-F Azaresveratrol analog A (112)	IC ₅₀ = 44.89 µg/mL on monophenolase inhibitory activity	[83]
Azaresveratrol analog B (113)	IC ₅₀ = 72.58 µg/mL on monophenolase inhibitory activity	
Azaresveratrol analog C (114)	IC ₅₀ = 160.1 µg/mL on monophenolase inhibitory activity	
Azaresveratrol analog D (115)	IC ₅₀ = 28.66 µg/mL on monophenolase inhibitory activity	
Azaresveratrol analog E (116)	IC ₅₀ = 49.47 µg/mL on monophenolase inhibitory activity	
Azaresveratrol analog F (117)	IC ₅₀ = 147.96µg/mL on monophenolase inhibitory activity	

Table 3 Antityrosinase activity of synthetic compounds (continue)

Compound	Tyrosinase inhibitory activity	Reference
Caffeic acid <i>N</i> -nonyl ester (118)	Mixed inhibitor at lower concentration than 50 μ M Irreversible inhibitor at higher concentration than 50 μ M IC ₅₀ = 37.5 μ M on diphenolase inhibitory activity	[84]
Coumarin-resveratrol hybrids 1-8 Coumarin-resveratrol hybrid 1 (119) Coumarin-resveratrol hybrid 2 (120) Coumarin-resveratrol hybrid 3 (121) Coumarin-resveratrol hybrid 4 (122) Coumarin-resveratrol hybrid 5 (123) Coumarin-resveratrol hybrid 6 (124) Coumarin-resveratrol hybrid 7 (125) Coumarin-resveratrol hybrid 8 (126)	IC ₅₀ > 0.1 mM on diphenolase inhibitory activity IC ₅₀ > 0.1 mM on diphenolase inhibitory activity IC ₅₀ > 0.1 mM on diphenolase inhibitory activity IC ₅₀ = 1.56 mM on diphenolase inhibitory activity IC ₅₀ > 0.1 mM on diphenolase inhibitory activity IC ₅₀ = 3.68 mM on diphenolase inhibitory activity IC ₅₀ > 0.1 mM on diphenolase inhibitory activity IC ₅₀ = 0.27 mM on diphenolase inhibitory activity	[81]
Curcumin-diaryl pentanoid analogues Curcumin-diaryl pentanoid analogue 4 (127)	IC ₅₀ = 79.05 \pm 3.92 μ M on diphenolase inhibitory activity	[85]
Curcumin-diaryl pentanoid analogue 10 (128) Curcumin-diaryl pentanoid analogue 15 (129) Curcumin-diaryl pentanoid analogue 16 (130) Curcumin-diaryl pentanoid analogue 22 (131)	IC ₅₀ > 250 μ M on diphenolase inhibitory activity IC ₅₀ > 250 μ M on diphenolase inhibitory activity IC ₅₀ > 250 μ M on diphenolase inhibitory activity IC ₅₀ > 250 μ M on diphenolase inhibitory activity	
(2 <i>RS</i> ,4 <i>R</i>)-2-(2,4-Dihydroxyphenyl)thiazolidine-4-carboxylic acid (132)	IC ₅₀ = 1.81 \pm 0.90 μ M on diphenolase inhibitory activity	[86]
Furfural (133)	IC ₅₀ = 3.38 mM on diphenolase inhibitory activity	[87]
Furfuryl alcohol (134)	IC ₅₀ = 17.75 mM on diphenolase inhibitory activity	[87]
Furoic acid (135)	Uncompetitive inhibitor IC ₅₀ = 10.00 mM on diphenolase inhibitory activity	[87]
Glabridin (136)	Noncompetitive inhibitor IC ₅₀ = 0.43 μ M on diphenolase inhibitory activity	[88]
Hydroxypyridinone derivatives Hydroxypyridinone derivative 6a (137) Hydroxypyridinone derivative 6b (138) Hydroxypyridinone derivative 6c (139) Hydroxypyridinone derivative 6d (140) Hydroxypyridinone derivative 6e (141) Hydroxypyridinone derivative 12a (142) Hydroxypyridinone derivative 12b (143) Hydroxypyridinone derivative 12c (144)	IC ₅₀ = 11.76 μ M on diphenolase inhibitory activity IC ₅₀ = 28.71 μ M on diphenolase inhibitory activity IC ₅₀ = 15.62 μ M on diphenolase inhibitory activity IC ₅₀ = 12.48 μ M on diphenolase inhibitory activity IC ₅₀ = 1.95 μ M on diphenolase inhibitory activity IC ₅₀ = 2.79 μ M on diphenolase inhibitory activity IC ₅₀ = 6.93 μ M on diphenolase inhibitory activity IC ₅₀ = 14.26 μ M on diphenolase inhibitory activity	[89]
5-Hydroxy-4-acetyl-2,3-dihydronaphtho[1,2- <i>b</i>]furans derivatives: 1-(2-Ethoxy-5-hydroxy-2,3-dihydronaphtho[1,2- <i>b</i>]furan-4-yl)ethanone (145) 1-(5-Hydroxy-2-propoxy-2,3-dihydronaphtho[1,2- <i>b</i>]furan-4-yl)ethanone (146) 1-(5-Hydroxy-2-isobutoxy-2,3-dihydronaphtho[1,2- <i>b</i>]furan-4-yl)ethanone (147) 1-(2-Butoxy-5-hydroxy-2,3-dihydronaphtho[1,2- <i>b</i>]furan-4-yl)ethanone (148) 1-(5-Hydroxy-2-methoxy-2-methyl-2,3-dihydronaphtho[1,2- <i>b</i>]furan-4-yl)ethanone (149) 1-(<i>trans</i> -2-Ethoxy-5-hydroxy-3-methyl-2,3-dihydronaphtho[1,2- <i>b</i>]furan-4-yl)ethanone (150) <i>cis</i> -1-(5-Hydroxy-6b,7,8,9a-tetrahydrofuro[2,3- <i>b</i>]naphtho[2,1- <i>d</i>]furan-6-yl)ethanone (151) <i>cis</i> -1-(5-Hydroxy-7,8,9,10a-tetrahydro-6bH-naphtho[2',1':4,5]furo[2,3- <i>b</i>]pyran-6-yl)ethanone (152) 1-(5-Hydroxy-2-methyl-2-phenyl-2,3-dihydronaphtho[1,2- <i>b</i>]furan-4-yl)ethanone (153) 1-(5-Hydroxy-2-methyl-2-phenyl-2,3-dihydronaphtho[1,2- <i>b</i>]furan-4-yl)ethanone (154) 1-(5-Hydroxy-2-(4-methoxyphenyl)-2,3-dihydronaphtho[1,2- <i>b</i>]furan-4-yl)ethanone (155) 2-Phenylacetic acid (156)	IC ₅₀ = 83.17 \pm 0.12 μ g/mL on diphenolase inhibitory activity Competitive inhibitor IC ₅₀ = 8.91 \pm 0.24 μ g/mL on diphenolase inhibitory activity IC ₅₀ = 59.56 \pm 0.95 μ g/mL on diphenolase inhibitory activity IC ₅₀ = 69.82 \pm 0.72 μ g/mL on diphenolase inhibitory activity IC ₅₀ > 100 μ g/mL on diphenolase inhibitory activity IC ₅₀ = 30.61 \pm 0.91 μ g/mL on diphenolase inhibitory activity IC ₅₀ > 100 μ g/mL on diphenolase inhibitory activity IC ₅₀ = 50.00 \pm 0.82 μ g/mL on diphenolase inhibitory activity IC ₅₀ > 100 μ g/mL on diphenolase inhibitory activity IC ₅₀ > 100 μ g/mL on diphenolase inhibitory activity IC ₅₀ > 100 μ g/mL on diphenolase inhibitory activity Uncompetitive inhibitor IC ₅₀ = 2.38 mM on diphenolase inhibitory activity	[90]
		[91]

Table 3 Antityrosinase activity of synthetic compounds (continue)

Compound	Tyrosinase inhibitory activity	Reference
2-Phenylacetaldehyde (157)	Uncompetitive inhibitor IC ₅₀ = 0.39 mM on diphenolase inhibitory activity	[91]
2-Phenylethanol (158)	Mixed inhibitor IC ₅₀ = 3.04 mM on diphenolase inhibitory activity	[91]
Rhododendrol derivatives:		[92]
Rhododendrol derivative 3 (159)	IC ₅₀ = 4.72 ± 0.58 μM on diphenolase inhibitory activity	
Rhododendrol derivative 4 (160)	IC ₅₀ = 2.30 ± 0.15 μM on diphenolase inhibitory activity	
Rhododendrol derivative 5 (161)	IC ₅₀ = 2.17 ± 0.20 μM on diphenolase inhibitory activity	
Rhododendrol derivative 6 (162)	IC ₅₀ = 1.78 ± 0.10 μM on diphenolase inhibitory activity	
Rhododendrol derivative 7 (163)	IC ₅₀ = 4.56 ± 0.48 μM on diphenolase inhibitory activity	
Rhododendrol derivative 8 (164)	IC ₅₀ = 1.72 ± 0.17 μM on diphenolase inhibitory activity	
Rhododendrol derivative 9 (165)	IC ₅₀ = 3.83 ± 0.45 μM on diphenolase inhibitory activity	
Rhododendrol derivative 10 (166)	IC ₅₀ = 1.51 ± 0.10 μM on diphenolase inhibitory activity	
Rhododendrol derivative 11 (167)	IC ₅₀ = 4.13 ± 0.69 μM on diphenolase inhibitory activity	
Rhododendrol derivative 12 (168)	IC ₅₀ = 1.98 ± 0.17 μM on diphenolase inhibitory activity	
Rhododendrol derivative 20 (169)	IC ₅₀ = 9.15 ± 0.71 μM on diphenolase inhibitory activity	
Rhododendrol derivative 21 (170)	IC ₅₀ = 0.56 ± 0.02 μM on diphenolase inhibitory activity	

**Figure 13** Structure of synthetic compounds of tyrosinase inhibitors

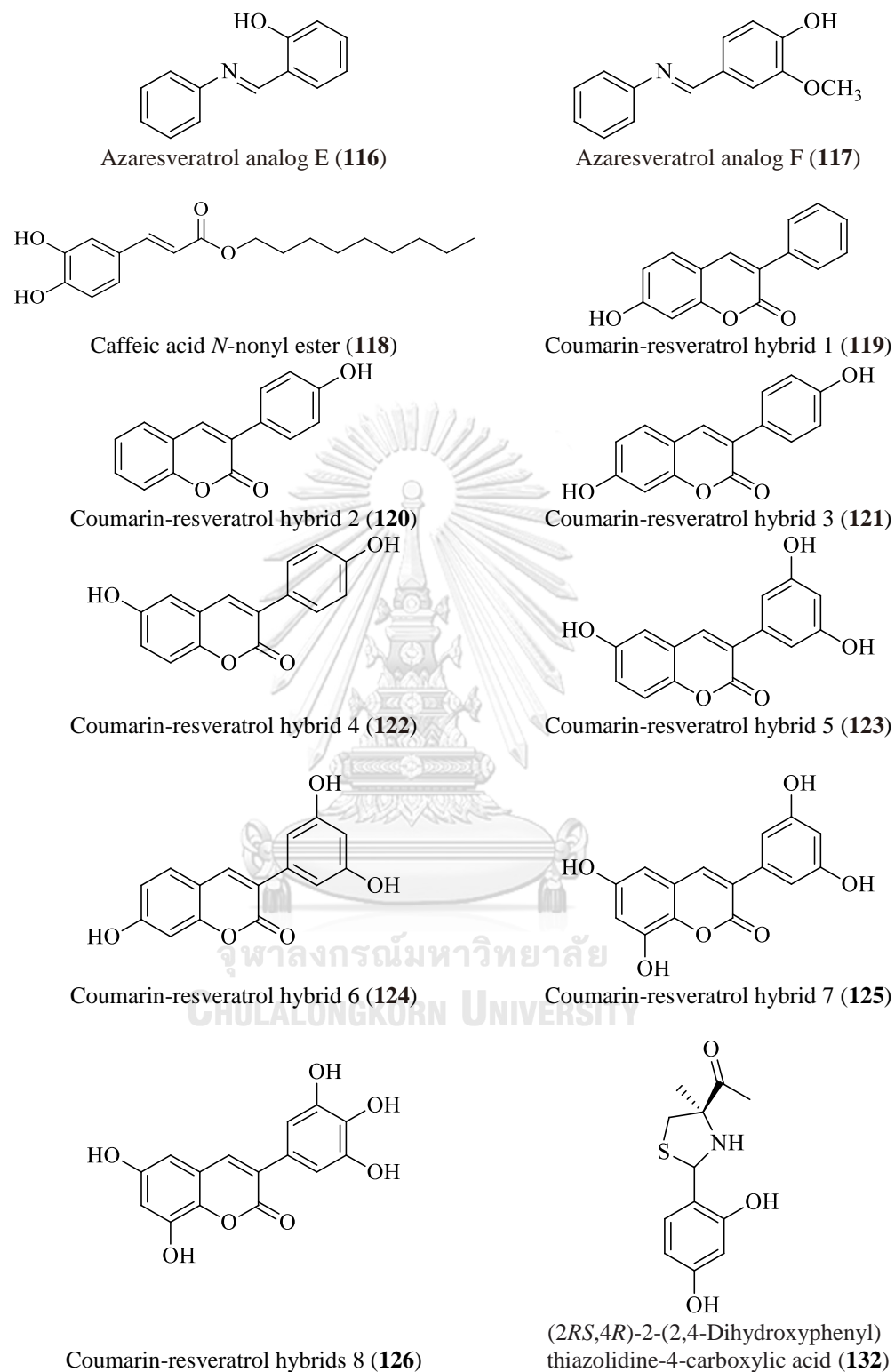
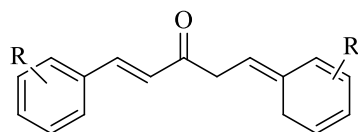
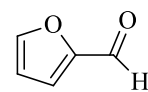
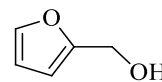
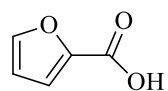
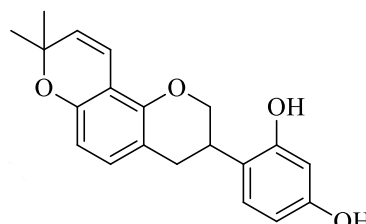
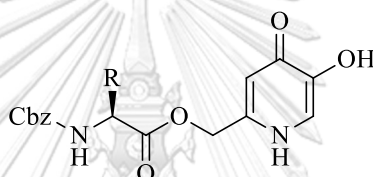
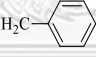
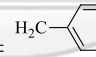


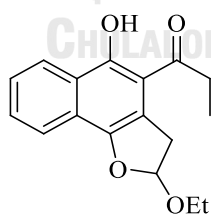
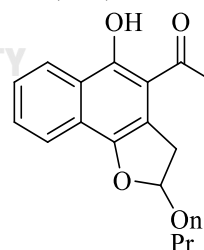
Figure 13 Structure of synthetic compounds of tyrosinase inhibitors (continue)



- Curcumin-diaryl pentanoid analogue 4 (**127**): R = 4-OH
 Curcumin-diaryl pentanoid analogue 10 (**128**): R = 4-F
 Curcumin-diaryl pentanoid analogue 15 (**129**): R = 3-OCH₃, 4-OH
 Curcumin-diaryl pentanoid analogue 16 (**130**): R = 2-F, 4-OCH₃
 Curcumin-diaryl pentanoid analogue 22 (**131**): R = 4-OH

Furfural (**133**)Furfuryl alcohol (**134**)Furoic acid (**135**)Glabridin (**136**)

- Hydroxypyridinone derivative 6a (**137**): R = CH₃
 Hydroxypyridinone derivative 6b (**138**): R = CH₃CH(CH₃)₂
 Hydroxypyridinone derivative 6c (**139**): R = (CH₃)CHCH₂CH₃
 Hydroxypyridinone derivative 6d (**140**): R = CH(CH₃)₂
 Hydroxypyridinone derivative 6e (**141**): R = 
 Hydroxypyridinone derivative 12a (**142**): R = 
 Hydroxypyridinone derivative 12b (**143**): R = CH₂CH(CH₃)₂
 Hydroxypyridinone derivative 12c (**144**): R = CH(CH₃)₂

1-(2-Ethoxy-5-hydroxy-2,3-dihydro
naphtho[1,2-b]furan-4-yl)ethanone (**145**)1-(5-Hydroxy-2-propoxy-2,3-dihydro
naphtho[1,2-b]furan-4-yl)ethanone (**146**)**Figure 13** Structure of synthetic compounds of tyrosinase inhibitors (continue)

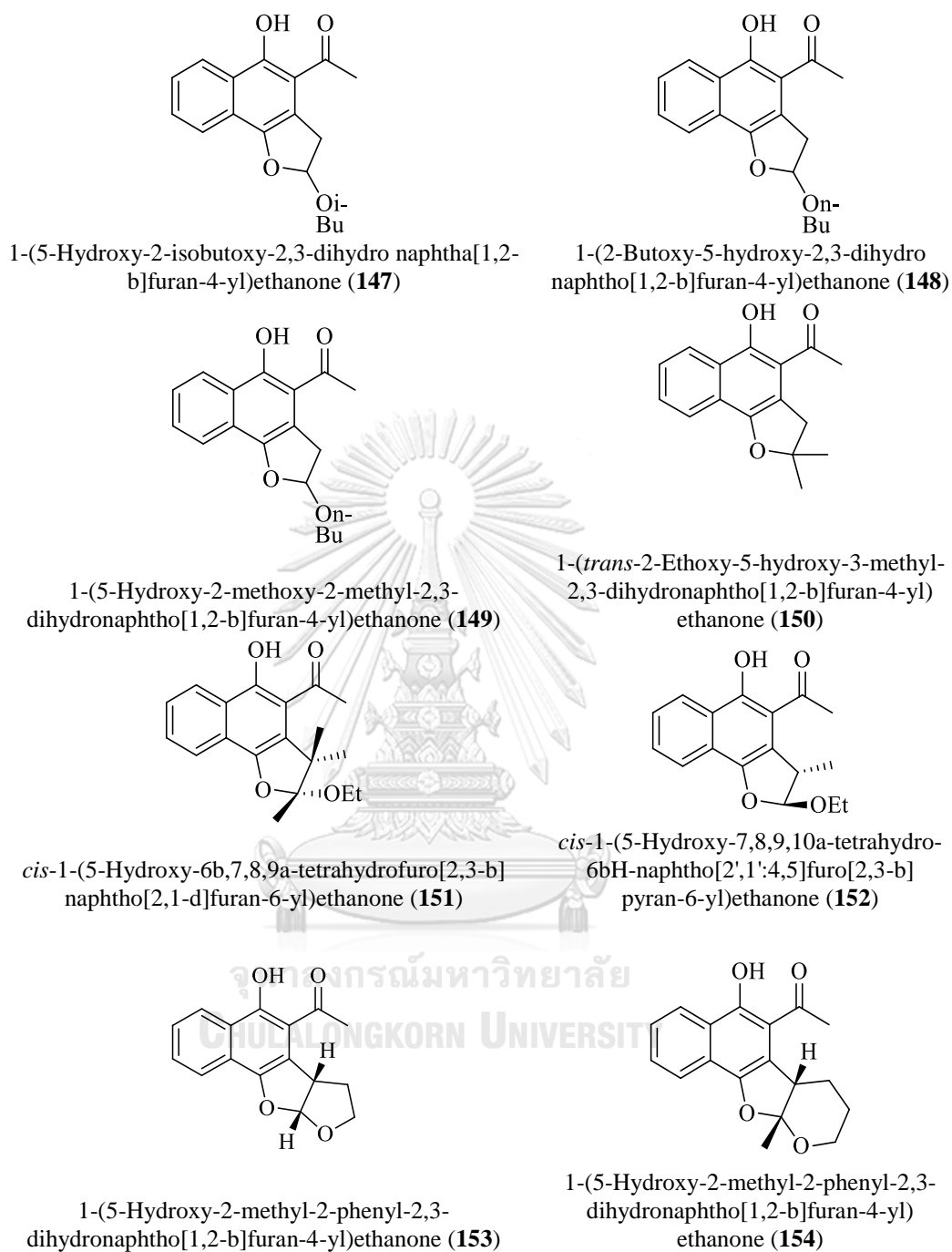
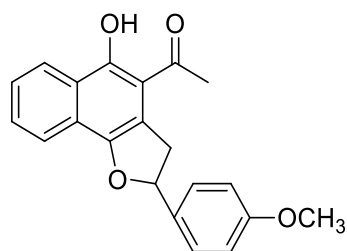
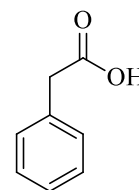


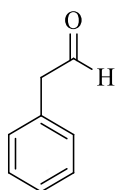
Figure 13 Structure of synthetic compounds of tyrosinase inhibitors (continue)



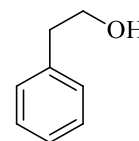
1-(5-Hydroxy-2-(4-methoxyphenyl)-2,3-dihydronaphtho[1,2-b]furan-4-yl)ethanone (**155**)



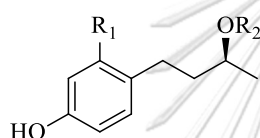
2-Phenylacetic acid (**156**)



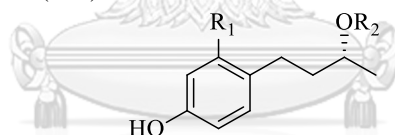
2-Phenylacetaldehyde (**157**)



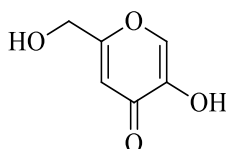
2-Phenylethanol (**158**)



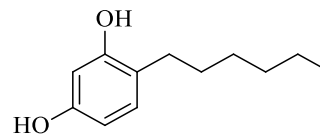
- Rhododendrol derivative 3 (**159**): $R_1 = OH$ $R_2 = Glc$
 Rhododendrol derivative 5 (**161**): $R_1 = OH$ $R_2 = H$
 Rhododendrol derivative 7 (**163**): $R_1 = OH$ $R_2 = Xyl$
 Rhododendrol derivative 9 (**165**): $R_1 = OH$ $R_2 = Cel$
 Rhododendrol derivative 11 (**167**): $R_1 = OH$ $R_2 = Mal$



- Rhododendrol derivative 4 (**160**): $R_1 = OH$ $R_2 = Glc$
 Rhododendrol derivative 6 (**162**): $R_1 = OH$ $R_2 = H$
 Rhododendrol derivative 8 (**164**): $R_1 = OH$ $R_2 = Xyl$
 Rhododendrol derivative 10 (**166**): $R_1 = OH$ $R_2 = Cel$
 Rhododendrol derivative 12 (**168**): $R_1 = OH$ $R_2 = Mal$



Rhododendrol derivative 20 (**169**)



Rhododendrol derivative 21 (**170**)

Figure 13 Structure of synthetic compounds of tyrosinase inhibitors (continue)

2.6 *Manilkara zapota* Linn.

2.6.1 Botanical

M. zapota belongs to the Sapotaceae family. The genus *Manilkara* are found only four species in Thailand; *M. hexandra*, *M. littoralis*, *M. kauki* and *M. zapota*. Thai

name of *M. zapota* is called Lamut, Cha-wa-ni-lo (Pattani) and general name of *M. zapota* is called Lamut farang. It is a native of South America and is widely cultivated in tropical zones. This tree grows up to 6 m tall. Branches are reddish brown and leaves are elliptic oblong, 1.3-2.6 cm long. Solitary flower is 2-2.5 cm long and reddish brown tomentose. Ellipsoid fruits are 5-6 cm long. Ripe fruits are edible, soft and sweet [15].

2.6.2 Phytochemical and biological activities

M. zapota contains many phytochemical compounds like triterpenoid such as 3-acetyltaraxer-14-en-12-one, 3-acetyltaraxerol, beturinic acid and lupeol. These compounds were isolated from *M. zapota* barks and showed cytotoxicity against the human Caucasian prostate adenocarcinoma cell line PC-3 [93]. Antioxidant compound, methyl-4-*O*-galloylchlorogenate was isolated from *M. zapota* fruits and displayed antioxidant activity on DPPH radical scavenging with IC₅₀ value of 12.9 μM [94]. Moreover, ethanol extract of *M. zapota* fruits showed DPPH and ABTS radical scavenging with IC₅₀ values of 37.63 ± 1.18 and 73.14 ± 2.84 μg/mL, respectively. Ethanol extract of *M. zapota* fruits inhibited matrix metalloproteinases types MMP-1, MMP-2 and elastase activities with IC₅₀ values of 89.61 ± 0.96, 86.47 ± 3.04 and 35.73 ± 0.61 μg/mL, respectively [95]. Myricetin-3-*O*-α-*L*-rhamnoside was isolated from *M. zapota* leaves and showed antityrosinase activity (% diphenolase inhibition = 30% at 100 μg/mL) and DPPH radical scavenging activity (% radical scavenging = 94% at 40 μg/mL). *D*-Quercitol and saccharose were isolated from *M. zapota* seeds [96]. Acetone extract of *M. zapota* leaves showed antimicrobial activity against *Klebsiella pneumoniae* with zone of inhibition value of 15 ± 0.29 mm [18]. Aqueous extract of *M. zapota* fruit pulps and leaves showed *in vivo* antidiabetic and antipidemic activities on metabolic parameter of Wistar rats [16]. Ethyl acetate extract of stem barks showed antitumor activity against *Ehrlich ascites* carcinoma cell bearing mice that the weight gain was reduced with 200 mg/kg dose extract and showed antimicrobial activity against gram positive and negative bacteria with the average value of 7-13.5 mm zone of inhibition at the concentration of 400 μg/disc [97]. Manilkoraside, a pentacyclic triterpenoid saponin was isolated from ethanol extract. It showed anticancer activity with the half maximal effective concentration values (EC₅₀) of 20 and 48 μg/mL against human promyelocytic leukemia (HL-60 and HL-29), respectively [98]. Aqueous extract

of *M. zapota* leaves showed acaricidal activity against *Rhipicephalus microplus* with IC_{50} value of 16.72 mg/L [99]. Acetone extract of *M. zapota* seeds showed antibacterial activity againsts *Vibrio cholerae* with an IC_{50} value 93 μ g/mL [100]. Acetone extract of *M. zapota* seeds showed DPPH free radical scavenging activity with IC_{50} value of 400 μ g/mL [101]. Ethyl acetate extract of *M. zapota* seed coats exhibited tyrosinase inhibitory activity with IC_{50} value of 138 μ g/mL [102]. Phytochemicals and biological activities of *Manilkara* genus are summarized in Table 4. Structure of phytochemicals of genus *Manilkara* is shown in Figure 14.

Table 4 Phytochemical and biological activities of genus *Manilkara*

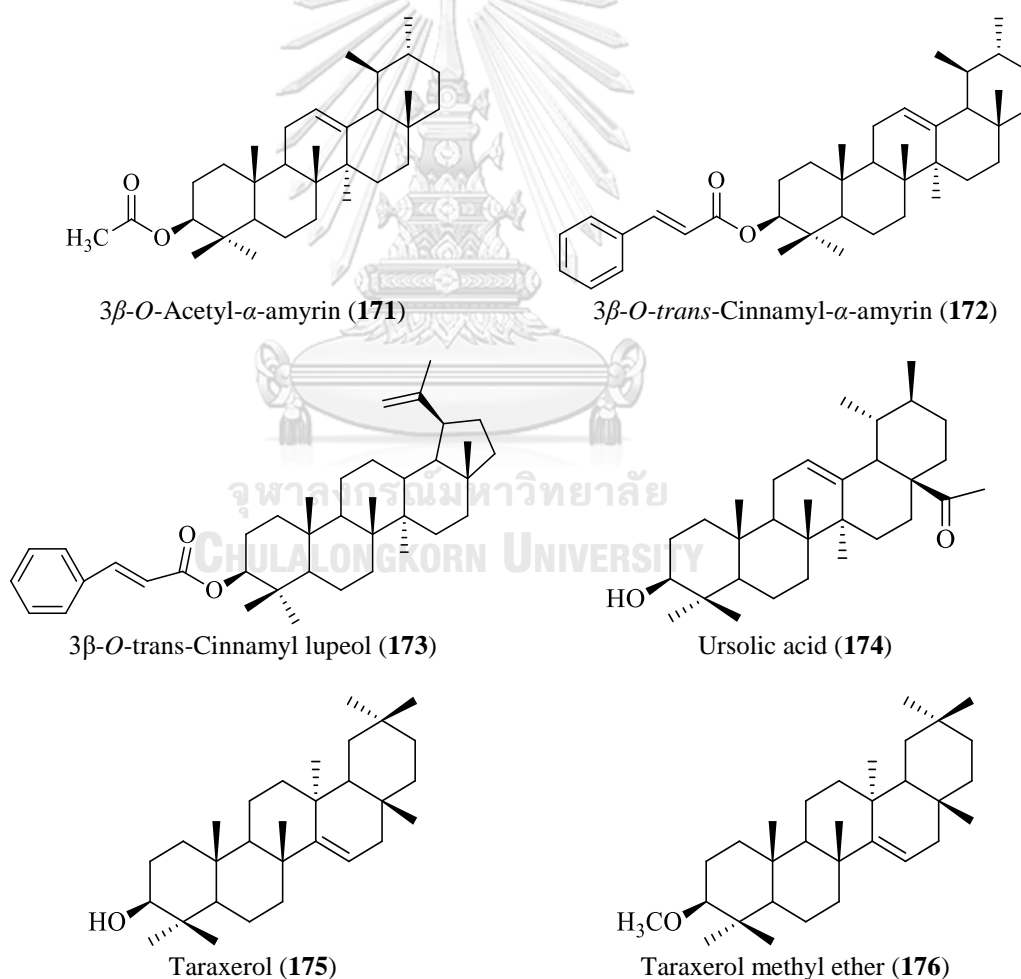
Scientific name	Plant part	Crude extract/phytochemical	Reference
<i>Manilkara bidentata</i>	Resin	3 β -O-Acetyl- α -amyrin (171) 3 β -O-trans-Cinnamyl- α -amyrin (172) 3 β -O-trans-Cinnamyl Lupeol (173)	[103]
<i>Manilkara caffra</i>	Leaves	Ursolic acid (174) Antiplasmodial activity (IC_{50} = 6.8 μ g/mL)	[104]
<i>Manilkara obtusifolia</i>	Stem barks	Taraxerol (175) Antiplasmodial activity (IC_{50} > 100 μ g/mL) Taraxerol methyl ether (176) Antiplasmodial activity (IC_{50} > 100 μ g/mL)	[104]
<i>Manilkara subsericea</i>	Fruits	α -Amyrin acetate (177) β -Amyrin acetate (178) α -Amyrin caproate (179) β -Amyrin caproate (180) α -Amyrin caprylate (181) β -Amyrin caprylate (182) Hexadecanoic acid (183) Hexadecanoic acid ethyl ester (184) Octadecanoic acid ethyl ester (185) (<i>E</i>)-9-Octadecanoic acid ethyl ester (186)	[105]
<i>Manilkara zapota</i>	Barks	3-Acetyloleanolic acid (187) (IC_{50} = 16.2 \pm 0.7 μ g/mL on cytotoxic activity against the human Caucasian prostate adenocarcinoma cell line PC-3) 3-Acetyltaraxer-14-en-12-one (188) (IC_{50} = 27.8 \pm 0.5 μ g/mL on cytotoxic activity against the human Caucasian prostate adenocarcinoma cell line PC-3) α -Amyrin (189) β -Amyrin (190) Betulinic acid (191) (IC_{50} = 19.8 \pm 0.6 μ g/mL on cytotoxic activity against the human Caucasian prostate adenocarcinoma cell line PC-3) Lupeol (192) (IC_{50} = 30.6 \pm 0.9 μ g/mL on cytotoxic activity against the human Caucasian prostate adenocarcinoma cell line PC-3) Lupeol acetate (193) (IC_{50} = 61.2 \pm 0.7 μ g/mL on cytotoxic activity against the human Caucasian prostate adenocarcinoma cell line PC-3) Lupeone (194) Oleanolic acid (195) 7-Oxobetulinic acid (196) (IC_{50} = 14.1 \pm 0.5 μ g/mL on cytotoxic activity against the human Caucasian prostate adenocarcinoma cell line PC-3) 3-Oxolup-20(29)-en-28-oic acid (197) (IC_{50} = 24.8 \pm 0.8 μ g/mL on cytotoxic activity against the human Caucasian prostate adenocarcinoma cell line PC-3)	[93]

Table 4 Phytochemical and biological activities of genus *Manilkara* (continue)

Scientific name	Plant part	Crude extract/phytochemical	Reference	
<i>Manilkara zapota</i>	Fruits	Taraxerone (198) (IC ₅₀ = 62.5 ± 0.6 µg/mL on cytotoxic activity against the human Caucasian prostate adenocarcinoma cell line PC-3)	[106]	
		Ethanol extract		
		DPPH radical scavenging (IC ₅₀ = 37.63 ± 1.18 µg/mL)		
		ABTS radical scavenging (IC ₅₀ = 73.14 ± 2.84 µg/mL)		
		Collagenase inhibition on MMP-1 (IC ₅₀ = 89.61 ± 0.96 µg/mL)		
		Collagenase inhibition on MMP-1 (IC ₅₀ = 86.47 ± 3.04 µg/mL)		
		Elastase inhibition (IC ₅₀ = 35.73 ± 0.61 µg/mL)		
		4-Caffeoylquinic acid (199)		[94]
		Methyl-4- <i>O</i> -Galloylchlorogenate (200)		
		DPPH radical scavenging (IC ₅₀ = 12.9 µM)		
		Cytotoxicity against the HCT-116 and SW-480 human colon cancer cell lines (IC ₅₀ = 154 and 134 µM)		
		4- <i>O</i> -Galloylchlorogenic acid (201)		
		Methyl chlorogenate (202)		
		Dihydromyricetin (203)		
	Quercitrin (204)			
	Fruit pulps, leaves	Aqueous extract	[16]	
	Leaves	<i>In vivo</i> antidiabetic and antipidemic activities	[99]	
		Aqueous extract	[99]	
		Acaricidal activity against <i>Rhipicephalus microplus</i> (IC ₅₀ = 16.72 mg/L)	[18]	
		Acetone extract	[18]	
		Antimicrobial activity against <i>Klebsiella pneumoniae</i> (zone of inhibition = 15 ± 0.29 mm)	[96]	
		Myricetin-3- <i>O</i> - α -L- rhamnoside (205) (% diphenolase inhibition = 30% at 100 µg/mL) (% elastase inhibition = 34% at 40 µg/mL) (% radical scavenging = 94% at 40 µg/mL)	[96]	
		(+)-Catechin (206)		
		(-)-Epicatechin (207)		
		(+)-Gallocatechin (208)		
		Gallic acid (82)		
	Seeds	Acetone extract	[100]	
	Antibacterial activity againsts <i>Vibrio cholerae</i> (IC ₅₀ = 93 µg/mL)	[101]		
	Acetone extract	[101]		
	DPPH radical scavenging (IC ₅₀ = 400 µg/mL)	[96]		
	D-quercitol (209)	[96]		
	Saccharose (210)	[96]		
	2-(4-Hydroxyphenethyl) tetratriacontanoate (211) (IC ₅₀ = 8.50 ± 0.55 µg/mL on DPPH radical scavenging)	[107]		
	Mixture of phenylethanoyls (IC ₅₀ = 62.52 ± 1.25 µg/mL on DPPH radical scavenging)	[107]		
	2-(4-Hydroxyphenethyl) tetracosanoate (212)			
	2-(4-Hydroxyphenethyl) docosanoate (213)			
	2-(4-Hydroxyphenethyl) eicosanoate (214)			
	2-(4-Hydroxyphenethyl) octadecanoate (215)			
	2-(4-Hydroxyphenethyl) hexadecanoate (216)			
	β -Amyrin (190) (IC ₅₀ = 201.14 ± 4.53 µg/mL on DPPH radical scavenging)	[107]		
	Oleanolic acid (195) (IC ₅₀ = 151.80 ± 2.00 µg/mL on DPPH radical scavenging)	[107]		

Table 4 Phytochemical and biological activities of genus *Manilkara* (continue)

Scientific name	Plant part	Crude extract/phytochemical	Reference
		Lupeol (192)	[107]
		(IC ₅₀ = 223.11 ± 5.64 µg/mL on DPPH radical scavenging)	
		Betulinic acid (191)	[107]
		DPPH radical scavenging	
		(IC ₅₀ = 105.20 ± 0.41 µg/mL)	
		Stigmasterol-3-O-β-D-glucopyranoside (217)	[107]
		Stigmasterol (218)	[107]
		β-Sitosterol (89)	[107]
	Seed coats	Ethyl acetate extract	[102]
		Tyrosinase inhibitory activity	
		(IC ₅₀ = 138 µg/ml)	
	Stem barks	Ethyl acetate extract	[97]
		Antitumor activity against EAC	
		Antimicrobial activity against gram positive and negative bacteria	
		(zone of inhibition range 7-13.5 mm)	
		Manilkoraside (219)	[98]
		Anticancer activity against HL-60	
		(EC ₅₀ = 20 µg/mL)	
		Anticancer activity against HL-29	
		(EC ₅₀ = 48 µg/mL)	

**Figure 14** Phytochemical structure of genus *Manilkara*

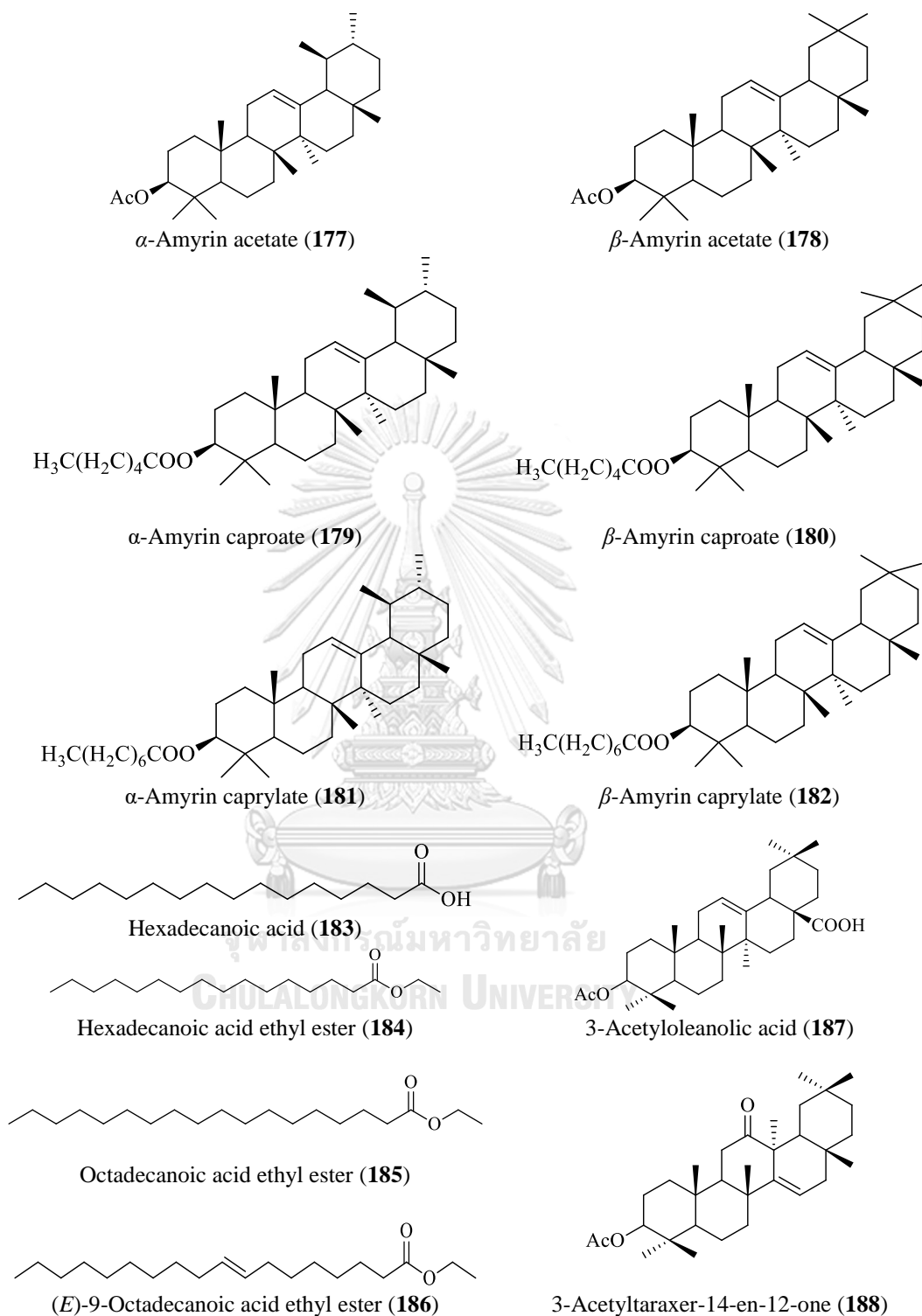


Figure 14 Phytochemical structure of genus *Manilkara* (continue)

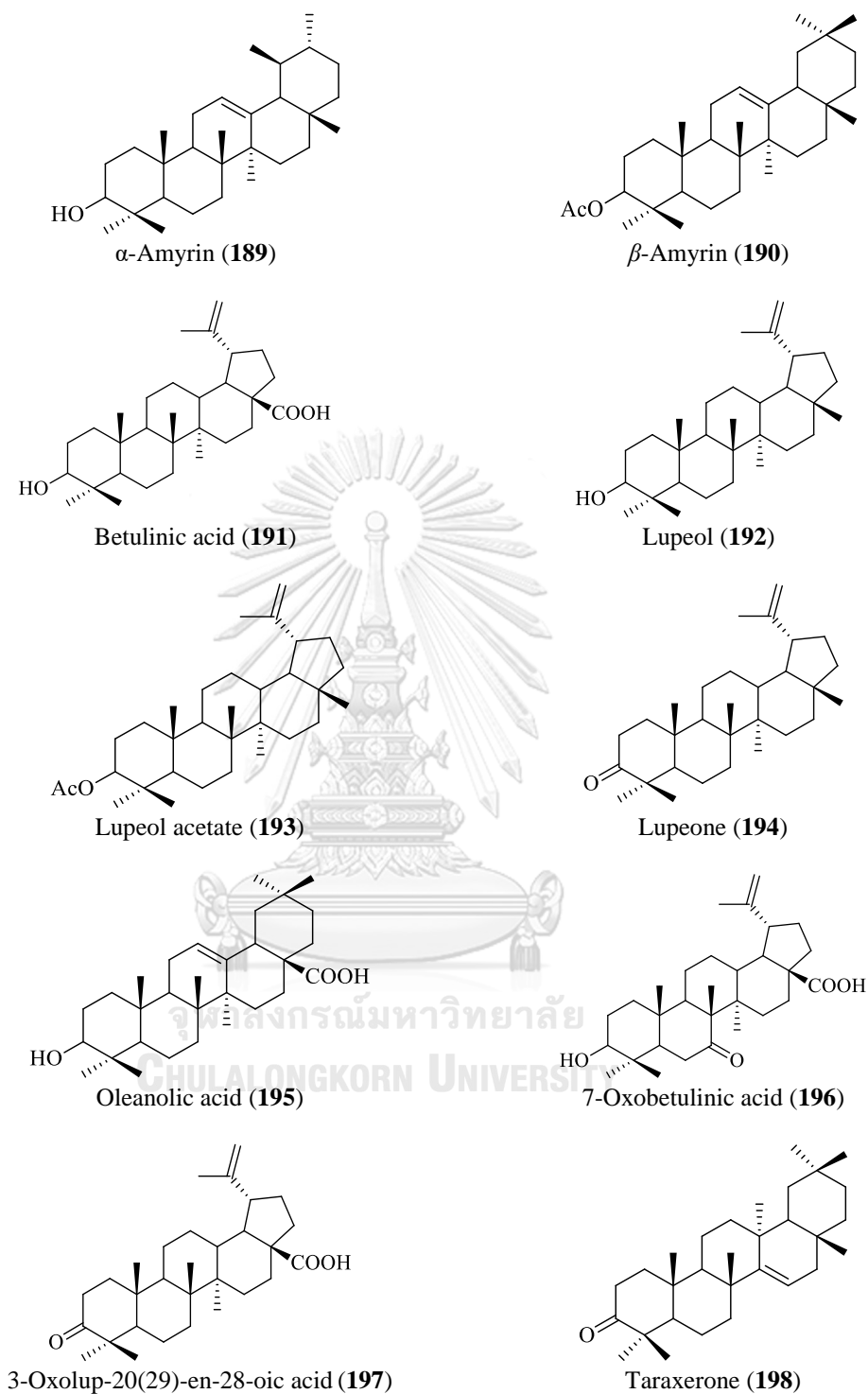


Figure 14 Phytochemical structure of genus *Manilkara* (continue)

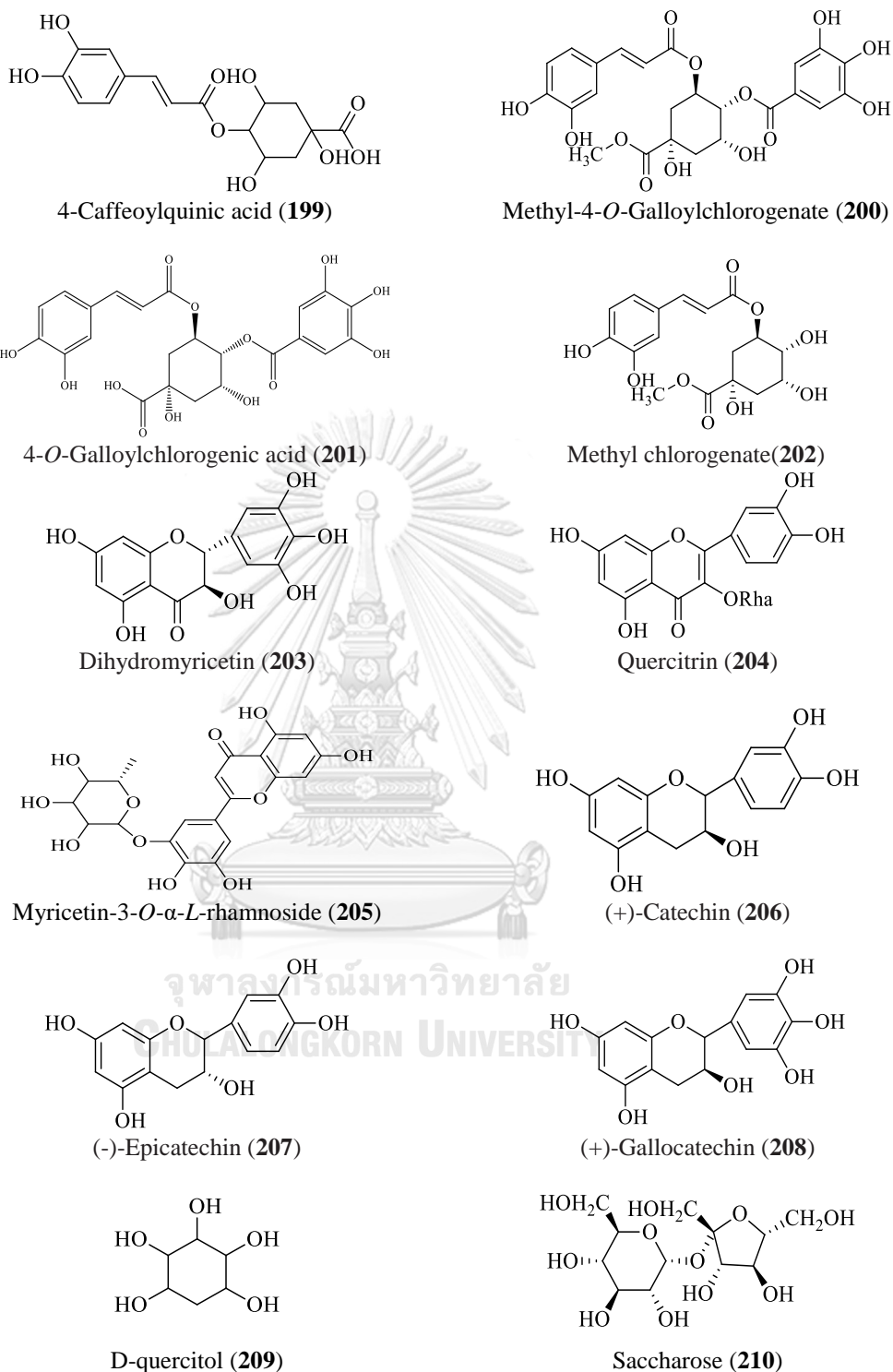


Figure 14 Phytochemical structure of genus *Manilkara* (continue)

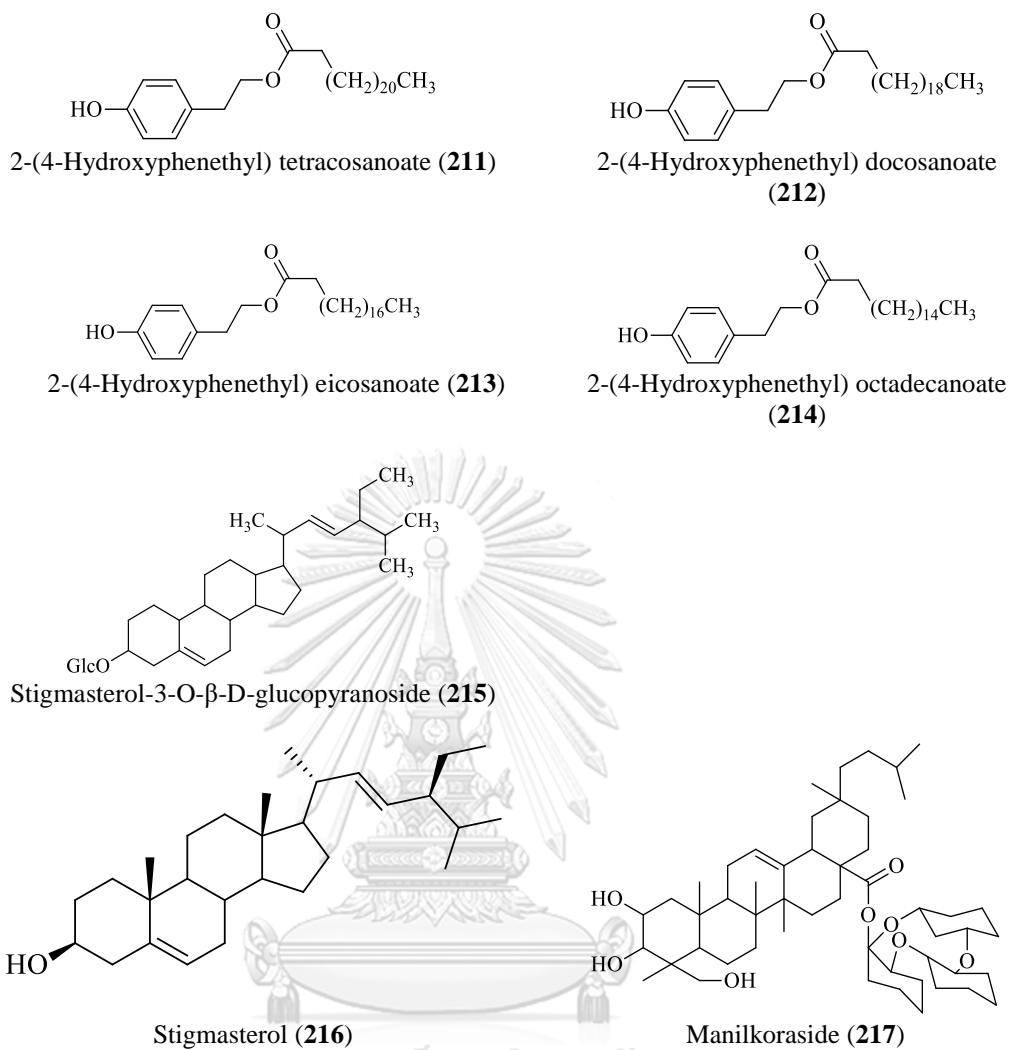


Figure 14 Phytochemical structure of genus *Manilkara* (continue)

CHAPTER III

MATERIALS AND METHODS

3.1 Materials

3.1.1 Plant material of *M. zapota*

The barks, flowers, fruits, leaves, roots and seeds of *M. zapota* were collected from Saraburi Province, Thailand in May 2013. A voucher specimen (BKF No. 187749) was deposited at the Forest Herbarium, Department of National Parks, Wildlife and Plant Conservation, Bangkok, Thailand.

3.1.2 Chemicals and reagents

3.1.2.1 All commercial grade solvents were distilled prior to use such as hexane, dichloromethane, ethyl acetate, acetone and methanol.

3.1.2.2 All HPLC grade solvents were used for HPLC analysis such as acetonitrile, methanol and DDI water (Sigma, Germany).

3.1.2.3 All analytical grade chemicals, monosodium phosphate, disodium phosphate, dimethyl sulfoxide (DMSO), absolute ethanol, sulfuric acid, vanillin reagent, *L*-tyrosine, *L*-DOPA, kojic acid, chloroform-*d*, acetone-*d*₆ were purchased from Merck (Germany). Mushroom tyrosinase was purchased from Sigma-Aldrich (USA).

3.2 General techniques and procedures

3.2.1 Thin layer chromatography (TLC)

Techniques:	One dimension
Stationary phase:	Silica gel 60 F ₂₅₄ (Merck, Germany) pre-coated plate
Layer thickness:	0.2 mm
Distance of mobile phase:	4 cm
Mobile phase:	Various solvent systems
Detection:	a. UV light at 254 and 365 nm b. dipping in 10% sulfuric acid in aqueous ethanol and heating on hot plate

3.2.2 Preparative thin layer chromatography (PTLC)

Techniques:	One dimension
Stationary phase:	Silica gel 60 F ₂₅₄ (Merck, Germany) glass-coated plate
Layer thickness:	1 mm
Distance of mobile phase:	18 cm
Mobile phase:	Various solvent systems
Detection:	a. UV light at 254 and 365 nm b. dipping in 10% sulfuric acid in aqueous ethanol and heating on hot plate

3.2.3 Column chromatography (CC)

Stationary phase:	Silica gel 60, 70-230 mesh ASTM (Merck, Germany) and Sephadex LH-20, 8-111 μm (Bioscience, USA)
Mobile phase:	Various solvent systems
Packing method:	Dry and wet packing
Detection:	Eluted fractions were monitored by TLC

3.2.4 High performance liquid chromatography (HPLC)

Stationary phase:	Hypersyl ODS Cyano column (4.6 mm \times 25 cm, 5 μm , Thermo Hypersil-Keystone, Germany)
Mobile phase:	Acetonitrile, methanol and DDI water
Injection value:	10 μL
Detection:	UV-Visible spectrophotometer, range of wavelength was 200-600 nm

3.2.5 UV-Visible spectrophotometer

UV spectra were recorded with a Microplate reader Multiscan GO (Thermo Fisher Scientific, USA).

3.2.6 Nuclear magnetic resonance spectrophotometer (NMR)

The one dimensional spectra (¹H-NMR, ¹³C-NMR, DEPT90 and DEPT135) and two dimensional spectra (correlation spectrophotometer (COSY), heteronuclear

multiple quantum coherence (HMQC), heteronuclear single quantum correlation (HSQC) and heteronuclear multiple bond correlation (HMBC)) were determined on a Bruker model Fourier 300 spectrometer instrument (Bruker Daltonics Inc, Bremen, Germany). The chemical shifts were recorded in ppm with the reference solvent signals. Tetramethylsilane (TMS) was used as an internal standard.

3.2.7 High resolution electron impact mass spectrophotometer

The high resolution mass spectra were obtained on Bruker model MICROTOF (Bruker Daltonics Inc, Bremen, Germany). The coupled mass spectrometer was carried on electron impact ionization (EI) mode. Range of scan was 25-3000 m/z.

3.3 Methods

3.3.1 Extraction

3.3.1.1 Extraction of different parts of *M. zapota*

The six different parts of *M. zapota*; barks, flowers, fruits, leaves, roots and seeds were chopped and dried in a hot air oven at 60 °C. Each dried sample (500 g) was extracted with methanol (2 × 0.5 L) and water (2 × 0.5 L) by maceration for 24 h at 30 °C. Then, the filtrate was evaporated *in vacuo* to give methanol and aqueous crude extracts.

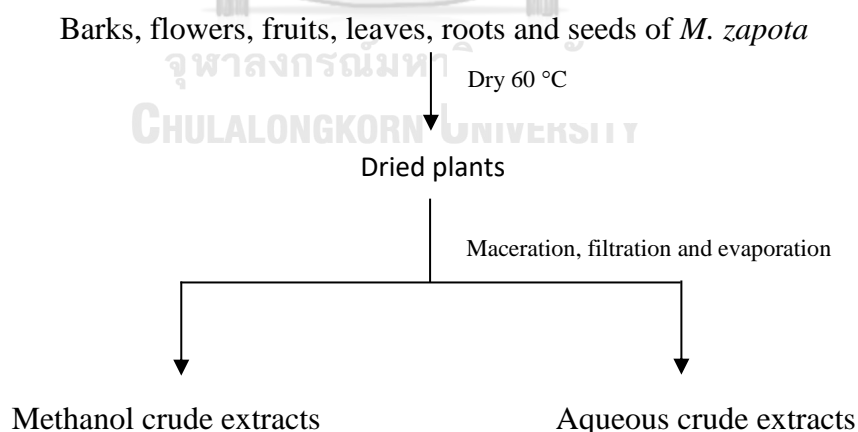


Figure 15 Extraction procedure of six different parts of *M. zapota*

3.3.1.2 Extraction of *M. zapota* barks

Fresh barks of *M. zapota* (175 kg) were collected and dried in an oven at 60 °C. The dried barks of *M. zapota* (7 kg) were then powdered and extracted by maceration with *n*-hexane (3 × 5.0 L), ethyl acetate (3 × 5.5 L), methanol (3 × 5.0 L) and water (3

× 3.5 L), respectively. Each the extract was filtrated and evaporated under *in vacuo* evaporator to get *n*-hexane crude extract (140 g), ethyl acetate crude extract (138 g), methanol crude extract (820 g) and aqueous crude extract (97 g). All crude extracts of *M. zapota* barks were evaluated for tyrosinase inhibitory activity.

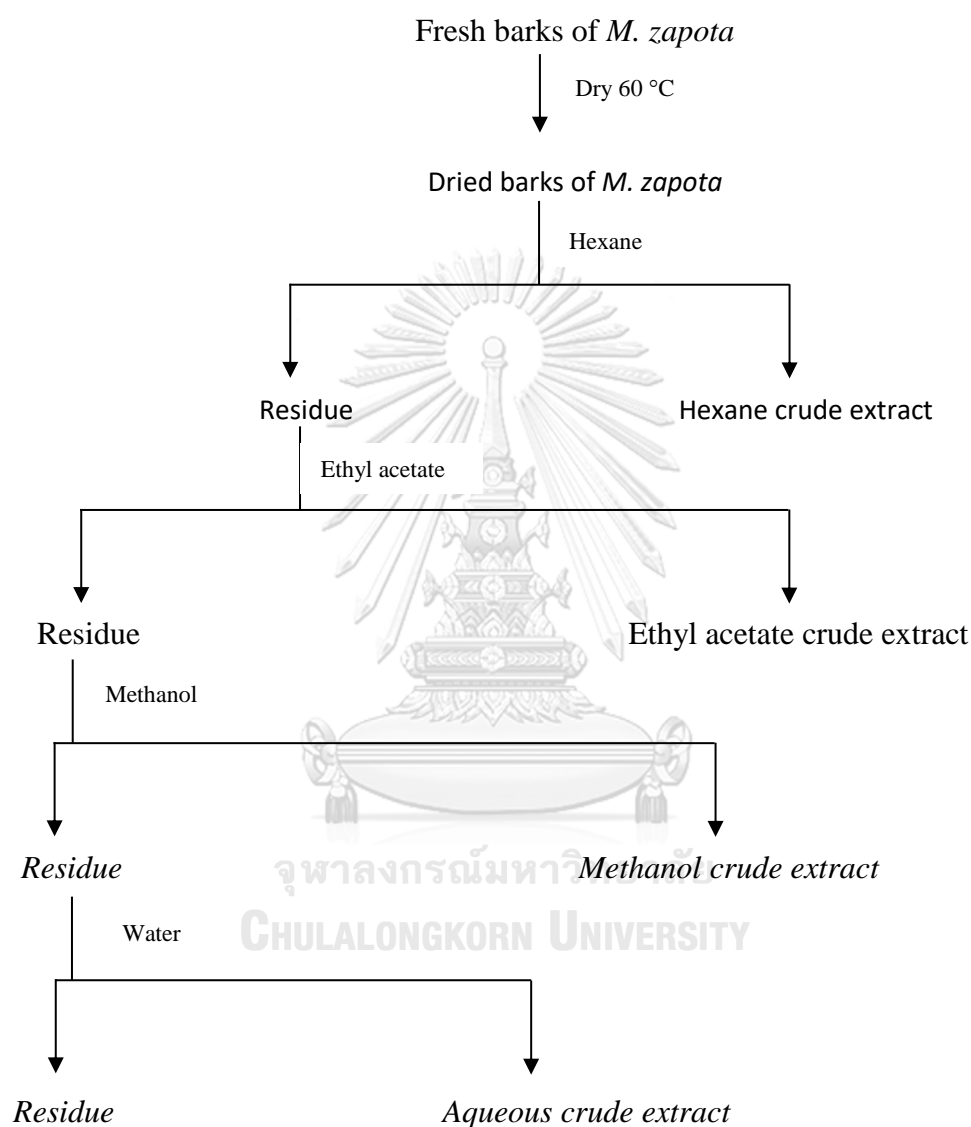


Figure 16 Extraction procedure of *M. zapota* barks

3.3.2 Total phenolic content

Total phenolic content was determined using the Folin-Ciocalteu assay according to the modified method of Dorman *et al* [22]. The 100 μ L of sample (1 mg/mL) was added to 6 mL of water. After that, 500 μ L of undiluted Folin–Ciocalteu reagent was added to the solution and incubated for 1 min at 30 °C. Then, 1.5 mL of 20% (w/v) Na_2CO_3 was added and the reaction mixture was made up to 10 mL of

volumetric flask with water. The absorbance was measured at 760 nm after 2 h incubation using the spectrophotometer. The total phenolic content was expressed as mg gallic acid equivalents (mg GAE)/g dry sample. The concentrations of standard curve were 50, 100, 200, 400 and 800 μ M, respectively.

3.3.3 Total flavonoid content

Total flavonoid content was determined by a modified method of Tohidi *et al* [23]. The 125 μ L of sample (1 mg/mL) was added to 75 μ L of 5% (w/v) NaNO₂. The mixture solution was incubated for 6 min at 30 °C and 150 μ L of 10% (w/v) AlCl₃ was then added. After 5 min of incubation, 750 μ L of 1 M NaOH was added and the final volume of the reaction mixture was made up to 2500 μ L with water. After incubation for 15 min at 30 °C, the absorbance was measured at 510 nm using the spectrophotometer. The total flavonoid content was expressed as mg quercetin equivalents (mg QE)/g dry sample using quercetin calibration curve. Standard curve was prepared at concentration of 50, 100, 200, 400 and 800 μ M, respectively.

3.3.4 Isolation of crude extracts of *M. zapota* barks

3.3.4.1 Bio-assay guided isolation of *n*-hexane crude extract

n-Hexane crude extract (135 g) was chromatographed on a silica gel quick column chromatography and eluted with *n*-hexane, a mixture of *n*-hexane:ethyl acetate (1:1 v/v), ethyl acetate and a mixture of ethyl acetate:methanol (19:1 v/v) to yield four fractions [108]. Fractions A-D were tested for tyrosinase inhibitory activity using *L*-DOPA as a substrate.

The fraction A (60 g) was applied for a silica gel column chromatography and eluted with *n*-hexane:dichloromethane (100:0, 19:1, 1:1 and 0:100 v/v) to obtain four subfractions (A1-A4). These subfractions were investigated for tyrosinase inhibitory activity. Fraction A1 (900.0 mg) was subjected to silica gel column chromatography using *n*-heptane, a mixture gradient of *n*-heptane:*n*-hexane (9:1 and 2:3 v/v) and *n*-hexane to afford four subfractions (A11-A14). Each subfractions was evaluated for tyrosinase inhibitory activity using *L*-DOPA as a substrate. Subfraction A14 was recrystallized in a mixture of dichloromethane and methanol (9:1 v/v) to give colorless crystal (60.8 mg). Moreover, fraction A2 was afforded as colorless crystal (26.2 mg).

Isolated crystal from subfractions A14 and A2 exhibited the same R_f value on TLC. Thus, subfractions A14 and A2 were obtained as compound **I** (87.0 mg).

The fraction C (1.3 g) was chromatographed by column chromatography on silica gel with eluents as *n*-heptane:*n*-hexane:dichloromethane (1:4:0, 0:100:0 and 0:9:1 v/v) to yield three subfractions (C1-C3). Each subfraction was investigated for tyrosinase inhibitory activity. Subfraction C3 (140.0 mg) was subjected to silica gel column chromatography and eluted with petroleum ether:dichloromethane (2:3 and 1:4 v/v) and dichloromethane:ethyl acetate (100:0 and 9:1 v/v) to give four subfractions (C31-C34). Subfractions C31-C34 were tested for antityrosinase activity.

3.3.4.2 Bio-assay guided isolation of ethyl acetate crude extract

Ethyl acetate crude extract (130 g) was chromatographed by a silica gel quick column chromatography and eluted with a mixture gradient of *n*-hexane:ethyl acetate (100:0, 1:1 and 0:100 v/v) and a mixture gradient of ethyl acetate:methanol (19:1 v/v) to yield four fractions (E-H). Fractions E-H were evaluated for tyrosinase inhibitory activity using *L*-DOPA as a substrate.

Fraction E (1.0 g) was chromatographed over silica gel column chromatography and eluted with *n*-hexane in dichloromethane (100:0, 9:1, 7:3, 3:2, 1:1, 4:5, 3:7 and 1:9 v/v) to give nine subfractions (E1-E9). Subfractions E2, E5, E6 and E8 were evaluated against tyrosinase activity. Subfraction E2 (25.0 mg) was separated on silica gel column chromatography and eluted with a mixture gradient of *n*-hexane:dichloromethane (9:1, 4:1, 7:3, 3:2, 3:7, 1:4, 1:9 and 0:100 v/v) to obtain eight subfractions (E21-E28). Only subfraction E22 was determined for tyrosinase inhibitory activity. Subfraction E5 (75.0 mg) was rechromatographed using preparative TLC with petroleum ether:dichloromethane (3:2 v/v) as eluent to give three subfractions (E51-E53).

Fraction F (19.0 g) was subjected to column chromatography over silica gel and eluted with a mixture gradient of *n*-hexane:ethyl acetate (4:1, 7:3, 3:2, 3:7, 1:4 and 0:100 v/v) to yield six subfractions (F1-F6). All subfractions F1-F6 were evaluated for tyrosinase inhibitory activity. Subfraction F1 (1.0 g) was fractionated by silica gel column chromatography and eluted with *n*-hexane:dichloromethane (9:1, 4:1, 7:3, 3:2, 3:7 and 1:9 v/v) to give six subfractions (F11-F16). From tyrosinase inhibitory activity,

subfraction F11 (120.0 mg) was chromatographed by silica gel column chromatography and eluted with a mixture gradient of *n*-hexane:dichloromethane (100:0, 9:1, 4:1, 3:2, 1:1 and 0:100 v/v) to afford six subfractions (F111-F116). Subfraction F113 (60.0 mg) was purified by silica gel column chromatography which eluted with dichloromethane:ethyl acetate (4:1, 7:3, 3:2, 1:1 and 1:4 v/v) to yield five subfractions (F1131-F1135). Subfractions F1131 and F1132 were tested for antityrosinase activity. Subfraction F1131 (25.0 mg) was chromatographed by silica gel column chromatography and eluted with petroleum ether:*n*-hexane (3:2 and 1:9 v/v), *n*-hexane:dichloromethane (100:0, 4:1, 7:3, 3:2, 1:9 and 0:100 v/v) to provide eight subfractions (F11311-F11318). Subfraction F2 (100 mg) was chromatographed by silica gel column chromatography and eluted with a mixture gradient of *n*-hexane:dichloromethane (9:1, 7:3 and 1:9 v/v) to obtain three subfractions (F21-F23). Subfraction F21 displayed as same R_f value on TLC as compound **I**. Subfraction F3 (9.6 g) was applied to silica gel column chromatography and eluted with a mixture solvent of *n*-hexane:ethyl acetate (4:1, 7:3, 3:7 and 0:100 v/v) to obtain four subfractions (F31-F34). TLC analysis of subfractions F31 and compound **I** showed the same R_f value. Thus subfractions F31 was compound **I**. Subfraction F4 (1.0 g) was subjected to silica gel column chromatography using a mixture gradient of *n*-hexane:ethyl acetate (100:0, 9:1, 7:3, 1:1, 1:4 and 0:100 v/v) as eluent to yield six subfractions (F41-F46). Subfraction F43 (100.0 mg) was further subjected to silica gel column chromatography eluting with *n*-hexane:ethyl acetate (4:1, 7:3, 1:1, 1:4 and 0:100 v/v) to yield five subfractions (F431-F435). Subfraction F433 (65.0 mg) was separated by silica gel column chromatography and eluted with gradient solvent of *n*-hexane:ethyl acetate (100:0, 4:1, 7:3, 1:1, 1:4 and 0:100 v/v) to obtain six subfractions (F4331-F4336). Subfraction F4332 (72.9 mg) was separated by preparative TLC and eluted with a mixture of *n*-hexane:ethyl acetate (7:3 v/v) to obtain two subfractions (F43321-F43322). Subfraction F4334 (10.0 mg) was fractionated on an analytical C_{18} column using an isocratic system of methanol and aqueous (3:2 v/v, 1 mL/min). The retention time of subfraction F4334 is 3.5 min to yield compound **II** (8.0 mg). Subfraction F4335 (5.0 mg) was submitted to Sephadex LH-20 column chromatography and used methanol as an eluent to afford three subfractions (F43351-F43353). Subfraction F43353 (2.4 mg) was purified by an analytical HPLC using an isocratic system of methanol and water (7:3 v/v, 0.5 mL/min)

to yield compound **III** (2.4 mg). Retention time of compound **III** was recorded at 5.9 min. Subfraction F5 (3.8 g) was separated by silica gel column chromatography and eluted with a mixture gradient of *n*-hexane:ethyl acetate (9:1, 4:1, 7:3, 3:2, 3:7, 1:4, 1:9 and 0:100 v/v) to afford nine subfractions (F51-F59). Subfraction F53 (70.0 mg) was separated by preparative TLC and eluted with a mixture gradient of *n*-hexane and ethyl acetate (9:1 v/v) to afford two subfractions (F531-F532). Subfraction F54 (17.9 mg) was separated by silica gel column chromatography and eluted with a mixture gradient of *n*-hexane:ethyl acetate (9:1, 7:3, 3:2, 1:4, 1:9 and 0:100 v/v) to afford six subfractions (F541-F546). Subfraction F59 (150.0 mg) was separated by silica gel column chromatography using a mixture gradient of *n*-hexane:acetone (9:1, 4:1, 7:3, 3:2, 1:1, 2:3, 3:7, 1:4 and 0:100 v/v) to afford ten subfractions (F591- F5910). Subfraction F596 was obtained as brown powder (60.0 mg, compound **IV**). Subfraction F6 (1.0 g) was separated by silica gel column chromatography and eluted with a mixture gradient of *n*-hexane:ethyl acetate (100:0, 4:1 and 7:3 v/v) to give three subfractions (F61-F63). Subfraction F62 (20.0 mg) was separated by silica gel column chromatography and eluted with a mixture of *n*-hexane:dichloromethane (4:1, 7:3, 1:4, 1:9 and 0:100 v/v) to give six subfractions (F621-F626).

Subfraction G (4.0 g) was separated by silica gel column chromatography and eluted with a mixture gradient of *n*-hexane:dichloromethane:ethyl acetate (100:0:0, 1:4:0 and 0:7:3 v/v) to give five subfractions (G1-G5). Subfraction G3 (150 mg) was separated by silica gel column chromatography and eluted with a mixture gradient of *n*-hexane:ethyl acetate (100:0, 4:1 and 2:3 v/v) and ethyl acetate:methanol (9.5:0.5 v/v) to give four subfractions (G31-G34). Subfraction G33 (45.0 mg) was separated using silica gel column chromatography and eluted with *n*-heptane:dichloromethane (9:1, 7:3 and 1:9 v/v) to give three subfractions (G331-G333). Subfraction G332 (24.0 mg) was further purified by preparative TLC and eluted with a mixture of petroleum ether and dichloromethane (7:3 v/v) to obtain two subfractions (G3321-G3322). Subfraction G3322 was obtained as white crystal (10.5 mg, compound **V**). Subfraction G333 was obtained as white crystal (15.4 mg, compound **VI**). Subfraction G5 (180.0 mg) was separated by silica gel column chromatography and eluted with a mixture gradient of *n*-hexane:ethyl acetate (3:7 and 2:8 v/v) to obtain two subfractions (G51-G52). Subfraction G51 (80.0 mg) was further separated by silica gel column chromatography

and eluted with a mixture of dichloromethane:ethyl acetate (3:7 and 1:9 v/v) to obtain two subfractions (G511-G512). Subfraction G511 was obtained as white powder (20.0 mg, compound **VII**).

3.3.5 Tyrosinase inhibitory activity

Antityrosinase activity was determined using a modified protocol of Dej-adisai *et al.* [26]. *L*-Tyrosine and *L*-DOPA were used as substrates for monophenolase and diphenolase inhibitory activities, respectively. Briefly, test sample (1 mg/mL) was dissolved in 20% dimethyl sulfoxide (DMSO) in ethanol. The reaction mixture of control without test sample (A) consisted of 50 μ L of tyrosinase solution (200 U/mL), 150 μ L of 0.2 M sodium phosphate buffer (pH 6.8) and 50 μ L of 20% DMSO in ethanol. The reaction mixture of blank of control (B) consisted of 200 μ L of 0.2 M sodium phosphate buffer and 50 μ L of 20% DMSO in ethanol. The reaction mixture of test sample and positive control (C) consisted of 50 μ L of tyrosinase solution, 150 μ L of 0.2 M sodium phosphate buffer (pH 6.8) and 50 μ L of test sample. The reaction mixture of blank of test sample and positive control (D) consisted of 200 μ L of 0.2 M sodium phosphate buffer (pH 6.8) and 50 μ L of test sample. The reaction was mixed and incubated for 10 min at 30 $^{\circ}$ C. After that, 50 μ L of substrate solution (500 μ M for *L*-tyrosine or *L*-DOPA) was added and absorbance was immediately measured ($t = 0$ min) at 490 nm. The assay mixture was then incubated for 20 min at 30 $^{\circ}$ C and the absorbance was measured at 490 nm ($t = 20$ min). The percentage of inhibition was calculated using the following equation:

$$\% \text{ inhibition} = \left[\frac{(A-B)-(C-D)}{(A-B)} \right] \times 100$$

Where A is the difference of the absorbance of control without test sample at $t = 0$ min and $t = 20$ min, B is the difference of the absorbance of blank of control at $t = 0$ min and $t = 20$ min, C is the difference of the absorbance of test sample and positive control at $t = 0$ min and $t = 20$ min and D is the difference of the absorbance of blank of test sample and positive control at $t = 0$ min and $t = 20$ min.

3.3.6 Antioxidant activities

3.3.6.1 2,2-Diphenyl-1-picrylhydrazyl (DPPH) radical scavenging activity

The scavenging activity on DPPH radical of test sample was determined as previously reported [109]. Briefly, the reaction mixture consisted of 50 μL of test sample (100 mg/mL) and 150 μL of 0.05 M DPPH solution in methanol. Then, the reaction mixture was mixed and incubated for 30 min in the dark at 30 $^{\circ}\text{C}$. The absorbance was measured at 517 nm using spectrophotometer. Trolox was used as a positive control. DPPH scavenging effect was calculated using the following equation:

$$\text{DPPH radical scavenging activity (\%)} = \left[1 - \frac{A_s - A_b}{A_d} \right] \times 100$$

Where A_s is the absorbance of the isolated compound mixed with DPPH solution, A_b is the absorbance of the sample without DPPH solution and A_d is the absorbance of DPPH solution without sample.

3.3.6.2 ABTS radical scavenging activity

The ABTS scavenging capacity was determined in accordance with a reported method [110]. The stock solution consisted of 100 mL of 7.0 mM ABTS solution and 100 mL of 2.4 mM potassium persulfate solution. Then, the stock solution was left in the dark for 14 h at 30 $^{\circ}\text{C}$. The solution was diluted by 1 mL of ABTS solution with 60 mL of absolute ethanol to determine an absorbance of 0.700 ± 0.001 absorbance units at 734 nm using the spectrophotometer. Five hundred μL of test sample (100 mg/mL) were reacted with 500 μL of the ABTS solution and measured at 734 nm after incubation for 7 min using the spectrophotometer. The results were compared with a trolox standard and percentage scavenging was calculated with equation below:

$$\text{ABTS radical scavenging activity (\%)} = \left[\left(\frac{A_c - A_s}{A_c} \right) \times 100 \right]$$

Where A_c is the absorbance of ABTS radical with absolute ethanol and A_s is the absorbance of ABTS radical with test sample or positive control.

3.3.6.3 The ferric reducing antioxidant power (FRAP) assay

Reducing power was evaluated using a modification of the FRAP assay as followed protocol [110]. The FRAP reagent consisted of 25 mL of 0.3 M acetate buffer

(pH 3.6), 2.5 mL of 20 mM ferric chloride solution, 2.5 mL of 10 mM 4,6-tripyridyls-triazine and made up to a last volume of 50 mL using 40 mM HCl solution. Then, the FRAP reagent put on water bath for about half an hour at 50 °C. Then, 600 µL of FRAP reagent was added to 25 µL of test sample (100 mg/mL). The absorbance was measured at 595 nm after incubation for 4 min at room temperature using the spectrophotometer. Trolox was used as a positive control. The ferric reducing capacity was expressed as ferrous sulphate equivalent.

3.3.7 *In vitro* cytotoxicity assay

Cytotoxic activity of isolated compounds was tested using the MTT assay which following described [111]. In this study, five human cancer cell lines were evaluated including breast carcinoma (BT474, ATCC[®] HTB20TM), lung bronchus carcinoma (ChaGo-K-1, National Cancer Institute, Thailand), liver carcinoma (HepG₂, ATCC[®] HB8065TM), gastric carcinoma (KATO-III, ATCC[®]HTB103TM) and colon carcinoma (SW620, ATCC[®] CCL227TM). Human diploid lung fibroblasts (Wi-38, ATCC[®]CCL75TM) were used as the comparison. Culturing of these cell lines were derived in complete medium including RPMI-1640 medium, 5% v/v of fetal bovine serum, 25 mM HEPES, 0.25% w/v of sodium bicarbonate and kanamycin (100 µg/mL). Doxorubicin and DMSO were used as reference control. The culture medium of cell lines (198 µL) were added into each well of 96 plate and incubated with 5% (v/v) CO₂ for 24 h at 37 °C. Then the culture cells were treated with 2 µL/well of the test sample and further incubated for 72 h at 37 °C. Two µL of MTT solution (5 mg/mL) in normal saline were added in each well of plate and incubated for 4 h. The medium solution was discarded and the mixture of 25 µL of 0.1 M glycine and 150 µL of DMSO were added. The plates were mixed for dissolving the purple-blue crystal before its absorbance was determined using the spectrophotometer at 540 nm. Relative of the cell survival and a percentage of the DMSO as only control which set 100% were calculated using the formula:

$$\text{The percentage of cell survival} = \left[\frac{A_s}{A_c} \times 100 \right]$$

Where A_s is the absorbance of test sample and A_c is the absorbance of control.

3.3.8 Statistics

All expressed data are the mean \pm standard deviation (SD) of experiment. All statistical of the three experiments carried out in triplicate and used GraphPad Prism 6 and SPSS 24. Difference were evaluated statistically significant at $p < 0.05$.



CHAPTER IV

RESULTS AND DISCUSSIONS

M. zapota contained many phytochemical constituents such as phenolic compound, triterpenoid, saponin and steroid. The reviews were reported on biological of crude extracts and phytochemical of *M. zapota* such as antibacterial, anticancer, antidiabetic, antioxidant and antityrosinase activities. However, little research on tyrosinase inhibitory activity of *M. zapota* had been previously reported. In the present study, the quantity of total phenolic content was evaluated for a correlation with total flavonoid content, antioxidant activities with DPPH, ABTS radical scavenging, FRAP assays and antityrosinase activities of crude extracts of six different parts. Consequently, tyrosinase inhibitors and mechanism of tyrosinase inhibition of isolated compounds from *M. zapota* barks.

4.1 Extraction of different parts of *M. zapota*

The barks, flowers, fruits, leaves, roots and seeds of *M. zapota* were macerated with methanol and water. The yield of methanol crude extracts of six different parts of *M. zapota* was ranged between 6.71-39.67% and the yield of aqueous crude extracts was ranged between 5.38-34.00% (Table 5).

Table 5 Extraction yield of crude extracts of different parts of *M. zapota*

Plant part	Solvent extract	Appearance	Extraction yield (% w/w dry weight)
Barks	Aqueous	Brown gum	12.52
	Methanol	Brown gum	14.45
Flowers	Aqueous	Yellow gum	9.40
	Methanol	Yellow gum	6.71
Fruits	Aqueous	Brown gum	34.00
	Methanol	Brown gum	39.67
Leaves	Aqueous	Brown gum	20.67
	Methanol	Brown gum	20.11
Roots	Aqueous	Brown gum	11.55
	Methanol	Brown gum	11.01
Seeds	Aqueous	Brown gum	5.38
	Methanol	Brown gum	7.25

4.2 Determination of total phenolic and total flavonoid contents of different parts of *M. zapota*

The results of total phenolic content of methanol and aqueous crude extracts of six different parts of *M. zapota* are shown in Table 6. Total phenolic content was estimated using a standard calibration curve of gallic acid (Figure 31) and expressed as mg gallic acid equivalents (mg GAE)/g dry sample. Methanol crude extract of flowers showed the highest amount of total phenolic content of 368.73 ± 0.65 mg GAE/g, followed by methanol crude extract of barks with total phenolic value of 343.44 ± 0.50 mg GAE/g and methanol crude extract of seeds with total phenolic value of 341.68 ± 0.60 mg GAE/g. Whereas, aqueous crude extract of flowers showed the lowest amount of total phenolic content of 114.03 ± 0.94 mg GAE/g.

4.2.2 Total flavonoid content

The results of total flavonoid content of methanol and aqueous crude extracts of six different parts of *M. zapota* are shown in Table 6. Total flavonoid content was determined using calibration curve of quercetin (Figure 32) and expressed as mg quercetin equivalents (mg QE)/g dry sample. Methanol crude extract of seeds displayed the highest amount of total flavonoid content of 90.21 ± 0.57 mg QE/g which followed by methanol crude extract of roots with total flavonoid value of 89.03 ± 1.00 mg QE/g and aqueous crude extract of seeds with total flavonoid value of 82.56 ± 1.34 mg QE/g. While, aqueous crude extract of roots showed the lowest amount of total flavonoid content of 24.32 ± 0.82 mg QE/g.

Table 6 Total phenolic and total flavonoid contents of crude extracts of different parts of *M. zapota*

Plant part	Solvent extract	Total phenolic content (mg GAE/g)	Total flavonoid content (mg QE/g)
Barks	Aqueous	286.97 ± 0.28	38.15 ± 0.54
	Methanol	343.44 ± 0.50	49.62 ± 1.68
Flowers	Aqueous	114.03 ± 0.94	43.15 ± 0.54
	Methanol	368.73 ± 0.65	54.32 ± 0.48
Fruits	Aqueous	246.97 ± 0.11	59.32 ± 1.01
	Methanol	141.97 ± 0.36	67.56 ± 1.08
Leaves	Aqueous	209.91 ± 0.60	32.26 ± 0.97
	Methanol	271.67 ± 0.72	71.68 ± 0.53
Roots	Aqueous	305.21 ± 0.76	24.32 ± 0.82
	Methanol	145.50 ± 0.65	89.03 ± 1.00
Seeds	Aqueous	299.62 ± 0.53	82.56 ± 1.34
	Methanol	341.68 ± 0.60	90.21 ± 0.57

These results showed that total phenolic and total flavonoid contents were differences in crude extracts of six different parts of *M. zapota*. Total phenolic and total flavonoid contents are the two role factors for representation the antioxidant activity. Previous research of this plant has reported that the ethanol crude extract of fruit pulps showed total phenolic value of 38.56 ± 1.98 mg GAE/g [106]. While, acetone, aqueous, ethyl acetate and toluene crude extracts of leaves showed total phenolic contents of 241.06 ± 0.81 , 106.19 ± 1.99 , 137.63 ± 1.12 and 4.45 ± 0.09 mg GAE/g, respectively [18]. Amount of total flavonoid content of acetone, aqueous, ethyl acetate and toluene crude extracts of leaves was 166.84 ± 0.31 , 37.04 ± 0.37 , 127.63 ± 0.20 and 59.84 ± 0.59 mg QE/g, respectively [18]. Total phenolic content of acetone, ethyl acetate and aqueous crude extracts of *M. zapota* seeds was 2.26 ± 0.01 , 2.54 ± 0.02 and 1.21 ± 0.01 mg GAE/g, respectively [101]. Moreover, total flavonoid content of acetone, ethyl acetate and aqueous crude extracts of *M. zapota* seeds was 2.19 ± 0.01 , 1.01 ± 0.02 and 0.74 ± 0.01 mg QE/g, respectively [101]. In this study, crude extracts of six different parts of *M. zapota* showed high total phenolic and total flavonoid contents than the previous reported. The results conducted that the different parts of plant and polarity solvents can affect the total phenolic and total flavonoid contents of crude extract of *M. zapota*.

4.3 Determination of antioxidant and antityrosinase activities of different parts of *M. zapota*

4.3.1 Antioxidant activities

4.3.1.1 DPPH radical scavenging activity

The results of DPPH radical scavenging activity of methanol and aqueous crude extracts of six different parts of *M. zapota* are shown in Table 7. Methanol crude extracts of six different parts of *M. zapota* showed higher DPPH radical scavenging activity than aqueous crude extracts of six different parts of *M. zapota*. Methanol crude extracts of seeds, flowers and barks showed strong DPPH radical scavenging capacity with IC₅₀ values of 282.05 ± 0.60 , 297.18 ± 0.49 and 299.53 ± 0.31 µg/mL, respectively. Whereas, aqueous crude extract of seeds exhibited the weakest DPPH radical scavenging capacity with IC₅₀ value of 670.31 ± 0.24 µg/mL. Trolox was used as a positive control and exhibited stronger DPPH radical scavenging activity than all crude extracts of six different parts of *M. zapota* with IC₅₀ value of 124.84 ± 0.78 µg/mL.

4.3.1.2 ABTS radical scavenging activity

The results of ABTS radical scavenging activity of crude extracts of six different parts of *M. zapota* are shown in Table 7. Methanol crude extracts of *M. zapota* displayed stronger ABTS radical scavenging activity than aqueous crude extracts of *M. zapota*. Methanol crude extracts of seeds, roots and flowers exhibited potent scavenger of ABTS radical with IC₅₀ values of 205.11 ± 0.89 , 262.80 ± 0.51 and 308.51 ± 0.57 µg/mL, respectively. While, aqueous crude extract of barks showed the lowest scavenger of ABTS radical with IC₅₀ value of 942.47 ± 0.26 µg/mL. Trolox exhibited a significant strong ABTS radical scavenging capacity with IC₅₀ value of 164.09 ± 0.21 µg/mL.

4.3.1.3 FRAP activity

The results of reducing capacity of crude extracts of six different parts of *M. zapota* are shown in Table 7. FRAP values were calculated using calibration curve of ferrous sulphate (Figure 33). Methanol crude extract of seeds displayed the highest reducing capacity with FRAP value of 296.46 ± 0.08 mg TEAC/g, followed by methanol crude extracts of flowers and roots with FRAP values of 292.27 ± 0.09 and

278.46 ± 0.02 mg TEAC/g, respectively. Trolox exhibited strong reducing capacity with FRAP value of 349.18 ± 0.06 mg TEAC/g. While, aqueous and methanol crude extracts of fruits showed the lowest reducing capacity with FRAP values of 155.18 ± 0.08 and 150.27 ± 0.06 mg TEAC/g, respectively.

Table 7 Antioxidant activities of crude extracts of different parts of *M. zapota*

Plant part	Solvent extract	IC ₅₀ (µg/mL)		FRAP (mg TEAC/g)
		DPPH	ABTS	
Barks	Aqueous	453.23 ± 0.72	942.47 ± 0.26	222.27 ± 0.06
	Methanol	299.53 ± 0.31	649.13 ± 0.40	252.27 ± 0.02
Flowers	Aqueous	369.05 ± 0.10	447.91 ± 0.67	168.64 ± 0.06
	Methanol	297.18 ± 0.49	308.51 ± 0.57	292.27 ± 0.09
Fruits	Aqueous	424.10 ± 0.21	564.25 ± 0.25	155.18 ± 0.08
	Methanol	444.59 ± 0.56	514.35 ± 0.24	150.27 ± 0.06
Leaves	Aqueous	431.11 ± 0.65	497.75 ± 0.14	251.73 ± 0.02
	Methanol	341.89 ± 0.94	378.85 ± 0.26	258.27 ± 0.08
Roots	Aqueous	586.22 ± 0.84	651.08 ± 0.35	225.00 ± 0.01
	Methanol	428.64 ± 0.49	262.80 ± 0.51	278.46 ± 0.02
Seeds	Aqueous	670.31 ± 0.24	725.45 ± 0.42	217.73 ± 0.02
	Methanol	282.05 ± 0.60	205.11 ± 0.89	296.46 ± 0.08
Trolox ^a		124.84 ± 0.78	164.09 ± 0.21	349.18 ± 0.06

^a Trolox was used as a positive control.

The results of this study showed that methanol crude extract of seeds displayed the highest antioxidant activities on DPPH, ABTS and FRAP assays. In the literature, acetone crude extract of *M. zapota* leaves showed more scavenger DPPH radical than ascorbic acid with IC₅₀ values of 7.6 and 11.4 µg/mL, respectively [18]. On the other hand, this study indicated that aqueous and methanol crude extracts of leaves showed lower scavenger DPPH radical than the previous research of Kaneria *et al* [18]. While, ethanol crude extract of *M. zapota* fruit pulps exhibited lower antioxidant activities on DPPH and ABTS radicals than ascorbic acid with IC₅₀ values of 37.63 ± 1.18 and 73.14 ± 2.84 µg/mL, respectively [106]. In this study, aqueous and methanol crude extracts of fruits showed less antioxidant activity on DPPH and ABTS radicals than that of reported by Pientaweeratch *et al* [106].

4.3.2 Antityrosinase activities

4.3.2.1 Monophenolase inhibitory activity

The results of monophenolase inhibitory activity of crude extracts of six different parts of *M. zapota* are shown in Table 8. The methanol crude extracts of barks, roots, leaves and aqueous crude extract of roots showed high monophenolase inhibitory activity with IC₅₀ values of 0.81 ± 0.06 , 0.81 ± 0.92 , 0.94 ± 0.38 and 0.97 ± 0.88 mg/mL, respectively. While, methanol crude extract of fruits showed weak monophenolase inhibitory activity with IC₅₀ value of 4.84 ± 0.49 mg/mL. However, kojic acid showed the strongest tyrosinase activity on monophenolase inhibitory activity with IC₅₀ value of 0.09 ± 0.11 mg/mL.

4.3.2.2 Diphenolase inhibitory activity

The results of diphenolase inhibitory activity of crude extracts of six different parts of *M. zapota* are shown in Table 8. Methanol crude extracts of roots, flowers, leaves, barks and fruits displayed stronger diphenolase inhibitory activity than other crude extracts with IC₅₀ values of 0.55 ± 0.50 , 0.60 ± 0.97 , 0.62 ± 0.87 , 0.71 ± 0.39 and 0.73 ± 0.51 mg/mL, respectively. Whereas, aqueous crude extract of barks exhibited diphenolase inhibitory activity less than other crude extracts with IC₅₀ value of 4.30 ± 0.66 mg/mL. The IC₅₀ value of kojic acid was 0.10 ± 0.03 mg/mL.

Table 8 Antityrosinase activities of crude extracts of different parts of *M. zapota*

Plant part	Solvent extract	IC ₅₀ (mg/mL)	
		Monophenolase inhibitory activity	Diphenolase inhibitory activity
Barks	Aqueous	1.71 ± 0.82	4.30 ± 0.66
	Methanol	0.81 ± 0.06	0.71 ± 0.39
Flowers	Aqueous	1.66 ± 0.88	2.04 ± 0.16
	Methanol	1.66 ± 0.38	0.60 ± 0.97
Fruits	Aqueous	2.60 ± 0.55	3.12 ± 0.69
	Methanol	4.84 ± 0.49	0.73 ± 0.51
Leaves	Aqueous	1.28 ± 0.43	3.04 ± 0.50
	Methanol	0.94 ± 0.38	0.62 ± 0.87
Roots	Aqueous	0.97 ± 0.88	1.01 ± 0.39
	Methanol	0.81 ± 0.92	0.55 ± 0.50
Seeds	Aqueous	2.06 ± 0.69	1.02 ± 0.14
	Methanol	1.66 ± 0.66	1.35 ± 0.17
Kojic acid ^a		0.09 ± 0.11	0.10 ± 0.03

^a Kojic acid was used as a positive control.

A previous report indicated that methanol crude extract of *M. zapota* leaves showed antityrosinase activity on monophenolase inhibitory activity with percentage

inhibition value of 39% at a concentration of 40 $\mu\text{g/mL}$ [96]. This study indicated that methanol crude extracts of barks, leaves and roots showed potent antityrosinase activity on monophenolase and diphenolase inhibitory activities. However, methanol crude extracts of flowers and fruits exhibited higher diphenolase inhibitory activity than monophenolase inhibitory activity.

4.4 Correlations

Quantity of total phenolic and total flavonoid contents were evaluated for correlations with antioxidant activities by DPPH, ABTS radical scavenging and FRAP assays and with antityrosinase activities on monophenolase and diphenolase inhibitory activities of crude extracts of six different parts of *M. zapota*.

4.4.1 Correlations between total phenolic content and antioxidant activities

The correlations between total phenolic content in crude extracts of *M. zapota* with their DPPH and ABTS radical scavenging activities and reducing capacity with FRAP were investigated (Table 9). Total phenolic content and ABTS radical scavenging activity of six different parts of *M. zapota* showed the highest positive correlation ($r = 0.90$). In addition, relationship of total phenolic content with DPPH radical scavenging activity and with FRAP assay also showed positive correlation with r values of 0.79 and 0.69, respectively (Figures 34-36). It was similar to the previous report that indicated the high correlation between total phenolic content and ABTS radical scavenging activity of *M. zapota* fruits with r value of 0.99 [112]. These results suggested that crude extracts of *M. zapota* which contained high total phenolic content lead to express high antioxidant activity. The indicator of correlation between total phenolic content and antioxidant activity could be used an electron transfer in mechanism [101].

Table 9 Correlation values of total phenolic content and antioxidant activities of crude extracts of different parts of *M. zapota*

	Antioxidant activities		
	DPPH radical scavenging activity	ABTS radical scavenging activity	FRAP activity
Total phenolic content	0.79	0.90	0.69

4.4.2 Correlations between total phenolic content and antityrosinase activities

The correlations between total phenolic content and antityrosinase activities of crude extracts of *M. zapota* were investigated (Table 10). Correlation between total phenolic content and monophenolase inhibitory activity was negative related ($r = -0.01$). Moreover, there was very low correlation between total phenolic content and diphenolase inhibitory activity with r value of 0.10 (Figures 37-38). These results suggested that classes of phenolic compound of crude extracts of *M. zapota* could not inhibit tyrosinase activities.

Table 10 Correlation values of total phenolic content and antityrosinase activities of crude extracts of different parts of *M. zapota*

	Antityrosinase activities	
	Monophenolase inhibitory activities	Diphenolase inhibitory activity
Total phenolic content	-0.01	0.10

4.4.3 Correlations between total phenolic content and total flavonoid content

The correlations between total phenolic and total flavonoid contents of crude extracts of *M. zapota* were investigated. Total phenolic content showed low positive correlation with total flavonoid contents ($r = 0.28$) (Figure 39). Phenolic compounds are a large group of chemical compounds that contain antioxidant, anti-inflammatory, anti-carcinogenic and other biological properties. Phenolic compounds are divided into several groups, one of which is represented by flavonoids. Flavonoids are further divided in several subclasses such as anthocyanins, flavonols, flavanones, flavanols, flavones and isoflavonones. These results suggested that amount of flavonoids in each crude extract of *M. zapota* might not depend on total phenolic content of crude extract of *M. zapota*.

4.4.4 Correlations between total flavonoid content and antioxidant activities

The correlations between total flavonoid content and antioxidant activities on DPPH radical scavenging activity, ABTS radical scavenging activity and FRAP activity of crude extracts of *M. zapota* were investigated (Table 11). Correlations between total flavonoid content and antioxidant activities with DPPH, ABTS and FRAP assays were evaluated as r values of 0.35, 0.29 and 0.39, respectively (Figures 40-42).

These results indicated that flavonoids in crude extracts of *M. zapota* might not be acted as reducing agents for antioxidant activities.

Table 11 Correlation values of total flavonoid content and antioxidant activities of crude extracts of different parts of *M. zapota*

	Antioxidant activities		
	DPPH radical scavenging activity	ABTS radical scavenging activity	FRAP activity
Total flavonoid content	0.35	0.29	0.39

4.4.5 Correlations between total flavonoid content and antityrosinase activities

The correlations between total flavonoid content and antityrosinase activities of crude extracts of *M. zapota* were investigated (Table 12). No correlation between total flavonoid content and monophenolase inhibitory activity was observed ($r = -0.07$). Relationship of total flavonoid content and monophenolase inhibitory activity was not correlated ($r = 0.14$) (Figures 43-44). These results indicated that flavonoids in crude extracts of *M. zapota* should not be connected to inhibit tyrosinase activity.

Table 12 Correlation values of total flavonoid content and antityrosinase activities of crude extracts of different parts of *M. zapota*

	Antityrosinase activities	
	Monophenolase inhibitory activities	Diphenolase inhibitory activity
Total flavonoid content	-0.07	0.14

4.4.6 Correlations between antityrosinase and antioxidant activities

The correlations between antityrosinase and antioxidant activities of crude extracts of *M. zapota* were investigated (Table 13). It was no correlation between antityrosinase and antioxidant activities. (Figures 45-50). These results were similar to previous report on the correlation between antityrosinase and antioxidant activities of ethanol crude extract of *Dioscorea opposita* root tubers [113]. In contrast, diphenolase inhibitory activity and antioxidant activity of *Macaranga* sp. extract showed positive correlation with R^2 value of 0.787 [114]. This study confirmed that mechanism tyrosinase activity is independent from mechanism of antioxidant activity as previously described [115].

Table 13 Correlation values of antityrosinase and antioxidant activities of crude of extracts of different parts of *M. zapota*

	Antioxidant activities		
	DPPH radical scavenging activity	ABTS radical scavenging activity	FRAP activity
Monophenolase inhibitory activity	-0.10	-0.10	-0.09
Diphenolase inhibitory activity	0.02	0.06	0.02

Among crude extracts of six different parts of *M. zapota*, the highest total phenolic content was found in methanol crude extract of flowers and the maximum of total flavonoid content was found in methanol crude extract of roots. Moreover, methanol crude extract of seeds showed potent antioxidant activities with DPPH and ABTS radical scavenging activities and reducing capacity of FRAP activity. Methanol crude extract of barks and seeds displayed significant monophenolase inhibitory activity and methanol crude extract of roots exhibited the most potent diphenolase inhibitory activity. Total phenolic content of *M. zapota* showed a positive relationship with antioxidant activities but showed weak correlation with antityrosinase activities. Total flavonoid content of *M. zapota* exhibited low correlation with both antioxidant and antityrosinase activities. Furthermore, this study indicated that no correlation between antityrosinase and antioxidant activities. So phenolic compounds of *M. zapota* do not relate to antityrosinase activity. Methanol crude extracts of six different parts of *M. zapota* exhibited potent tyrosinase inhibitory activity. For next step, barks of *M. zapota* were extracted by organic solvents and isolated using chromatography techniques.

4.5 Extraction of *M. zapota* barks

The fresh barks of *M. zapota* (175 kg) were dried in a hot air oven at 60 °C. The dried barks (7 kg) were ground and macerated with various polarity organic solvents such as *n*-hexane, ethyl acetate, methanol and water, respectively. Each extract was filtrated and evaporated under *in vacuo* to afford four crude extracts. *n*-Hexane crude extract was obtained as yellow green gum (139.60 g, 1.99% w/dried weight of barks). Ethyl acetate crude extract was dark green gum (138.13 g, 1.97% w/dried weight of barks). Methanol crude extract was dark brown gum (819.96 g, 11.71% w/dried weight

of barks) and aqueous crude extract was brown gum (96.79 g, 1.38% w/dried weight of barks). All crude extracts were screened for antityrosinase activity by DOPAchrome method (Table 14). *n*-Hexane, ethyl acetate and methanol crude extracts showed high tyrosinase inhibitory effect with percentage inhibition of $85.85 \pm 0.03\%$, $82.80 \pm 0.50\%$ and $77.23 \pm 0.94\%$, respectively at concentration of 1.0 mg/mL. Aqueous crude extract showed the lowest antityrosinase activity with percentage inhibition of $24.86 \pm 0.54\%$ at concentration of 1.0 mg/mL. Kojic acid exhibited tyrosinase inhibitory activity with percentage inhibition of $96.19 \pm 0.13\%$ at concentration of 0.1 mg/mL. These results indicated that *n*-hexane, ethyl acetate and methanol crude extracts might contain tyrosinase inhibitor. So, they were conducted to isolate active compounds by bioassay-guided fractionation on tyrosinase inhibitory activity.

Table 14 Extraction yield and tyrosinase inhibitory activity of crude extracts of *M. zapota* barks

Crude extract	Appearance	Yield (g) (%, w/dried weight of barks)	Percentage of inhibitory activity (%)
<i>n</i> -Hexane	Yellow green gum	139.60 (1.99)	$85.85 \pm 0.03^*$
Ethyl acetate	Dark green gum	138.13 (1.97)	$82.80 \pm 0.50^*$
Methanol	Dark brown gum	819.96 (11.71)	$77.23 \pm 0.94^*$
Aqueous	Brown gum	96.79 (1.38)	$24.86 \pm 0.54^*$
Kojic acid ^a			$96.19 \pm 0.13^{**}$

^a Kojic acid was used as a positive control.

* Concentration of crude extract was 1.0 mg/mL.

** Concentration of kojic acid was 0.1 mg/mL.

4.6 Isolation of crude extracts of *M. zapota* barks

4.6.1 Isolation of *n*-hexane crude extract

n-Hexane crude extract was chromatographed on a silica gel quick column chromatography and eluted with *n*-hexane, a mixture of *n*-hexane:ethyl acetate, ethyl acetate and a mixture of ethyl acetate:methanol to yield four fractions [108]. They were investigated for tyrosinase inhibitory activity using *L*-DOPA as a substrate. The results are shown in Table 15. Fraction A exhibited the strongest antityrosinase activity with percentage inhibition value of $82.63 \pm 0.31\%$. While, fraction B ($42.95 \pm 0.10\%$) showed inhibitory tyrosinase activity less than fraction C ($62.71 \pm 0.43\%$). Thus, fraction A was further purified to obtain tyrosinase inhibitors.

Table 15 Tyrosinase inhibitory activity of fractions A-D of *n*-hexane crude extract

Fraction	Appearance	Yield (g) (%, w/weight of <i>n</i> -hexane crude extract)	Percentage of inhibitory activity (%)
A	Yellow gum	63.05 (46.70)	82.63 ± 0.31
B	Yellow gum	20.97 (15.53)	42.95 ± 0.10
C	Brown gum	1.40 (1.04)	62.71 ± 0.43
D	Brown gum	4.91 (3.64)	NA

NA = No activity.

The fraction A was subjected to silica gel column chromatography and eluted with a mixture gradient of *n*-hexane:dichloromethane to obtain four subfractions (A1-A4). All subfractions were investigated for tyrosinase inhibitory activity using *L*-DOPA as a substrate (Table 16). Subfractions A1 and A2 showed potent tyrosinase inhibition activity with percentage inhibition values of 70.18 ± 0.10% and 87.60 ± 0.14%, respectively. Subfraction A2 was recrystallized in a mixture of dichloromethane:methanol to afford compound **I**.

Table 16 Tyrosinase inhibitory activity of subfractions A1-A4 of fraction A

Subfraction	Appearance	Yield (g) (%), w/weight of fraction A)	Percentage of inhibitory activity (%)
A1	White powder	0.94 (1.49)	70.18 ± 0.10
A2	Colorless crystal	0.03 (0.05)	87.60 ± 0.14
A3	Colorless gum	47.92 (76.18)	NA
A4	White powder	14.01 (22.27)	NA

NA = No activity.

Fraction A1 was subjected to silica gel column chromatography using a gradient system of *n*-heptane and *n*-hexane to obtain four subfractions (A11-A14). All four subfractions were tested for tyrosinase inhibitory activity using *L*-DOPA as a substrate (Table 17). Subfraction A11 showed lower tyrosinase inhibitory activity than subfraction A14. Subfraction 14 was recrystallized to give compound **I**. The ¹H-NMR of subfraction A14 is similar to that of compound **I**.

Table 17 Tyrosinase inhibitory activity of subfractions A11-A14 of subfraction A1

Subfraction	Appearance	Yield [115] (%, w/weight of subfraction A1)	Percentage of inhibitory activity (%)
A11	White powder	17.0 (1.81)	46.11 ± 0.14
A12	Yellow gum	716.0 (76.17)	NA
A13	Yellow gum	105.2 (11.19)	NA
A14	White powder	60.8 (6.47)	71.58 ± 0.18

NA = No activity.

Fraction C showed moderate antityrosinase activity so it was then chromatographed by column chromatography on silica gel and eluted with a gradient system of *n*-heptane:*n*-hexane and *n*-hexane:dichloromethane to yield three subfractions (C1-C3). All three subfractions were investigated for tyrosinase inhibitory activity (Table 18). Both subfractions C1 and C2 exhibited low antityrosinase activity with percentage inhibition values of 15.91 ± 0.84% and 25.72 ± 0.52%, respectively. While subfraction C3 showed moderate tyrosinase inhibitory activity with percentage inhibition value of 52.27 ± 0.39%. The results indicated that subfraction C3 might consist of moderate tyrosinase inhibitors.

Table 18 Tyrosinase inhibitory activity of subfractions C1-C3 of fraction C

Subfraction	Appearance	Yield [115] (%, w/weight of fraction C)	Percentage of inhibitory activity (%)
C1	Yellow gum	617.1 (44.08)	15.91 ± 0.84
C2	Yellow solid	473.8 (33.84)	25.72 ± 0.52
C3	White powder	147.3 (10.52)	52.27 ± 0.39

Subfraction C3 was subjected to silica gel column chromatography to give four subfractions (C31-C34). Each of subfraction was tested for tyrosinase inhibitory activity using *L*-DOPA as a substrate (Table 19). Subfraction C33 showed the highest antityrosinase activity when compared with the other subfractions of subfraction C3 with percentage inhibition value of 48.70 ± 0.33%. Unfortunately, subfraction C3 was not a pure compound.

Table 19 Tyrosinase inhibitory activity of subfractions C31-C34 of subfraction C3

Subfraction	Appearance	Yield [115] (%, w/weight of subfraction C3)	Percentage of inhibitory activity (%)
C31	Yellow gum	39.7 (26.95)	17.53 ± 0.23
C32	White solid	19.7 (13.37)	16.56 ± 0.32
C33	White solid	45.8 (31.09)	48.70 ± 0.33
C34	White solid	30.3 (20.57)	32.31 ± 0.23

4.6.2 Isolation of ethyl acetate crude extract

Ethyl acetate crude extract was chromatographed by a silica gel quick column chromatography to yield four fractions (E-H). Fractions E-H were determined for tyrosinase inhibitory activity (Table 20). Fraction F showed the highest tyrosinase inhibitory activity with percentage inhibition value of $82.10 \pm 0.04\%$. Moreover, fraction G showed higher antityrosinase activity than fraction E with percentage inhibition values of $75.52 \pm 0.04\%$ and $55.73 \pm 0.10\%$, respectively. Fraction H showed no tyrosinase inhibitory activity. The results indicated that fractions E-G might contain tyrosinase inhibitors.

Table 20 Tyrosinase inhibitory activity of fractions E-H of ethyl acetate crude extract

Fraction	Appearance	Yield (g) (% , w/weight of ethyl acetate crude extract)	Percentage of inhibitory activity (%)
E	Brown gum	37.27 (28.67)	55.73 ± 0.10
F	Brown gum	20.08 (15.45)	82.10 ± 0.04
G	Brown gum	4.75 (3.65)	75.52 ± 0.04
H	Brown gum	4.91 (3.78)	NA

NA = No activity.

Fraction E was chromatographed over silica gel column chromatography. Isolation of fraction E was eluted with mixtures gradient of *n*-hexane and dichloromethane to give nine subfractions (E1-E9). Subfractions E2, E5, E6 and E8 were determined for tyrosinase inhibitory activity (Table 21). Subfractions E2, E5 and E6 showed weak antityrosinase activity with percentage inhibition values of $24.93 \pm 0.99\%$, $30.40 \pm 0.40\%$ and $14.05 \pm 0.40\%$, respectively. Subfraction E5 was rechromatographed, although it showed weak antityrosinase activity. Preparative TLC

method was used for isolation of subfraction E5 and eluent was petroleum ether:dichloromethane. Three bands of separation were collected and determined by $^1\text{H-NMR}$. Subfractions E51 (18.3 mg, 23.19% w/w), E52 (28.6 mg, 36.25% w/w) and E53 (5.0 mg, 6.34% w/w) were obtained as white powders. Unfortunately, subfraction E5 was not a pure compound.

Table 21 Tyrosinase inhibitory activity of subfractions E1-E9 of fraction E

Subfraction	Appearance	Yield [115] (%, w/weight of fraction E)	Percentage of inhibitory activity (%)
E1	Yellow oil	8.9 (0.02)	ND
E2	Yellow oil	26.9 (0.07)	24.93 \pm 0.99
E3	White powder	2.8 (0.01)	ND
E4	White powder	8.0 (0.02)	ND
E5	White powder	78.9 (0.21)	30.40 \pm 0.40
E6	White powder	26.8 (0.07)	14.05 \pm 0.40
E7	White powder	2.7 (0.01)	ND
E8	Yellow oil	84.8 (0.23)	NA
E9	Yellow oil	9.4 (0.03)	ND

NA = No activity.

ND = No detection.

Fraction F was fractionated by column chromatography to yield six subfractions (F1-F6). Six subfractions were determined for tyrosinase inhibitory activity (Table 22). Subfractions F2, F3, F4 and F5 exhibited significant tyrosinase inhibitory activity with percentage inhibition values of 70.91 \pm 0.30%, 71.34 \pm 1.91%, 74.90 \pm 0.07% and 80.15 \pm 1.15%, respectively. While, subfractions F1 and F6 showed moderate tyrosinase inhibitory activity with percentage inhibition values of 64.11 \pm 0.14% and 51.20 \pm 1.45%, respectively.

Table 22 Tyrosinase inhibitory activity of subfractions F1-F6 of fraction F

Subfraction	Appearance	Yield (g) (% w/weight of fraction F)	Percentage of inhibitory activity (%)
F1	White powder	1.26 (6.27)	64.11 \pm 0.14
F2	White powder	0.03 (0.15)	70.91 \pm 0.30
F3	White powder	10.63 (52.94)	71.34 \pm 1.91
F4	Green gum	1.43 (7.12)	74.90 \pm 0.07
F5	Brown gum	4.40 (21.91)	80.15 \pm 1.15
F6	Brown gum	1.24 (6.18)	51.20 \pm 1.45

Subfraction F1 was fractionated by column chromatography. Fractionation was used gradient elution of *n*-hexane and dichloromethane to give six subfractions (F11-F16). Subfractions F11-F13 were determined for tyrosinase inhibitory activity (Table 23). Subfractions F14-F16 were not tested tyrosinase inhibitory activity because amount of subfraction F14-F16 was not enough to test tyrosinase inhibitory activity. Subfractions F11 and F13 showed strong tyrosinase inhibitory activity with percentage inhibition values of $81.62 \pm 0.91\%$ and $81.90 \pm 0.27\%$, respectively.

Table 23 Tyrosinase inhibitory activity of subfractions F11-F16 of subfraction F1

Subfraction	Appearance	Yield [115] (% of subfraction F1)	Percentage of inhibitory activity (%)
F11	White powder	126.3 (12.63)	81.62 ± 0.91
F12	Yellow gum	115.4 (11.54)	29.21 ± 0.89
F13	White crystal	5.4 (0.54)	81.90 ± 0.27
F14	Yellow gum	2.4 (0.24)	ND
F15	Yellow gum	4.3 (0.43)	ND
F16	Yellow gum	4.3 (0.43)	ND

ND = No detection.

Subfraction F11 was rechromatographed and eluted with mixture gradient of *n*-hexane and dichloromethane to afford six subfractions (F111-F116). Both subfractions F112 and F113 were evaluated for antityrosinase activity (Table 24). Subfraction F113 showed higher antityrosinase activity than subfraction F112 with percentage inhibition values of $62.62 \pm 5.22\%$ and $12.25 \pm 0.48\%$, respectively.

Table 24 Tyrosinase inhibitory activity of subfractions F111-F116 of subfraction F11

Subfraction	Appearance	Yield [115] (% w/weight of subfraction F11)	Percentage of inhibitory activity (%)
F111	Yellow oil	2.5 (2.08)	ND
F112	White powder	30.6 (25.50)	12.25 ± 0.48
F113	White powder	71.8 (54.67)	62.62 ± 5.22
F114	White powder	2.5 (2.08)	ND
F115	White powder	9.7 (8.08)	ND
F116	White powder	9.1 (7.58)	ND

ND = No detection.

Subfraction F113 was further purified by silica gel column chromatography and eluted with mixture of dichloromethane:ethyl acetate in increasing of polarity to yield five subfractions (F1131-F1135). Subfractions F1131 and F1132 showed strong

antityrosinase activity with percentage inhibition values of $71.79 \pm 0.22\%$ and $87.31 \pm 0.15\%$, respectively (Table 25). Subfractions F1133-F1135 did not evaluated for antityrosinase activity because of limitation of amount of them.

Table 25 Tyrosinase inhibitory activity of subfractions F1131-F1135 of subfraction F113

Subfraction	Appearance	Yield [115] (%, w/weight of subfraction F113)	Percentage of inhibitory activity (%)
F1131	White powder	30.7 (51.17)	71.79 ± 0.22
F1132	White powder	5.8 (9.67)	87.31 ± 0.15
F1133	Yellow oil	6.9 (11.5)	ND
F1134	Yellow oil	7.2 (12.0)	ND
F1135	Yellow oil	3.2 (5.33)	ND

ND = No detection.

Subfraction F1131 was rechromatographed by silica gel and eluted with mixture gradient of petroleum ether:*n*-hexane and *n*-hexane:dichloromethane to provide eight subfractions (F11311-F11318). Subfractions F11313 and F11316 showed potent antityrosinase activity with percentage inhibition values of $72.22 \pm 0.22\%$ and $70.62 \pm 0.36\%$, respectively. Antityrosinase activity of other subfractions was not tested (Table 26). As the attempted isolation of fraction F1, it was unsuccessful to obtain pure compounds.

Table 26 Tyrosinase inhibitory activity of subfractions F11311-F11315 of subfraction F1131

Subfraction	Appearance	Yield [115] (%, w/weight of subfraction F1131)	Percentage of inhibitory activity (%)
F11311	Yellow oil	1.3 (42.35)	ND
F11312	Clear oil	4.2 (13.68)	ND
F11313	White powder	4.1 (13.36)	72.22 ± 0.22
F11314	Yellow oil	4.1 (13.36)	ND
F11315	Yellow oil	0.9 (2.93)	ND
F11316	White powder	5.0 (16.29)	70.62 ± 0.36
F11317	White powder	3.7 (12.05)	ND
F11318	White powder	5.1 (16.61)	ND

ND = No detection.

Subfraction F2 was chromatographed by silica gel column chromatography with gradient of *n*-hexane and dichloromethane as eluent to obtain three subfractions

(F21-F23). Subfraction F21 showed strong antityrosinase activity with percentage inhibition value of $81.39 \pm 0.89\%$ (Table 27). Its TLC pattern showed a single spot and its R_f value exhibited subfraction F21 was compound **I**. Moreover, $^1\text{H-NMR}$ spectrum of subfraction F21 was compound **I**.

Table 27 Tyrosinase inhibitory activity of subfractions F21-F23 of subfraction F2

Subfraction	Appearance	Yield [115] (% w/weight of subfraction F2)	Percentage of inhibitory activity (%)
F21	Clear crystal	27.0 (23.40)	81.39 ± 0.89
F22	Yellow gum	3.7 (3.21)	ND
F23	White powder	1.4 (1.21)	ND

ND = No detection.

Subfraction F3 was applied to silica gel column chromatography and eluted with gradient of *n*-hexane and ethyl acetate to obtain four subfractions (F31-F34). Subfraction F31 showed strong antityrosinase activity with percentage inhibition value of $82.10 \pm 0.32\%$ (Table 28). $^1\text{H-NMR}$ spectra of subfraction F31 and compound **I** were compared. The results indicated that subfraction F31 was compound **I**.

Table 28 Tyrosinase inhibitory activity of subfractions F31-F34 of subfraction F3

Subfraction	Appearance	Yield (g) (% w/weight of subfraction F3)	Percentage of inhibitory activity (%)
F31	White crystal	0.01 (0.09)	82.10 ± 0.32
F32	Yellow gum	0.04 (0.38)	ND
F33	Yellow gum	0.73 (6.87)	ND
F34	Brown gum	9.84 (92.57)	ND

ND = No detection.

Subfraction F4 was subjected to silica gel column chromatography with a step gradient elution with *n*-hexane and ethyl acetate to yield six subfractions (F41-F46). Subfraction F43 showed the strongest antityrosinase activity with percentage inhibition value of $73.69 \pm 0.11\%$. Subfractions F41, F44, F45 and F46 showed weak antityrosinase activity with percentage inhibition values of $20.60 \pm 0.72\%$, $12.74 \pm 0.97\%$, $24.31 \pm 0.25\%$ and $10.54 \pm 0.93\%$, respectively (Table 29). Thus, subfraction F43 was selected for further isolation of tyrosinase inhibitors.

Table 29 Tyrosinase inhibitory activity of subfractions F41-F46 of subfraction F4

Subfraction	Appearance	Yield [115] (% , w/weight of subfraction F4)	Percentage of inhibitory activity (%)
F41	Yellow powder	90.2 (6.31)	20.60 ± 0.72
F42	White powder	2.0 (0.14)	ND
F43	White powder	133.7 (9.35)	73.69 ± 0.11
F44	Yellow solid	14.7 (1.03)	12.74 ± 0.97
F45	Brown solid	105.6 (7.38)	24.31 ± 0.25
F46	Brown gum	83.2 (5.82)	10.54 ± 0.93

ND = No detection.

Subfraction F43 was further subjected to silica gel column chromatography to yield five subfractions (F431-F435). Subfraction F433 showed strong antityrosinase activity with percentage inhibition value of 91.59 ± 0.87% (Table 30). Therefore, subfraction F433 was collected for further isolation of active compounds.

Table 30 Tyrosinase inhibitory activity of subfractions F431-F435 of subfraction F43

Subfraction	Appearance	Yield [115] (% , w/weight of subfraction F43)	Percentage of inhibitory activity (%)
F431	White powder	18.2 (18.20)	NA
F432	Yellow gum	5.8 (5.80)	ND
F433	Yellow gum	115.2 (70.20)	91.59 ± 0.87
F434	Brown gum	1.2 (1.20)	ND
F435	Brown gum	4.6 (4.60)	ND

NA = No activity.

ND = No detection.

Subfraction F433 was separated by silica gel column chromatography and eluted with a stepwise mixture of *n*-hexane and ethyl acetate to obtain six subfractions (F4331-F4336). Subfractions F4332, F4334 and F4335 showed strong antityrosinase activity with percentage inhibition values of 87.22 ± 0.41%, 90.21 ± 0.95% and 90.01 ± 1.00%, respectively. Subfraction F4331 exhibited no activity against mushroom tyrosinase (Table 31). Subfractions F4332, F4334 and F4335 were collected for further tyrosinase-guided fractionation.

Table 31 Tyrosinase inhibitory activity of subfractions F4331-F4336 of subfraction F433

Subfraction	Appearance	Yield [115] (%, w/weight of subfraction F433)	Percentage of inhibitory activity (%)
F4331	Yellow oil	4.4 (3.82)	NA
F4332	White powder	72.9 (63.28)	87.22 ± 0.41
F4333	Clear gum	2.0 (1.74)	ND
F4334	White powder	13.2 (11.46)	90.21 ± 0.95
F4335	Yellow powder	12.9 (11.20)	90.01 ± 1.00
F4336	Brown gum	9.7 (8.42)	ND

NA = No activity.

ND = No detection.

Subfraction F4332 was separated by preparative TLC and eluted with a mixture of *n*-hexane and ethyl acetate to obtain two subfractions (F43321-F43322). Subfraction F43321 showed stronger antityrosinase activity than subfraction F43322 with percentage inhibition values of 93.00 ± 0.60% and 6.04 ± 0.42%, respectively (Table 32). Subfraction F43321 was obtained as white powder. Subfraction F43321 was identified as compound **I**.

Table 32 Tyrosinase inhibitory activity of subfractions F43321-F43322 of subfraction F4332

Subfraction	Appearance	Yield [115] (%, w/weight of subfraction F4332)	Percentage of inhibitory activity (%)
F43321	White powder	8.9 (24.45)	93.00 ± 0.60
F43322	White powder	27.5 (75.55)	6.04 ± 0.42

Subfraction F4334 was fractionated on an analytical C₁₈ column using an isocratic system of methanol and aqueous (3:2 v/v) in the flow rate of 1 mL/min to yield compound **II** (8 mg) at retention time 3.5 min. Compound **II** was obtained as yellow powder. Subfraction F4335 was submitted to Sephadex LH-20 column chromatography and used methanol as eluent to afford three subfractions (F43351-F43353). Subfraction F43353 showed high antityrosinase activity with percentage inhibition value of 95.94 ± 0.20% (Table 33). Subfraction F43353 (2.4 mg) was purified by HPLC using C₁₈ column and an isocratic system of methanol and water (7:3 v/v) in the flow rate of 0.5 mL/min to yield yellow powder (compound **III**, 2.4 mg) at retention time 5.9 min.

Table 33 Tyrosinase inhibitory activity of subfractions F43351-F43353 of subfraction F4335

Subfraction	Appearance	Yield [115] (% w/weight of subfraction F4335)	Percentage of inhibitory activity (%)
F43351	White powder	9.5 (73.64)	NA
F43352	Yellow powder	1.0 (7.75)	ND
F43353	Yellow powder	2.4 (18.60)	95.94 ± 0.20

NA = No activity.

ND = No detection.

Subfraction F5 was separated by silica gel column chromatography and eluted with a mixture gradient of *n*-hexane:ethyl acetate to afford nine subfractions (F51-F59). Subfraction F59 showed the highest tyrosinase inhibitory activity with percentage inhibition value of 88.38 ± 0.76% when compared with other eluted subfractions from subfraction F5. Subfraction F53 showed moderate tyrosinase inhibitory activity with percentage inhibition value of 61.90 ± 0.85%. Subfractions F52, F54 and F55 showed weak tyrosinase inhibitory activity with percentage inhibition values of 20.12 ± 0.97%, 40.98 ± 0.42% and 22.22 ± 0.51%, respectively (Table 34).

Table 34 Tyrosinase inhibitory activity of all subfractions F51-F59 of subfraction F5

Subfraction	Appearance	Yield (g) (% w/w)	Percentage of inhibitory activity (%)
F51	Yellow gum	0.05 (1.14)	NA
F52	Yellow gum	2.38 (54.09)	20.12 ± 0.97
F53	Yellow gum	0.08 (1.82)	61.90 ± 0.85
F54	Brown gum	0.11 (2.50)	40.98 ± 0.42
F55	Brown gum	0.22 (5.0)	22.22 ± 0.51
F56	Brown gum	0.13 (2.95)	NA
F57	White powder	0.04 (0.91)	NA
F58	Brown gum	0.45 (10.23)	NA
F59	Brown gum	0.12 (2.73)	88.38 ± 0.76

NA = No activity.

Subfraction F53 was separated by preparative TLC and eluted with a mixture gradient of *n*-hexane and ethyl acetate to afford two subfractions (F531-F532). The results of subfractions F531-F532 are shown in Table 35. As the attempted isolation of subfraction F53, it could not get pure compounds.

Table 35 Isolation of subfractions F531-F532 of subfraction F53

Fraction	Appearance	Yield [115] (% w/weight of subfraction F53)
F531	White powder	68.8 (86.00)
F532	White powder	1.2 (1.50)

Subfraction F54 was separated by silica gel column chromatography to afford six subfractions (F541-F546). The results of subfractions F541-F546 are shown in Table 36. Unfortunately, isolation of subfraction F54 was not successful to get pure compounds.

Subfraction F59 was separated by silica gel column chromatography and eluted with *n*-hexane, a mixture gradient of *n*-hexane:acetone, acetone and acetone:methanol to afford ten subfractions (F591-F5910). Subfraction F596 showed high antityrosinase activity with percentage inhibition values of $84.21 \pm 0.44\%$. Subfraction F596 was recrystallized to obtain brown powder (compound **IV**). The results of subfractions F591-F5910 are shown in Table 36.

Table 36 Tyrosinase inhibitory activity of subfractions F591-F5910 of subfraction F59

Subfraction	Appearance	Yield [115] (% w/weight of subfraction F59)	Percentage of inhibitory activity (%)
F591	Yellow gum	7.4 (3.43)	ND
F592	Yellow gum	6.4 (2.96)	ND
F593	White powder	5.1 (2.36)	ND
F594	Yellow gum	6.0 (2.78)	ND
F595	Yellow gum	9.1 (4.21)	ND
F596	Brown powder	60.0 (27.78)	84.21 ± 0.44
F597	Yellow gum	7.1 (3.29)	ND
F598	Yellow gum	8.0 (3.70)	ND
F599	Yellow gum	9.4 (4.35)	ND
F5910	Yellow gum	6.2 (2.87)	ND

ND = No detection.

Subfraction F6 (42.1 mg) was further separated by silica gel column chromatography and eluted with hexane and a mixture gradient of *n*-hexane:ethyl acetate to give three subfractions (F61-F63). Subfraction F62 showed moderated antityrosinase activity with percentage inhibition value of $52.76 \pm 0.60\%$. While, subfraction F63 showed weak antityrosinase activity with percentage inhibition value of $15.89 \pm 0.81\%$. The results of subfractions F61-F63 are shown in Table 37.

Table 37 Tyrosinase inhibitory activity of subfractions F61-F63 of subfraction F6

Subfraction	Appearance	Yield [115] (%, w/weight of subfraction F6)	Percentage of inhibitory activity (%)
F61	Yellow gum	3.7 (0.30)	ND
F62	White powder	24.9 (2.01)	52.76 ± 0.60
F63	Brown gum	12.5 (1.01)	15.89 ± 0.81

ND = No detection.

Subfraction F62 was separated by silica gel column chromatography and eluted with *n*-hexane, a mixture gradient of *n*-hexane:dichloromethane and dichloromethane to give six subfractions (F621-F626). The results of subfractions F621-F626 are shown in Table 38. Unfortunately, isolation of subfraction F62 did not succeed to obtain pure compounds.

Table 38 Isolation of subfractions F621-F626 of subfraction F62

Fraction	Appearance	Yield [115] (% , w/weight of subfraction F62)
F621	Yellow gum	1.6 (6.43)
F622	White powder	4.8 (19.28)
F623	White powder	2.8 (11.24)
F624	White powder	1.3 (5.22)
F625	White powder	8.2 (32.93)
F626	Brown gum	1.3 (5.22)

Fraction G was separated by silica gel column chromatography to give five subfractions (G1-G5). Subfractions G3 and G5 exhibited strong tyrosinase inhibitory activity with percentage inhibition values of 80.10 ± 0.90 and 81.30 ± 0.51%, respectively. Subfractions G1, G2 and G4 showed weak tyrosinase inhibitory activity with percentage inhibition values of 16.97 ± 0.15%, 11.58 ± 0.71% and 31.09 ± 0.54%, respectively. The results of subfractions G1-G5 are shown in Table 39.

Table 39 Tyrosinase inhibitory activity of subfractions G1-G5 of fraction G

Subfraction	Appearance	Yield (g) (% , w/weight of fraction G)	Percentage of inhibitory activity (%)
G1	Yellow gum	0.77 (16.21)	16.97 ± 0.15
G2	Yellow gum	2.06 (43.37)	11.58 ± 0.71
G3	White powder	0.20 (4.21)	80.10 ± 0.90
G4	Green gum	0.14 (2.95)	31.09 ± 0.54
G5	Green gum	0.20 (4.21)	81.30 ± 0.51

Subfraction G3 was further separated by silica gel column chromatography and eluted with *n*-hexane, a mixture gradient of *n*-hexane:ethyl acetate and ethyl acetate:methanol to give four subfractions (G31-G34). Subfraction G33 showed higher antityrosinase activity than subfraction G32 with percentage inhibition values of $70.60 \pm 0.03\%$ and $30.50 \pm 0.03\%$, respectively. The results of subfractions G31-G34 are shown in Table 40.

Table 40 Tyrosinase inhibitory activity of subfractions G31-G34 of subfraction G3

Subfraction	Appearance	Yield [115] (% w/weight of subfraction G3)	Percentage of inhibitory activity (%)
G31	White powder	61.1 (30.55)	NA
G32	Clear gum	41.6 (20.80)	30.50 ± 0.03
G33	White powder	51.1 (25.55)	70.60 ± 0.03
G34	White powder	41.8 (20.90)	NA

NA = No activity.

Subfraction G33 was separated by silica gel column chromatography and eluted with a mixture gradient of *n*-heptane:dichloromethane to give three subfractions (G331-G333). Subfractions G332 and G333 showed strong antityrosinase activity with percentage inhibition values of $84.90 \pm 0.22\%$ and $90.12 \pm 0.42\%$. The results of subfractions G331-G333 are shown in Table 41.

Table 41 Tyrosinase inhibitory activity of subfractions G331-G333 of subfraction G33

Subfraction	Appearance	Yield [115] (% w/weight of subfraction G33)	Percentage of inhibitory activity (%)
G331	White powder	11.1 (21.72)	NA
G332	White powder	24.6 (4.81)	84.90 ± 0.22
G333	Colorless crystal	15.4 (30.14)	90.12 ± 0.42

NA = No activity.

Subfraction G332 was purified by preparative TLC and eluted with a mixture of petroleum ether and dichloromethane to obtain two subfractions (G3321-G3322). Subfraction G3322 exhibited antityrosinase activity with percentage inhibition value of $84.27 \pm 0.12\%$. Subfraction G3322 (compound **V**) was obtained as white powder (10.5 mg). The results of subfractions G3321-G3322 are shown in Table 42. Subfraction

G333 was recrystallized with methanol to give colorless crystal (15.4 mg, compound **VI**).

Table 42 Tyrosinase inhibitory activity of subfractions G3321-G3322 of subfraction G332

Subfraction	Appearance	Yield [115] (% w/weight of subfraction G332)	Percentage of inhibitory activity (%)
G3321	White powder	13.4 (55.83)	NA
G3322	White powder	10.5 (43.75)	84.27 ± 0.12

NA = No activity.

Subfraction G5 was separated by silica gel column chromatography and eluted with a mixture of *n*-hexane:ethyl acetate to obtain two subfractions (G51-G52). The results of subfractions G51-G52 are shown in Table 43.

Table 43 Tyrosinase inhibitory activity of subfractions G51-G52 of subfraction G5

Subfraction	Appearance	Yield [115] (% w/weight of subfraction G5)	Percentage of inhibitory activity (%)
G51	White powder	100.0 (50.00)	62.66 ± 0.33
G52	Green gum	71.3 (35.60)	38.68 ± 0.45

Subfraction G51 was separated by silica gel column chromatography and eluted with a mixture of dichloromethane and ethyl acetate to obtain two subfractions (G511-G512). Subfraction G511 was obtained as white powder (compound **VII**). The results of subfractions G511-G512 are shown in Table 44.

Table 44 Tyrosinase inhibitory activity of subfractions G511-G512 of subfraction G51

Subfraction	Appearance	Yield [115] (% w/weight of subfraction G51)	Percentage of inhibitory activity (%)
G511	White powder	20.0 (20.00)	75.31 ± 0.04
G512	White powder	60.0 (60.00)	10.71 ± 0.11

Among the isolation of crude extracts of *M. zapota* barks, compound **I** was isolated from *n*-hexane crude extract and compounds **II-VII** were isolated from ethyl acetate crude extract. Moreover, compounds **I-VII** were elucidated by spectroscopic data (NMR and HR-EI-MS), analyzed by physical properties (melting point and the optical rotation) and compared with previously reported. Compounds **I-VII** were evaluated for antityrosinase activities on monophenolase and diphenolase inhibitory

activities, antioxidant activities with DPPH, ABTS and FRAP assays and cytotoxic activity. Isolated compounds could reveal with these biological activities.

4.7 Elucidation of isolated compounds I-VII

4.7.1 Elucidation of compound I

Compound **I** was obtained as white powder (132.9 mg, 0.06% w/w of hexane crude extract and 0.03% of ethyl acetate crude extract) with melting point of 278-280 °C. The optical rotation was as $[\alpha]_D^{28} +8.3$ (CHCl₃; c 0.63). The ¹H-NMR spectrum (Figure 51) showed seven signals of methyl proton at δ 1.06 (3H, s, H-27), 0.94 (3H, s, H-29), 0.93 (3H, s, H-23), 0.90 (3H, s, H-24), 0.89 (6H, s, H-28 and H-30), 0.80 (3H, s, H-26) and 0.76 (3H, s, H-25) ppm. One signal of methoxy proton showed at δ 3.33 (s, H-1') ppm. One signal of olefinic proton showed at δ 5.51 (1H, dd, $J = 8.1, 3.3$ Hz, H-15) ppm. Four signals of methine proton showed at 2.61 (1H, dd, $J = 11.7, 4.2$ Hz, H-3), 1.42 (1H, m, H-9), 1.39 (1H, m, H-18) and 0.85 (1H, d, $J = 3.6$ Hz, H-5), ppm. Sixteen signals of methylene proton showed at δ 2.00 (1H, dt, $J = 12.0, 3.0$ Hz, H-19a), 1.89 (1H, dd, $J = 15.0, 3.0$ Hz, H-1a), 1.65 (1H, m, H-7a), 1.64 (1H, m, H-7b), 1.60 (1H, m, H-1b), 1.57 (2H, m, H-6a and H-21a), 1.51 (2H, m, H-11a and H-21b), 1.44 (1H, m, H-11b), 1.37 (1H, m, H-6b), 1.36 (1H, m, H-12a and H-22a), 1.34 (1H, m, H-19b), 1.31 (1H, m, H-16a), 1.25 (2H, m, H-16b and H-22b), 1.00 (1H, m, H-12b), 0.96 (1H, m, H-2a), 0.95 (1H, m, H-2b) ppm.

The ¹³C-NMR spectrum (Figure 52) showed thirty one carbon atoms. DEPT90 and DEPT135 experiments (Figures 53-54), two signals of olefinic carbon showed signal δ 158.3 and 116.8 ppm suggested that the chemical shift were C-14 and C-15. A signal carbon at 88.9 ppm indicated a C-3 substituted methoxy carbon (OCH₃, C-1'). Eight signals of methyl carbon displayed at δ 33.5 (C-29), 30.1 (C-28), 30.0 (C-26), 28.2 (C-23), 26.1 (C-27), 21.5 (C-30), 15.5 (C-24) and 16.3 (C-25) ppm. Nine signals of methylene carbon showed at δ 37.9 (C-7), 37.8 (C-1), 36.8 (C-16), 35.3 (C-12), 33.8 (C-21), 33.2 (C-22), 28.2 (C-2), 18.8 (C-6) and 17.7 (C-11) ppm. Five signals of methine carbon showed at δ 88.9 (C-3), 55.9 (C-5), 49.1 (C-18), 48.9 (C-9) and 41.5 (C-19) ppm. Six signals of quaternary carbon appeared at δ 39.2 (C-8 and C-10), 38.8 (C-4), 37.9 (C-13 and C-17) and 28.9 (C-20) ppm.

Experiments of HSQC, HMBC and COSY analysis (Figures 55-57) were confirmed the structure of compound **I**. HMBC spectrum (Figure 56) showed correlation peaks of H-3/C-1, 2 and 3, H-5/C-4, 6 and 10, H-6/C-4, 5 and 7, H-9/C-6, 8 and 11, H-11/C-9, 12 and 13, H-15/C-13, 14 and 16, H-19/C-18, 20 and 30, H-23/C-3, 4 and 5, H-24/C-4 and 5, H-25/C-1, 5 and 10, H-26/C-6, 7 and 8, H-27/C-12, 13 and 15, H-28/C-16, 17 and 18, H-29/C-18, 19 and 20 and H-30/C-17, 21 and 22 (Figure 17).

Comparison of NMR data of compound **I** and reported literature [116] are shown in Table 45.

Table 45 Comparison of NMR data of compound **I** and taraxerol methyl ether

Position	Chemical shift (ppm)			
	Taraxerol methyl ether		Compound I	
	δ_{H}	δ_{C}	δ_{H}	δ_{C}
1	1.56 (m), 1.61 (m)	33.9	1.89 (dd, 15.0, 3.0), 1.60 (m)	37.8
2	1.40 (m), 1.76 (m)	22.1	0.96 (m), 0.96 (m)	28.2
3	2.63 (dd, 11.7, 4.3)	88.9	2.61 (dd, 11.7, 4.2)	88.9
4	-	39.2	-	38.8
5	0.75 (m)	56.3	0.85 (d, 3.6)	55.9
6	1.48 (m), 1.58 (m)	18.8	1.57 (m), 1.37 (m)	18.8
7	1.34 (m), 2.04 (m)	41.5	1.65 (m), 1.64 (m)	37.9
8	-	38.8	-	39.2
9	1.40 (m)	49.4	1.42 (m)	48.9
10	-	37.8	-	39.2
11	1.48 (m), 1.63 (m)	17.7	1.51 (m), 1.44 (m)	17.7
12	0.93 (m), 0.91 (m)	29.0	1.36 (m), 1.00 (m)	35.3
13	-	38.2	-	37.9
14	-	158.3	-	158.3
15	5.53 (dd, 8.3, 3.3)	117.0	5.51 (dd, 8.1, 3.3)	116.8
16	1.63 (m), 1.90 (m)	37.9	1.31 (m), 1.25 (m)	36.8
17	-	35.9	-	37.9
18	0.94 (m)	48.9	1.39 (m)	49.1
19	1.03 (m), 1.36 (m)	35.3	2.00 (dt, 12.0, 3.0), 1.34 (m)	41.5
20	-	37.7	-	28.9
21	0.99 (m), 1.31 (m)	36.8	1.57 (m), 1.51 (m)	33.8
22	1.26 (m), 1.34 (m)	33.2	1.36 (m), 1.25 (m)	33.2
23	0.96 (s)	28.2	0.93 (s)	28.2
24	0.78 (s)	16.4	0.90 (s)	15.5
25	0.93 (s)	15.6	0.76 (s)	16.3
26	1.08 (s)	26.1	0.80 (s)	30.0
27	0.91 (s)	21.5	1.06 (s)	26.1
28	0.91 (s)	30.1	0.89 (s)	30.1
29	0.95 (s)	33.5	0.94 (s)	33.5
30	0.82 (s)	30.0	0.89 (s)	21.5
1'	3.35 (s)	57.7	3.33 (s)	56.3

The HR-EI-MS spectrum (Figure 58) of compound **I** showed $[\text{M}+\text{Na}]^+$ at m/z 463.3249. A molecular formula was predicted as $\text{C}_{31}\text{H}_{52}\text{ONa}$ and it was calculated as 463.3916. Therefore, compound **I** was identified as taraxerol methyl ether. The

structure of compound **I** is shown in Figure 18.

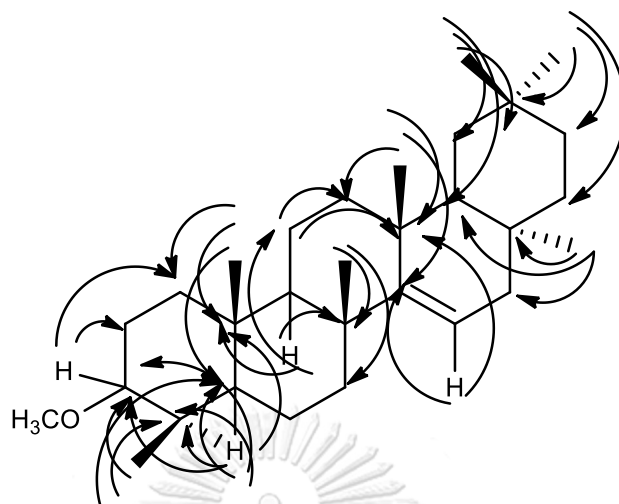


Figure 17 HMBC correlations of compound **I**

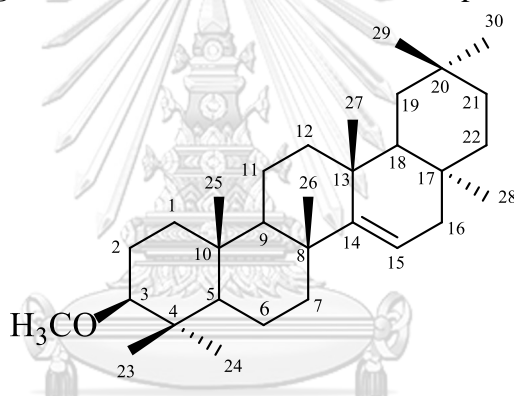


Figure 18 The structure of compound **I**

Taraxerol methyl ether was isolated from *Echinochloa crusgallis* L. [116], leaves of *Bosistoa sapindiformis* [117] and stem barks of *Mimusops obtusifolia* [104]. It showed cytotoxic activity against HeLa, HL-60 and MCF-7 with IC_{50} value $> 50 \mu\text{M}$ [116] and displayed antiplasmodial activity with IC_{50} value $> 100 \mu\text{g/mL}$ [104].

4.7.2 Elucidation of compound **II**

Compound **II** was afforded as yellow powder (8.0 mg, 0.0006% w/w of ethyl acetate crude extract) with melting point of 180-182 °C. The optical rotation was determined as $[\alpha]_D^{28} -1.2$ (DMSO; c 1.05). The $^1\text{H-NMR}$ spectrum (Figure 59) showed five aromatic protons at δ 7.53 (1H, dd, $J = 8.1, 1.5$ Hz, H-2' and H-6'), δ 7.39 (1H, m, H-3', H-4' and H-5'), 7.23 (1H, d, $J = 3.3$ Hz, H-5), 7.06 (1H, dd, $J = 9.0, 3.3$ Hz, H-7) and 6.96 (1H, dd, $J = 9.0, 3.3$ Hz, H-8) ppm. Two signals of methylene proton displayed

at 3.08 (1H, $J = 16.8, 12.9$ Hz, H-3) and 2.83 (1H, $J = 16.8, 3.0$ Hz, H-3) ppm. One signal of methine proton showed at δ 5.48 (1H, dd, $J = 13.2, 3.0$ Hz, H-2) ppm.

The ^{13}C -NMR spectrum (Figure 60) showed one carbonyl carbon signal at δ 194.3 ppm (C-4) and one signal of methylene carbon showed at δ 45.6 (C-3) ppm. One signal of methine carbon showed at δ 81.0 (C-2) ppm. The remaining signals displayed aromatic carbons at δ 156.8 (C-9), 153.1 (C-6), 140.8 (C-1'), 129.7 (C-3' and C-5'), 129.5 (C-4'), 127.3 (C-2' and C-6'), 126.0 (C-7) and 122.4 (C-10) ppm.

Experiments of HSQC, HMBC and COSY (Figures 61-63) analysis were confirmed the structure of compound **II** and HMBC spectrum (Figure 62) showed correlation peaks of H-2/C-3 and 1', H-3/C-2, 4 and 5, H-5/C-6 and 10, H-7/C-6 and 8, H-8/C-7 and 9, H-2'/C-1' and 3', H-3'/C-2' and 4', H-4'/C-3' and 5', H-5'/C-4' and 6' and H-6'/C-1' and 5' (Figure 19).

Compound **II** was identified by comparison of NMR data with reported in the literature [118] (Table 46).

Table 46 Comparison of NMR data of compound **II** and 6-hydroxyflavanone

Position	Chemical shift (ppm)			
	6-hydroxyflavanone		Compound II	
	δ_{H}	δ_{C}	δ_{H}	δ_{C}
1	-	-	-	-
2	5.51 (dd, $J = 13.0, 2.8$ Hz)	79.2	5.48 (dd, $J = 13.2, 3.0$ Hz)	81.0
3	3.13 (dd, $J = 16.9, 13.0$ Hz) 2.75 (dd, $J = 16.9, 2.9$ Hz)	44.2	3.08 ($J = 16.8, 12.9$ Hz) 2.83 ($J = 16.8, 3.0$ Hz)	45.6
4	-	192.2	-	194.3
5	7.09 (d, $J = 2.9$ Hz)	110.4	7.23 (d, $J = 3.3$ Hz)	111.5
6	-	152.1	-	153.1
7	7.00 (dd, $J = 8.8, 3.0$ Hz)	124.9	7.06 (dd, $J = 9.0, 3.3$ Hz)	125.9
8	6.92 (d, $J = 8.8$ Hz)	119.5	6.96 (dd, $J = 9.0, 3.3$ Hz)	120.2
9	-	154.9	-	156.8
10	-	121.4	-	122.4
1'	-	139.7	-	140.8
2'	7.35 (d, $J = 8.4$ Hz)	127.0	7.53 (dd, $J = 8.1, 1.5$ Hz)	127.3
3'	7.36 (m)	129.0	7.39 (m)	129.7
4'	7.36 (m)	128.9	7.39 (m)	129.5
5'	7.36 (m)	129.0	7.39 (m)	129.7
6'	7.35 (d, $J = 8.4$ Hz)	127.0	7.53 (dd, $J = 8.1, 1.5$ Hz)	127.3

The HR-EI-MS spectrum (Figure 64) of compound **II** displayed $[\text{M}+\text{H}]^+$ at m/z 263.0685. A molecular formula was assigned and calculated as $\text{C}_{15}\text{H}_{12}\text{O}_3\text{Na}$ (263.0684). Thus, compound **II** was elucidated as 6-hydroxyflavanone. The structure of compound **II** is shown in Figure 20.

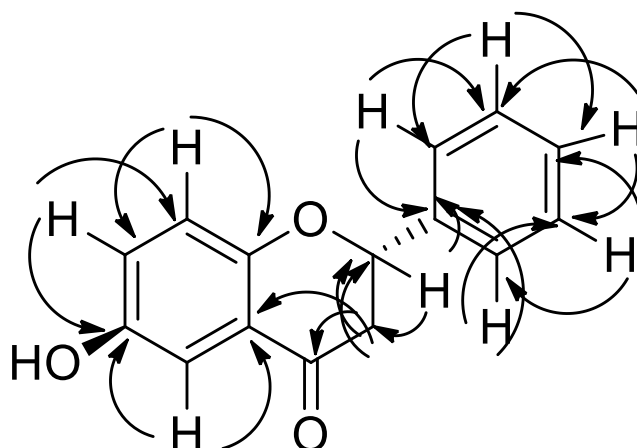


Figure 19 HMBC correlations of compound **II**

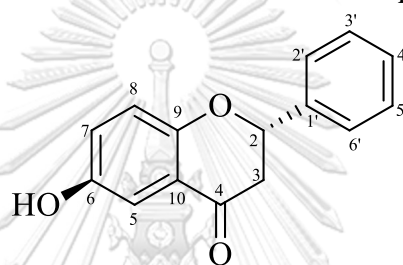


Figure 20 The structure of compound **II**

This study, 6-hydroxyflavanone was isolated for the first time in *M. zapota* barks. Herath *et al* reported that 6-hydroxyflavone was fermented with *Beauveria bassiana* to afford 6-hydroxyflavanone [118]. Mikell *et al* studied that 6-hydroxyflavanone was fermented by *Cunninghamella blakesleeana* to yield 6-hydroxyflavanone derivatives such as flavanone 6-*O*- β -*D*-glucopyranoside, flavanone 6-sulfate and 6-hydroxyflavanone-7-sulfate [119]. 6-Hydroxyflavanone showed cytotoxic activity against human epithelial adenocarcinoma (HeLa) cell lines and human breast cancer cell lines (BT474) [120, 121].

4.7.3 Elucidation of compound **III**

Compound **III** was obtained as yellow powder (2.4 mg, 0.0017% w/w of ethyl acetate crude extract) with melting point of 228-230 °C. The optical rotation was recorded as $[\alpha]_D^{28} +26.4$ (CH₃OH; c 0.12). The ¹H-NMR spectrum (Figure 65) showed four aromatic protons at δ 7.41 (2H, d, *J* = 8.4 Hz, H-2' and 6'), 6.89 (2H, d, *J* = 8.7 Hz, H-3' and 5'), 5.98 ppm (1H, d, *J* = 2.1 Hz, H-8) and 5.94 (1H, d, *J* = 2.1 Hz, H-6) ppm. Two signals methine proton showed at 5.08 (1H, d, *J* = 11.4 Hz, H-2) and 4.64 (1H, d,

$J = 11.7$ Hz, H-3) ppm. Hydroxy proton substitution signal displayed at δ 11.67 (4H, s, OH) ppm.

The ^{13}C -NMR spectrum (Figure 66) showed one ketone carbon signal at δ 198.3 (C-4) ppm. Two signals of methine carbon showed at δ 84.3 (C-2) and 73.1 (C-3) ppm. Nine signals of aromatic carbon displayed at δ 168.7 (C-7), 165.0 (C-5), 164.2 (C-9), 158.8 (C-4'), 130.3 (C-2' and C-6'), 129.1 (C-1'), 115.9 (C-3' and C-5'), 101.5 (C-10), 97.0 (C-8) and 96.0 (C-6) ppm.

Experiments of HSQC, HMBC and COSY (Figures 67-69) analysis were confirmed the structure of compound **III** and HMBC spectrum (Figure 68) showed correlation peaks of H-3/C-3 and 4, H-6/C-5 and 7, H-8/C-7 and 9, H-2'/C-1', 3' and 6', H-3'/C-2', 4' and 5', H-5'/C-3', 4' and 6' and H-6'/C-1', 2' and 5' (Figure 21).

Compound **III** was identified by comparison of NMR data with reported in the literature [122] (Table 47).

Table 47 Comparison of NMR data of compound **III** and dihydrokaempferol

Position	Chemical shift (ppm)			
	dihydrokaempferol		Compound III	
	δ_{H}	δ_{C}	δ_{H}	δ_{C}
1	-	-	-	-
2	5.09 (1H, d, $J = 11.6$ Hz)	84.4	5.08 (1H, d, $J = 11.4$ Hz)	84.3
3	4.66 (1H, d, $J = 11.6$ Hz)	73.1	4.64 (1H, d, $J = 11.7$ Hz)	73.1
4	-	198.2	-	198.3
5	-	165.0	-	165.0
6	5.96 (1H, d, $J = 2.0$ Hz)	97.2	5.94 (1H, d, $J = 2.1$ Hz)	96.0
7	-	167.9	-	168.7
8	6.00 ppm (1H, d, $J = 2.0$ Hz)	96.1	5.98 ppm (1H, d, $J = 2.1$ Hz)	97.0
9	-	164.2	-	164.2
10	-	101.5	-	101.5
1'	-	129.1	-	129.1
2'	7.42 (2H, d, $J = 8.6$ Hz)	130.2	7.41 (2H, d, $J = 8.4$ Hz)	130.3
3'	6.90 (2H, d, $J = 8.6$ Hz)	115.9	6.89 (2H, d, $J = 8.7$ Hz)	115.9
4'	-	158.8	-	158.8
5'	6.90 (2H, d, $J = 8.6$ Hz)	115.9	6.89 (2H, d, $J = 8.7$ Hz)	115.9
6'	7.42 (2H, d, $J = 8.6$ Hz)	130.2	7.41 (2H, d, $J = 8.4$ Hz)	130.3

The HR-EI-MS spectrum (Figure 69) of compound **III** displayed $[\text{M}+\text{H}]^+$ at m/z 311.0387. A molecular formula was assigned and calculated as $\text{C}_{15}\text{H}_{13}\text{O}_6$ (311.0532). Thus, compound **III** was elucidated as (+)-dihydrokaempferol. The structure of compound **III** is shown in Figure 22.

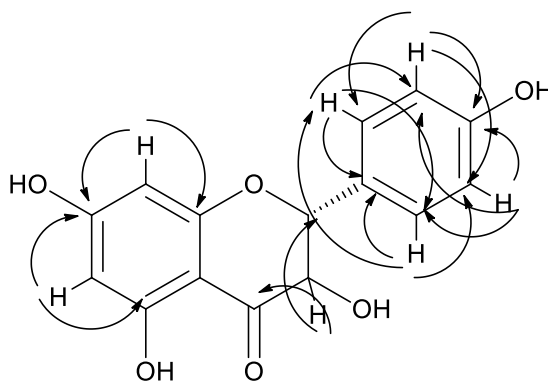


Figure 21 HMBC correlations of compound **III**

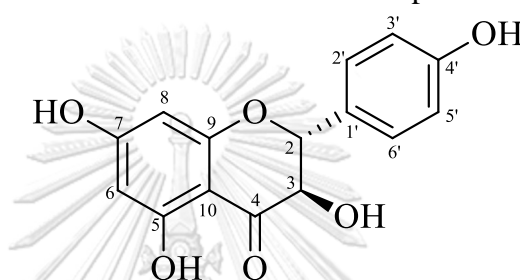


Figure 22 The structure of compound **III**

This is the first report on isolation of (+)-dihydrokaempferol from *M. zapota* barks. However, flavonoid compounds were found in *M. zapota* such as (+)-catechin, dihydromiricetin and quercitrin. (+)-Dihydrokaempferol was isolated from roots of *Polygonum amplexicaule* [122], barks of *Juglans mandshurica* [36] and twigs of *Morus alba* [123]. (+)-Dihydrokaempferol displayed antityrosinase activity on monophenolase inhibitory activity with IC_{50} value of $> 200 \mu\text{M}$ [123]. In addition, it showed antityrosinase activity on diphenolase inhibitory activity with IC_{50} value of $2.7 \pm 0.7 \text{ mM}$ [36].

4.7.4 Elucidation of compound **IV**

Compound **IV** was obtained as brown powder (60.0 mg, 0.0434% w/w of ethyl acetate crude extract) with melting point of 220-222 °C. The optical rotation was determined as $[\alpha]_D^{28} +13.3$ (CH_3COCH_3 ; c 1.33). The $^1\text{H-NMR}$ spectrum (Figure 70) showed three aromatic proton signals at δ 7.52 (1H, d, $J = 2.1 \text{ Hz}$, H-2), 7.47 (1H, d, $J = 8.1, 1.8 \text{ Hz}$, H-6) and 6.89 (1H, d, $J = 8.4 \text{ Hz}$, H-5) ppm.

The ^{13}C -NMR spectrum (Figure 71) showed carboxylic carbon signal appeared at δ 167.5 (C-1') ppm. Three signals of methine aromatic carbon showed at δ 123.6 (C-6), 117.5 (C-2) and 115.6 (C-5) ppm. Three signals of quaternary aromatic carbon appeared at δ 150.7 (C-4), 145.6 (C-3) and 123.1 (C-1) ppm.

Experiments of HSQC, HMBC and COSY (Figures 72-74) analysis were confirmed the structure of compound **IV** and HMBC spectrum (Figure 73) showed correlation peaks of H-2/C-1 and 6, H-3/C-2 and 4 and H-6/C-1 and 5 (Figure 23).

Compound **IV** was elucidated by comparison of NMR data with reported in the literature [124] (Table 48).

Table 48 Comparison of NMR data of compound **IV** and 3,4-dihydroxybenzoic acid

Position	Chemical shift (ppm)			
	3,4-dihydroxybenzoic acid		Compound IV	
	δ_{H}	δ_{C}	δ_{H}	δ_{C}
1	-	122.2	-	123.1
2	7.54 (1H, d, $J = 2.4$ Hz)	116.8	7.52 (1H, d, $J = 2.1$ Hz)	117.5
3	-	150.3	-	145.6
4	-	144.9	-	150.7
5	6.88 (1H, d, $J = 8.0$ Hz)	123.1	6.89 (1H, d, $J = 8.4$ Hz)	115.6
6	7.45 (1H, d, $J = 10.27$ Hz)	115.1	7.47 (1H, d, $J = 8.1, 1.8$ Hz)	123.6
1'	-	207.0	-	167.5

The HR-EI-MS spectrum (Figure 75) of compound **IV** displayed $[\text{M}+\text{H}]^+$ at m/z 177.0125. A molecular formula was assigned and calculated as $\text{C}_7\text{H}_6\text{O}_4$ (177.0164). Thus, compound **IV** was elucidated as 3,4-dihydroxybenzoic acid. The structure of compound **IV** is shown in Figure 24.

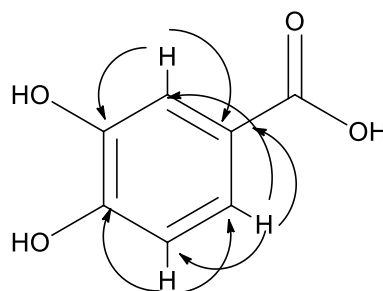


Figure 23 HMBC correlations of compound **IV**

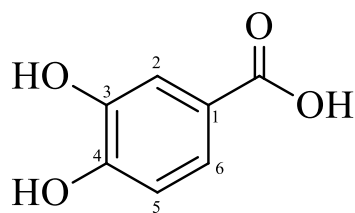


Figure 24 The structure of compound **IV**

In this study, 3,4-dihydroxybenzoic acid was isolated for the first time from *M. zapota* barks. 3,4-Dihydroxybenzoic acid was found in leaves of *Ageratum conyzoides* [125] and stem barks of *Musanga cecropioides* [124]. Benzoic acid derivatives showed biological activities such as antimicrobial and antioxidant activities [126].

4.7.5 Elucidation of compound **V**

Compound **V** was obtained as white crystal (10.5 mg, 0.00076% w/w of ethyl acetate crude extract) with melting point of 284-286 °C. The optical rotation was determined as $[\alpha]_D^{28} +0.7$ (CH₃Cl₃; c 3.24). The ¹H-NMR spectrum (Figure 76) showed seven signals of methyl proton at δ 1.09 (3H, s, H-27), 0.98 (1H, s, H-23), 0.95 (1H, s, H-29), 0.93 (1H, s, H-24), 0.91 (2H, s, H-26 and H-30), 0.82 (1H, s, H-28) and 0.80 (1H, s, H-25) ppm. One signal of olefinic proton showed at δ 5.53 (1H, dd, $J = 8.1, 3.3$ Hz, H-15) ppm. Four signals of methine proton showed at δ 0.76 (1H, d, $J = 2.7$ Hz, H-5), 3.19 (1H, dd, $J = 8.1, 3.3$ Hz, H-3), 1.44 (m, H-18) and 0.76 (1H, d, $J = 2.7$ Hz, H-5) ppm. Thirteen signals of methylene proton displayed at δ 1.92 ppm (1H, dd, $J = 14.7, 3.0$ Hz, H-16a), 2.03 (1H, dt, $J = 11.7, 3.0$ Hz, H-19a), 1.65 (2H, m, H-2a and H-21a), 1.64 (2H, m, H-6a and H-11a), 1.62 (2H, m, H-1a and H-22a), 1.58 (3H, m, H-1b, H-6b and H-21b), 1.39 (1H, m, H-11b), 1.38 (1H, m, H-22b), 1.33 (1H, m, H-19b), 1.31 (2H, m, H-7a and H-12a), 1.30 (1H, m, H-16b), 1.25 (1H, m, H-2b) and 1.02 (1H, m, H-7b, H-9 and H-12b) ppm.

The ¹³C-NMR spectrum (Figure 77) showed thirty carbon atoms. Two signals of olefinic carbons showed at δ 158.2 and 117.0 ppm and suggested that these chemical shifts were C-14 and C-15. A signal carbon at 79.2 ppm indicated a C-3 substituted hydroxyl group (OH). Seven signals of methyl carbon displayed at δ 33.5 (C-29), 30.1 (C-28), 30.0 (C-26), 28.1 (C-23), 26.1 (C-27), 21.5 (C-30) and 15.6 (C-24 and C-25) ppm. Eight signals of methylene carbon showed at δ 37.9 (C-1), 36.8 (C-16), 35.3 (C-

7 and C-12), 33.8 (C-21), 33.2 (C-22), 27.3 (C-2), 18.9 (C-6) and 17.7 (C-11) ppm. Five signals of methine carbon showed at δ 79.2 (C-3), 55.7 (C-5), 49.4 (C-18), 48.9 (C-9) and 41.5 (C-19) ppm. Six signals of quaternary carbon appeared at δ 39.1 (C-8), 38.9 (C-4), 38.2 (C-17), 37.7 (C-13), 35.9 (C-10) and 29.0 (C-20) ppm.

Experiments of HSQC, HMBC and COSY analysis (Figures 80-82) were confirmed the structure of compound **V** and HMBC spectrum (Figure 81) showed correlation peaks of H-3/C-1, 2 and 4, H-5/C-6 and 10, H-7/C-6 and 8, H-9/C-10 and 11, H-15/C-14 and 16, H-18/C-13 and 19, H-23/C-3, 4 and 5, H-24/C-3, 4 and 5, H-25/C-1, 5 and 10, H-26/C-7, 8 and 9, H-27/C-11, 12 and 13, H-28/C-16, 17 and 22, H-29/C-18, 19 and 20 and H-30/C-20, 21 and 22 (Figure 25).

Comparison of NMR data of compound **V** and reported literature [116] are shown in Table 49.

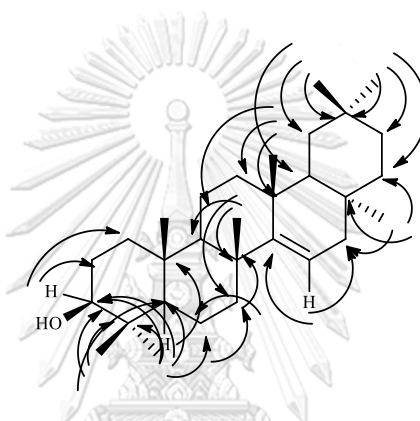
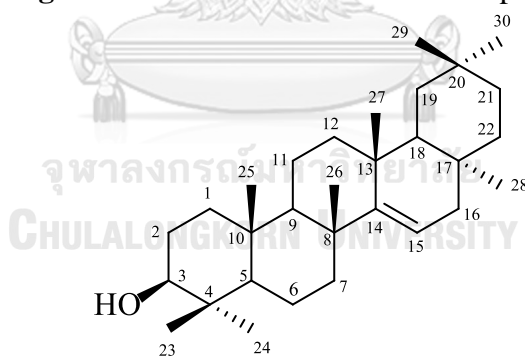
Table 49 Comparison of NMR data of compound **V** and taraxerol

Position	Chemical shift (ppm)			
	Taraxerol δ_H	Taraxerol δ_C	Compound V δ_H	Compound V δ_C
1		38.0	1.62 (m), 1.58 (m)	37.9
2		27.2	1.65 (m), 0.96 (m)	27.3
3		79.1	3.19 (dd, 8.1, 3.3)	79.2
4		39.0	-	38.9
5		55.6	0.76 (d, 2.7)	55.7
6		18.8	1.57 (m), 1.58 (m)	18.9
7	2.0 (dt, 12.6, 3.1)	35.1	1.31 (m), 1.64 (m)	35.3
8		38.8	-	39.1
9		48.8	1.42 (m)	48.9
10		37.6	-	35.9
11		17.5	1.64 (m), 1.39 (m)	17.7
12		35.8	1.31 (m), 1.00 (m)	35.3
13		37.6	-	37.7
14		158.1	-	158.3
15	5.53 (dd, 8.2, 3.2)	116.9	5.53 (dd, 8.1, 3.3)	116.8
16	1.9 (dd, 14.6, 3.0)	36.7	1.64 (m), 1.30 (m)	36.8
17		37.7	-	38.2
18		49.3	1.44 (m)	49.4
19		41.3	2.03 (dt, 11.7, 3.0), 1.33 (m)	41.5
20		28.8	-	29.0
21		33.7	1.65 (m), 1.58 (m)	33.8
22		33.1	1.62 (m), 1.38 (m)	33.2
23	0.98 (s)	28.0	0.98 (s)	28.1
24	0.80 (s)	15.4	0.93 (s)	15.6
25	0.93 (s)	15.5	0.80 (s)	15.6
26	1.09 (s)	29.8	0.91 (s)	30.0
27	0.91 (s)	25.9	1.09 (s)	26.1
28	0.82 (s)	39.9	0.82 (s)	30.1

Table 49 Comparison of NMR data of compound **V** and taraxerol (continue)

Position	Chemical shift (ppm)			
	Taraxerol		Compound V	
	δ_{H}	δ_{C}	δ_{H}	δ_{C}
29	0.95 (s)	33.4	0.95 (s)	33.5
30	0.90 (s)	21.3	0.91 (s)	21.5

The HR-EI-MS spectrum (Figure 83) of compound **V** displayed $[\text{M}+\text{H}]^+$ at m/z 449.3748. A molecular formula was assigned and calculated as $\text{C}_{30}\text{H}_{50}\text{ONa}$ (449.3759). Thus, compound **V** was elucidated as taraxerol. The structure of compound **V** is shown in Figure 26.

**Figure 25** HMBC correlations of compound **V****Figure 26** The structure of compound **V**

Taraxerol was previously isolated from *M. obtusifolia* which showed antiplasmodial activity with IC_{50} value $> 100 \mu\text{g}/\text{mL}$ [104]. Moreover, taraxerol was produced from *Agrobacterium rhizogenes* transformed root cultured of *Clitoria ternatea* and showed anticancer activity [127]. Viswanadh *et al* reported that taraxerol was isolated from *Homonoia riparia* barks [128].

4.7.6 Elucidation of compounds **VI**

Compound **VI** was obtained as white crystal (15.4 mg, 0.0111% w/w of ethyl acetate crude extract) with melting point of 248-250 °C. The optical rotation was recorded as $[\alpha]_D^{28} +8.1$ (CHCl₃; c 1.60). The ¹H-NMR spectrum (Figure 84) showed six signals of methyl group at δ 1.14 (3H, s, H-27), 1.08 (6H, s, H-23 and H-25), 1.06 (3H, s, H-24), 0.95 (3H, s, H-29), 0.91 (6H, s, H-28 and H-30) and 0.83 (3H, s, H-26) ppm. One signal of olefinic proton showed at δ 5.56 (1H, dd, $J = 8.1, 2.1$ Hz, H-15) ppm. Three signals of methine proton showed at δ 2.58 (1H, m, H-3), 1.50 (2H, m, H-9 and H-18) and 1.33 (1H, m, H-5) ppm. Eleven signals of methylene proton displayed at δ 2.58 (1H, m, H-2a), 2.33 (1H, ddd, $J = 15.9, 6.3, 3.3$ Hz, H-2b), 2.31 (1H, m, H-21), 2.08 (1H, dt, $J = 12.9, 3.3$ Hz, H-19), 1.87 (1H, m, H-1a), 1.65 (2H, m, H-7 and H-12), 1.59 (1H, m, H-6), 1.58 (1H, m, H-11), 1.37 (1H, m, H-16), 1.32 (1H, m, H-22) and 0.99 (1H, m, H-1b) ppm.

The ¹³C-NMR spectrum (Figure 85) showed thirty carbon atoms. Two signals of olefinic carbon showed at δ 157.6 (C-14) and 117.3 (C-15) ppm. One signal of carbonyl carbon showed at δ 217.6 (C-3) ppm. Eight signals of methyl carbon appeared at δ 33.5 (C-29), 30.0 (C-26), 30.1 (C-28), 26.2 (C-23), 25.7 (C-27), 21.6 (C-24), 21.5 (C-30) and 14.9 (C-25) ppm. Eight signals of methylene carbon displayed at δ 38.5 (C-1), 36.8 (C-16), 35.2 (C-7 and C-12), 33.7 (C-21), 33.2 (C-22), 28.2 (C-2), 20.1 (C-6) and 17.6 (C-11) ppm. Three signals of methine carbon showed at δ 55.9 (C-5), 48.9 (C-9 and C-18) and 40.8 (C-19) ppm. Five signals of quaternary carbon appeared at 47.7 (C-4), 39.0 (C-8), 37.7 (C-10), 37.9 (C-13 and C-17) and 28.9 (C-20) ppm.

Experiments of HSQC, HMBC and COSY (Figures 88-90) analysis were confirmed the structure of compound **VI** and HMBC spectrum (Figure 89) showed correlation peaks of H-5/C-4 and 10, H-6/C-5, 7 and 8, H-9/C-10 and 11, H-11/C-10 and 12, H-15/C-14 and 16, H-16/C-17, 18 and 22, H-18/C-13, 19 and 20, H-23/C-3, 4 and 5, H-24/C-3, 4 and 5, H-25/C-1, 2 and 5, H-26/C-7, 8 and 14, H-27/C-12, 13 and 14, H-28/C-17, 21 and 22, H-29/C-18, 19 and 20 and H-30/C-19, 20 and 21 (Figure 27).

Comparison of NMR data of compound **VI** and reported literature [128] are shown in Table 50.

Table 50 Comparison of NMR data of compound **VI** and taraxerone

Position	Chemical shift (ppm)			
	Taraxerone δ_{H}	δ_{C}	Compound VI δ_{H}	δ_{C}
1		38.3	1.87 (1H, m) 0.99 (1H, m)	38.5
2	2.52 (2H, m)	34.1	2.33 (1H, ddd, $J = 15.9, 6.3, 3.3$ Hz) 2.58 (1H, m)	28.2
3		217.5	-	217.6
4		47.6	-	47.7
5		55.6	1.33 (1H, m)	55.9
6		20.0	1.59 (1H, m)	20.1
7		35.8	1.65 (2H, m)	35.2
8		38.9	-	39.0
9		48.7	1.50 (2H, m)	48.9
10		37.5	-	37.7
11		17.4	1.58 (1H, m)	17.6
12		29.9	1.65 (2H, m)	35.2
13		37.7	-	37.9
14		157.6	-	157.6
15	5.56 (1H, dd, $J = 8.4, 4.0$ Hz)	117.9	5.56 (1H, dd, $J = 8.1, 2.1$ Hz)	117.3
16		33.1	1.37 (1H, m)	36.8
17		40.6	-	37.9
18		47.8	1.50 (2H, m)	48.9
19		40.6	2.08 (1H, dt, $J = 12.9, 3.3$ Hz)	40.8
20		28.8	-	28.9
21		33.6	2.31 (1H, m)	33.7
22		28.8	1.32 (1H, m)	33.2
23	0.98 (3H, s)	26.1	1.08 (3H, s)	26.2
24	0.88 (3H, s)	21.5	1.06 (3H, s)	21.6
25	1.08 (3H, s)	14.6	1.08 (3H, s)	14.9
26	1.05 (3H, s)	29.9	0.83 (3H, s)	30.0
27	1.05 (3H, s)	25.6	1.14 (3H, s)	25.7
28	0.81 (3H, s)	29.9	0.91 (3H, s)	30.1
29	0.88 (3H, s)	33.6	0.95 (3H, s)	33.5
30	0.94 (3H, s)	21.4	0.91 (3H, s)	21.5

The HR-EI-MS spectrum (Figure 91) of compound **VI** displayed $[\text{M}+\text{H}]^+$ at m/z 447.3590. A molecular formula was assigned and calculated as $\text{C}_{30}\text{H}_{48}\text{ONa}$ (447.3602). Thus, compound **VI** was elucidated as taraxerone. The structure of compound **VI** is shown in Figure 28.

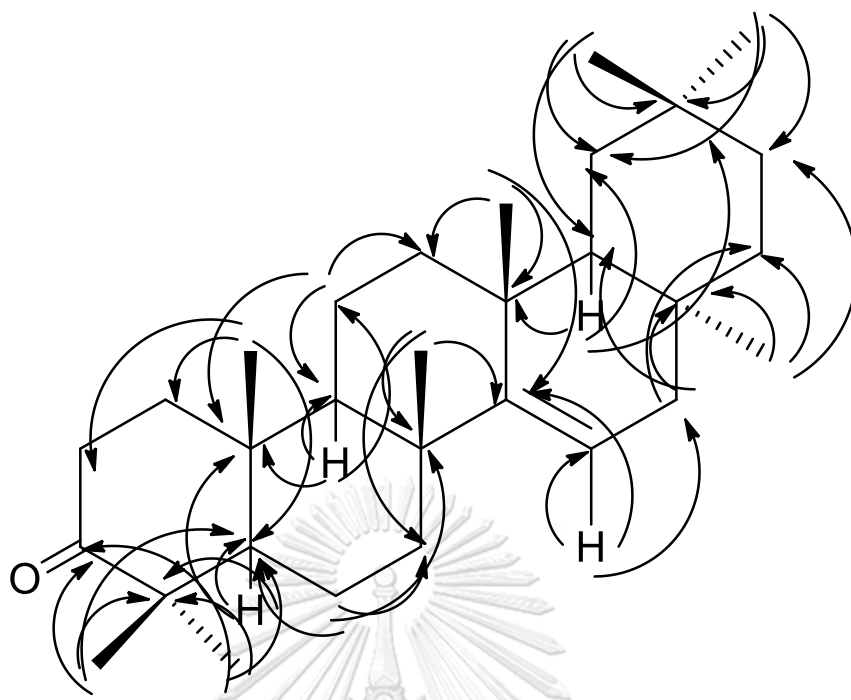


Figure 27 HMBC correlations of compound **VI**

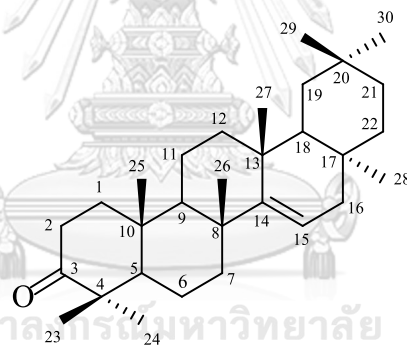


Figure 28 The structure of compound **VI**

Taraxerone was previously reported that it was isolated from *M. zapota* barks and showed cytotoxic activity against the human Caucasian prostate adenocarcinoma with IC_{50} value of $24.8 \pm 0.8 \mu\text{g/ml}$ [94]. Furthermore, taraxerone was isolated from barks of *Homonoia riparia* [128] and leaves of *Sedum sarmentosum* [129].

4.6.7 Elucidation of compounds **VII**

Compound **VII** was obtained as white powder (20.0 mg, 0.0145% w/w of ethyl acetate crude extract) with melting point of 210-212 °C. The optical rotation was recorded as $[\alpha]_D^{28} +45.1$ (CHCl_3 ; c 1.76). The $^1\text{H-NMR}$ spectrum (Figure 92) showed seven signals of methyl proton appeared at δ 2.04 (3H, s, H-2'), 1.03 (3H, s, H-23), 0.94

(3H, s, H-27), 0.85 (3H, s, H-26), 0.84 (3H, s, H-25), 0.83 (3H, s, H-24), 0.78 (3H, s, H-28). Two signals of olefinic proton appeared at δ 4.68 (1H, $J = 1.5$ Hz, H-29a) and 4.58 (1H, dd, $J = 1.2, 0.6$ Hz, H-29b) ppm. Six signals of methine proton showed at δ 4.47 (1H, dd, $J = 6.3, 3.6$ Hz, H-3), 2.37 (1H, dt, $J = 9.6, 3.6$ Hz, H-19), 1.34 (m, H-18), 1.30 (m, H-9), 0.98 (m, H-13) and 0.81 (1H, dd, $J = 4.5, 2.7$ Hz, H-5) ppm. Seventeen signals of methylene proton appeared at δ 2.04 (s, H-2'), 1.91 (m, H-21a and H-30a), 1.67 (m, H-15a), 1.62 (m, H-2a and H-12a), 1.59 (m, H-1a), 1.51 (m, H-6a), 1.49 (m, H-16a), 1.41 (m, H-2b and H-11a), 1.40 (m, H-16b and H-22a), 1.39 (m, H-6b), 1.38 (m, H-7a), 1.35 (m, H-7b), 1.25 (m, H-21b and H-30b), 1.21 (m, H-11b and H-22b), 1.06 (m, H-12b), 0.96 (m, H-1b) and 0.86 (m, H-15b) ppm.

The ^{13}C -NMR spectrum (Figure 93) showed thirty two carbon atoms. Two signals of olefinic carbon showed at δ 151.1 (C-20) and 109.5 (C-19) ppm. One signal of carbonyl carbon showed at δ 171.4 (C-1') ppm. Eight signals of methyl carbon displayed at δ 28.1 (C-23), 21.5 (C-2'), 19.4 (C-30), 18.1 (C-28), 16.6 (C-26), 16.3 (C-24), 16.1 (C-25) and 14.6 (C-27) ppm. Ten signals of methylene carbon appeared at δ 40.1 (C-22), 38.5 (C-1), 35.7 (C-16), 34.4 (C-7), 30.0 (C-21), 27.6 (C-15), 25.2 (C-12), 23.9 (C-2), 21.1 (C-11) and 18.3 (C-6) ppm. Six signals of methine carbon showed at δ 81.2 (C-3), 55.5 (C-5), 50.5 (C-9), 48.2 (C-18), 48.4 (C-19) and 38.2 (C-13) ppm. Four signals of quaternary carbon appeared at δ 43.1 (C-14 and C-17), 41.0 (C-8), 37.9 (C-4) and 37.2 (C-10) ppm.

Experiments of HSQC, HMBC and COSY analysis (Figures 96-98) were confirmed the structure of compound **VII** and HMBC spectrum (Figure 99) showed correlation peaks of H-3/C-1 and 2, H-5/C-4, 6 and 10, H-9/C-10 and 11, H-13/C-11, 12 and 18, H-15/C-14, 16 and 17, H-23/C-3, 4 and 5, H-24/C-3, 4 and 5, H-25/C-1, 5 and 10, H-26/C-7, 8 and 9, H-27/C-7, 8 and 14, H-28/C-17, 18 and 22 and H-29/C-19, 20 and 30 (Figure 29).

Comparison of NMR data of compound **VII** and reported literature [130] are shown in Table 51.

Table 51 Comparison of NMR data of compound **VII** and lupeol acetate

Position	Chemical shift (ppm)			
	lupeol acetate		Compound VII	
	δ_{H}	δ_{C}	δ_{H}	δ_{C}
1		38.3	1.59 (m), 0.96 (m)	38.5
2		23.7	1.62 (m), 1.41 (m)	23.9
3	4.44 (1H, dd, $J = 10.8, 5.8$ Hz)	80.9	4.47 (1H, dd, $J = 6.3, 3.6$ Hz)	81.2
4		37.7	-	37.9
5	0.76 (1H, dd, $J = 10.8, 5.8$ Hz)	55.3	0.81 (1H, dd, $J = 4.5, 2.7$ Hz)	55.5
6		18.1	1.51 (m) 1.39 (m)	18.3
7		34.2	1.38 (m), 1.35 (m)	34.4
8		40.8	-	41.0
9		50.3	1.30 (m)	50.5
10		37.0	-	37.2
11		20.9	1.41 (m) 1.21 (m)	21.1
12		25.0	1.62 (m), 1.06 (m)	25.2
13		38.0	0.98 (m)	38.2
14		42.8	-	43.1
15		27.4	1.67 (m), 0.86 (m)	27.6
16		35.5	1.49 (m) 1.40 (m)	35.7
17		42.9	-	43.1
18		48.0	1.34 (m)	48.2
19	2.33 (1H, dt, $J = 11.1, 5.6$ Hz)	48.2	2.37 (1H, dt, $J = 9.6, 3.6$ Hz)	48.4
20		150.9	-	151.1
21	1.82-1.93 (2H, m)	29.8	1.91 (m) 1.25 (m)	30.0
22		39.9	1.40 (m), 1.21 (m)	40.1
23	0.82 (3H, s)	28.2	1.03 (3H, s)	28.1
24	0.82 (3H, s)	15.9	0.83 (3H, s)	16.3
25	0.82 (3H, s)	16.1	0.84 (3H, s)	16.1
26	1.00 (3H, s)	16.4	0.85 (3H, s)	16.6
27	0.91 (3H, s)	14.5	0.94 (3H, s)	14.6
28	0.81 (3H, s)	17.9	0.78 (3H, s)	18.1
29	4.66 (1H, s)	109.3	4.68 (1H, d, $J = 1.5$ Hz)	109.5
	4.54 (1H, s)		4.58 (1H, dd, $J = 1.2, 0.6$ Hz)	
30	1.66 (3H, s)	19.0	1.91 (m), 1.25 (m)	19.4
1'		171.0	-	171.4
2'	2.01 (3H, s)	21.3	2.04 (3H, s)	21.5

The HR-EI-MS spectrum (Figure 100) of compound **VII** displayed $[M+H]^+$ at m/z 464.3328. A molecular formula was assigned and calculated as $C_{32}H_{53}ONa$ (464.3994). Thus, compound **VII** was elucidated as lupeol acetate. The structure of compound **VII** is shown in Figure 30.

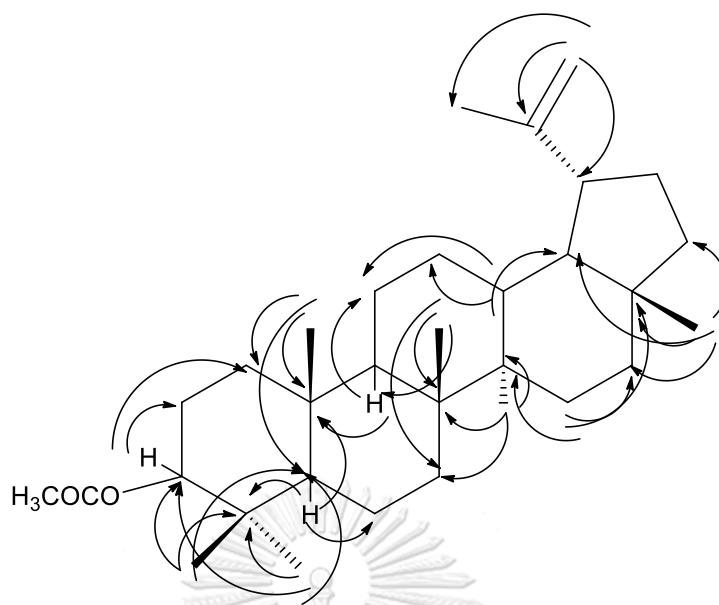


Figure 29 HMBC correlations of compound **VII**

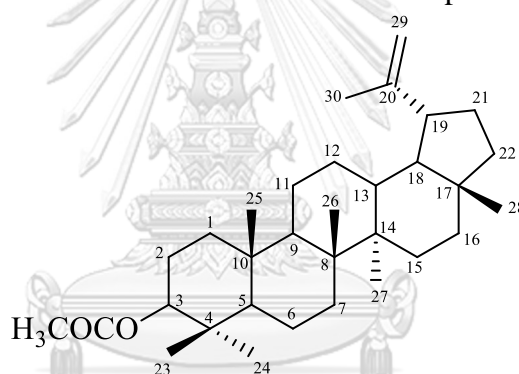


Figure 30 The structure of compound **VII**

Lupeol acetate was previously isolated from *M. zapota* barks and showed cytotoxic activity against the human Caucasian prostate adenocarcinoma with IC_{50} value of $61.2 \pm 0.7 \mu\text{g/mL}$ [94]. Lupeol acetate was isolated from *Diospiros rubra* stem and showed antimicrobial activity against *Corynebacterium diphtheriae* (NCTC 10356) with minimum inhibitory concentrations (MIC) value of $64 \mu\text{g/mL}$ [130].

The investigation of the chemical constituents of *M. zapota* using tyrosinase activity guided fractionation was performed. It was found that three kinds of isolated compounds **I-VII** were distinguished as triterpenoid, flavonoid and phenolic compounds. Triterpenoid consisted of taraxerol methyl ether (**I**), taraxerol (**V**) and

taraxerone (**VI**). Flavonoid had two compounds as 6-hydroxyflavanone (**II**) and (+)-dihydrokaempferol (**III**). 3,4-dihydroxy benzoic acid (**IV**) was a phenolic compound.

4.8 Antityrosinase activities of isolated compounds I-VII

Tyrosinase inhibitory activity is the assay for skin whitening agent. The tyrosinase inhibitory activity of compounds **I-VII** was evaluated. Kojic acid and arbutin were used as positive controls. (+)-Dihydrokaempferol (**III**) showed the strongest tyrosinase inhibitory activity on monophenolase inhibitory activity with IC_{50} value of $32.17 \pm 0.32 \mu\text{M}$ and compared with the positive standard, kojic acid ($IC_{50} 40.21 \pm 0.63 \mu\text{M}$) and arbutin ($IC_{50} 116.30 \pm 0.45 \mu\text{M}$). 6-Hydroxyflavanone (**II**) and kojic acid exhibited similar inhibition of monophenolase activity with IC_{50} values of 41.76 ± 0.20 and $40.21 \pm 0.63 \mu\text{M}$, respectively. While, 6-hydroxyflavanone (**II**) exhibited higher antityrosinase activity than arbutin ($IC_{50} 116.30 \pm 0.45 \mu\text{M}$). 3,4-Dihydroxybenzoic acid (**IV**), taraxerone (**VI**) and lupeol acetate (**VII**) displayed moderate monophenolase inhibitory activity with IC_{50} values of 55.21 ± 0.70 , 70.63 ± 0.36 and $71.17 \pm 0.33 \mu\text{M}$, respectively, when compared with kojic acid ($IC_{50} 40.21 \pm 0.63 \mu\text{M}$). Taraxerol methyl ether (**I**) and taraxerol (**V**) showed weak monophenolase inhibitory activity with IC_{50} values of 106.53 ± 0.34 and $103.37 \pm 0.22 \mu\text{M}$, respectively.

For diphenolase inhibitory activity, (+)-dihydrokaempferol (**III**) and kojic acid displayed similar antityrosinase activity with IC_{50} values of 31.60 ± 0.73 and $30.07 \pm 0.32 \mu\text{M}$, respectively, while (+)-dihydrokaempferol (**III**) showed stronger against tyrosinase activity than the other compounds and arbutin ($IC_{50} 370.65 \pm 0.90 \mu\text{M}$). 6-Hydroxyflavanone (**II**), 3,4-dihydroxybenzoic acid (**IV**), taraxerone (**VI**) and lupeol acetate (**VII**) showed moderate antityrosinase activity with IC_{50} values of 63.10 ± 0.73 , 43.91 ± 0.21 , 90.60 ± 0.26 and $87.50 \pm 0.63 \mu\text{M}$, respectively. Taraxerol methyl ether (**I**) and taraxerol (**V**) exhibited weak diphenolase inhibitory activity with IC_{50} values of 283.33 ± 0.59 and $272.10 \pm 0.16 \mu\text{M}$, respectively. The IC_{50} values of compounds **I-VII** for antityrosinase activity are shown in Table 4.43.

These results showed that (+)-dihydrokaempferol (**III**) showed more antityrosinase activity on diphenolase inhibitory activity with IC_{50} value of $31.60 \pm 0.73 \mu\text{M}$ than previous study by Hou *et al* [36]. Hou *et al* reported that flavanone, dihydrokaempferol showed diphenolase inhibitory activity with IC_{50} value of 2.7 ± 0.7

mM [36]. Flavanone, artocarpanone showed diphenolase inhibitory activity with IC₅₀ value of 147.55 μ M [25]. The structure of artocarpanone had methoxy group that substituted at 7 position and three hydroxy groups at 5, 2' and 4' positions. It is suggested that methoxy group and the number of hydroxy group affected tyrosinase inhibitory activity.

Table 52 The IC₅₀ values of compounds **I-VII** for antityrosinase activities

Compound	IC ₅₀ (μ M)	
	Monophenolase inhibitory activity	Diphenolase inhibitory activity
Taraxerol methyl ether (I)	106.53 \pm 0.34	283.33 \pm 0.59
6-Hydroxyflavanone (II)	41.76 \pm 0.20	63.10 \pm 0.73
(+)-Dihydrokaempferol (III)	32.17 \pm 0.32	31.60 \pm 0.73
3,4-Dihydroxybenzoic acid (IV)	55.21 \pm 0.70	43.91 \pm 0.21
Taraxerol (V)	103.37 \pm 0.22	272.10 \pm 0.16
Taraxerone (VI)	70.63 \pm 0.36	90.60 \pm 0.26
Lupeol acetate (VII)	71.17 \pm 0.33	87.50 \pm 0.63
Kojic acid ^a	40.21 \pm 0.63	30.07 \pm 0.32
Arbutin ^a	116.30 \pm 0.45	370.65 \pm 0.90

^a Kojic acid and arbutin were used as positive controls.

4.9 Determination of antioxidant activities of isolated compounds I-VII

Antioxidant activities of isolated compounds **I-VII** were determined on DPPH radical scavenging activity, ABTS radical scavenging activity and FRAP activity (Table 54).

4.9.1 DPPH radical scavenging activity

(+)-Dihydrokaempferol (**III**) showed the strongest scavenging DPPH capacity with IC₅₀ value of 2.21 \pm 0.77 μ M, followed by 6-hydroxyflavanone (**II**) and 3,4-dihydroxybenzoic acid (**IV**) with IC₅₀ values of 3.21 \pm 0.70 and 4.71 \pm 0.10 μ M, respectively. While, taraxerol methyl ether (**I**), taraxerol (**V**), taraxerone (**VI**) and lupeol acetate (**VII**) displayed weak DPPH radical scavenging with IC₅₀ values of 77.31 \pm 0.60, 16.28 \pm 0.33, 10.20 \pm 0.40 and 87.10 \pm 0.31 μ M, respectively. Trolox showed a significant free radical scavenging DPPH capacity with IC₅₀ value of 1.92 \pm 0.22 μ M.

4.9.2 ABTS radical scavenging activity

(+)-Dihydrokaempferol (**III**) displayed the highest free radical scavenging ABTS activity with IC_{50} value of $214.83 \pm 0.51 \mu\text{M}$. 6-Hydroxyflavanone (**II**) exhibited stronger ABTS radical scavenging activity than 3,4-dihydroxybenzoic acid (**IV**) with IC_{50} values of 225.53 ± 0.95 and $290.14 \pm 0.95 \mu\text{M}$, respectively. Whereas, taraxerol methyl ether (**I**), taraxerol (**V**), taraxerone (**VI**) and lupeol acetate (**VII**) showed low ABTS radical scavenging activity with IC_{50} values of 520.22 ± 0.30 , 630.84 ± 0.54 , 334.83 ± 0.99 and $669.62 \pm 0.42 \mu\text{M}$, respectively. Trolox exhibited strong ABTS radical scavenging activity with IC_{50} value of $188.39 \pm 0.43 \mu\text{M}$.

4.9.3 FRAP activity

(+)-Dihydrokaempferol (**III**) showed the highest reducing capacity with FRAP value of $6.23 \pm 0.10 \mu\text{M}$, followed by 6-hydroxyflavanone (**II**) and 3,4-dihydroxybenzoic acid (**IV**) with FRAP values of 4.12 ± 0.12 and $3.00 \pm 0.40 \mu\text{M}$, respectively. However, taraxerol methyl ether (**I**), taraxerol (**V**), taraxerone (**VI**) and lupeol acetate (**VII**) exhibited weak reducing capacity with FRAP values of 1.31 ± 0.16 , 1.46 ± 0.11 , 1.12 ± 0.13 , and $1.28 \pm 0.30 \mu\text{M}$, respectively. Trolox exhibited the greatest reducing activity with FRAP value of $6.10 \pm 0.28 \mu\text{M}$.

Table 53 Antioxidant activities of isolated compounds **I-VII**

Compound	IC_{50} (μM)		FRAP (μM)
	DPPH	ABTS	
Taraxerol methyl ether (I)	77.31 ± 0.60	520.22 ± 0.30	1.31 ± 0.16
6-Hydroxyflavanone (II)	3.21 ± 0.70	225.53 ± 0.95	4.12 ± 0.12
(+)-Dihydrokaempferol (III)	2.21 ± 0.77	214.83 ± 0.51	6.23 ± 0.10
3,4-Dihydroxybenzoic acid (IV)	4.71 ± 0.10	290.14 ± 0.95	3.00 ± 0.40
Taraxerol (V)	16.28 ± 0.33	630.84 ± 0.54	1.46 ± 0.11
Taraxerone (VI)	10.20 ± 0.40	334.83 ± 0.99	1.12 ± 0.13
Lupeol acetate (VII)	87.10 ± 0.31	669.62 ± 0.42	1.28 ± 0.30
Trolox ^a	1.92 ± 0.22	188.39 ± 0.43	6.10 ± 0.28

^a Trolox was used as positive control.

From this study, 6-hydroxyflavanone (**II**), (+)-dihydrokaempferol (**III**) and 3,4-dihydroxybenzoic acid (**IV**) showed potent antioxidant activity. 6-Hydroxyflavanone (**II**) showed antioxidant activity on lipid peroxidation with IC_{50} value of $33 \mu\text{M}$ [131]. (+)-Dihydrokaempferol (**III**) showed antioxidant activity with DPPH and ABTS

radical scavenging activities with IC_{50} values of 24.6 ± 0.41 and 25.4 ± 0.68 $\mu\text{g/mL}$, respectively [132]. 3,4-dihydroxybenzoic acid (**IV**) showed antioxidant activity with DPPH radical scavenging activities with EC_{50} value of 0.093 μM [126]. These results supported that phenolic compounds had property as electron donating agents or hydrogen donating agents. Ability to donate electrons of phenolic compounds depends on hydroxyl substitution.

4.10 Determination of cytotoxicity of isolated compounds I-VII

Many phytochemicals have been developed for anticancer drugs. However, mortality rate of cancer patients was increased. Compounds **I-VII** were evaluated for cytotoxicity against five human cancer cell lines including breast (BT474), lung (ChaGo-K-1), liver (HepG₂), stomach (KATO-III), colon (SW620) carcinoma cell lines using MTT assay. In addition, normal human diploid lung fibroblast (Wi-38) was used as the normal cell line. Doxorubicin was used as a positive control. The IC_{50} values for inhibition of cytotoxicity are shown in Table 55.

Taraxerol methyl ether (**I**) and taraxerone (**VI**) displayed no cytotoxicity on tested carcinoma cell lines. 6-Hydroxyflavanone (**II**) exhibited cytotoxic activity against BT474, ChaGo-K-1, HepG₂, KATO-III and SW620 cell lines with IC_{50} values of 86.16 ± 0.45 , 57.73 ± 1.08 , 65.76 ± 2.37 , 88.78 ± 3.70 and 82.79 ± 1.33 μM , respectively. (+)-Dihydrokaempferol (**III**) showed cytotoxic activity against BT474, ChaGo-K-1, HepG₂, KATO-III and SW620 cell lines with IC_{50} values of 11.66 ± 0.42 , 12.32 ± 0.73 , 13.67 ± 0.38 , 39.79 ± 0.38 and 41.11 ± 1.08 μM , respectively. 3,4-Dihydroxybenzoic acid (**IV**) exhibited inhibitory effect on ChaGo-K-1 and BT474 cell lines with IC_{50} values of 79.22 ± 4.02 and 85.21 ± 3.96 μM , respectively and displayed no cytotoxic activity against HepG₂, KATO-III and SW620 cell lines. *Taraxerol* (**V**) showed anticancer activity against BT474, ChaGo-K-1, HepG₂ and KATO-III cell lines with IC_{50} values of 19.24 ± 0.40 , 26.75 ± 0.97 , 20.41 ± 1.43 and 26.49 ± 0.57 μM , respectively. In contrast, Toze *et al* reported that taraxerone (**VI**) showed cytotoxicity against the human Caucasian prostate adenocarcinoma cell line [93]. Lupeol acetate (**VII**) showed cytotoxic activity against BT474 cell line with IC_{50} value of 60.20 ± 0.90 μM and showed weak anticancer activity against KATO-III, SW620 and ChaGo-K-1 cell lines. Taraxerol methyl ether (**I**) showed cytotoxic activity against HeLa, HL-60

and MCF-7 with IC_{50} value $> 50 \mu\text{M}$ [116]. 6-Hydroxyflavanone (**II**) was reported to show cytotoxic activity against HeLa and BT474 cell lines [120, 121]. This literature data supported that 6-hydroxyflavanone (**II**) showed anticancer activity against BT474 with IC_{50} value of $184.95 \pm 1.61 \mu\text{M}$.

Table 54 Cytotoxic activities of compounds **I-VII**

Isolated compound	IC_{50} of cell lines (μM)					
	BT474	ChaGo-K-1	HepG ₂	KATO-III	SW620	Wi-38
Taraxerol methyl ether (I)	184.95 ± 1.61	> 227.07	> 227.07	> 227.07	> 227.07	> 227.07
6-Hydroxyflavanone (II)	86.16 ± 0.45	57.73 ± 1.08	65.76 ± 2.37	88.78 ± 3.70	82.79 ± 1.33	416.22
(+)-Dihydrokaempferol (III)	11.66 ± 0.42	12.32 ± 0.73	13.67 ± 0.38	39.79 ± 0.38	41.11 ± 1.08	346.92
3,4-Dihydroxybenzoic acid (IV)	85.21 ± 3.96	79.22 ± 4.02	364.72 ± 2.27	507.53 ± 4.61	591.36 ± 0.71	648.85
Taraxerol (V)	19.24 ± 0.40	26.75 ± 0.97	20.41 ± 1.43	26.49 ± 0.57	> 234.34	234.34
Taraxerone (VI)	> 235.45	> 235.45	> 235.45	> 235.45	> 235.45	235.45
Lupeol acetate (VII)	60.20 ± 0.90	199.87 ± 0.30	> 213.33	136.68 ± 0.66	182.67 ± 1.51	213.33
Doxorubicin ^a	1.21 ± 0.20	1.58 ± 0.40	2.70 ± 0.83	1.78 ± 0.20	1.82 ± 0.39	183.99

^a Doxorubicin was used as a positive control.

BT474 = breast carcinoma cell line, ChaGo-K-1 = lung bronchus carcinoma cell line, HepG₂ = liver carcinoma cell line, KATO-III = gastric carcinoma cell line, SW620 = colon carcinoma cell line and Wi-38 = human diploid lung fibroblast.

CHAPTER V

CONCLUSION

The six different parts of *M. zapota* were extract with methanol and water for evaluation on correlation of total phenolic and total flavonoid contents with antioxidant and antityrosinase activities. Six different parts consisted of barks, flowers, fruits, leaves, roots and seeds. Methanol crude extract of flowers showed the highest amount of total phenolic content, followed by methanol crude extract of barks and methanol crude extract of seeds. Methanol crude extract of seeds showed the highest total flavonoid content, followed by methanol crude extract of roots and aqueous crude extract of seeds. Moreover, methanol crude extract of seeds showed potent antioxidant activities with DPPH radical scavenging activity, ABTS radical scavenging activity and FRAP activity. The methanol crude extracts of barks, roots, leaves and aqueous crude extract of roots showed high monophenolase inhibitory activity. Methanol crude extracts of roots, flowers, leaves, barks and fruits displayed stronger diphenolase inhibitory activity than other crude extracts. Correlations between total phenolic content and antioxidant activities of crude extract of six different parts of *M. zapota* were high positive. Total phenolic content of crude extracts of different parts of *M. zapota* and ABTS radical scavenging activity showed high correlation ($r = 0.90$), followed by DPPH radical scavenging activity ($r = 0.79$) and FRAP assay ($r = 0.69$). These results indicated high total phenolic content of *M. zapota* revealed high radical scavenging activity and reducing capacity. While, no correlation between total phenolic content with antityrosinase activities and with total flavonoid content of crude extracts of different parts of *M. zapota*. A low correlations were found between total total flavonoid content of crude extracts of different parts of *M. zapota* and antioxidant activities with DPPH radical scavenging activity ($r = 0.35$), ABTS radical scavenging activity ($r = 0.29$) and FRAP assay ($r = 0.39$). Likewise, correlation between total flavonoid content with antityrosinase activities and correlation between antityrosinase and antioxidant activities were not correlated in crude extract of different parts of *M. zapota*.

In this study, methanol crude extract of roots, leaves and barks showed potent antityrosinase activity. Thus, tyrosinase inhibitors from *M. zapota* barks were isolated by activity-guided fractionation. *M. zapota* barks were extracted with *n*-hexane, ethyl acetate, methanol and water, respectively. *n*-Hexane, ethyl acetate and methanol crude extracts showed high tyrosinase inhibitory effect with percentage inhibition. They were conducted to isolate active compounds by bioassay-guided fractionation on tyrosinase inhibitory activity. Taraxerol methyl ether (**I**) was isolated from *n*-hexane crude extract of *M. zapota* barks. 6-Hydroxyflavanone (**II**) exhibited moderate antityrosinase activities on monophenolase and diphenolase inhibitory activities. (+)-dihydrokaempferol (**III**) showed potent against tyrosinase activities on both monophenolase and diphenolase inhibitory activities with IC₅₀ value of 32.17 ± 0.32 and 31.60 ± 0.73 μM, respectively. 3,4-dihydroxybenzoic acid (**IV**) displayed moderate antityrosinase activities on both monophenolase and diphenolase inhibitory activities. Taraxerol (**V**), taraxerone (**VI**) and lupeol acetate (**VII**) showed weak antityrosinase activities on monophenolase and diphenolase inhibitory activities. For antioxidant activities, taraxerol methyl ether (**I**), taraxerol (**V**), taraxerone (**VI**) and lupeol acetate (**VII**) exhibited weak antioxidant activities with DPPH radical scavenging activity, ABTS radical scavenging activity and FRAP capacity. 6-Hydroxyflavanone (**II**) and 3,4-dihydroxybenzoic acid (**IV**) showed moderate antioxidant activities on DPPH, ABTS and FRAP capacity assays. (+)-Dihydrokaempferol (**III**) displayed strong antioxidant activities with DPPH, ABTS radical scavenging activities with IC₅₀ values of 2.21 ± 0.70 and 225.53 ± 0.95 μM, respectively and showed high reducing capacity with FRAP value of 6.23 ± 0.10 μM. Comparison of isolated compounds **I-VII** for cytotoxic activity, taraxerol methyl ether (**I**) and taraxerone (**IV**) showed no cytotoxic activity against carcinoma cell lines. 6-Hydroxyflavanone (**II**), (+)-dihydrokaempferol (**III**) and 3,4-dihydroxybenzoic acid (**IV**) showed cytotoxic activity against BT474, ChaGo-K-1, HepG₂, KATO-III and SW620. Lupeol acetate (**VII**) displayed cytotoxic activity against BT474 and ChaGo-K-1. From the results, (+)-dihydrokaempferol (**III**) could be attributed for active constituent in cosmetic ingredient.

REFERENCES

- [1] Jablonski, N.G., and Chaplin, G. Human skin pigmentation, migration and disease susceptibility. Philosophical Transactions of the Royal Society B: Biological Sciences 367(1590) (2012): 785-792.
- [2] Jacobs, M., Levine, S., Abney, K., and Davids, L. Fifty shades of African lightness: a bio-psychosocial review of the global phenomenon of skin lightening practices. Journal of Public Health in Africa 7(552) (2016): 67-70.
- [3] Kvam, E., and Dahle, J. Pigmented melanocytes are protected against ultraviolet-a-induced membrane damage. Journal of Investigative Dermatology 121(3) (2003): 564-569.
- [4] Wickett, R.R., and Visscher, M.O. Structure and function of the epidermal barrier. American Journal of Infection Control 34(10) (2006): S98-S110.
- [5] Chang, T.S. An updated review of tyrosinase inhibitors. International Journal of Molecular Sciences 10(6) (2009): 2440-2475.
- [6] Chang, T.S. Natural melagenesis inhibitors acting through the down-regulation of tyrosinase activity. Materials 5(9) (2012): 1661-1685.
- [7] Plonka, P.M., and Grabacka, M. Melanin synthesis in microorganisms- biotechnological and medical aspects. Acta Biochimica Polonica 53(3) (2006): 429-443.
- [8] Ebanks, J.P., Wickett, R.R., and Boissy, R.E. Mechanisms regulating skin pigmentation: the rise and fall of complexion coloration. International Journal of Molecular Sciences 10(9) (2009): 4066-4087.
- [9] Marrot, L., and Meunier, J.R. Skin DNA photodamage and its biological consequences. Journal of the American Academy of Dermatology 58(1) (2008): 139-148.
- [10] Park, K.C., Huh, S.Y., Choi, H.R., and Kim, D.S. Biology of melanogenesis and the search for hypopigmenting agents. Dermatologica Sinica 28(2) (2010): 53-58.
- [11] Seo, S.Y., Sharma, V.K., and Sharma, N. Mushroom tyrosinase: recent prospects. Journal of Agricultural and Food Chemistry 51(10) (2003): 2837-2853.

- [12] Loizzo, M.R., Tundis, R., and Menichini, F. Natural and synthetic tyrosinase inhibitors as antibrowning agents: an update. Comprehensive Reviews in Food Science and Food Safety 11(1) (2012): 378-398.
- [13] Lajis, A.F.B., Hamid, M., and Ariff, A.B. Depigmenting effect of kojic acid esters in hyperpigmented B16F1 melanoma cells. Journal of Biomedicine and Biotechnology 2012 (2012), doi: 10.1155/2012/952452.
- [14] Al-Saleh, I., Elkhatib, R., Al-Rouqi, R., Al-Enazi, S., and Shinwari, N. The dangers of skin-lightening creams. Toxicological and Environmental Chemistry Journal 94(1) (2012): 195-219.
- [15] Chantaranonthai, P. Sapotaceae. in Santisuk, T. and Balslev, H. (eds.), Flora of Thailand, pp. 610-655. Bangkok: Department of National Parks, Wildlife and Plant Conservative, 2014.
- [16] Barbalho, S.M., Dos Santos Bueno, P.C., Delazari, D.S., Guiguer, E.L., Coqueiro, D.P., Araújo, A.C., De Souza Mda, S., Farinazzi-Machado, F.M., Mendes, C.G., and Groppo, M. Antidiabetic and antilipidemic effects of *Manilkara zapota*. Journal of Medicinal Food 18(3) (2015): 385-391.
- [17] Ganguly, A., Mahmud, Z., Uddin, M.M.N., and Rahman, S.M.A. *In-vivo* anti-inflammatory and anti-pyretic activities of *Manilkara zapota* leaves in albino Wistar rats. Asian Pacific Journal of Tropical Disease 3(4) (2013): 301-307.
- [18] Kaneria, M., and Chanda, S. Evaluation of antioxidant and antimicrobial properties of *Manilkara zapota* L. (chiku) leaves by sequential soxhlet extraction method. Asian Pacific Journal of Tropical Biomedicine 2(3) (2012): S1526-S1533.
- [19] Baroni, A., Buommino, E., De Gregorio, V., Ruocco, E., Ruocco, V., and Wolf, R. Structure and function of the epidermis related to barrier properties. Clinics in Dermatology 30(3) (2012): 257-262.
- [20] Hwa, C., Bauer, E.A., and Cohen, D.E. Skin biology. Dermatologic Therapy 24(5) (2011): 464-470.
- [21] Brown, S.J., and Mclean, W.H. One remarkable molecule: filaggrin. Journal of Investigative Dermatology 132(3) (2012): 751-762.

- [22] Solano, F. Melanins: skin pigments and much more-types, structural, models, biological functions, and formation routes. New Journal of Science (2014), doi: 101155/2014498276.
- [23] Ando, H., Niki, Y., Ito, M., Akiyama, K., Matsui, M., Yarosh, D., and Ichihashi, M. Melanosomes are transferred from melanocytes to keratinocytes through the processes of packaging, release, uptake, and dispersion. Journal of Investigative Dermatology 132(4) (2012): 1222-1229.
- [24] Uchida, R., Ishikawa, S., and Tomoda, H. Inhibition of tyrosinase activity and melanine pigmentation by 2-hydroxytyrosol. Acta Pharmaceutica Sinica B 4(2) (2014): 141-145.
- [25] Dej-adisai, S., Meechai, I., Puripattanavong, J., and Kummee, S. Antityrosinase and antimicrobial activities from Thai medicinal plants. Archives of Pharmacal Research 37(4) (2014): 473-483.
- [26] Lee, C.C., Chen, Y.T., Chiu, C.C., Liao, W.T., Liu, Y.C., and Wang, H.M.D. *Polygonum cuspidatum* extracts as bioactive antioxiadaion, anti-tyrosinase, immune stimulation and anticancer agents. Journal of Bioscience and Bioengineering 119(4) (2015): 464-469.
- [27] Radhakrishnan, S., Shimmon, R., Conn, C., and Baker, A. Design, synthesis and biological evaluation of hydroxy substituted amino chalcone compounds for antityrosinase activity in B16 cells. Bioorganic Chemistry 62 (2015): 117-123.
- [28] Ben-Yosef, V.S., Sendovski, M., and Fishman, A. Directed evolution of tyrosinase for enhanced monophenolase/diphenolase activity ratio. Enzyme and Microbial Technology 47(7) (2010): 372-376.
- [29] Fang, D., Tsuji, Y., and Setaluri, V. Selective down-regulation of tyrosinase family gene TYRP1 by inhibition of the activity of melanocyte transcription. Nucleic Acids Research 30(14) (2002): 3096-3106.
- [30] Waldrop, G.L. A qualitative approach to enzyme inhibition. Biochemistry and Molecular Biology Education 37(1) (2009): 11-15.
- [31] Thoma, J.A., and Koshland, D.E.J. Competitive inhibition by substrate during enzyme action evidence for the induced-fit theory. Journal of the American Chemical Society 82(13) (1960): 3329-3333.

- [32] Dat, L.D., Thao, N.P., Luyen, B.T.T., Tai, B.H., Jeong, M.H., Woo, M.H., and Kim, Y.H. Identification of six new lupane-type triterpenoids from *Acanthopanax koreanum* leaves and their tyrosinase inhibitory activities. Bioorganic and Medicinal Chemistry Letters 26(3) (2016): 1061-1067.
- [33] Peralta, M.A., Santi, M.D., Agnese, A.M., Cabrera, J.L., and Ortega, M.G. Flavanoids from *Dalea elegans*: chemical reassignment and determination of kinetics parameters related to their anti-tyrosinase activity. Phytochemistry Letters 10(1) (2014): 260-267.
- [34] Prasad, K.N., Yang, B., Shi, J., Yu, C., Zhao, M., Xue, S., and Jiang, Y. Enhanced antioxidant and antityrosinase activities of longan fruit pericarp by ultra-high-pressure-assisted extraction. Journal of Pharmaceutical and Biomedical Analysis 51(2) (2010): 471-477.
- [35] Mapunya, M.B., Hussein, A.A., Rodriguez, B., and Lall, N. Tyrosinase activity of *Greyia flanaganii* (Bolus) constituents. Phytomedicine 18(11) (2011): 1006-1012.
- [36] Hou, S., Tan, T., Du, W., and Chen, G. Chemical constituents from the bark of *Juglans mandshurica* Maxim. and their phenol oxidase inhibitory effects. Archives of Phytopathology and Plant Protection 50(9-10) (2017): 463-472.
- [37] Prasad, K.N., Yang, B., Yang, S., Chen, Y., Zhao, M., Ashraf, M., and Jiang, Y. Identification of phenolic compounds and appraisal of antioxidant and antityrosinase activities from litchi (*Litchi sinensis* Sonn.) seeds. Food Chemistry 116(1) (2009): 1-7.
- [38] Narayanaswamy, N., Rohini, S., Duraisamy, A., and Balakrishnan, K.P. Antityrosinase and antioxidant activities of various parts of *Mimusops elengi*: a comparative study. International Journal of Cosmetic Science 1(1) (2011): 17-22.
- [39] Zhang, Y., Chen, J., Wang, L., Cao, J., and Xu, L. Chemical composition and biological activities of the essential oil from *Rubus pungens* var. *oldhamii*. Natural Product Research 31(12) (2017): 1454-1458.
- [40] Momtaz, S., Mapunya, B., Houghton, P.J., Edgerly, C., Hussein, A., Naidoo, S., and Lall, N. Tyrosinase inhibition by extracts and constituents of *Sideroxylon*

- inermis* L. stem bark, used in South Africa for skin lightening. Journal of Ethnopharmacology 119(3) (2008): 507-512.
- [41] Barbosa, A.F., Silva, K.C.B., De Oliveira, M.C.C., De Carvalho, M.G., and Srur, A.U.O.S. Effects of *Acmella oleracea* methanolic extract and fractions on the tyrosinase enzyme. Revista Brasileira de Farmacognosia 26(3) (2016): 321-325.
- [42] Nguyen, H.X., Nguyen, N.T., Nguyen, M.H.K., Le, T.H., Do, T.N.V., Hung, T.M., and Nguyen, M.T.T. Tyrosinase inhibitory activity of flavonoids from *Artocarpus heterophyllous*. Chemistry Central Journal 10 (2016), doi: 10.1186/s13065-016-0150-7.
- [43] Wang, B.S., Chang, L.W., Wu, H.C., Huang, S.L., Chu, H.L., and Huang, M.H. Antioxidant and antityrosinase activity of aqueous extracts of green asparagus. Food Chemistry 127(1) (2011): 141-146.
- [44] Aumeeruddy-Elalfi, Z., Gurib-Fakim, A., and Mahomoodally, M.F. Kinetic studies of tyrosinase inhibitory activity of 19 essential oils extracted from endemic and exotic medicinal plants. South African Journal of Botany 103(1) (2016): 89-94.
- [45] Zhang, C., Lu, Y., Tao, L., Tao, X., Su, X., and Wei, D. Tyrosinase inhibitory effects and inhibition mechanisms of nobliletin and hesperidin from citrus peel crude extracts. Journal of Enzyme Inhibition and Medicinal Chemistry 22(1) (2007): 83-90.
- [46] Chang, L.W., Juang, L.J., Wang, B.S., Wang, M.Y., Tai, H.M., Hung, W.J., Chen, Y.J., and Huang, M.H. Antioxidant and antityrosinase activity of mulberry (*Morus alba* L.) twigs and root bark. Food and Chemical Toxicology 49(4) (2011): 785-790.
- [47] Abdillahi, H.S., Finnie, J.F., and Staden, J.V. Anti-inflammatory, antioxidant, anti-tyrosinase and phenolic contents of four *Podocarpus* species used in traditional medicine in South Africa. Journal of Ethnopharmacology 136(3) (2011): 496-503.
- [48] Biswas, R., Mukherjee, P.K., Dalai, M.K., Mandal, P.K., and Nag, M. Tyrosinase inhibitory potential of purpurin in *Rubia cordifolia*-a bioactivity guided approach. Industrial Crops and Products 74(1) (2015): 319-326.

- [49] Dej-adisai, S., Parndaeng, K., and Wattanapiromsakul, C. Determination of phytochemical compounds, and tyrosinase inhibitory and antimicrobial activities of bioactive compounds from *Streblus ilicifolius* (S Vidal) Corner. Tropical Journal of Pharmaceutical Research 15(3) (2016): 497-506.
- [50] Ye, Y., Chou, G.X., Mu, D.D., Wang, H., Chu, J.H., Leung, A.K.M., Fong, W.F., and Yu, Z.L. Screening of Chinese herbal medicines for antityrosinase activity in a cell free system and B16 cells. Journal of Ethnopharmacology 129(3) (2010): 387-390.
- [51] Tan, Y.P., and Chan, E.W.C. Antioxidant, antityrosinase and antibacterial properties of fresh and processed leaves of *Anacardium occidentale* and *Piper betle*. Food Bioscience 6 (2014): 17-23.
- [52] Di Petrillo, A., González-Paramás, A.M., Era, B., Medda, R., Pintus, F., Santos-Buelga, C., and Fais, A. Tyrosinase inhibition and antioxidant properties of *Asphodelus microcarpus* extracts. BMC Complementary and Alternative Medicine 16(1) (2016): 453-461.
- [53] Salleh, W.M.N.H.W., Ahmad, F., Yen, K.H., and Zulkifli, R.M. Chemical composition and biological activities of essential oil of *Beilschmiedia pulverulenta*. Pharmaceutical Biology 54(2) (2016): 322-330.
- [54] Biswas, R., Mukherjee, P., and Chaudhary, S.K. Tyrosinase inhibition kinetic studies of standardized extract of *Berberis aristata*. Natural Product Research 30(12) (2015): 1451-1454.
- [55] Gupta, S., Adak, S., Rajak, R.C., and Banerjee, R. *In vitro* efficacy of *Bryophyllum pinnatum* leaf extracts as potent therapeutics. Preparative Biochemistry and Biotechnology 46(5) (2016): 489-494.
- [56] Özer, Ö., Mutlu, B., and Kivçak, B. Antityrosinase activity of some plant extracts and formulations containing ellagic acid. Pharmaceutical Biology 45(6) (2007): 519-524.
- [57] Rangkadilok, N., Sitthimonchai, S., Worasuttayangkurn, L., Mahidol, C., Ruchirawat, M., and Satayavivad, J. Evaluation of free radical scavenging and antityrosinase activities of standardized longan fruit extract. Food and Chemical Toxicology 45(2) (2011): 328-336.

- [58] Darusman, L.K., Batubara, I., Mitsunaga, T., Rahminiwati, M., Djauhari, E., and Yamauchi, K. Tyrosinase kinetic inhibition of active compounds from *Intsia palembanica*. Research Journal of Medicinal Plant 6(8) (2012): 615-620.
- [59] Lourith, N., Kanlayavattanakul, M., Chaikul, P., Chansriniyom, C., and Bunwatcharaphansakun, P. *In vitro* and cellular activities of the selected fruits residues for skin aging treatment. Anais da Academia Brasileira de Ciências 89(1 Suppl.) (2017): 577-589.
- [60] Brahmi, F., Hauchard, D., Guendouze, N., Madani, K., Kiendrebeogo, M., Kamagaju, L., Stévigny, C., Chibane, M., and Duez, P. Phenolic composition, *in vitro* antioxidant effects and tyrosinase inhibitory activity of three Algerian *Mentha* species: *M. spicata* (L.), *M. pulegium* (L.) and *M. rotundifolia* (L.) Huds (Lamiaceae). Industrial Crops and Products 72(1) (2015): 722-730.
- [61] Sarkhail, P., Sarkheil, P., Khalighi-Sigaroodi, F., Shafiee, A., and Ostad, N. Tyrosinase inhibitor and radical scavenger fractions and isolated compounds from aerial parts of *Peucedanum knappii* Bornm. Natural Product Research 27(10) (2013): 896-899.
- [62] Hashim, N.A., Ahmad, F., Jani, N.A., and Susanti, D. *In vitro* antioxidant, antityrosinase, antibacterial and cytotoxicity activities of the leaf and stem essential oil from *Piper magnibaccum* C. DC. Journal of Essential Oil Bearing Plants 20(1) (2017): 223-232.
- [63] Maack, A., and Pegard, A. *Populus nigra* (Salicaceae) absolute rich in phenolic acids, phenylpropanoids and flavonoids as a new potent tyrosinase inhibitor. Fitoterapia 111(1) (2016): 95-101.
- [64] Chiang, H.M., Chien, Y.C., Wu, C.H., Kuo, Y.H., Wu, W.C., Pan, Y.Y., Su, Y.H., and Wen, K.C. Hydroalcoholic extract of *Rhodiola rosea* L. (Crassulaceae) and its hydrolysate inhibit melanogenesis in B16F0 cells by regulating the CREB/MITF/tyrosinase pathway. Food and Chemical Toxicology 65(1) (2014): 129-139.
- [65] Solimine, J., Garo, E., Wedler, J., Rusanov, K., Fertig, O., Hamburger, M., Atanassov, I., and Butterweck, V. Tyrosinase inhibitory constituents from a polyphenol enriched fraction of rose oil distillation wastewater. Fitoterapia 108(1) (2016): 13-19.

- [66] Bravo, K., Alzate, F., and Osorio, E. Fruits of selected wild and cultivated Andean plants as sources of potential compounds with antioxidant and anti-aging activity. Industrial Crops and Products 85(1) (2016): 341-352.
- [67] Lai, J.S., Lin, C.C., and Chiang, T.M. Tyrosinase inhibitory activity and thermostability of the flavonoid complex from *Sophora japonica* L (Fabaceae). Tropical Journal of Pharmaceutical Research 13(2) (2014): 243-247.
- [68] Rao, G., Mukhopadhyay, T., and Radhakrishnan, N. Artoindonesianin F, a potent tyrosinase inhibitor from the roots of *Artocarpus heterophyllus* Lam. Indian Journal of Chemistry 49B (2010): 1264-1266.
- [69] Saewan, N., Koysomboon, S., and Chantrapromma, K. Anti-tyrosinase and anti-cancer activities of flavonoids from *Blumea balsamifera* DC. Journal of Medicinal Plants Research 5(6) (2011): 1018-1025.
- [70] Chang, C.T., Chang, W.L., Hsu, J.C., Shih, Y., and Chou, S.T. Chemical composition and tyrosinase inhibitory activity of *Cinnamomum cassia* essential oil. Botanical Studies 54 (2013), doi: 10.1186/1999/31105410.
- [71] Kim, J.E., Oh, T.H., Hyun, C.G., and Lee, N.H. Tyrosinase Inhibitory Chemical Constituents from *Cleyera japonica* Thunberg Branches. Rec. Nat. Prod. 8(3) (2014): 303-306.
- [72] Chen, Q.X., and Kubo, I. Kinetics of mushroom tyrosinase inhibition by quercetin. Journal of Agricultural and Food Chemistry 50(14) (2002): 4108-4112.
- [73] Jegal, J., Park, S., Chung, K., Chung, H.Y., Lee, J., Jeong, E.J., Kim, K.H., and Yang, M.H. Tyrosinase inhibitory flavonoid from *Juniperus communis* fruits. Bioscience, Biotechnology, and Biochemistry 80(12) (2016): 2311-2317.
- [74] Hua, X., Wang, M., Yan, G., Yu, M., Wang, H., and Hou, A. 2-Arylbzofuran and tyrosinase inhibitory constituents of *Morus notabilis*. Journal of Asian Natural Products Research 14(12) (2012): 1103-1108.
- [75] Chen, X.X., Liang, G., Chai, W.M., Feng, H.L., Zhou, H.T., Shi, Y., and Chen, Q.X. Antioxidant and antityrosinase proanthocyanidins from *Polyalthia longifolia* leaves. Journal of Bioscience and Bioengineering 118(5) (2014): 583-587.

- [76] Lu, T.M., and Ko, H.H. A new anthraquinone glycoside from *Rhamnus nakaharai* and anti-tyrosinase effect of 6-methoxysorigenin. Natural Product Research 30(23) (2016): 2655-2661.
- [77] Chen, H., Wang, C., Ye, J., Zhou, H., and Tao, R. Isolation of sulfuretin and butin from *Rhus verniciflua* stokes using medium-pressure liquid chromatography and their tyrosinase inhibitory effects. BioResources 11(1) (2016): 759-771.
- [78] Seong, Z.K., Kim, H.S., Won, Y.M., Kim, J.L., Song, H.H., Kim, D.Y., Oh, S.R., Cho, H.W., Cho, J.H., and Lee, H.K. Phenylacylphenol derivatives with anti-melanogenic activity from *Stewartia pseudocamellia*. Archives of Pharmacal Research 39(1) (2016): 636-645.
- [79] Jeong, C.H., and Shim, K.H. Tyrosinase inhibitor isolated from the leaves of *Zanthoxylum piperitum*. Bioscience, Biotechnology, and Biochemistry 68(9) (2004): 1984-1987.
- [80] Kubo, I., Chen, Q.X., Nihei, K.I., Calderón, J.S., and Céspedes, C.L. Tyrosinase inhibition kinetics of anisic acid. The Zeitschrift für Naturforschung 58(9-10) (2003): 713-718.
- [81] Fais, A., Corda, M., Era, B., Fadda, M.B., Matos, M.J., Quezada, E., Santana, L., Picciau, C., Podda, G., and Delogu, G. Tyrosinase inhibitor activity of coumarin-resveratrol hybrids. Molecules 14(7) (2009): 2514-2520.
- [82] Chen, X.X., Zhang, J., Chai, W.M., Feng, H.L., Xiang, Z.H., Shen, D.Y., and Chen, Q.X. Reversible and competitive inhibitory kinetics of amoxicillin on mushroom tyrosinase. International Journal of Bilological Macromolecules 62 (2013): 726-733.
- [83] Franco, D.C.Z., De Carvalho, G.S.G., Rocha, P.R., Da Silva Teixeira, R., Da Silva, A., and Raposo, N.R.B. Inhibitory effects of resveratrol analogs on mushroom tyrosinase activity. Molecules 17 (2012): 11816-11825.
- [84] Jia, Y., Zheng, J., Yu, F., Cai, Y., Zhan, X., Wang, H., and Chen, Q. Anti-tyrosinase kinetics and antibacterial process of caffeic acid *N*-nonyl ester in Chinese Olive (*Canarium album*) postharvest. International Journal of Bilological Macromolecules 91 (2016): 486-495.

- [85] Lee, K.H., Aziz, F.H.A., Syahida, A., Abas, F., Shaari, K., Israf, D.A., and Lajis, N.H. Synthesis and biological evaluation of curcumin-like diarylpentanoid analogues for anti-inflammatory, antioxidant and anti-tyrosinase activities. European Journal of Medicinal Chemistry 44(8) (2009): 3195-3200.
- [86] Han, Y., Park, Y., Ha, Y., Park, D., Lee, J., Lee, N., Yoon, J., Moon, H., and Chung, H. Characterization of a novel tyrosinase inhibitor, (2R,4R)-2-(2,4-dihydroxyphenyl)thiazolidine-4-carboxylic acid (MHY384). Biochimica et Biophysica Acta 1820 (2012): 542-549.
- [87] Chai, W.M., Liu, X., Hu, Y.H., Feng, H.L., Jia, Y.L., Guo, Y.J., Zhou, H.T., and Chen, Q.X. Antityrosinase and antimicrobial activities of furfuryl alcohol, furfural and furoic acid. International Journal of Biological Macromolecules 57(1) (2013): 151-155.
- [88] Chen, J., Yu, X., and Huang, Y. Inhibitory mechanisms of glabridin on tyrosinase. Spectrochimica Acta Part A: Molecular and Biomolecular Spectroscopy 168(1) (2016): 111-117.
- [89] Zhao, D.Y., Zhang, M.X., Dong, X.W., Hu, Y.Z., Dai, X.Y., Wei, X., Hider, R.C., Zhang, J.C., and Zhou, T. Design and synthesis of novel hydroxypyridinone derivatives as potential tyrosinase inhibitors. Bioorganic and Medicinal Chemistry Letters 26(1) (2016): 3103-3108.
- [90] Xia, L., Idhayadhulla, A., Lee, Y.R., Wee, Y.J., and Kim, S.H. Anti-tyrosinase, antioxidant, and antibacterial activities of novel 5-hydroxy-4-acetyl-2,3-dihydronaphtho[1,2-b]furans. European Journal of Medicinal Chemistry 86 (2014): 605-612.
- [91] Zhu, Y., Zhou, H., Hu, Y., Tang, J., Su, M., Guo, Y., Chen, Q., and Liu, B. Antityrosinase and antimicrobial activities of 2-phenylethanol, 2-phenylacetaldehyde and 2-phenylacetic acid. Food Chem 124 (2011): 298-302.
- [92] Iwadate, T., and Nihei, K. Rhododendrol glycosides as stereospecific tyrosinase inhibitors. Bioorganic and Medicinal Chemistry 23(20) (2015): 6650-6658.
- [93] Toze, F.a.A., Fomani, M., Nouga, A.B., Chouna, J.R., Kouam, A.F., Waffo, A.F.K., and Wansi, J.D. Taraxastane and lupane triterpenoids from the bark of *Manilkara zapota*. International Research Journal of Pure and Applied Chemistry 7(4) (2015): 157-164.

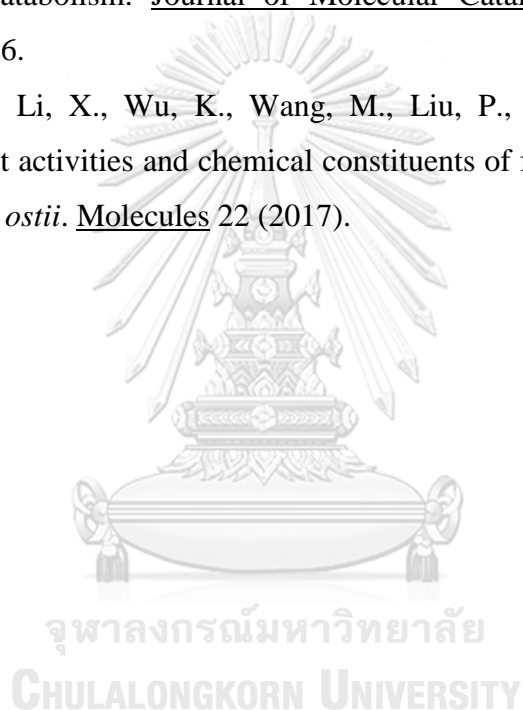
- [94] Ma, J., Luo, X.D., Protiva, P., Yang, H., Ma, C., Basile, M.J., Weinstein, I.B., and Kennelly, E.J. Bioactive novel polyphenols from the fruit of *Manilkara zapota* (Sapodilla). Journal of Natural Products 66(7) (2003): 983-986.
- [95] Pientaweeratch, S., Panapisal, V., and Tansirikongkol, A. Antioxidant, anti-collagenase and anti-elastase activities of *Phyllanthus emblica*, *Manilkara zapota* and silymarin: an *in vitro* comparative study for anti-aging applications. Pharm Biol 54(9) (2016): 1865-1872.
- [96] Rao, G.V., Sahoo, M.R., Madhavi, M.S.L., and Mukhopadhyay, T. Phytoconstituents from the leaves and seeds of *Manilkara zapota* Linn. Der Pharmacia Lettre 6(2) (2014): 69-73.
- [97] Osman, M.A., Rashid, M.M., Aziz, M.A., Habib, M.R., and Karim, M.R. Inhibition of Ehrlich ascites carcinoma by *Manilkara zapota* L. stem bark in Swiss albino mice. Asian Pacific Journal of Tropical Biomedicine 1(6) (2011): 448-451.
- [98] Awasare, S., Bhujbal, S., and Nanda, R. *In vitro* cytotoxic activity of novel oleanane type of triterpenoid saponin from stem bark of *Manilkara zapota* Linn. Asian Journal of Pharmaceutical and Clinical Research 5(4) (2012): 183-188.
- [99] Rajakumar, G., and Rahuman, A.A. Acaricidal activity of aqueous extract and synthesized silver nanoparticles from *Manilkara zapota* against *Rhipicephalus* (*Boophilus*) *microplus*. Research in Veterinary Science 93(1) (2012): 303-309.
- [100] Kothari, V., and Seshadri, S. *In vitro* antibacterial activity in seed extracts of *Manilkara zapota*, *Anona squamosa*, and *Tamarindus indica*. Biological Research 43(2) (2010): 165-168.
- [101] Shanmugapriya, K., Saravana, P.S., Payal, H., Mohammed, S.P., and Binnie, W. Antioxidant activity, total phenolic and flavenoid contents of *Artocarpus heterophyllus* and *Manilkara zapota* seeds and its reduction potential. International Journal of Pharmacy and Pharmaceutical Sciences 3(5) (2011): 256-260.
- [102] Kanlayavattanakul, M., and Lourith, N. Sapodilla seed coat as a multifunctional ingredient for cosmetic applications. Process Biochem 46(11) (2011): 2215-2218.

- [103] Rhourri-Frih, B., Renimel, I., Chaimbault, P., André, P., Herbette, G., and Lafosse, M. Pentacyclic triterpenes from *Manilkara bidentata* resin. Isolation, identification and biological properties. Fitoterapia 88 (2013): 101-108.
- [104] Simelane, M.B.C., Shonhai, A., Shode, F., Smith, P., Smith, M., and Opoku, A.R. Anti-plasmodial activity of some Zulu medicinal plants and of some triterpenes isolated from them. Molecules 18(10) (2013): 12313-12323.
- [105] Fernandes, C.P., Corrêa, A.L., Lobo, J.F.R., Caramel, O.P., De Almeida, F.B., Casto, E.S., Souza, K.F.C.S., Burth, P., Amorim, L.M.F., Santos, M.G., Ferreira, J.L.P., Falcão, D.Q., Carvalho, J.C.T., and Rocha, L. Triterpene esters and biological activities from edible fruits of *Manilkara subsericea* (Mart.) Dubard, Sapotaceae. BioMed Research International 2013 (2012), doi: 101155/2013280810.
- [106] Pientaweeratch, S., Panapisal, V., and Tansirikongkol, A. Antioxidant, anti-collagenase and anti-elastase activities of *Phyllanthus emblica*, *Manilkara zapota* and silymarin: an in vitro comparative study for anti-aging applications. Pharmaceutical Biology 54(9) (2016): 1865-1872.
- [107] Fomani, M., Nouga, A.B., Toze, F.a.A., Ndom, J.C., Waffo, A.F.K., and Wansi, J.D. Bioactive phenylethanoids from the seeds of *Manilkara zapota*. British Journal of Pharmaceutical Research 8(5) (2015): 1-5.
- [108] Espinosa-Diez, C., Miguel, V., Mennerich, D., Kietzmann, T., Sanchez-Perez, P., Cadenas, S., and Lamas, S. Antioxidant responses and cellular adjustments to oxidative stress. Redox Biol 6(1) (2015): 183-97.
- [109] Sulaiman, S., Yusoff, N., Eldeen, I., Seow, E., Sajak, A., and Ooi, K. Correlation between total phenolic and mineral contents with antioxidant activity of eight Malaysian bananas (*Musa* sp.). Journal of Food Composition and Analysis 24(1) (2011): 1-10.
- [110] Beard, P.C.W., Moran, A., and L, R. Stability of the total antioxidant capacity and total polyphenol content of 23 commercially available vegetable juices before and after in vitro digestion measured by FRAP, DPPH, ABTS and Folin-Ciocalteu methods. Food Research International 44(1) (2011): 217-224.
- [111] Nugitrangson, P., Puthong, S., Iempridee, T., Pimtong, W., Pornpakakul, S., and Chanchao, C. *In vitro* and *in vivo* characterization of the anticancer activity of

- Thai stingless bee (*Tetragonula laeviceps*) cerumen. Experimental Biology and Medicine 241(2) (2016): 166-176.
- [112] Parikh, B., and Patel, V.H. Quantification of phenolic compounds and antioxidant capacity of an underutilized Indian fruit: Rayan [*Manilkara hexandra* (Roxb.) Dubard]. Food Science and Human Wellness 6(1) (2017): 10-19.
- [113] Ya, W., Chun-Meng, Tao, G., Yi-Lin, Z., and Ping, Z. Preliminary screening of 44 plant extracts for anti-tyrosinase and antioxidant activities. Pakistan Journal of Pharmaceutical Sciences 28(5) (2015).
- [114] Mazlan, N.a.M., Mediani, A., Abas, F., Ahmad, S., Shaari, K., Khamis, S., and Lajis, N.H. Antioxidant, antityrosinase, anticholinesterase, and nitric oxide inhibition activities of three Malaysian *Macaranga* species. The Scientific World Journal 2013 (2013), doi: DOI10.1155/2013312741.
- [115] Barbosa, A., Silva, K., Oliveira, M., Carvalho, M., and Srur, A. Effects of *Acmella oleracea* methanolic extract and fractions on the tyrosinase enzyme. Revista Brasileira de Farmacognosia 26 (2016): 321–325.
- [116] Nguyen, T.T., Nguyen, D.H., Zhao, B.T., Le, D.D., Min, B.S., Kim, Y.H., and Woo, M.H. Triterpenoids and sterols from the grains of *Echinochloa utilis* Ohwi & Yabuno and their cytotoxic activity. Biomed Pharmacother 93(1) (2017): 202-207.
- [117] Obara, T., and Abe, S. Structure of sawamilletin from sawamillet oil. Bulletin of the Korean Chemical Society 21(6) (1957): 388-389.
- [118] Herath, W., Mikell, J.R., Hale, A.L., Ferreira, D., and Khan, I.A. Microbial metabolism Part 9. structure and antioxidant significance of the metabolites of 5,7-dihydroxyflavone (Chrysin), and 5- and 6-hydroxyflavones. Chemical and Pharmaceutical Bulletin 56(4) (2008): 418-422.
- [119] Mikell, J.R., Herath, W., and Khan, I.A. Eleven microbial metabolites of 6-hydroxyflavanone. Chemical and Pharmaceutical Bulletin 63(8) (2015): 579-583.
- [120] Zand, R.S.R., Jenkins, D.J.A., and Diamandis, E.P. Steroid hormone activity of flavonoids and related compounds. Breast Cancer Research and Treatment 62(1) (2000): 35-49.

- [121] Szliszka, E., Kostrzewa-Susłow, E., Bronikowska, J., Jaworska, D., Janeczko, T., Czuba, Z.P., and Krol, W. Synthetic flavanones augment the anticancer effect of tumor necrosis factor-related apoptosis-inducing ligand (trail). Molecules 17 (2017): 11693-11711.
- [122] Xiang, M., Su, H., Hu, J., and Yan, Y. Isolation, identification and determination of methyl caffeate, ethyl caffeate and other phenolic compounds from *Polygonum amplexicaule* var. *sinense*. Journal of Medicinal Plants Research 5(9) (2011): 1685-1691.
- [123] Zhang, L., Tao, G., Chen, J., and Zheng, Z.P. Characterization of a new flavone and tyrosinase inhibition constituents from the twigs of *Morus alba* L. Molecules 21 (2016), doi: 103390/21091130.
- [124] Ayinde, B.A., Onwukaeme, D.N., and Omogbai, E.K. Isolation and characterization of two phenolic compounds from the stem bark of *Musanga cecropioides* R. Brown (Moraceae). Acta Poloniae Pharmaceutica 64(2) (2007): 183-185.
- [125] Guria, M., Mitra, P., Ghosh, T., Gupta, S., Basu, B., and Mitra, P.K. 3,4-Dihydroxybenzoic acid isolated from the leaves of *Ageratum conyzoides* L. European Journal of Biotechnology and Bioscience 1(4) (2013): 25-28.
- [126] Friggeri, L., De Vita, D., Pandolfi, F., Tortorella, S., Costi, R., Di Santo, R., and Scipione, L. Design, synthesis and evaluation of 3,4-dihydroxybenzoic acid derivatives as antioxidants, bio-metal chelating agents and acetylcholinesterase inhibitors. Journal of Enzyme Inhibition and Medicinal Chemistry 30(1) (2015): 166-172.
- [127] Swain, S.S., Rout, K.K., and Chand, P.K. Production of triterpenoid anti-cancer compound taraxerol in *Agrobacterium*-transformed root cultures of Butterfly Pea (*Clitoria ternatea* L.). Applied Biochemistry and Biotechnology (2012), doi: 101007/1201001297918.
- [128] Viswanadh, G.S., Ramaiah, P.A., Laatsch, H., and Maskey, R. Chemical constituents of heartwood and bark of *Homonoia riparia*. Journal of Tropical Medicinal Plants 7(2) (2006): 267-273.
- [129] Mo, E.K., Han, B.H., Kim, S.M., Yang, S.A., Kang, S.K., Oh, C.J., Kim, R., Kim, G., Kang, H.J., and Sung, C.K. Identification of d-friedoolean-13-en-3-

- one (taraxerone) as an antioxidant compound from sedum (*Sedum sarmentosum*). Food Science and Biotechnology 21(2) (2012): 485-489.
- [130] Prachayasittikul, S., Saraban, P., Cherdtrakulkiat, R., Ruchirawat, S., and Prachayasittikul, V. New bioactive triterpenoids and antimalarial activity of *Diospyros rubra* Lec. Experimental and Clinical Sciences 9(1) (2010): 1-10.
- [131] Shindo, K., Kagiya, Y., Nakamura, R., Hara, A., Ikenaga, H., Furukawa, K., and Misawa, N. Enzymatic synthesis of novel antioxidant flavonoids by *Escherichia coli* cells expressing modified metabolic genes involved in biphenyl catabolism. Journal of Molecular Catalysis B: Enzymatic 23(1) (2003): 9-16.
- [132] Zhang, H., Li, X., Wu, K., Wang, M., Liu, P., Wang, X., and Deng, R. Antioxidant activities and chemical constituents of flavonoids from the flower of *Paeonia ostii*. Molecules 22 (2017).





APPENDIX

จุฬาลงกรณ์มหาวิทยาลัย
CHULALONGKORN UNIVERSITY

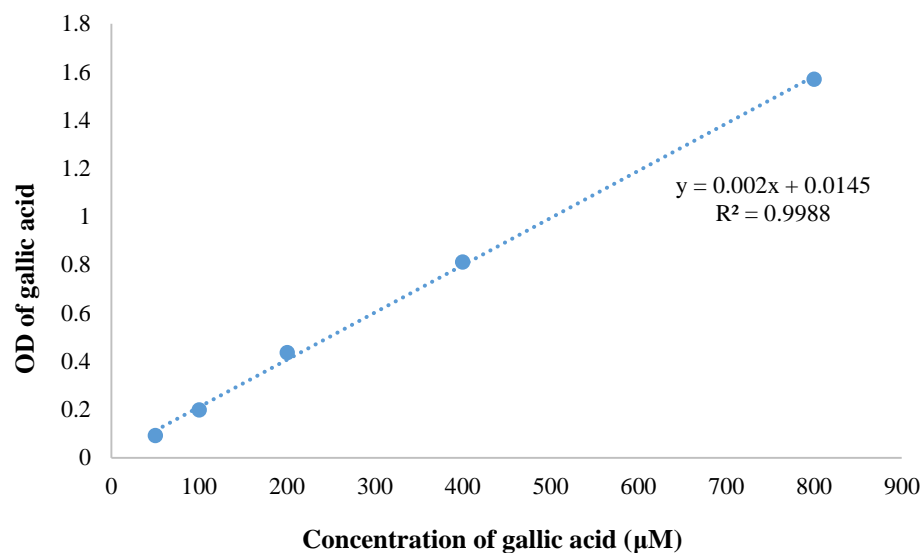


Figure 31 Calibration curve of gallic acid for total phenolic content of crude extract of different parts of *M. zapota*

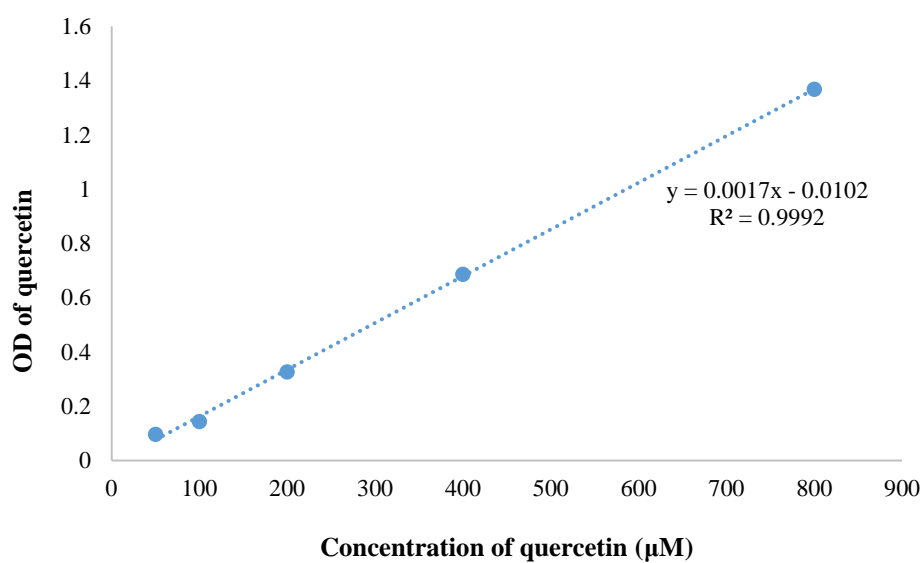


Figure 32 Calibration curve of quercetin for total flavonoid content of crude extract of different parts of *M. zapota*

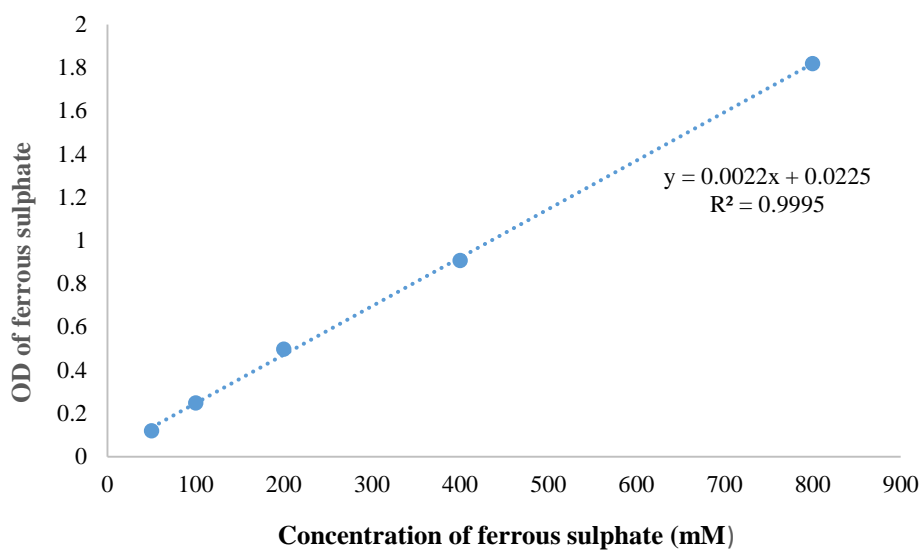


Figure 33 Calibration curve of ferrous sulphate of crude extract of different parts of *M. zapota*

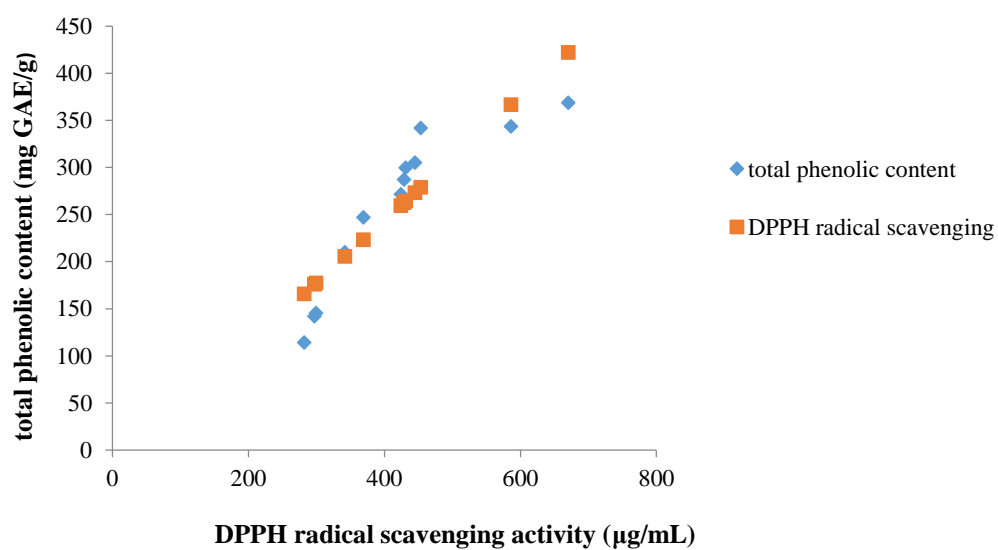


Figure 34 Correlation between total phenolic content and DPPH radical scavenging activity of crude extract of different parts of *M. zapota*

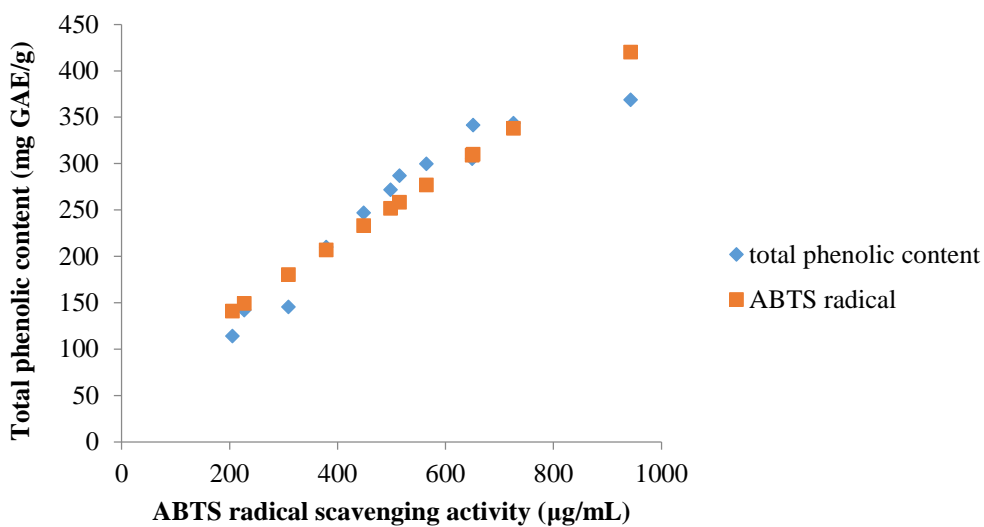


Figure 35 Correlation between total phenolic content and ABTS radical scavenging activity of crude extract of different parts of *M. zapota*

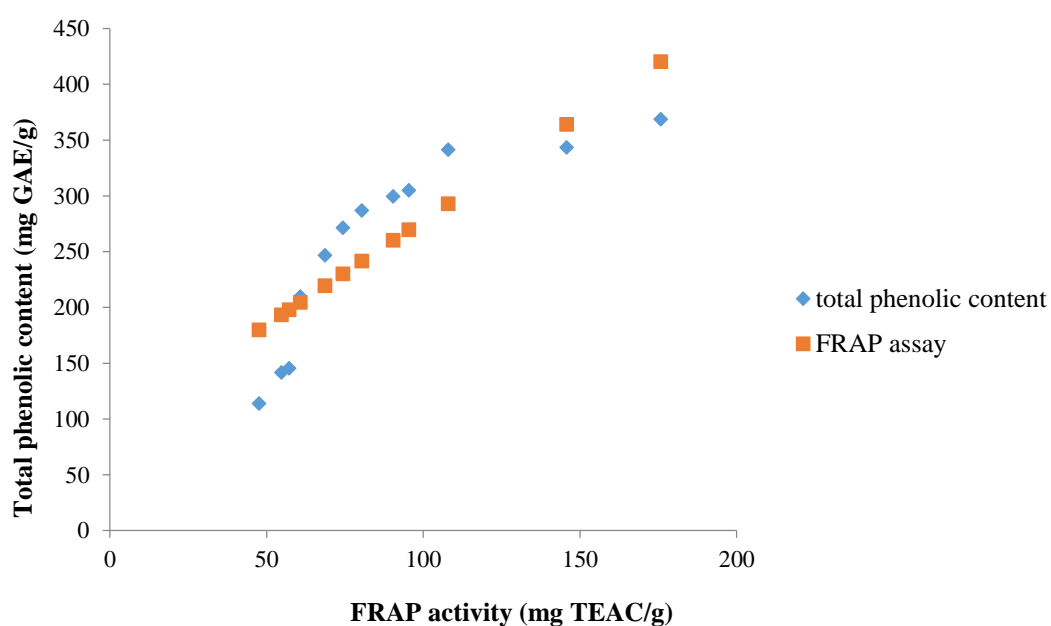


Figure 36 Correlation between total phenolic content and FRAP activity of crude extract of different parts of *M. zapota*

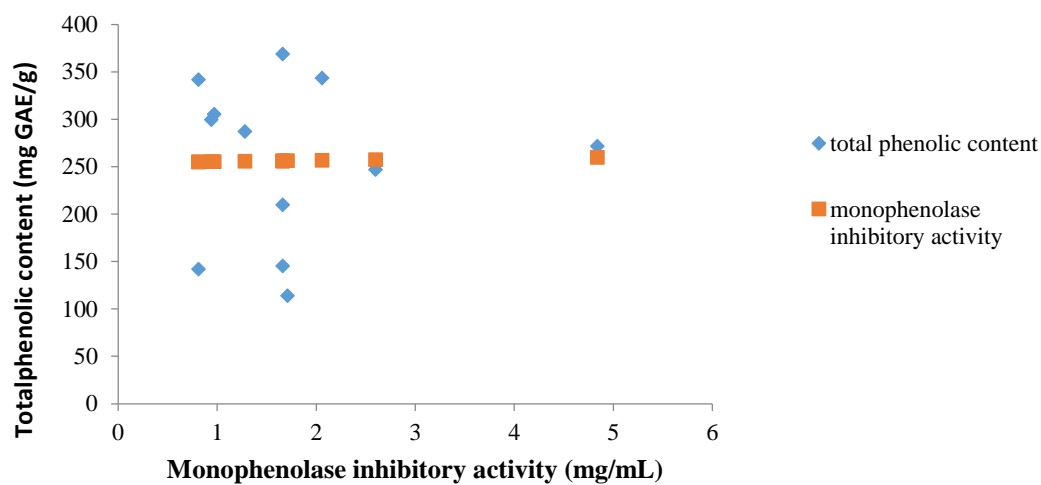


Figure 37 Correlation between total phenolic content and monophenolase inhibitory activity of crude extract of different parts of *M. zapota*

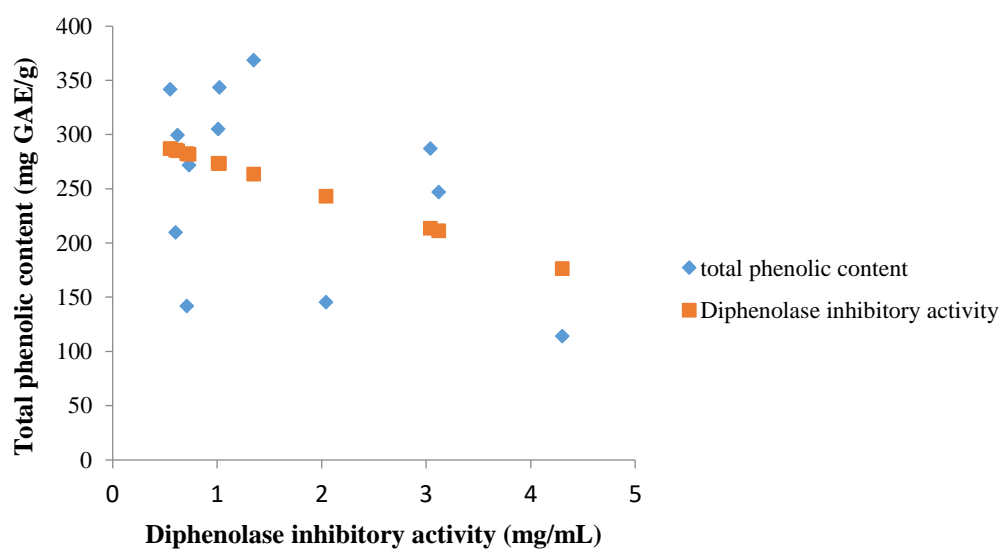


Figure 38 Correlation between total phenolic content and diphenolase inhibitory activity of crude extract of different parts of *M. zapota*

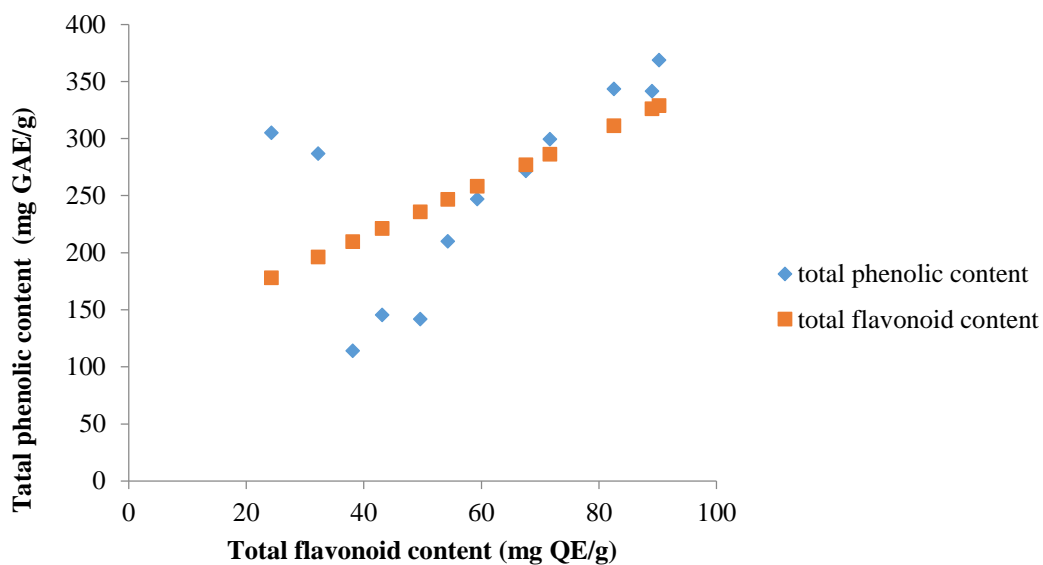


Figure 39 Correlation between total phenolic content and total flavonoid content of crude extract of different parts of *M. zapota*

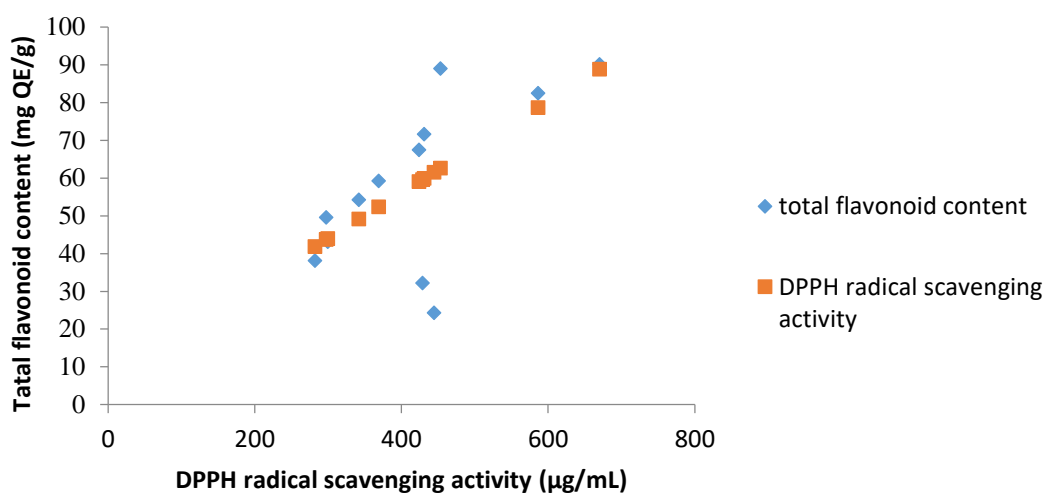


Figure 40 Correlation between total flavonoid content and DPPH radical scavenging activity of crude extract of different parts of *M. zapota*

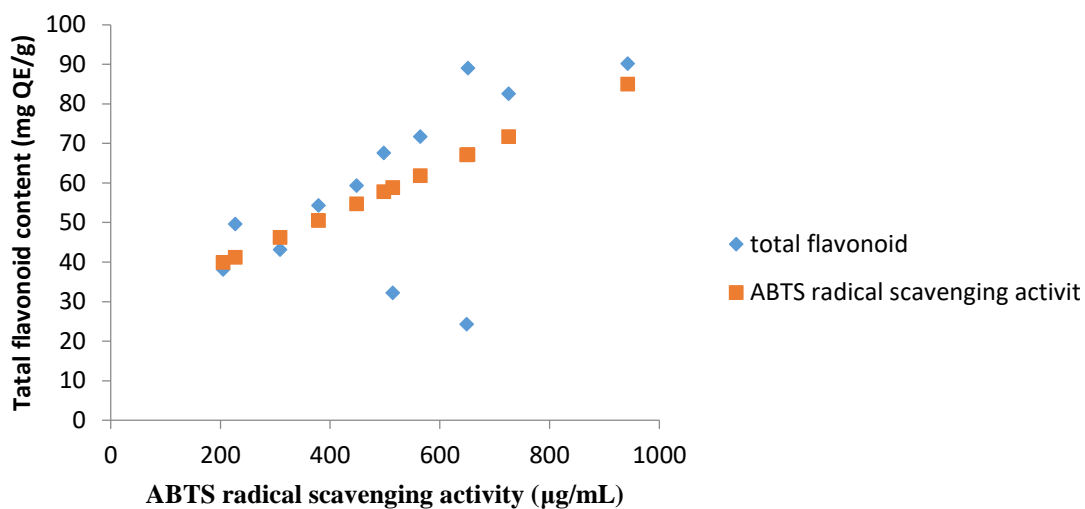


Figure 41 Correlation between total flavonoid content and ABTS radical scavenging activity of crude extract of different parts of *M. zapota*

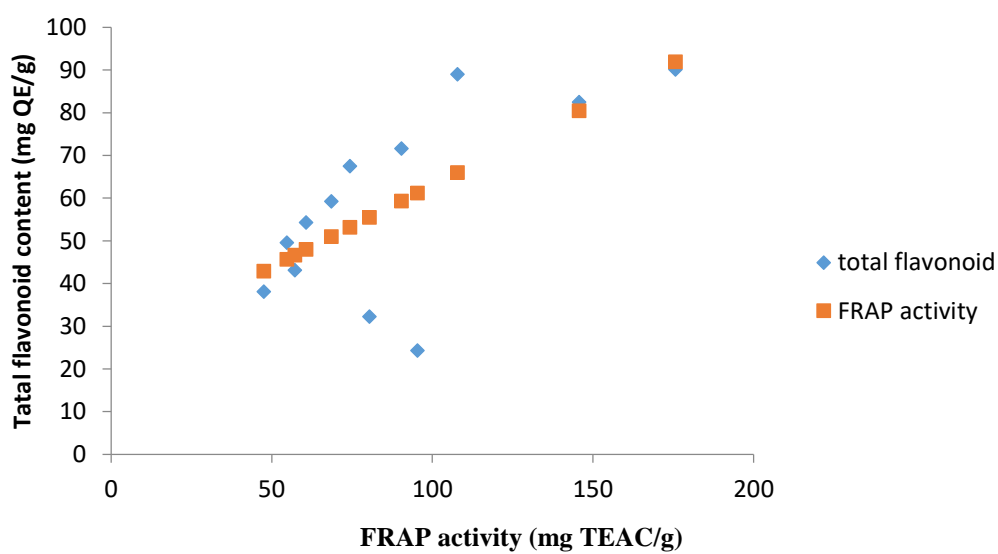


Figure 42 Correlation between total flavonoid content and FRAP activity of crude extract of different parts of *M. zapota*

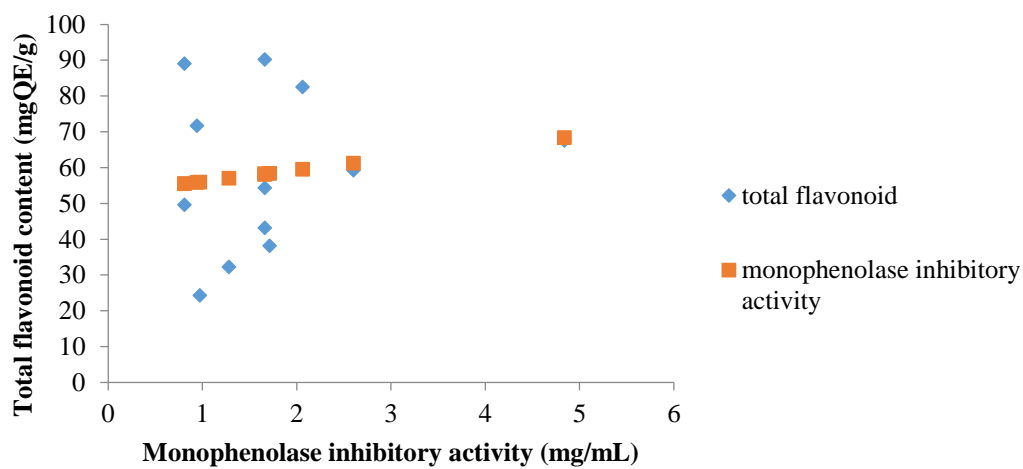


Figure 43 Correlation between total flavonoid content and monophenolase inhibitory activity of different parts of *M. zapota*

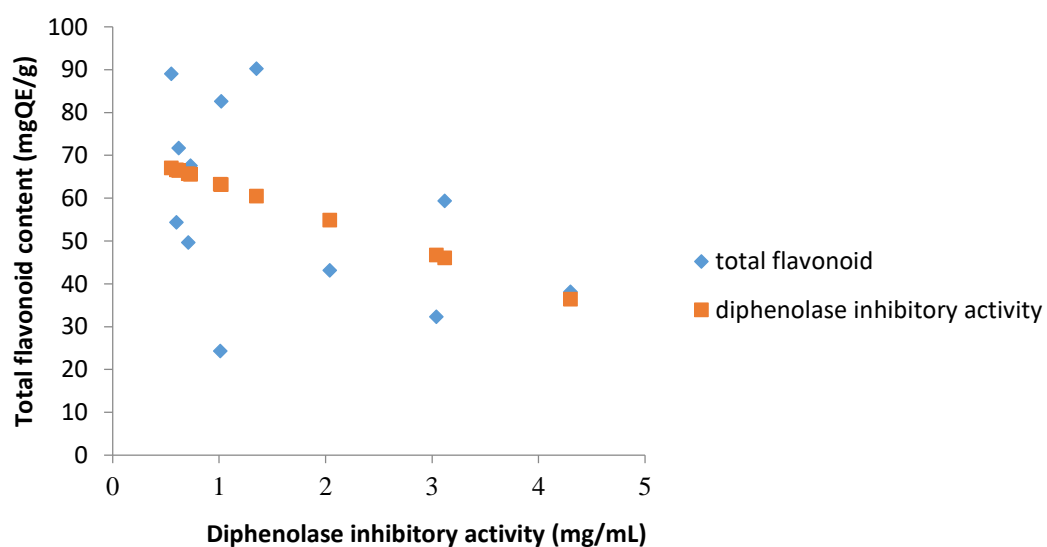


Figure 44 Correlation between total flavonoid content and diphenolase inhibitory activity of different parts of *M. zapota*

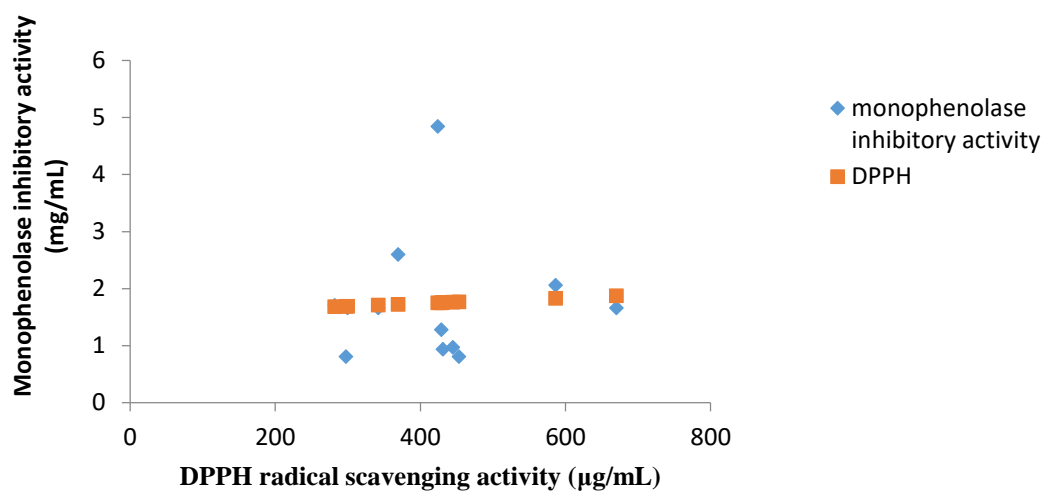


Figure 45 Correlation between monophenolase inhibitory activity and DPPH radical scavenging activity of different parts of *M. zapota*

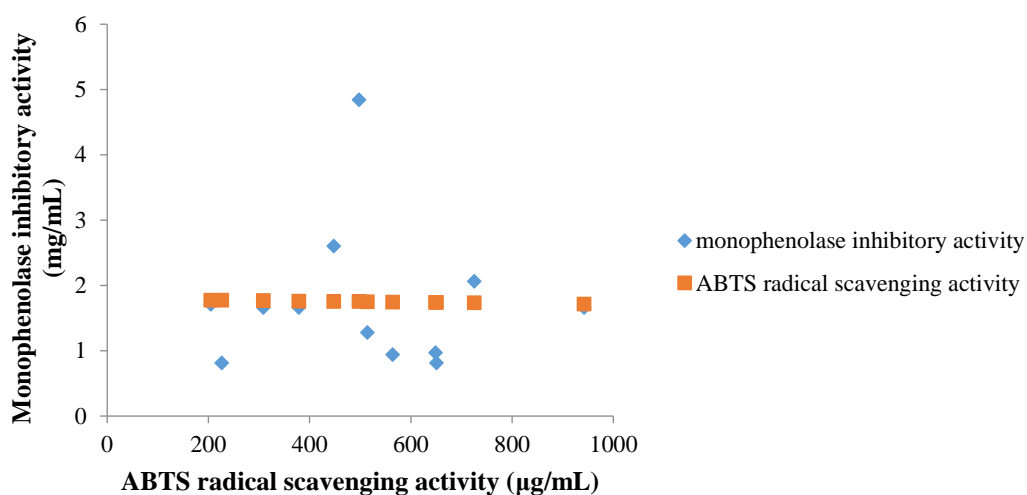


Figure 46 Correlation between monophenolase inhibitory activity and ABTS radical scavenging activity of different parts of *M. zapota*

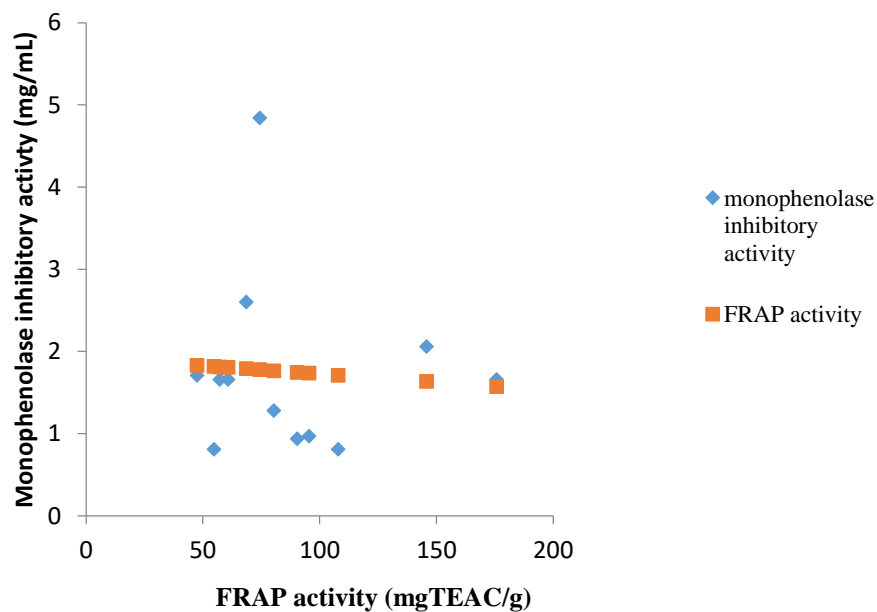


Figure 47 Correlation between monophenolase inhibitory activity and FRAP activity of different parts of *M. zapota*

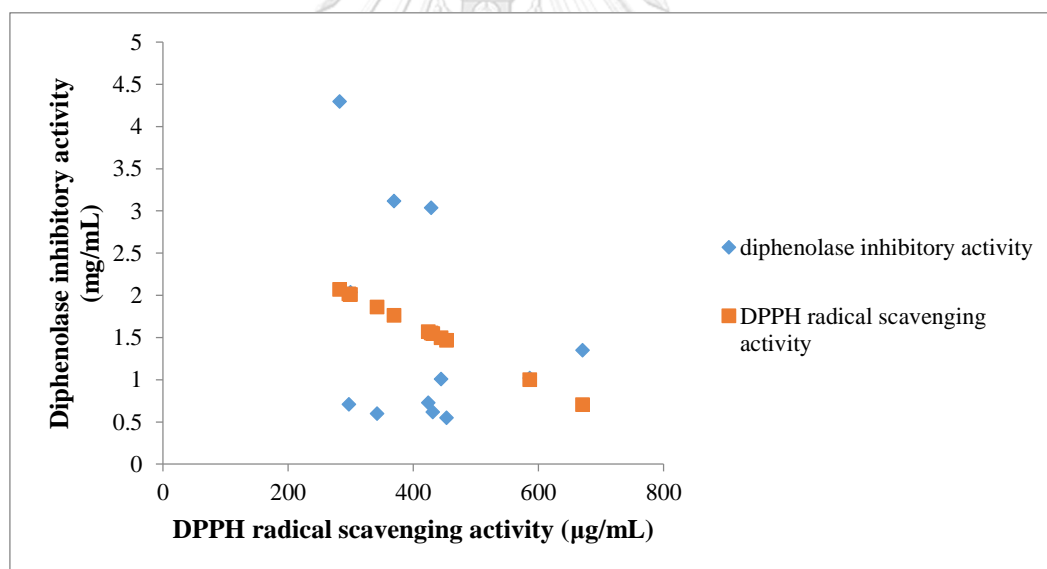


Figure 48 Correlation between diphenolase inhibitory activity and DPPH radical scavenging activity of different parts of *M. zapota*

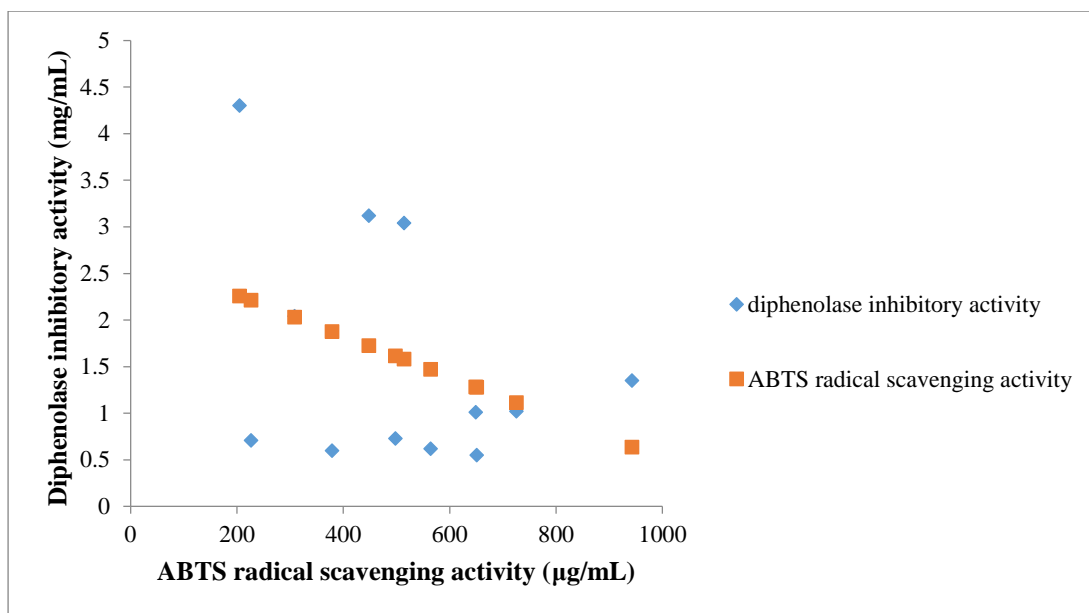


Figure 49 Correlation between diphenolase inhibitory activity and ABTS radical scavenging activity of different parts of *M. zapota*

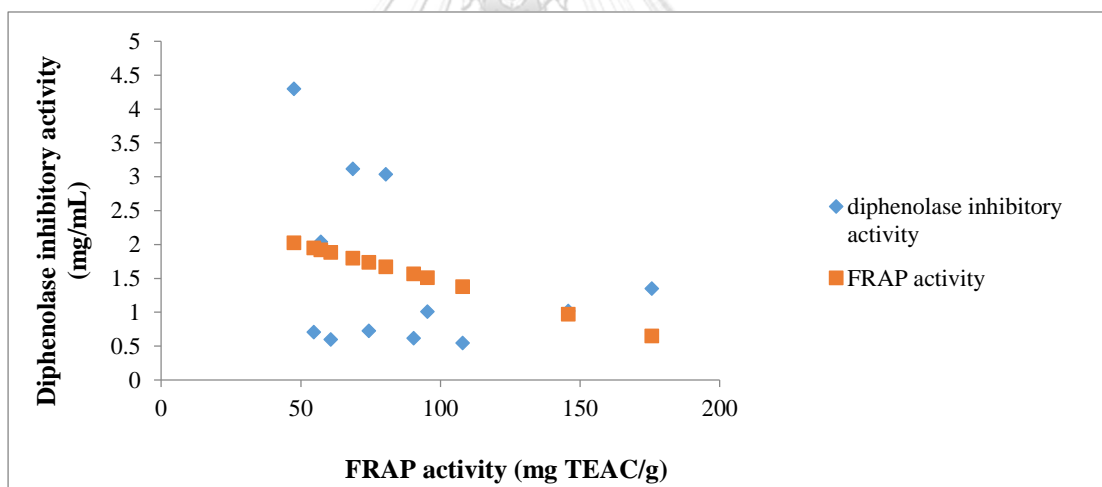


Figure 50 Correlation between diphenolase inhibitory activity and FRAP activity of different parts of *M. zapota*

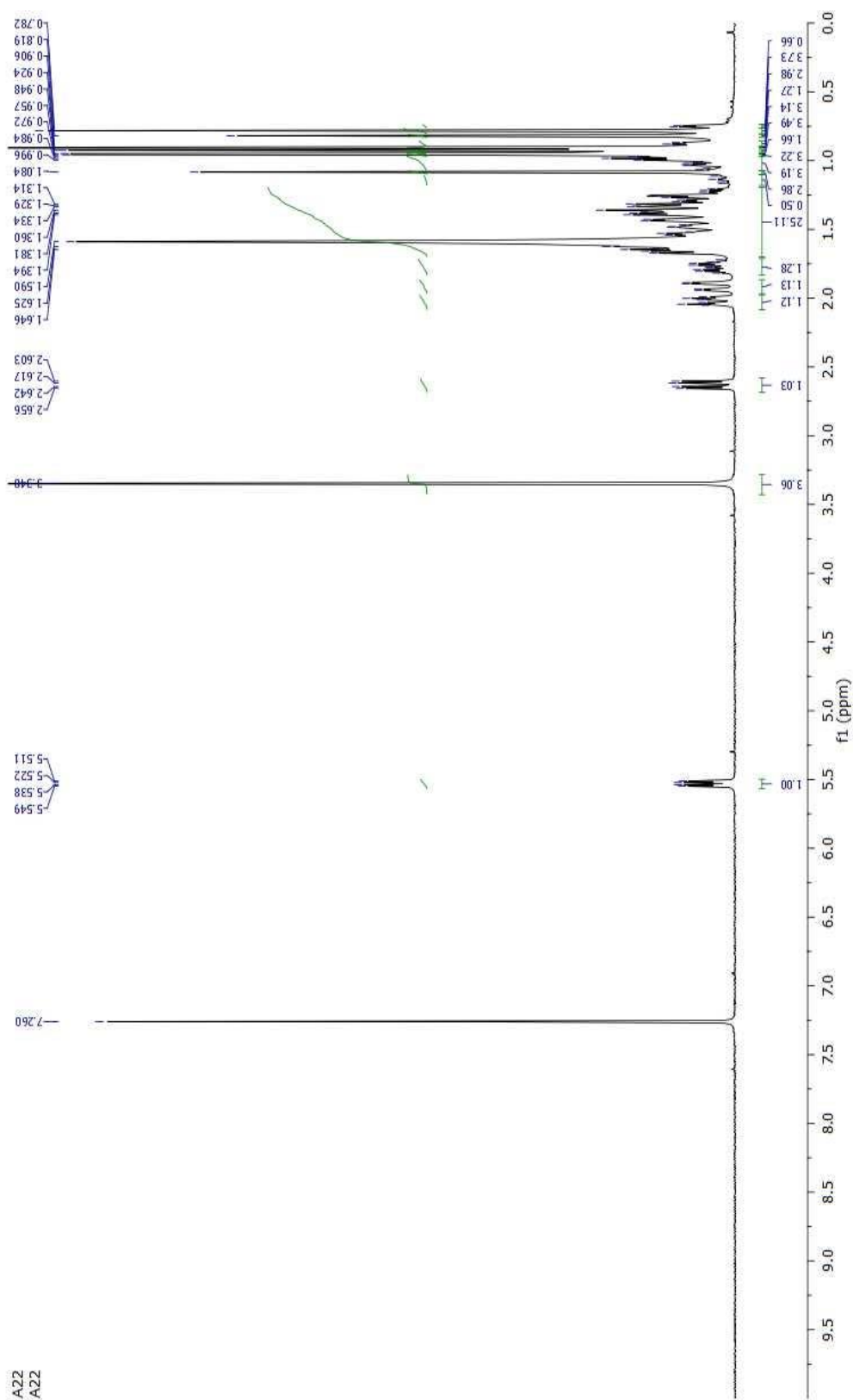


Figure 51 The ¹H-NMR spectrum of taraxerol methyl ether (I)

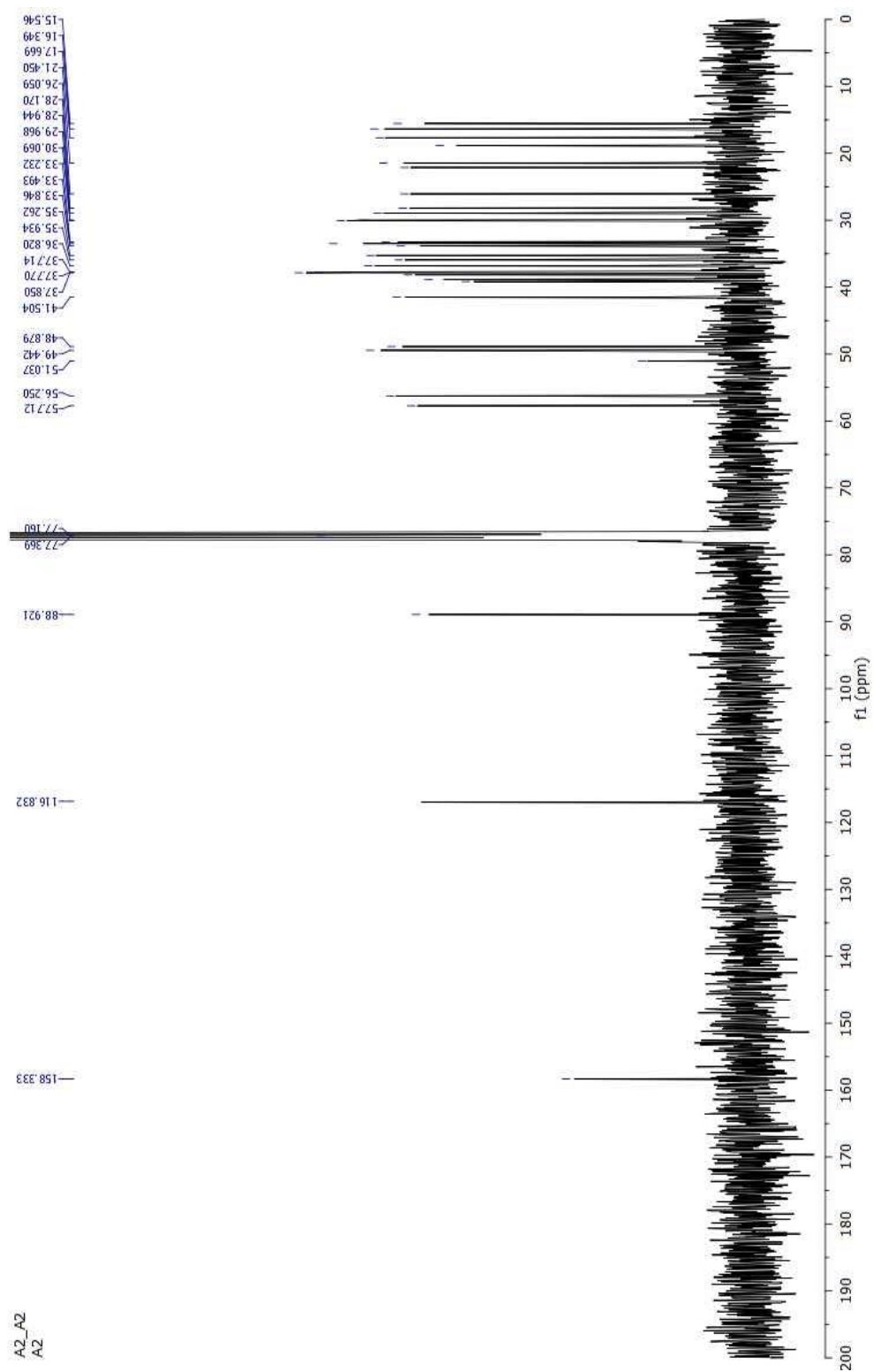


Figure 52 The ^{13}C -NMR spectrum of taraxerol methyl ether (I)

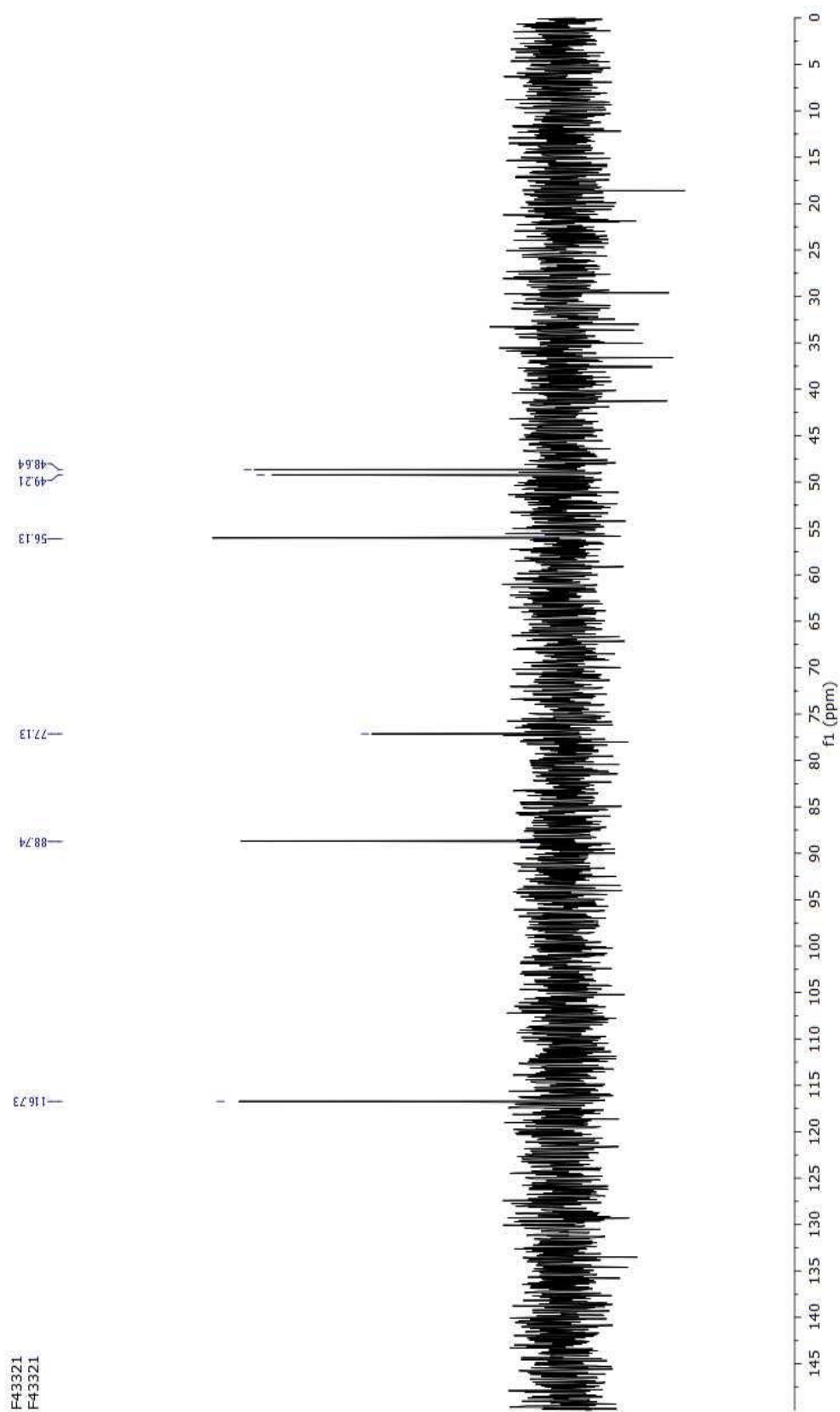


Figure 53 The DEPT90 spectrum of taraxerol methyl ether (**I**)

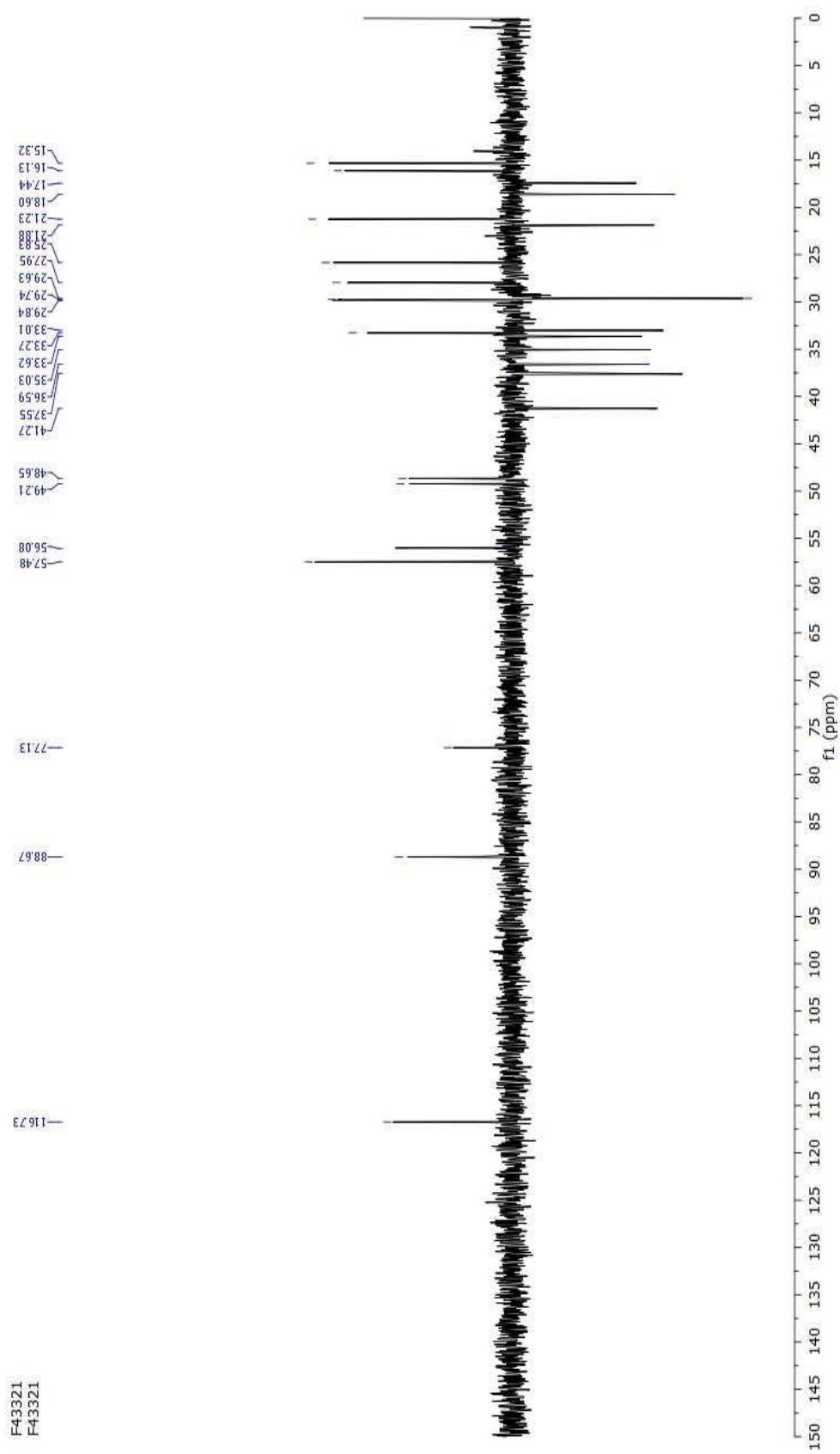


Figure 54 The DEPT135 spectrum of taraxerol methyl ether (**I**)

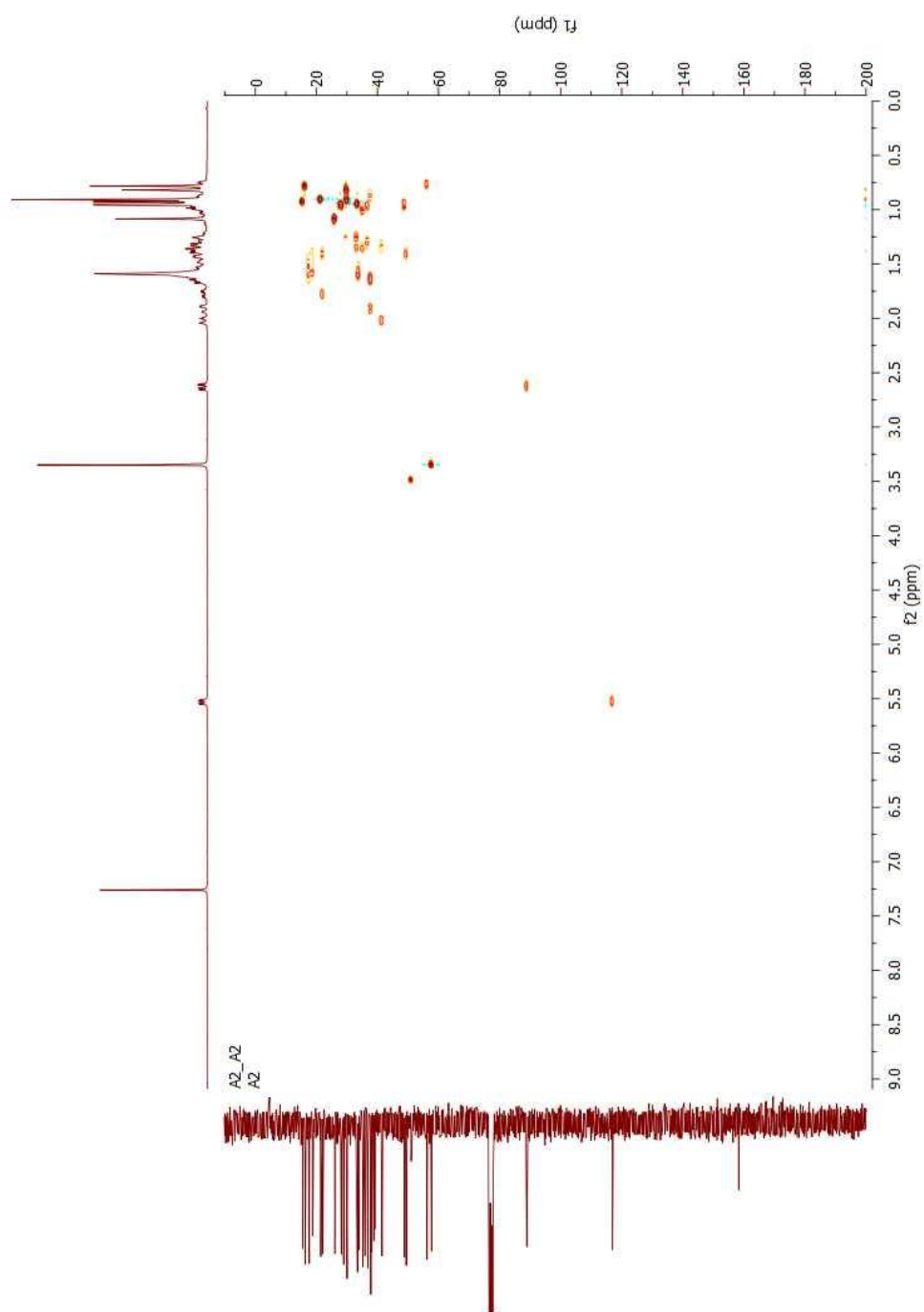


Figure 55 The HSQC spectrum of taraxerol methyl ether (**I**)

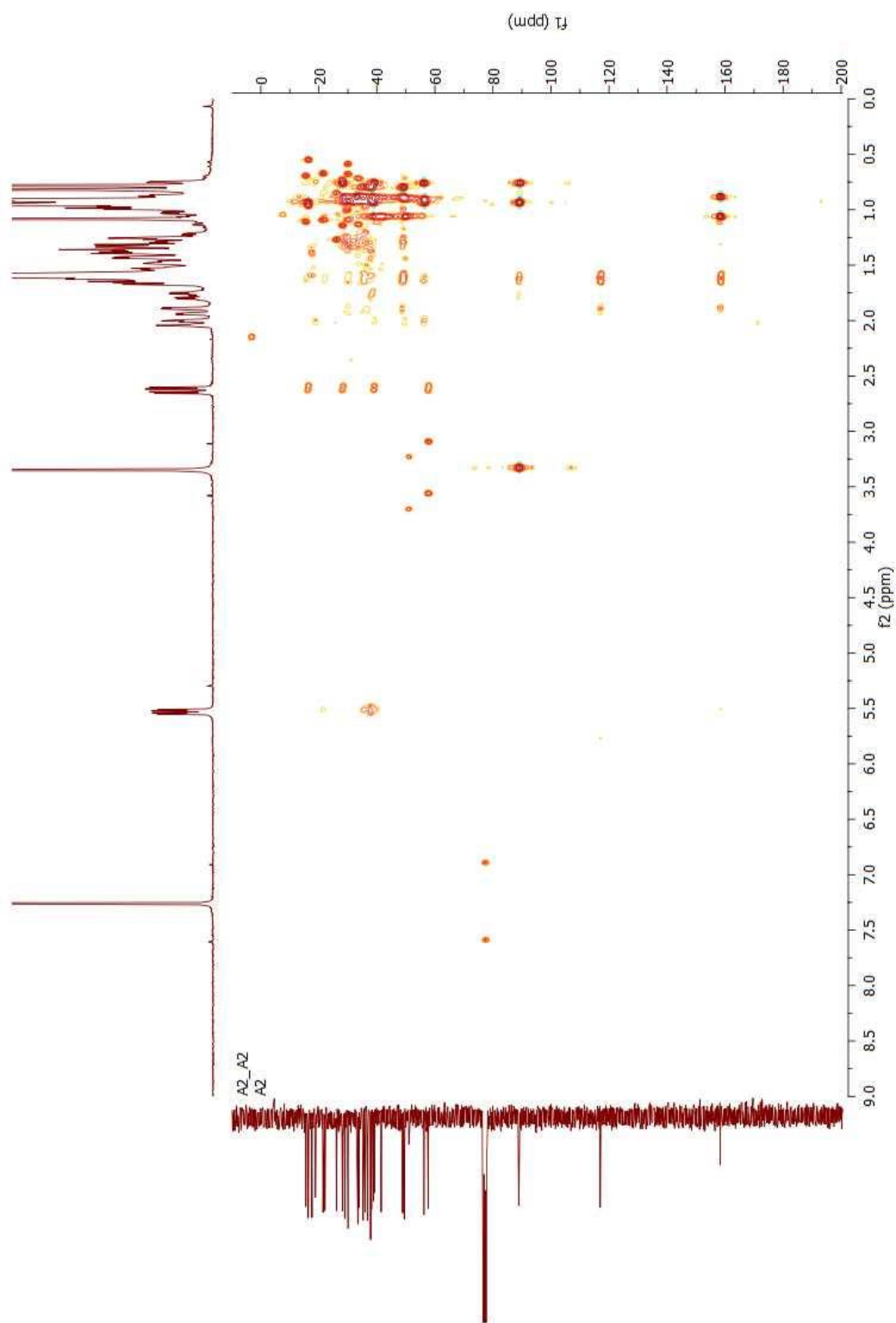
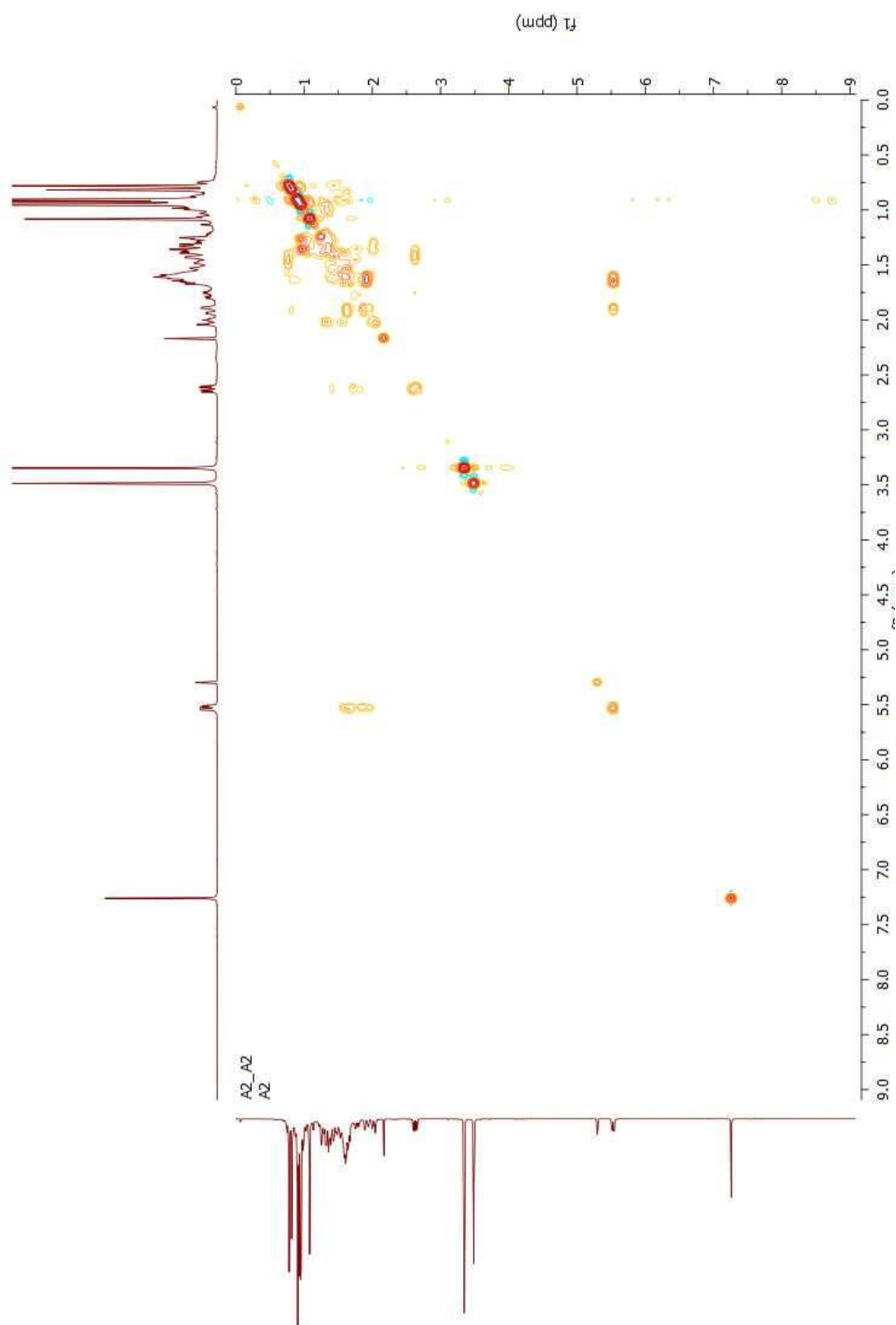


Figure 56 The HMBC spectrum of taraxerol methyl ether (**I**)



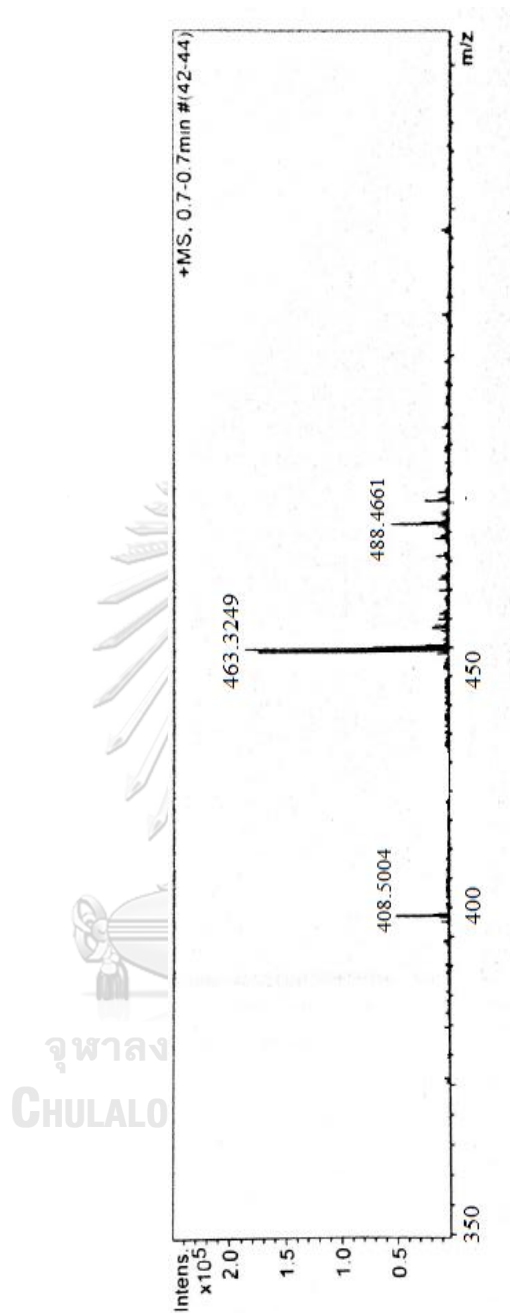
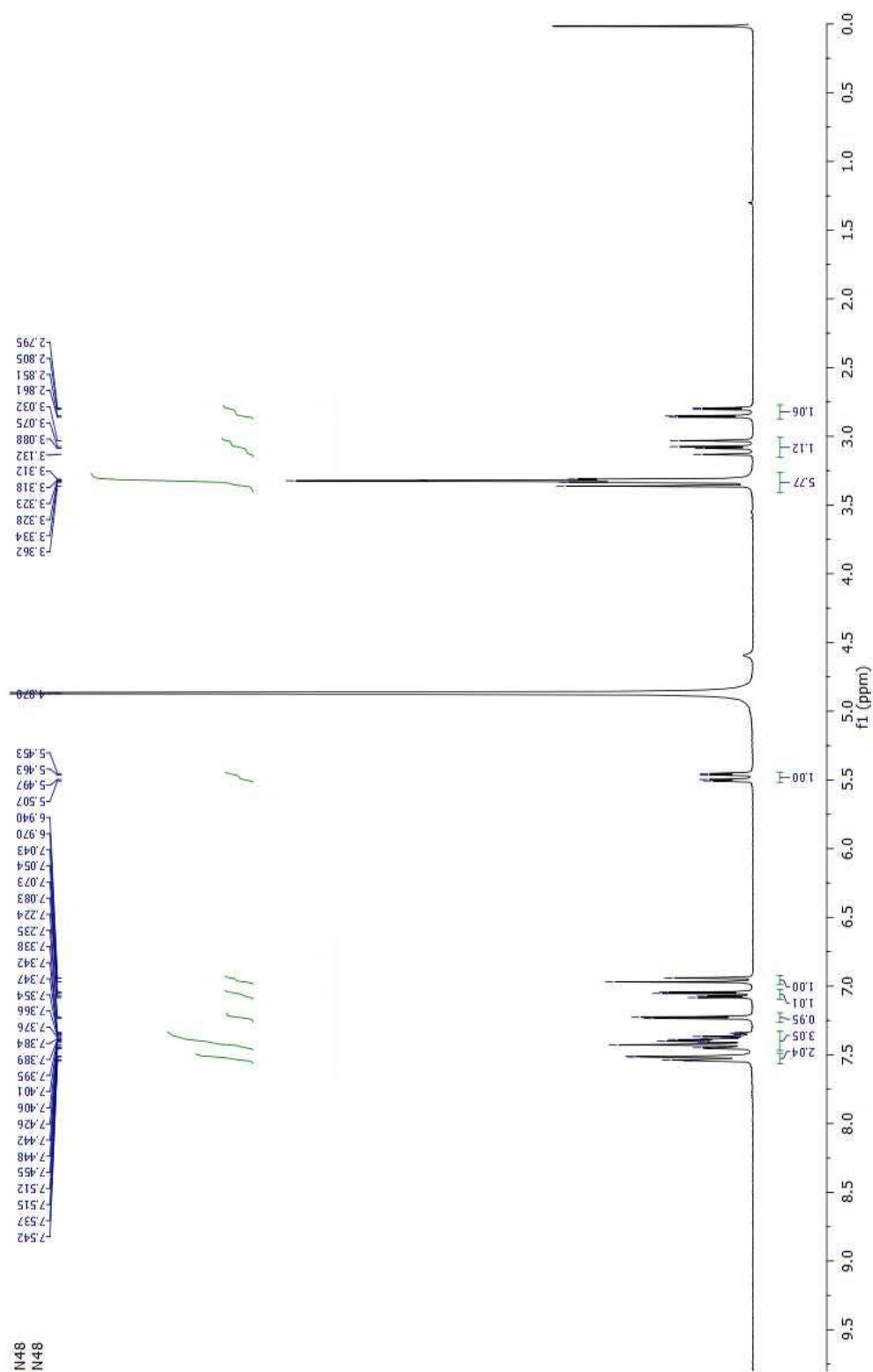


Figure 58 The HR-EI-MS spectrum of taraxerol methyl ether (**I**)



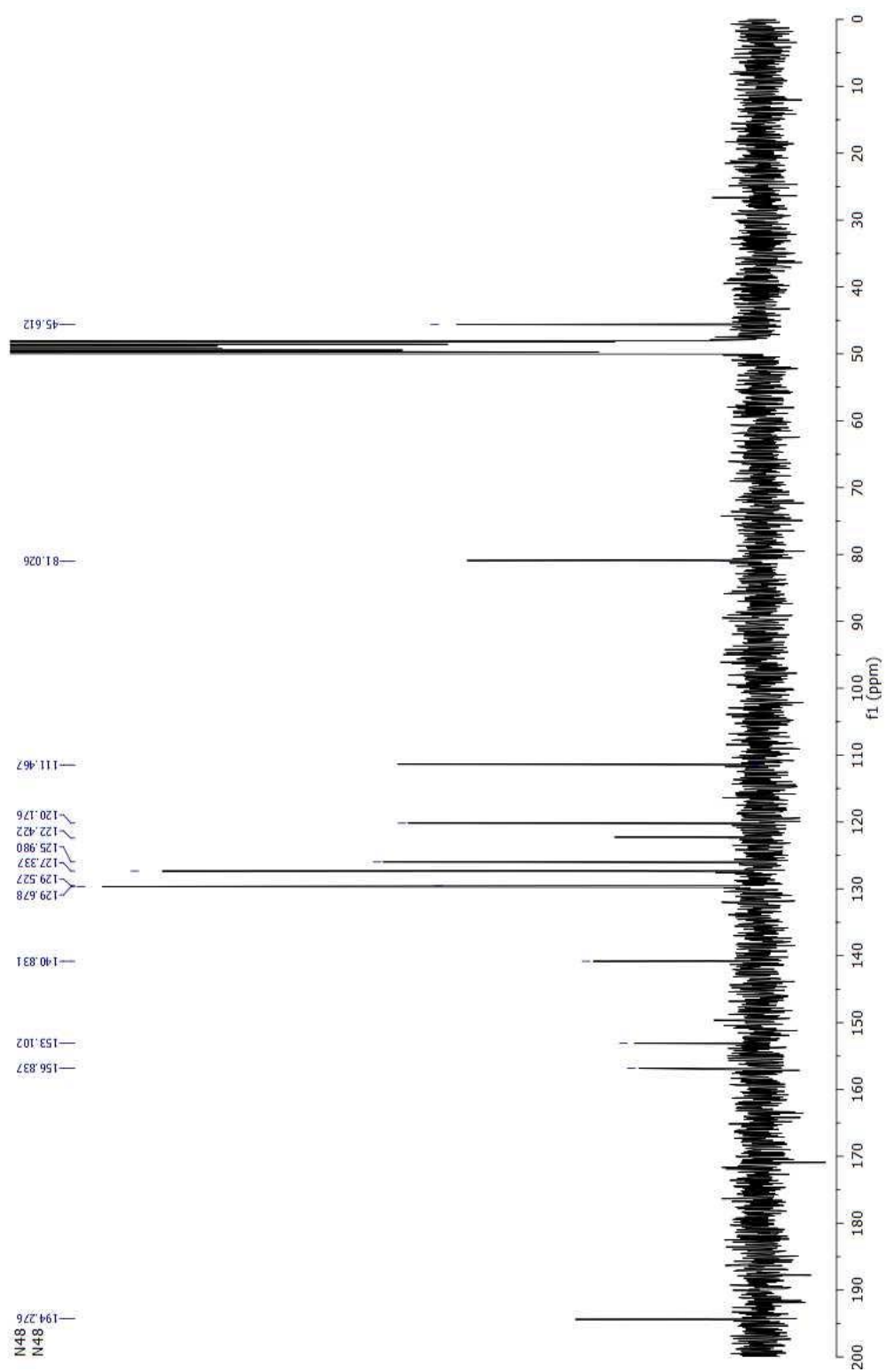


Figure 60 The ^{13}C -NMR spectrum of 6-hydroxyflavanone (II)

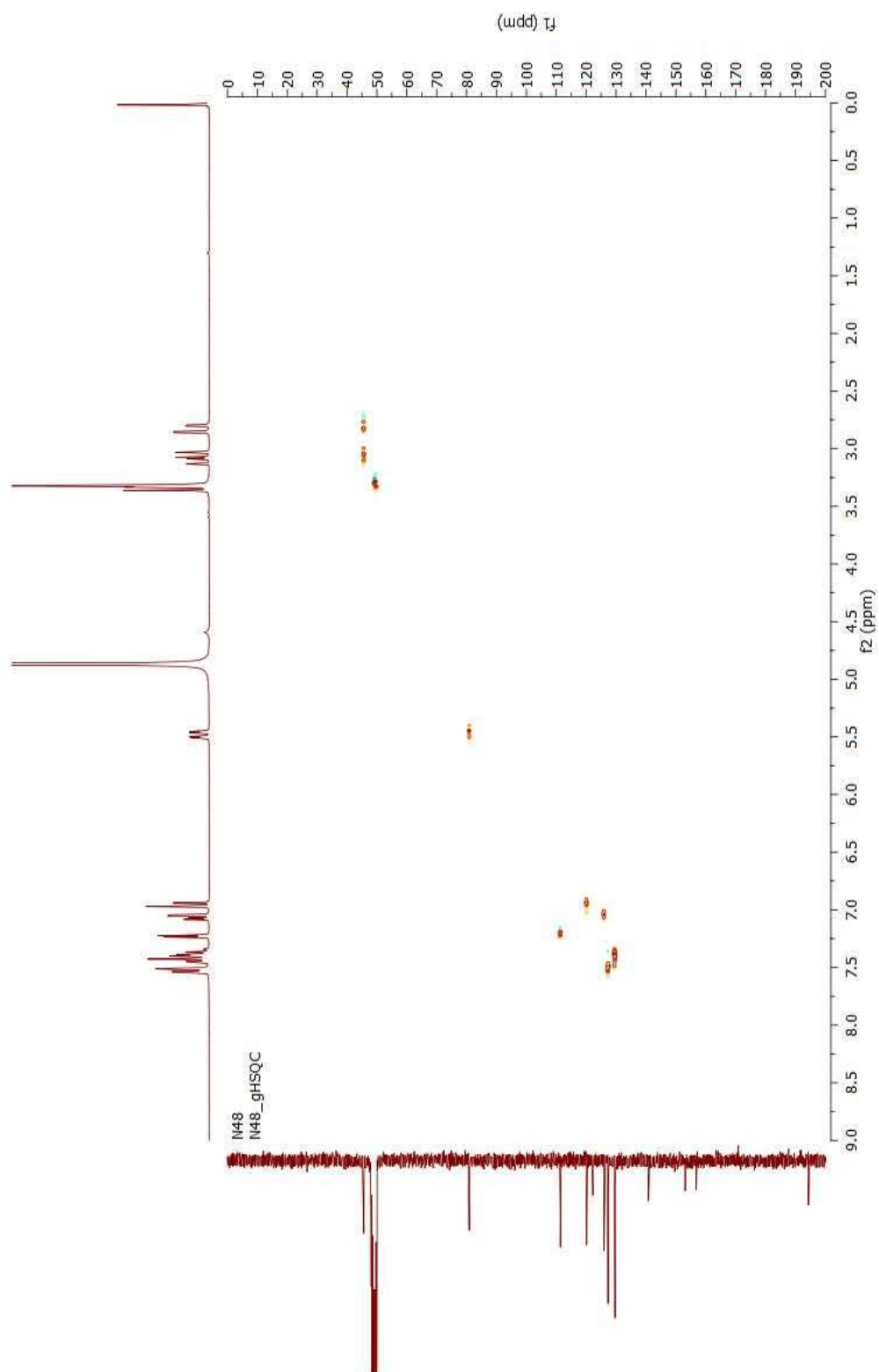


Figure 61 The HSQC spectrum of 6-hydroxyflavanone (II)

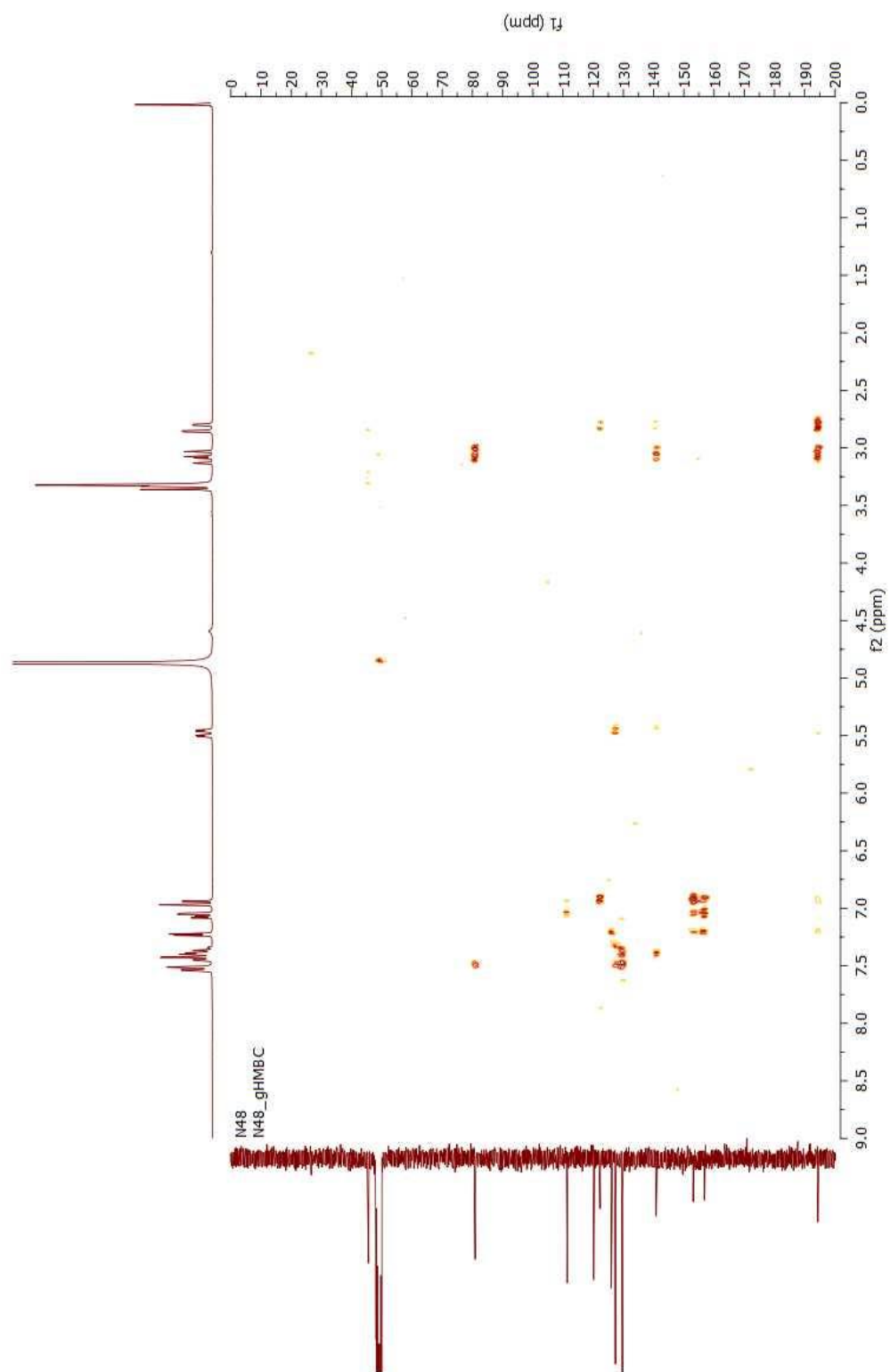


Figure 62 The HMBC spectrum of 6-hydroxyflavanone (II)

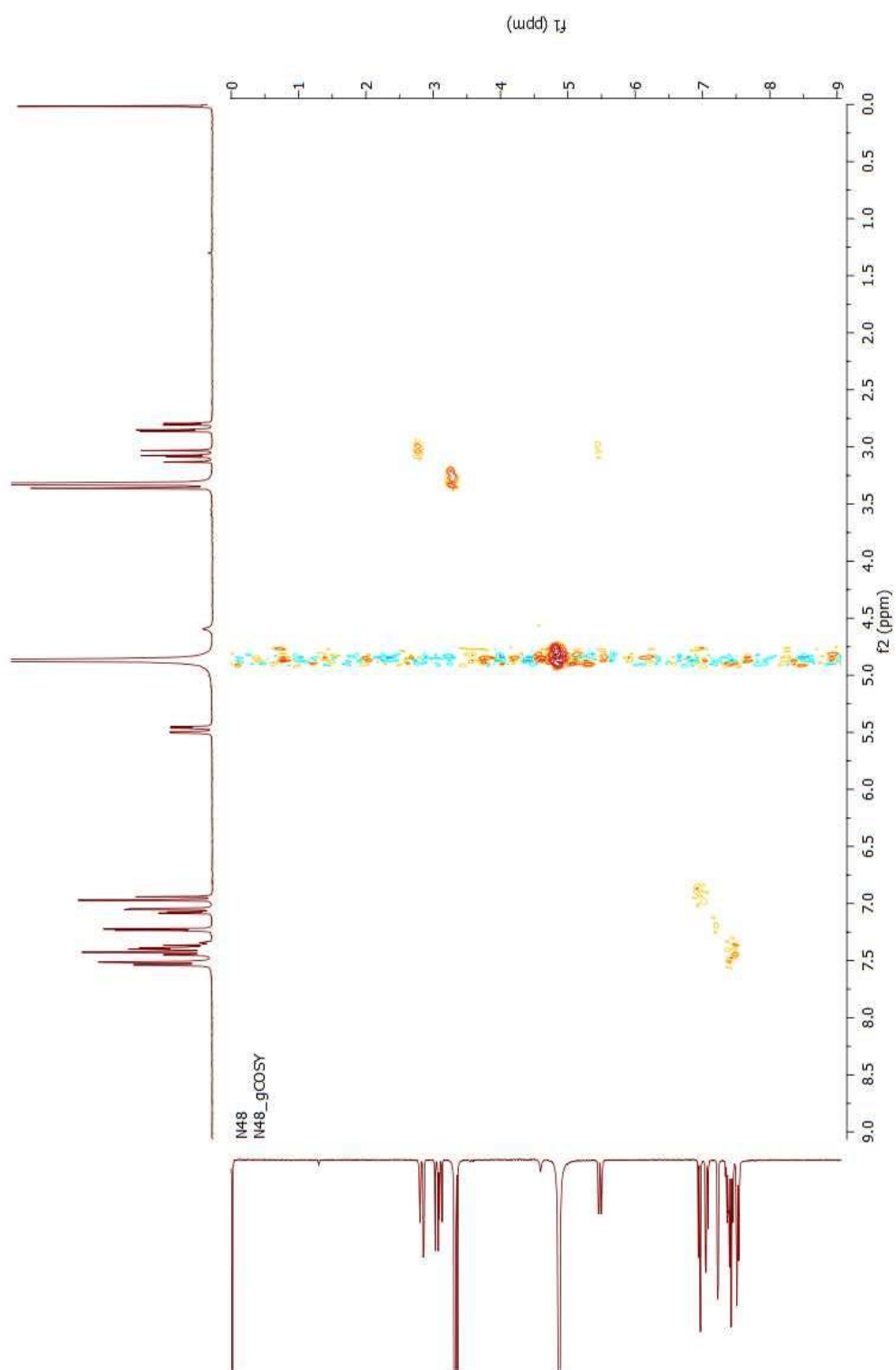


Figure 63 The COSY spectrum of 6-hydroxyflavanone (II)

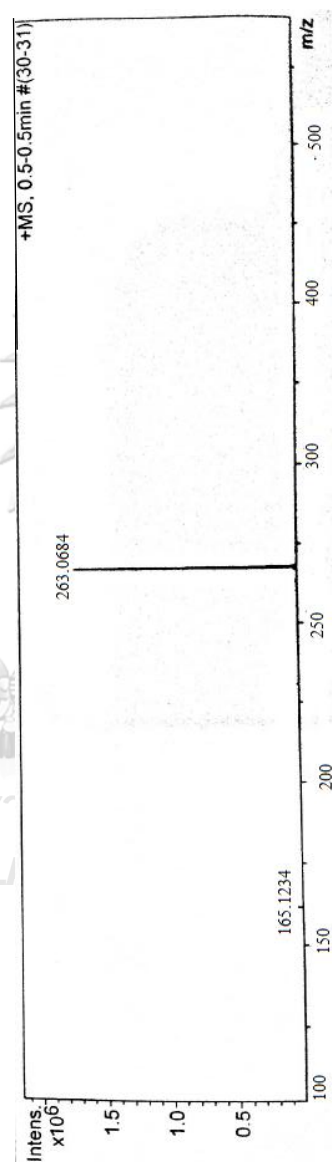


Figure 64 The HR-EI-MS spectrum of 6-hydroxyflavanone (II)

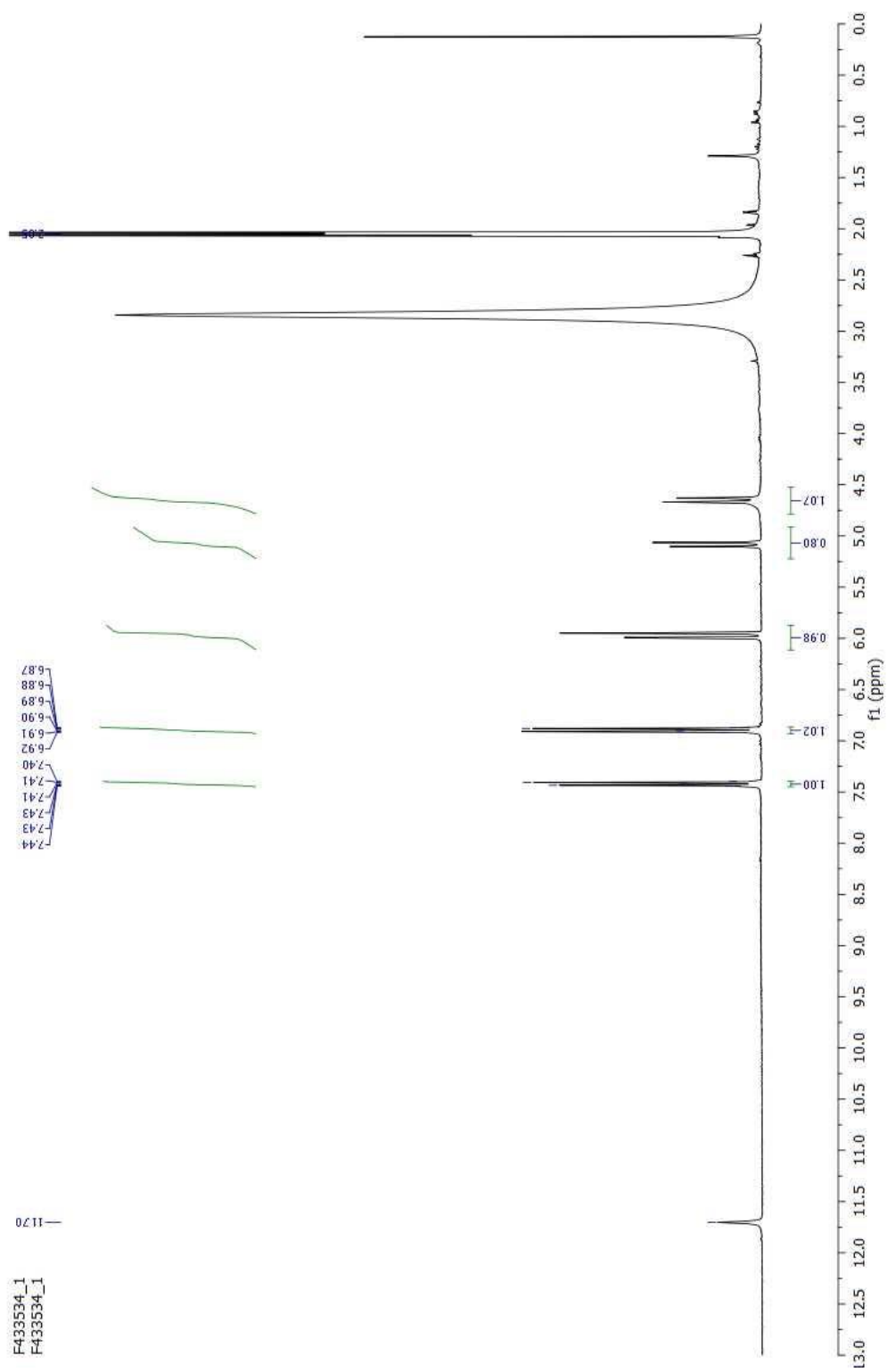


Figure 65 The ¹H-NMR spectrum of (+)-dihydrokampferol (III)

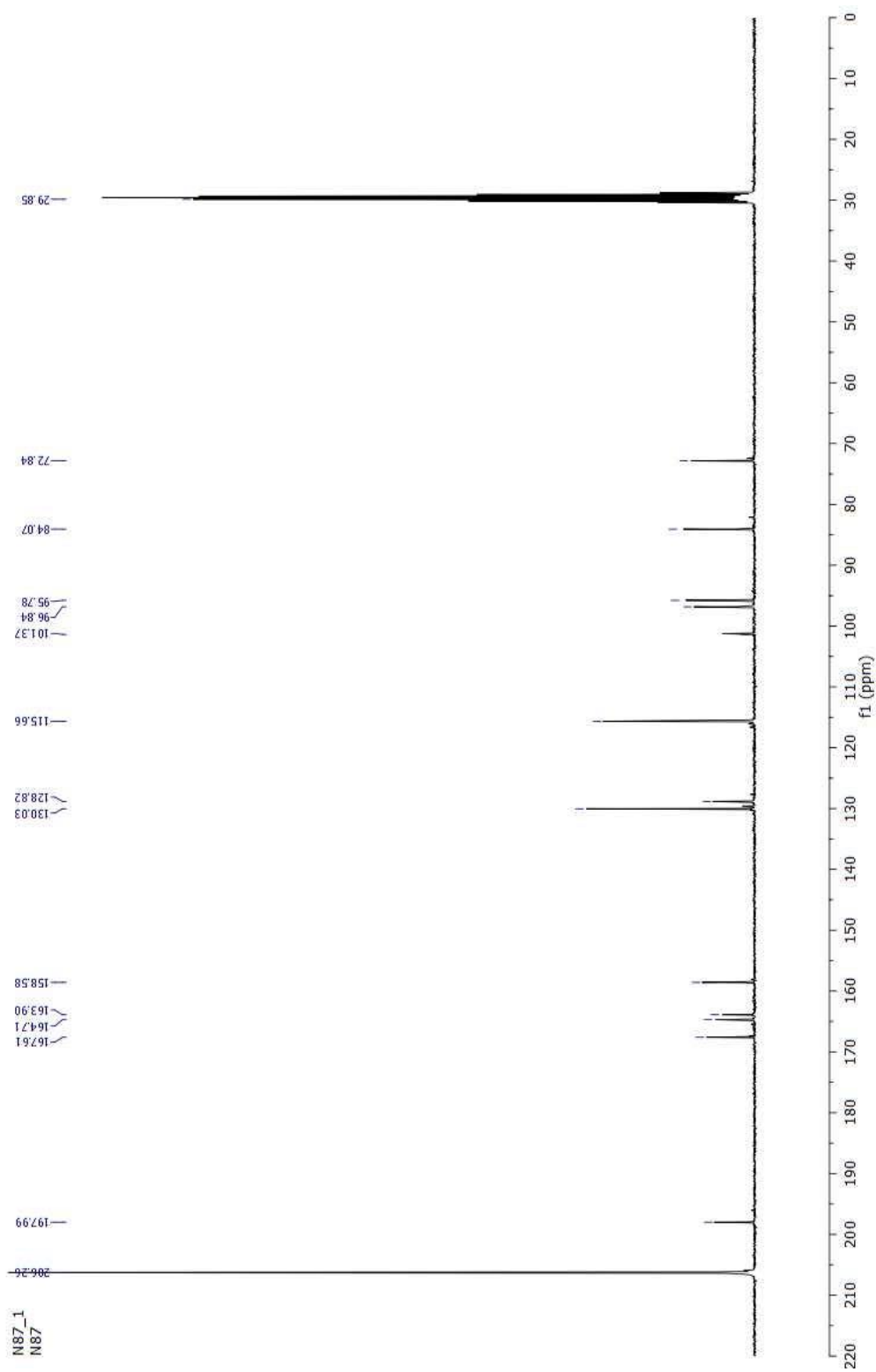


Figure 66 The ^{13}C -NMR spectrum of (+)-dihydrokeampferol (III)

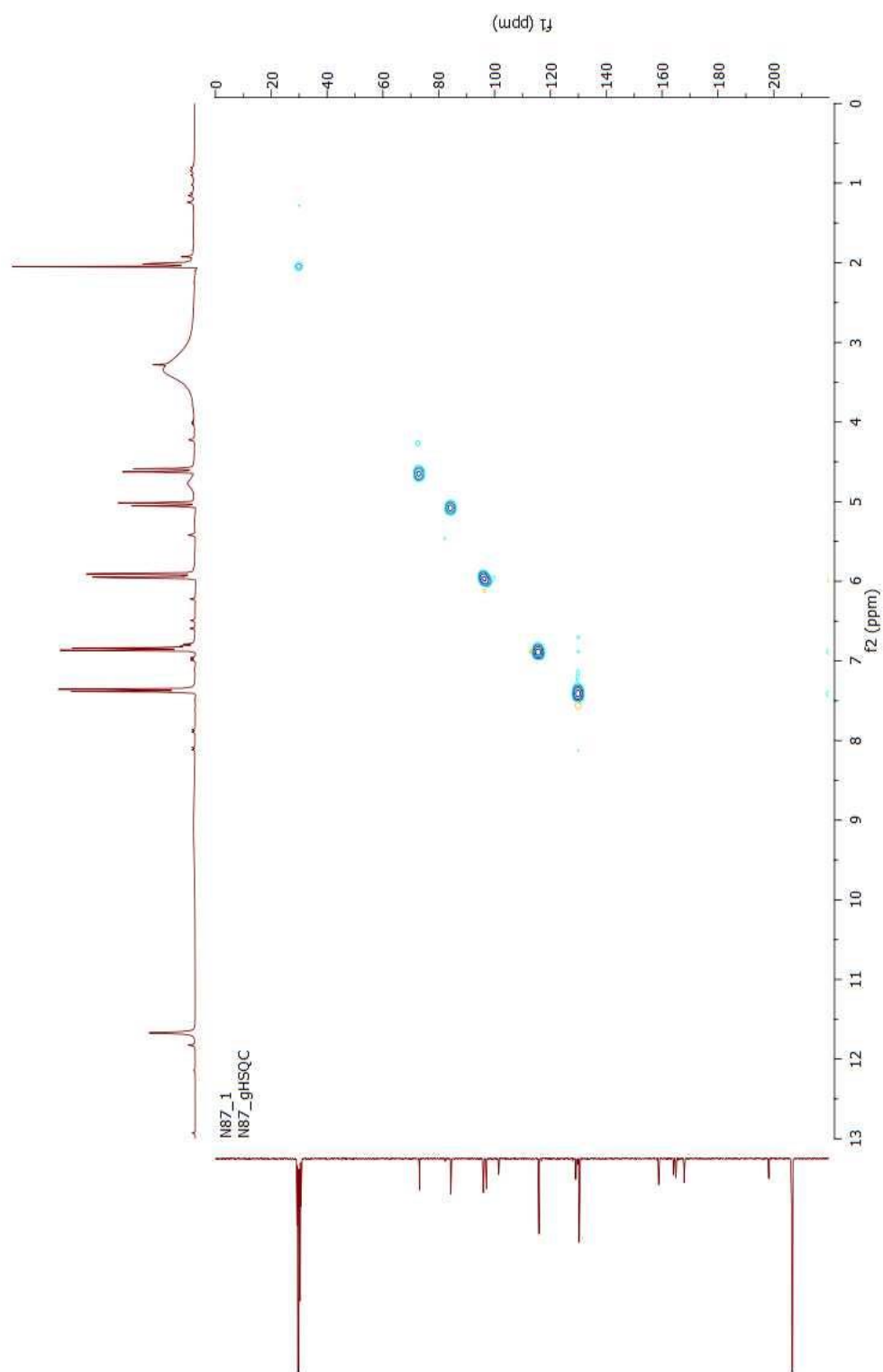


Figure 67 The HSQC spectrum of (+)-dihydrokampferol (III)

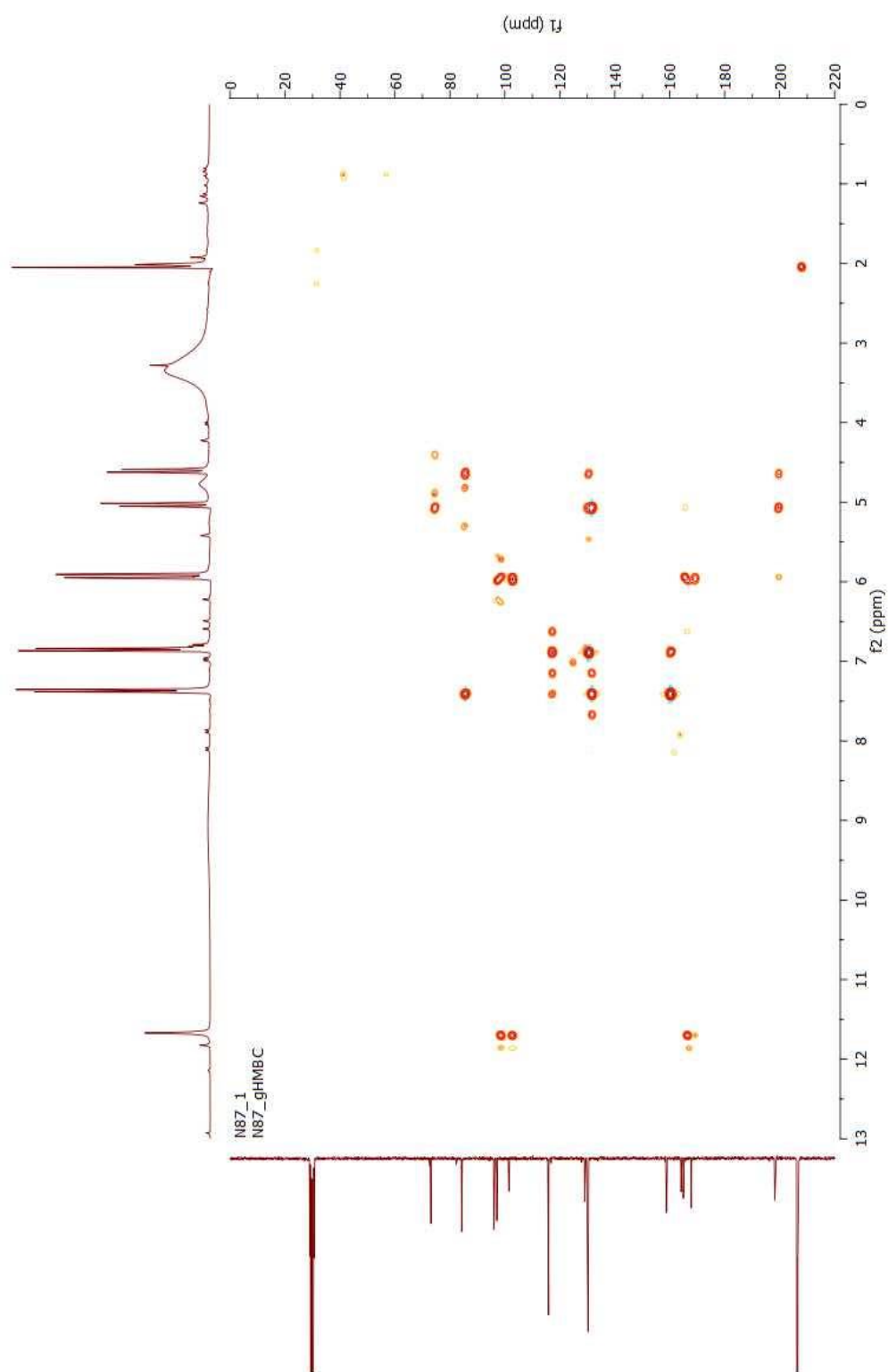


Figure 68 The HMBC spectrum of (+)-dihydrokampferol (III)

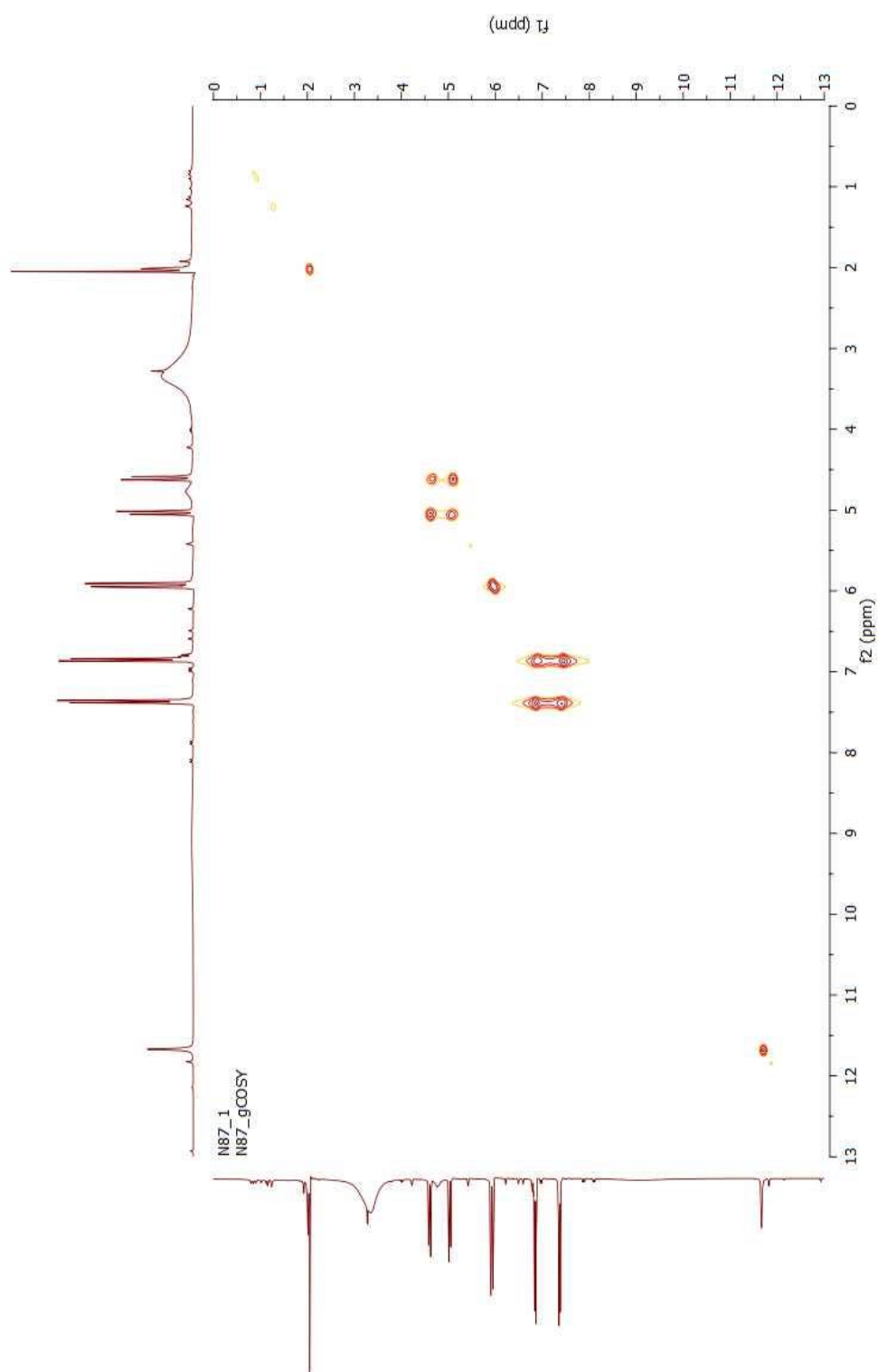


Figure 69 The COSY spectrum of (+)-dihydrokampferol (**III**)

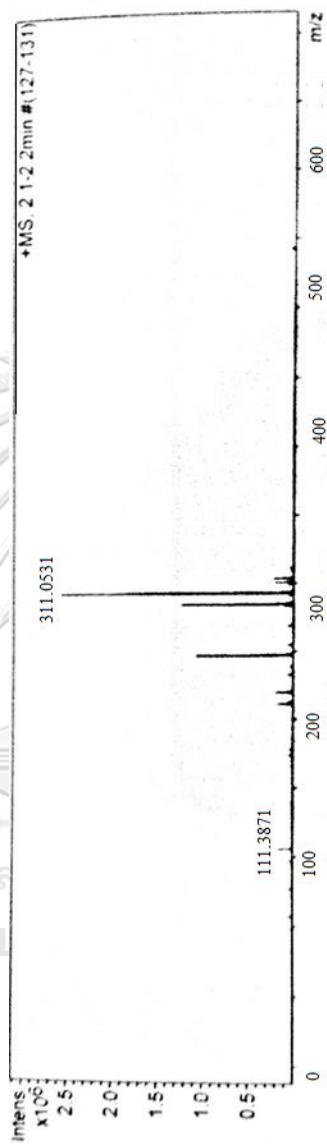


Figure 70 The HR-EI-MS spectrum of (+)-dihydrokeampferol (**III**)

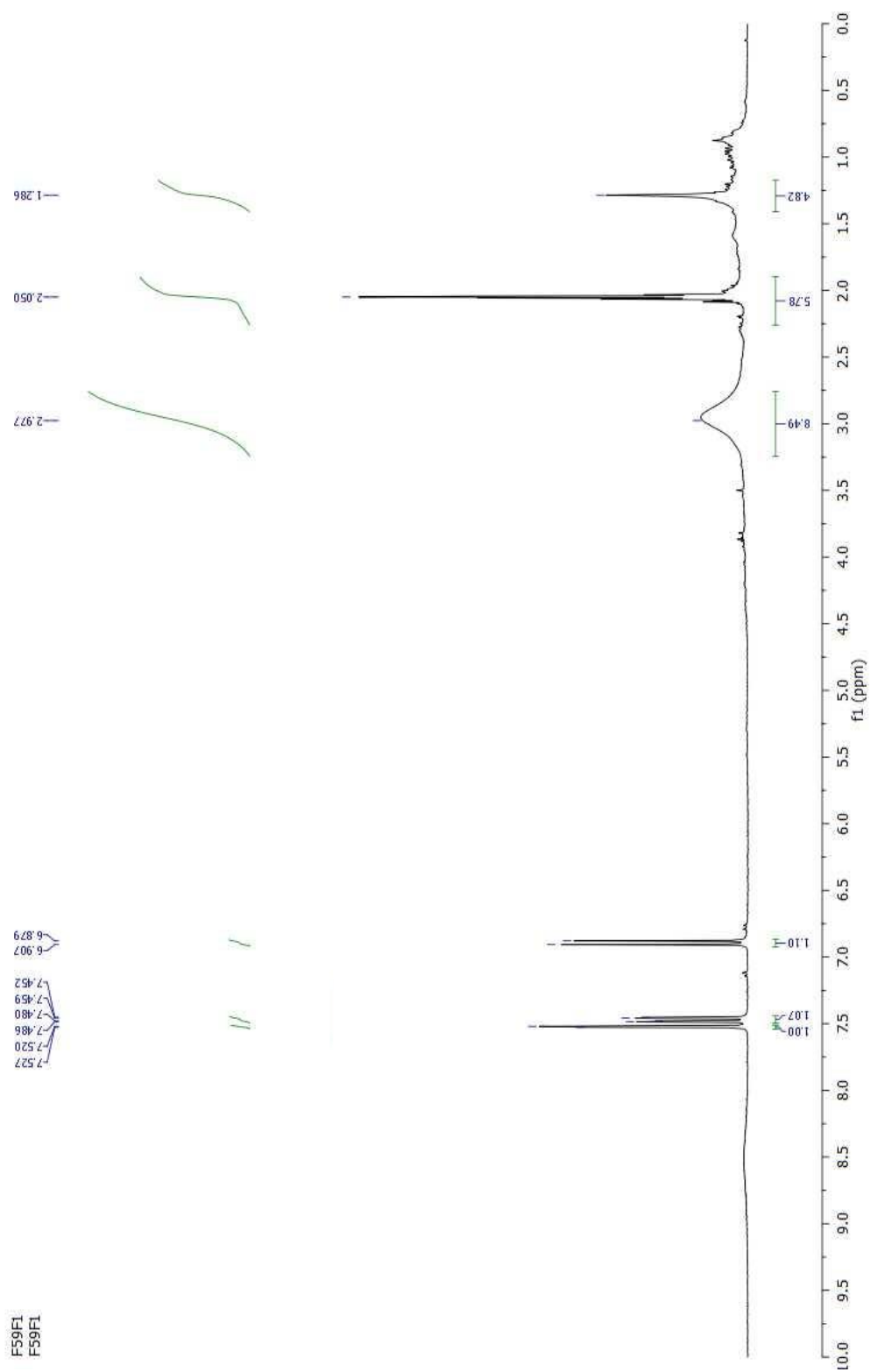


Figure 71 The ¹H-NMR spectrum of 3,4-dihydroxyflavanone (IV)

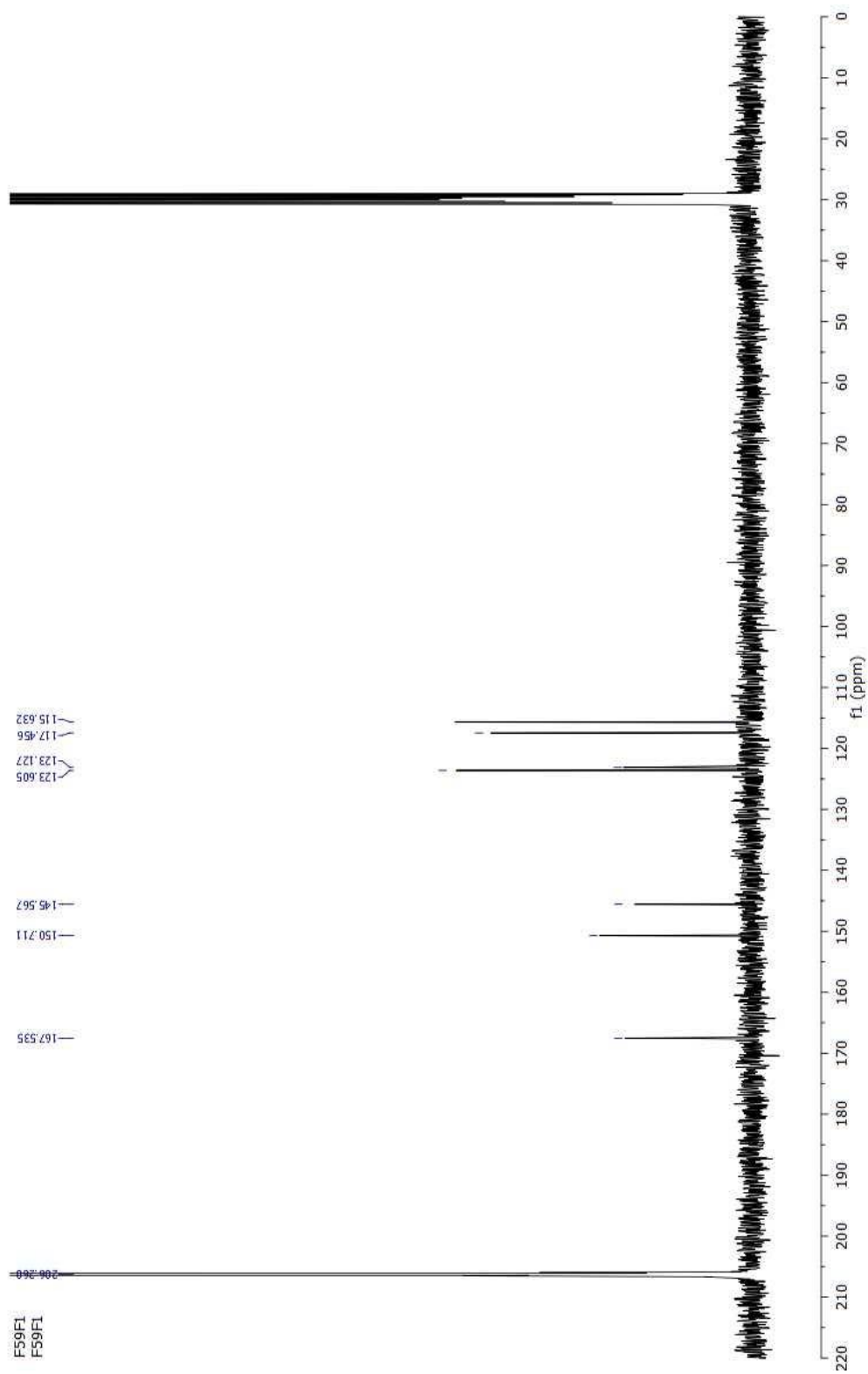


Figure 72 The ^{13}C -NMR spectrum of 3,4-dihydroxyflavanone (IV)

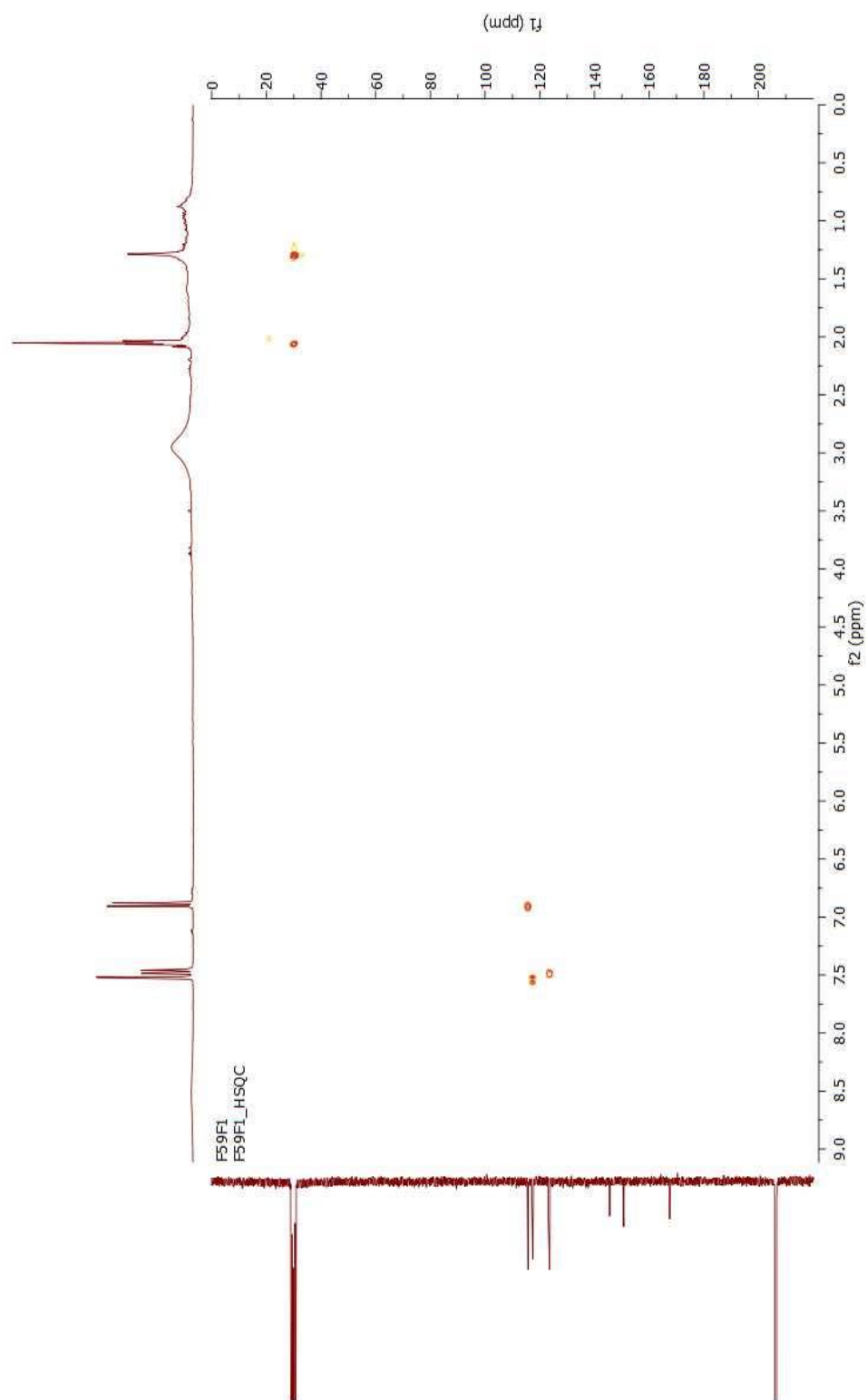


Figure 73 The HSQC spectrum of 3,4-dihydroxyflavanone (IV)

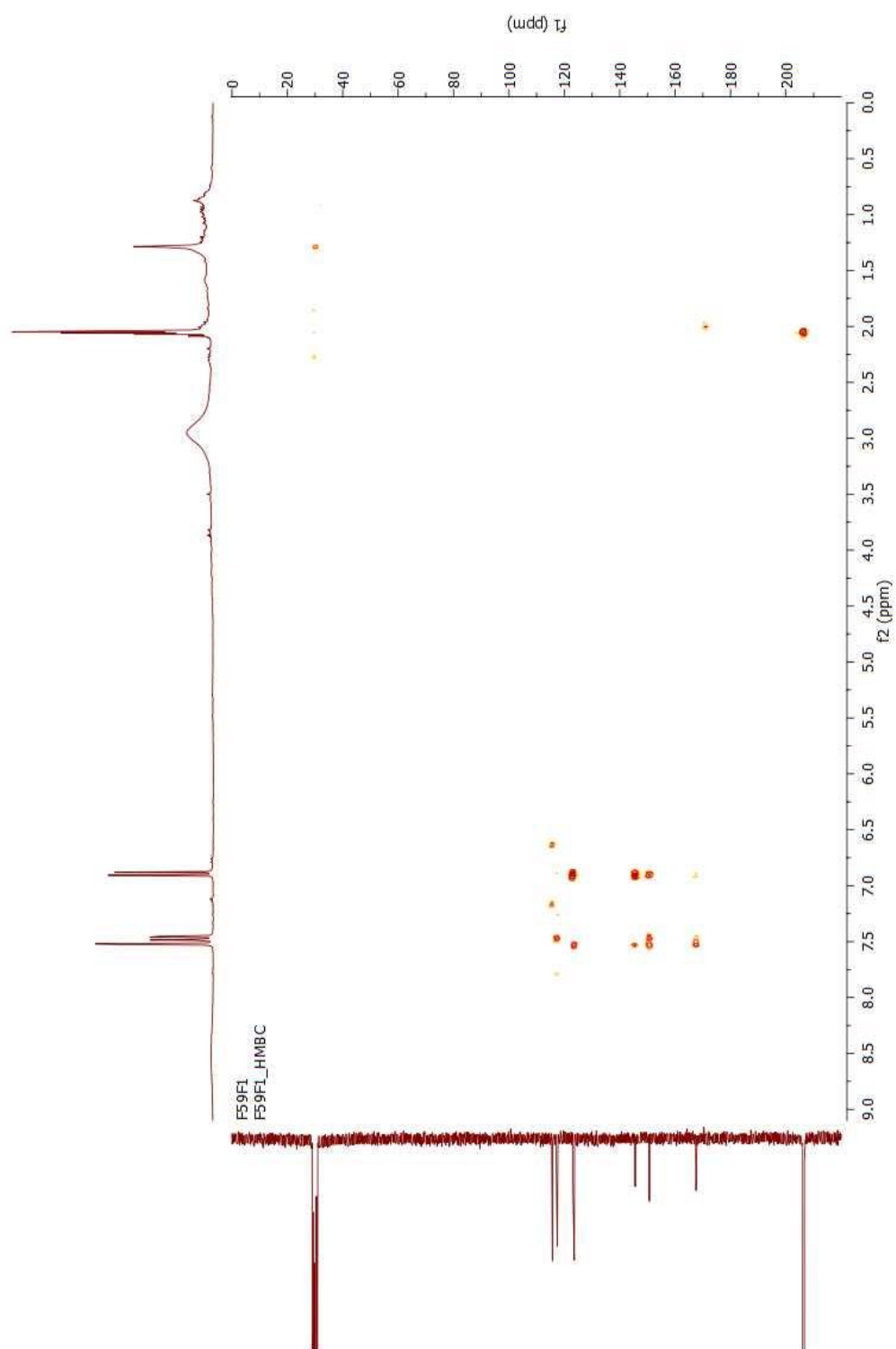


Figure 74 The HMBC spectrum of 3,4-dihydroxyflavanone (**IV**)

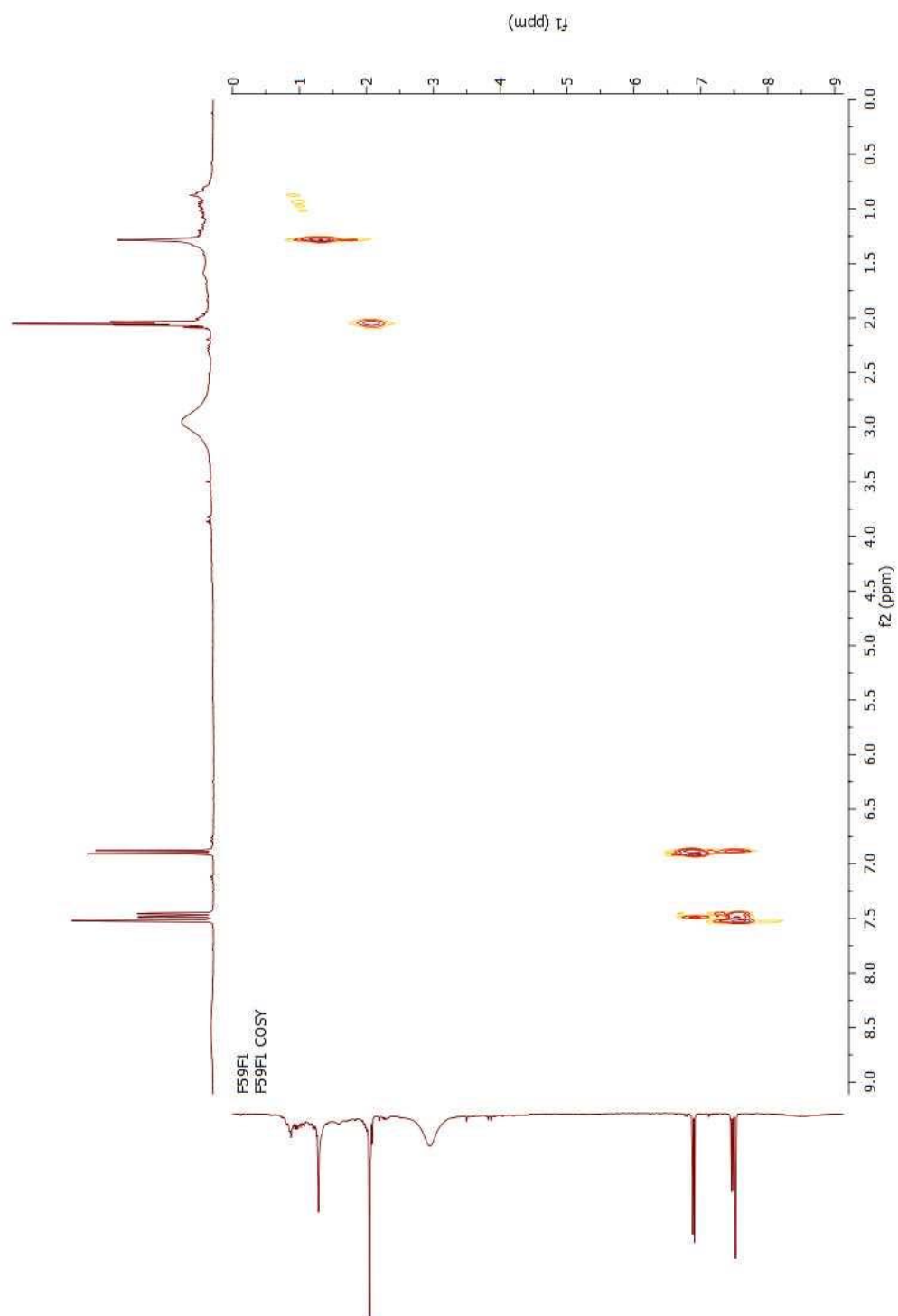


Figure 75 The COSY spectrum of 3,4-dihydroxyflavanone (**IV**)

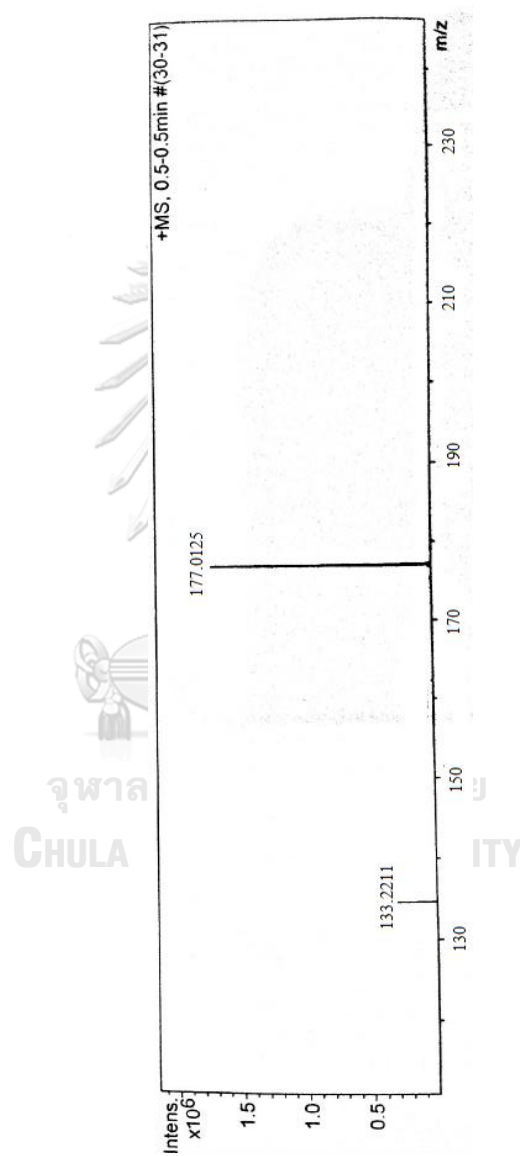


Figure 76 The HR-EI-MS spectrum of 3,4-dihydroxyflavanone (**IV**)

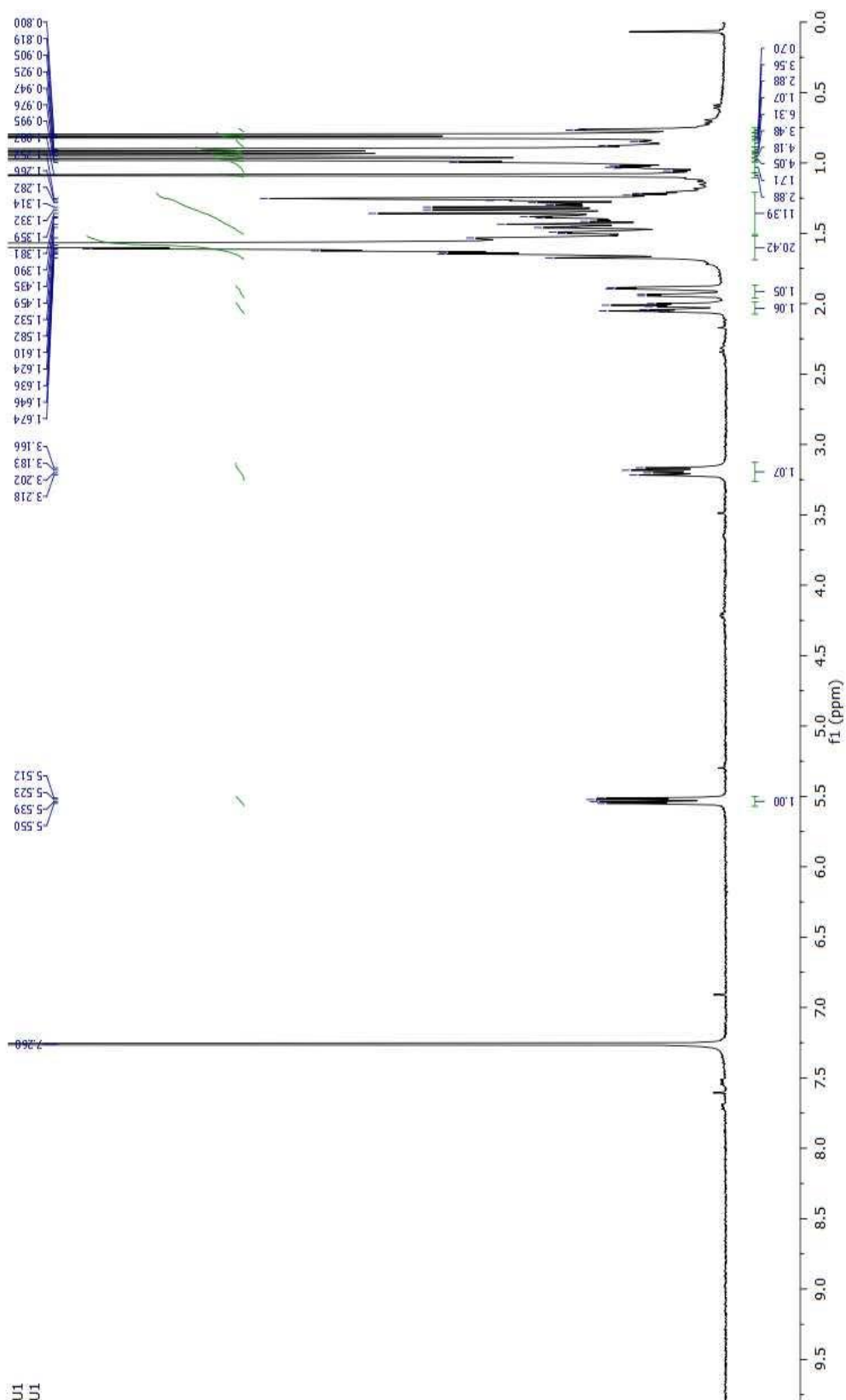


Figure 77 The $^1\text{H-NMR}$ spectrum of taraxerol (V)

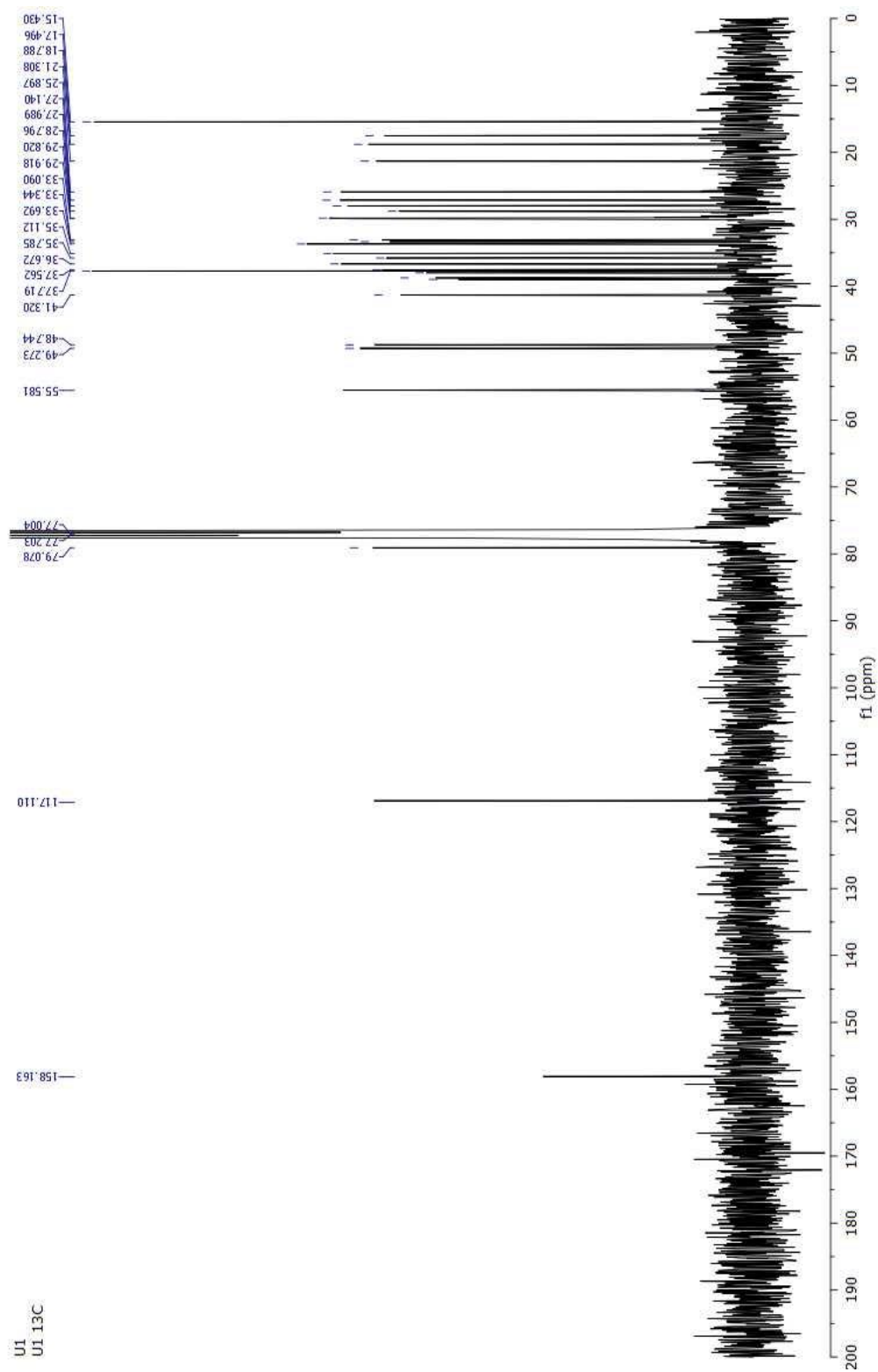


Figure 78 The ^{13}C -NMR spectrum of taraxerol (V)

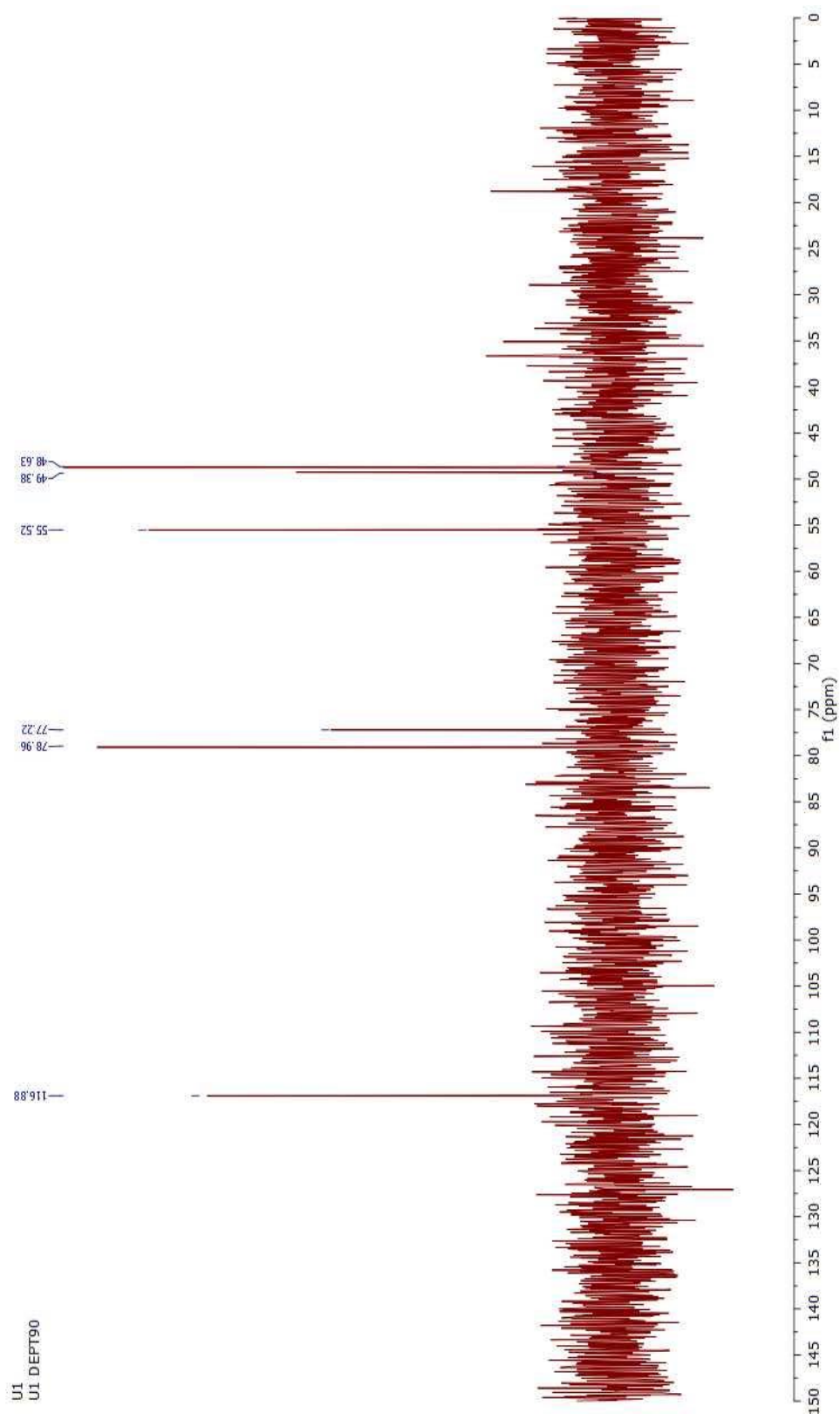


Figure 79 The DEPT90 spectrum of taraxerol (V)

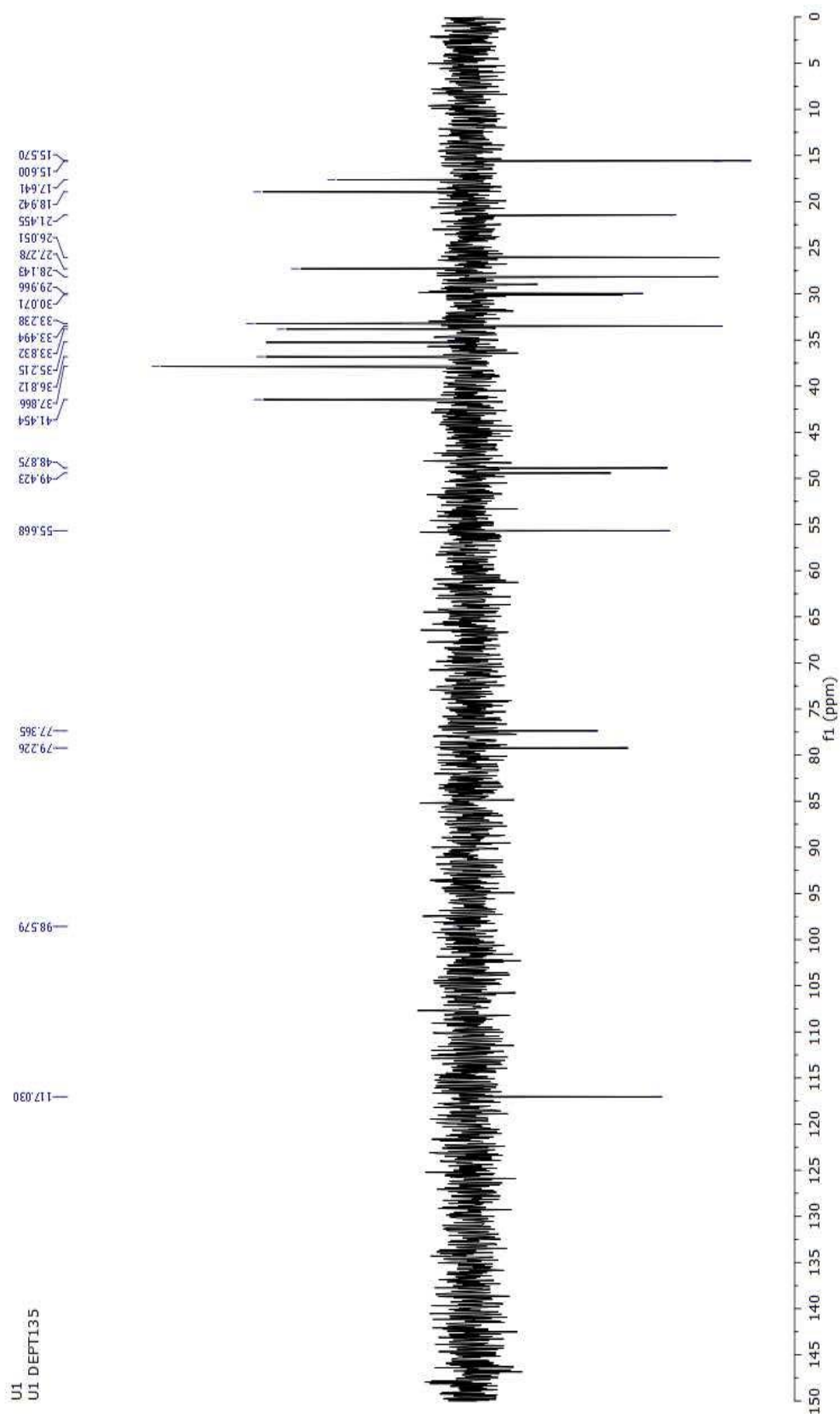


Figure 80 The DEPT135 spectrum of taraxerol (V)

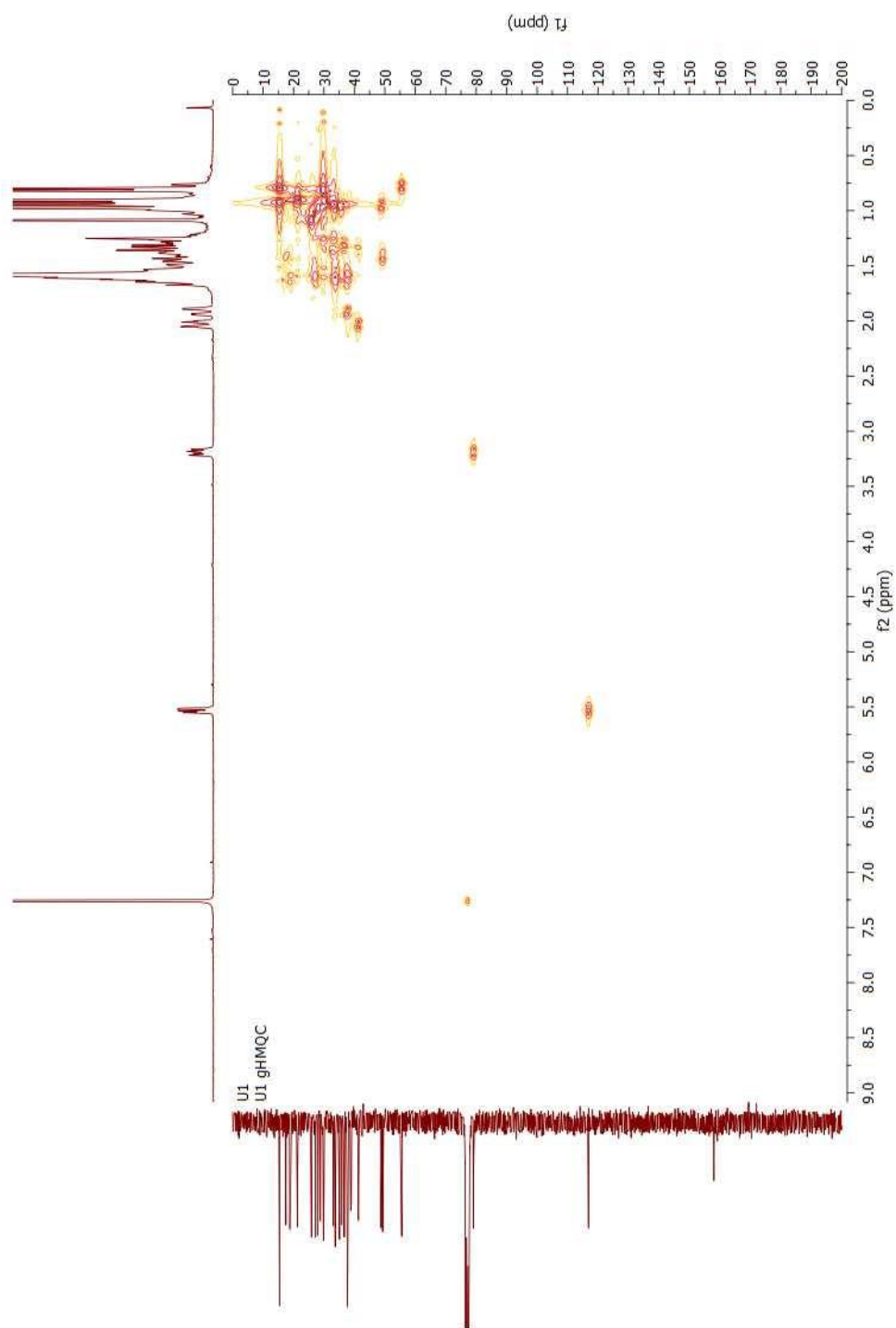


Figure 81 The HMQC spectrum of taraxerol (**V**)

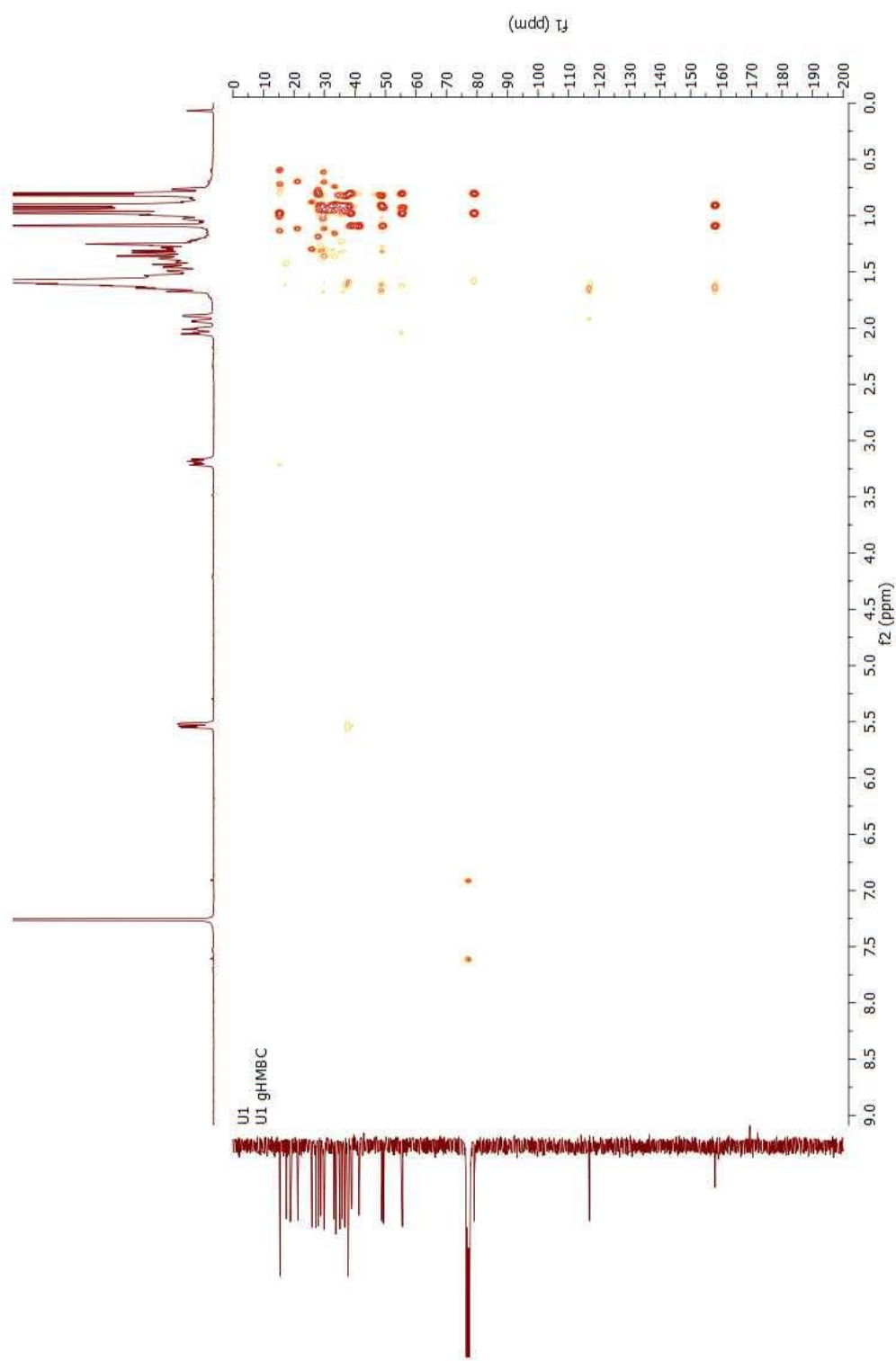


Figure 82 The HMBC spectrum of taraxerol (V)

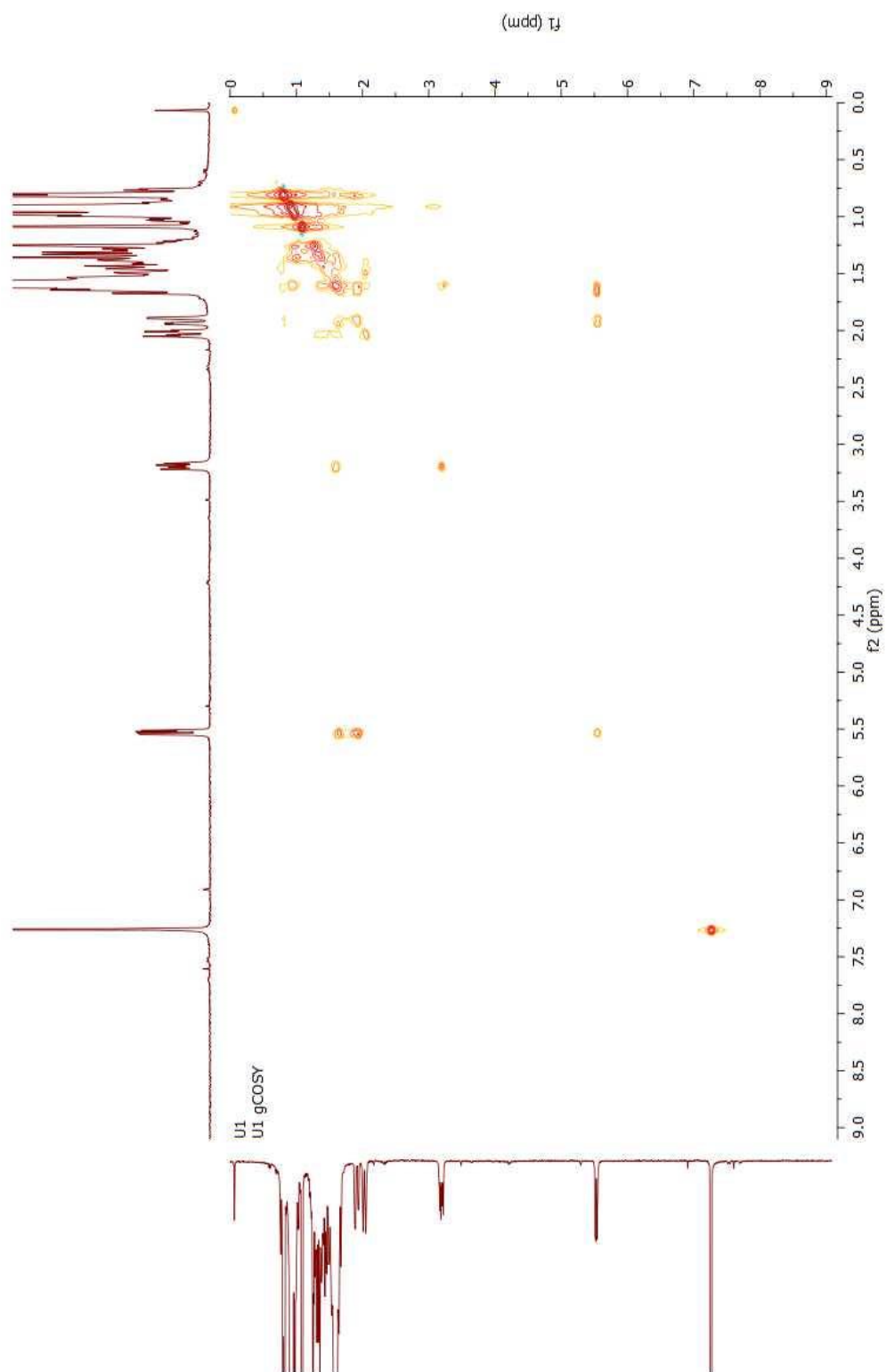


Figure 83 The COSY spectrum of taraxerol (V)

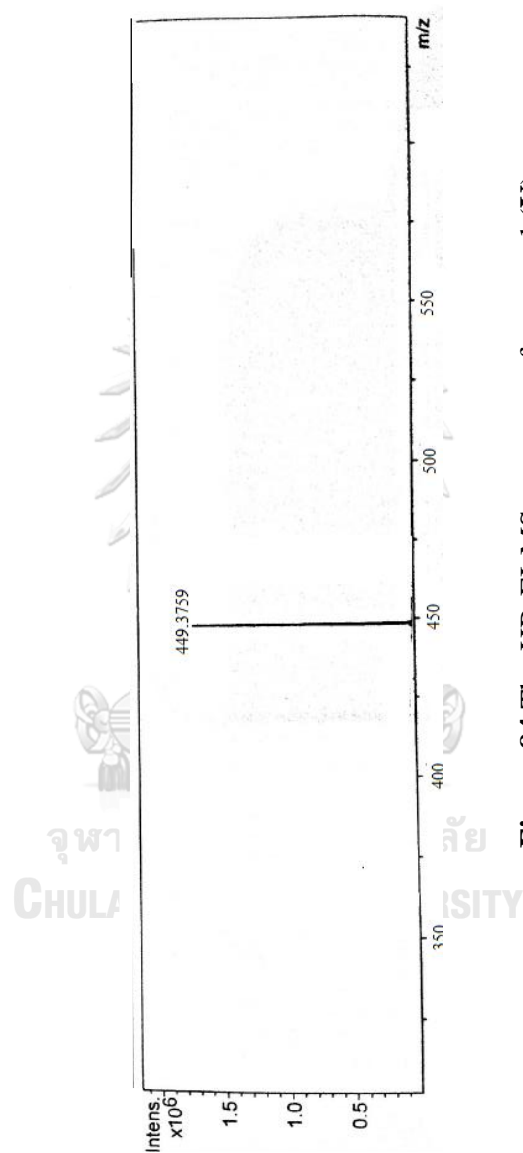
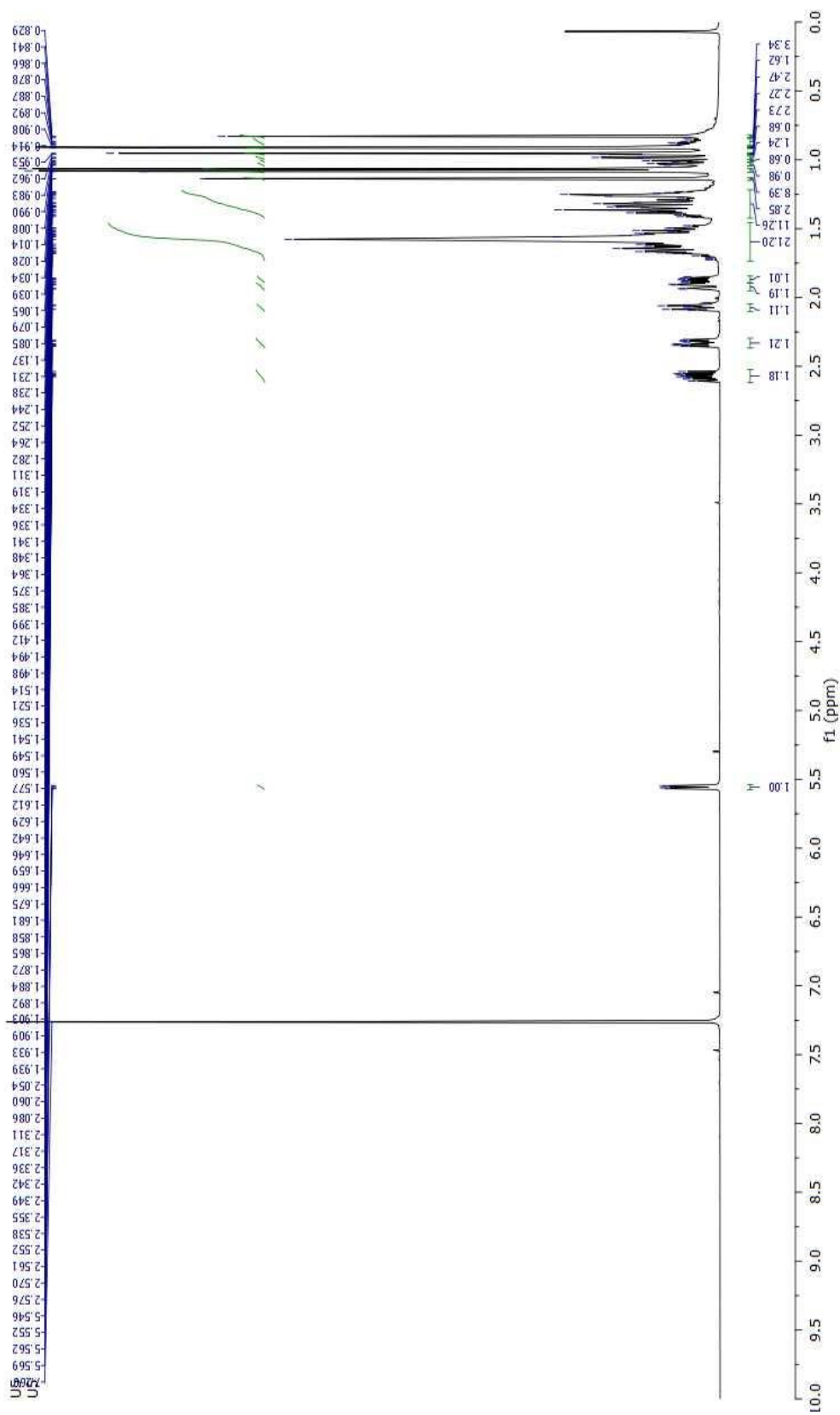


Figure 84 The HR-EI-MS spectrum of taraxerol (V)

Figure 85 The $^1\text{H-NMR}$ spectrum of taraxerone (VI)

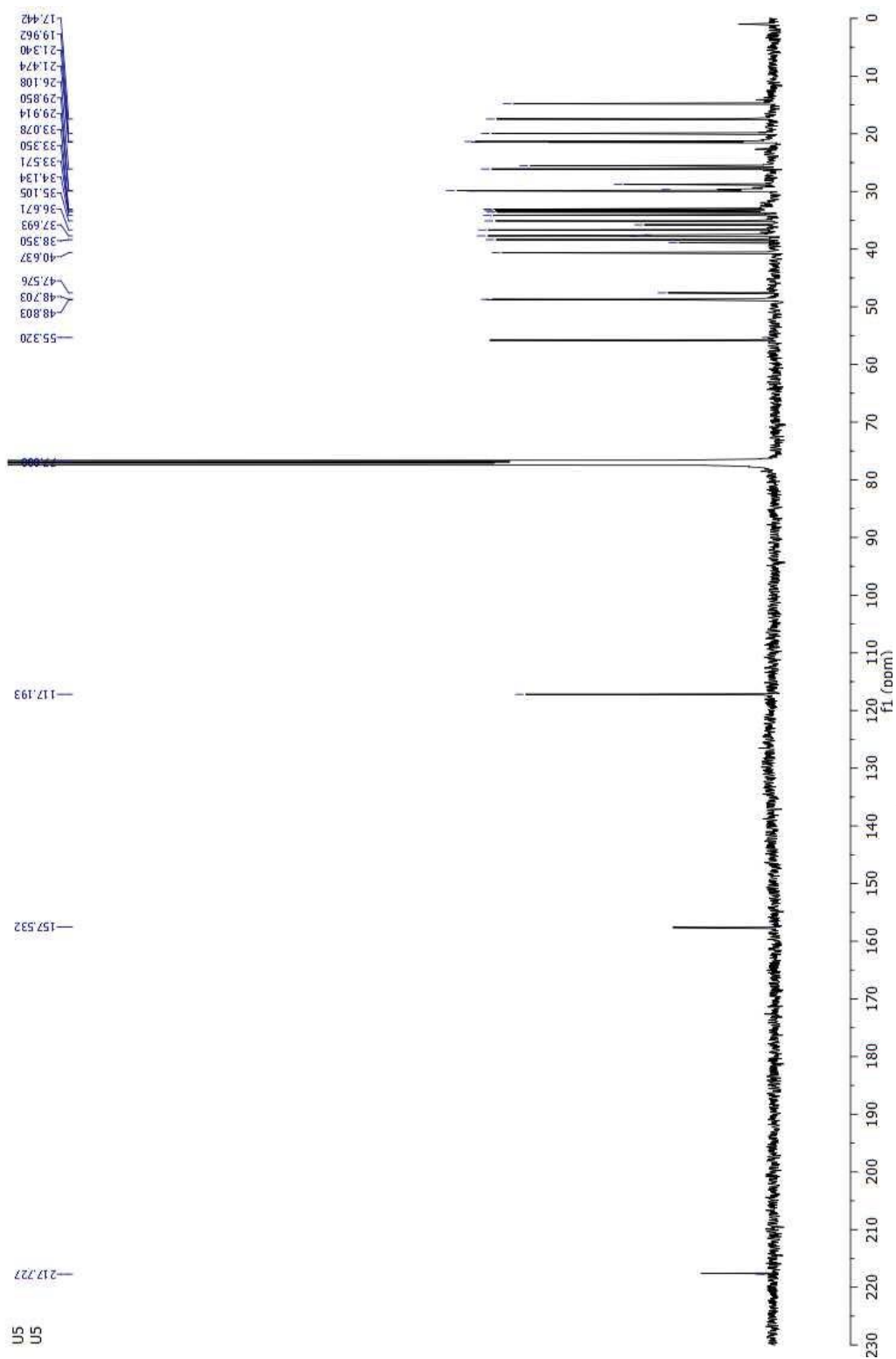


Figure 86 The ^{13}C -NMR spectrum of taraxerone (VI)

U5
U5

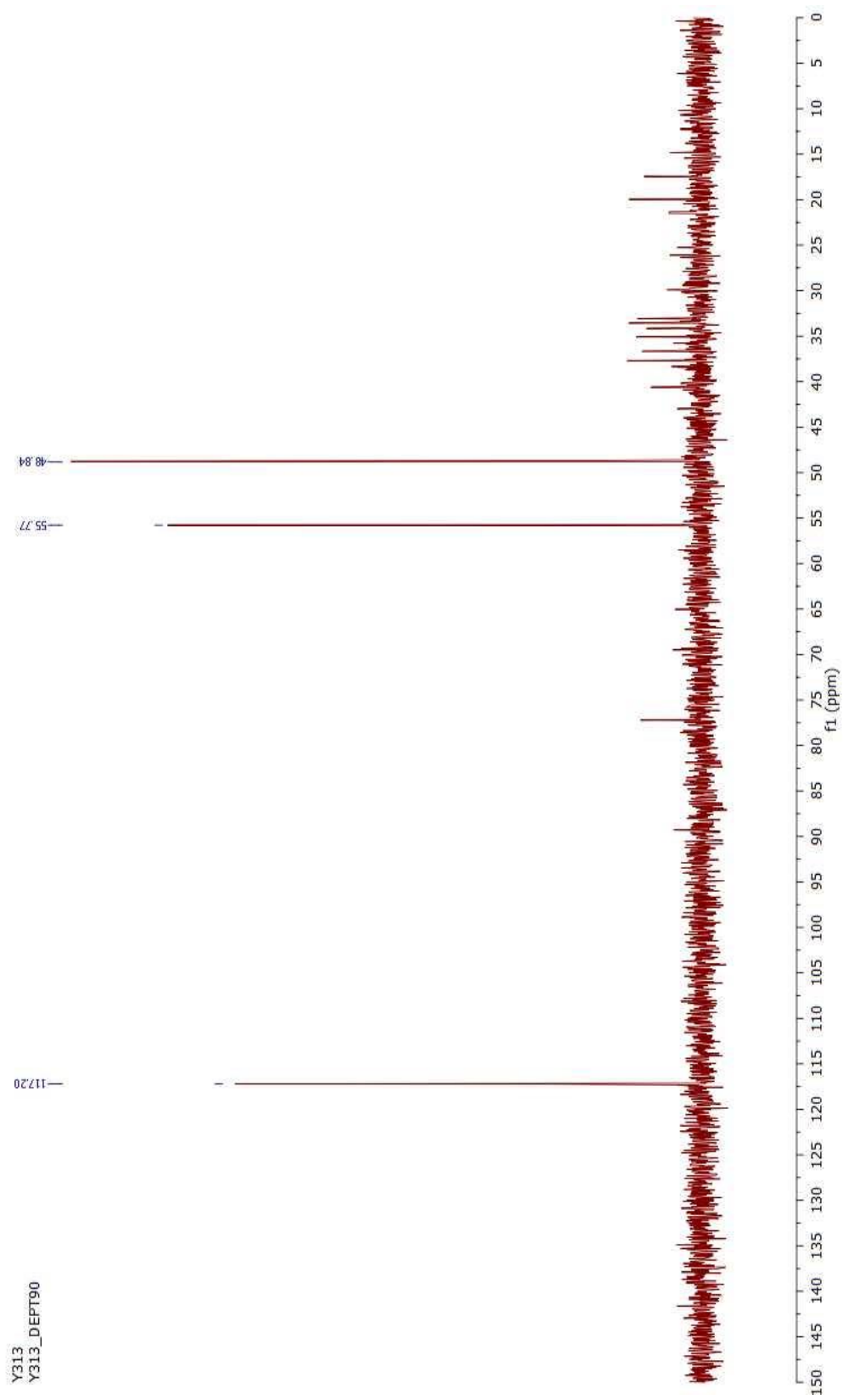
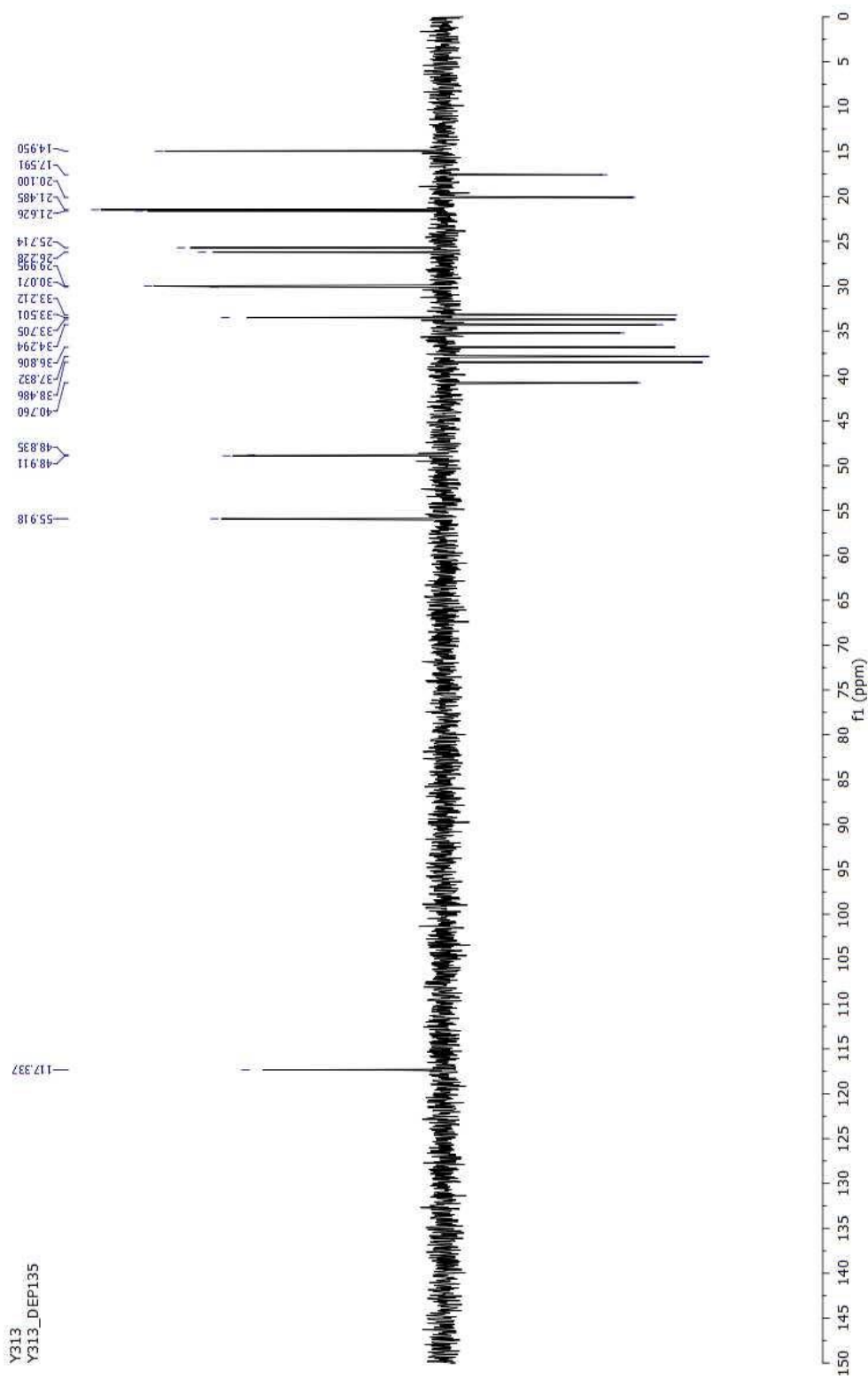


Figure 87 The DEPT90 spectrum of taraxerone (VI)

**Figure 88** The DEPT135 spectrum of taraxerone (VI)

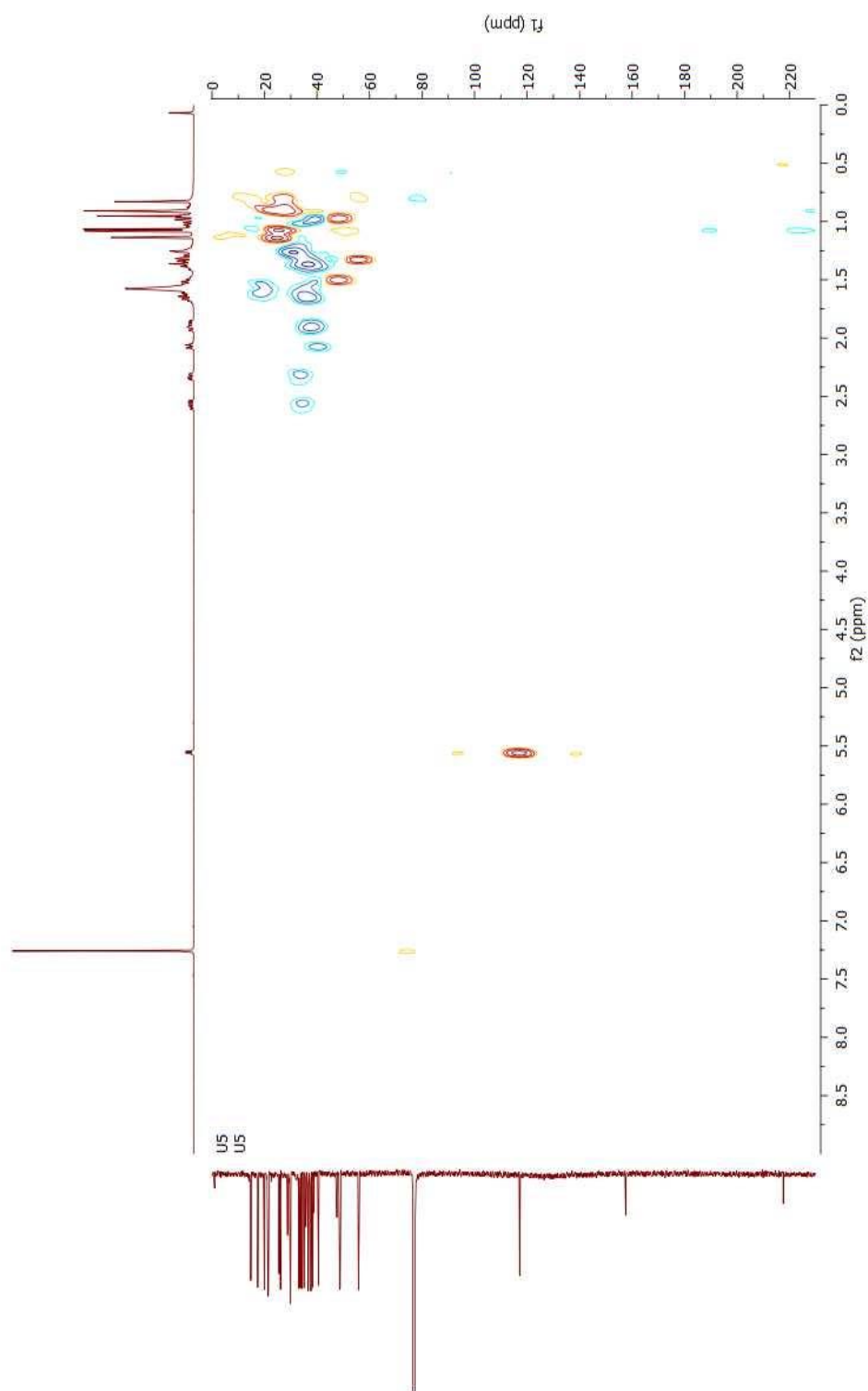


Figure 89 The HMQC spectrum of taraxerone (VI)

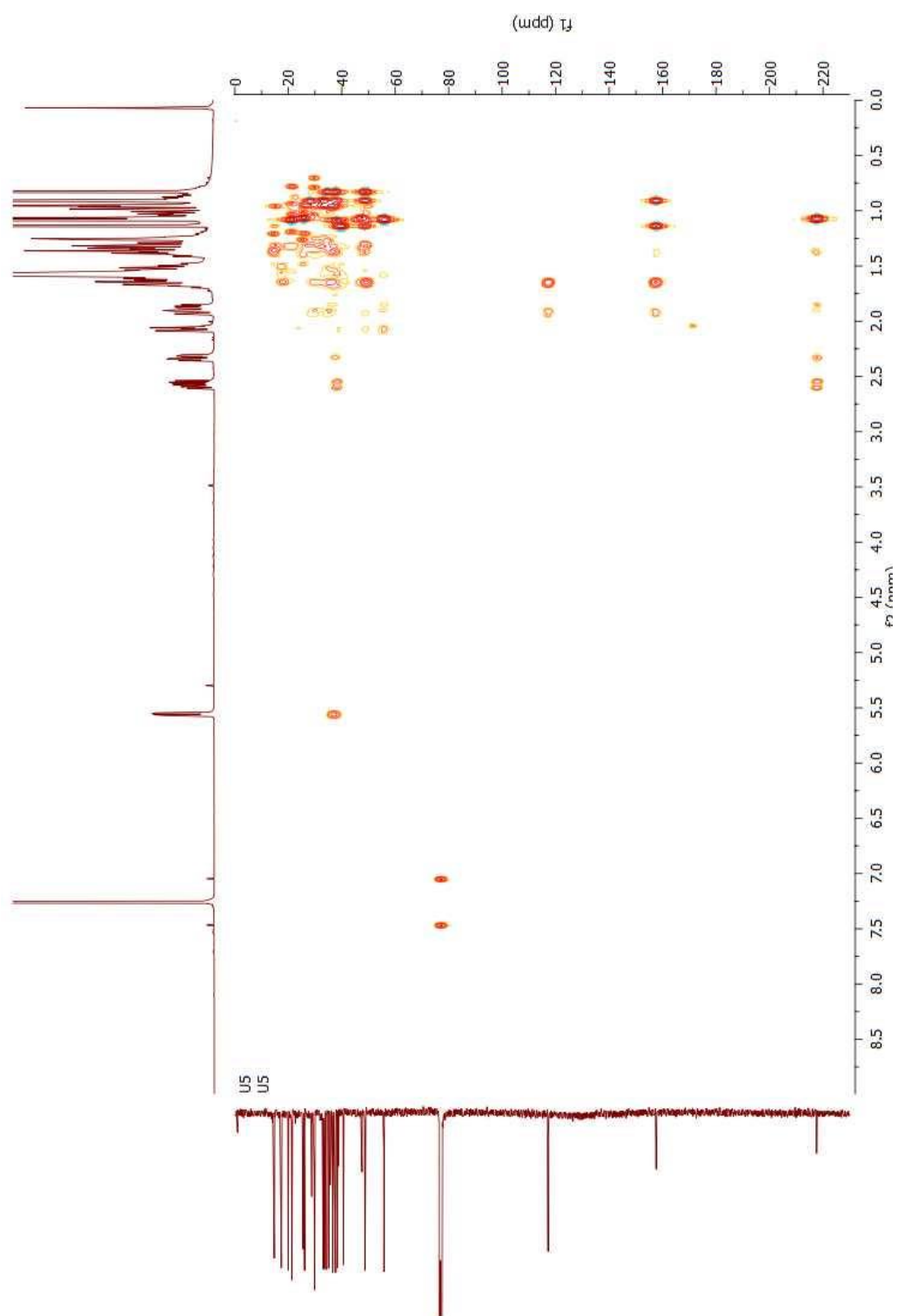


Figure 90 The HMBC spectrum of taraxerone (VI)

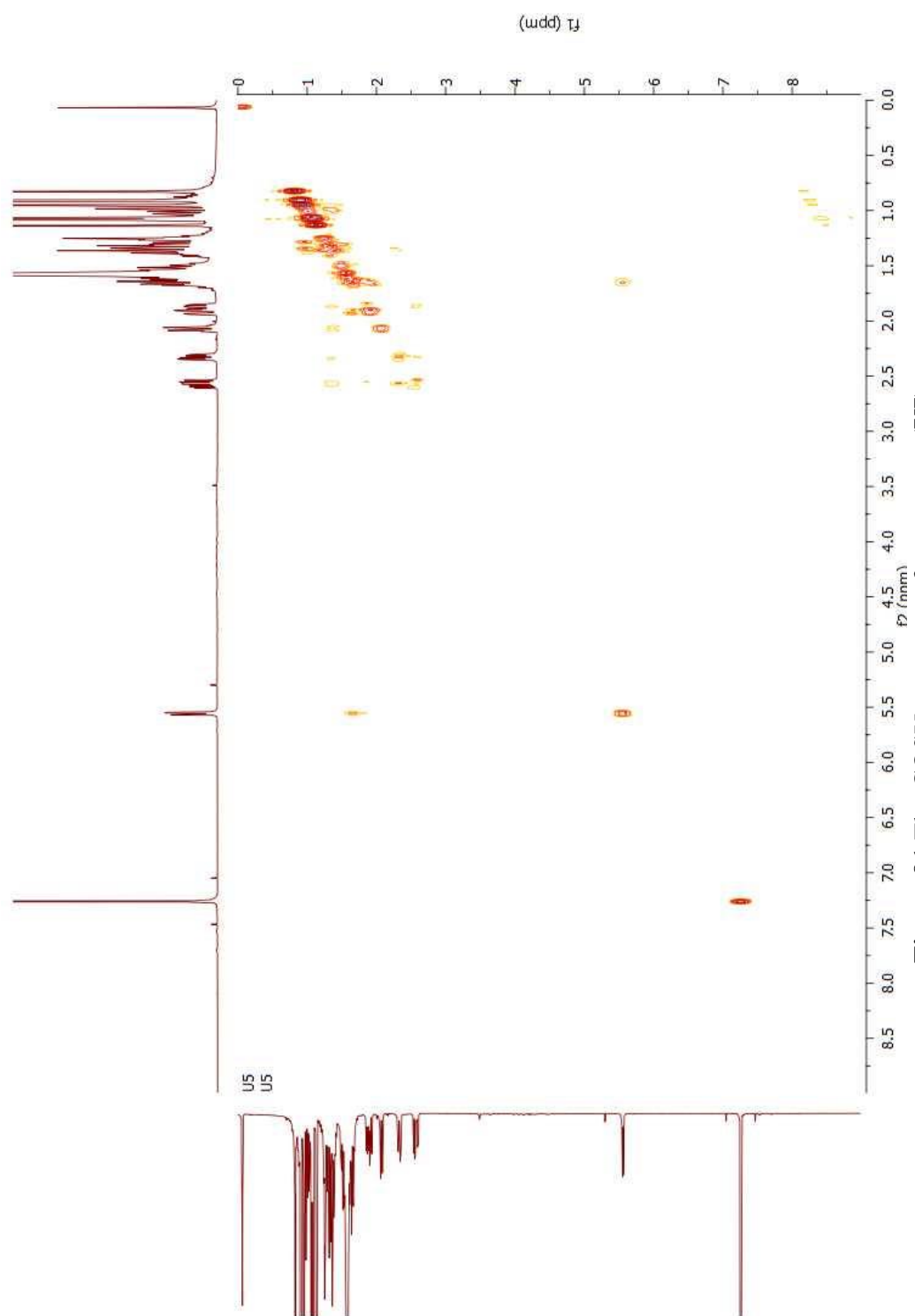


Figure 91 The COSY spectrum of taraxerone (VI)

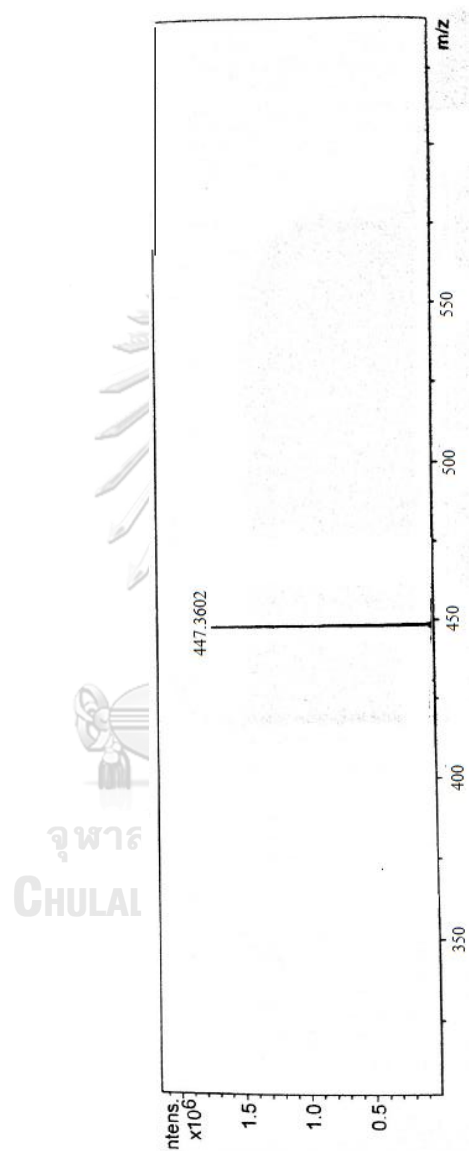
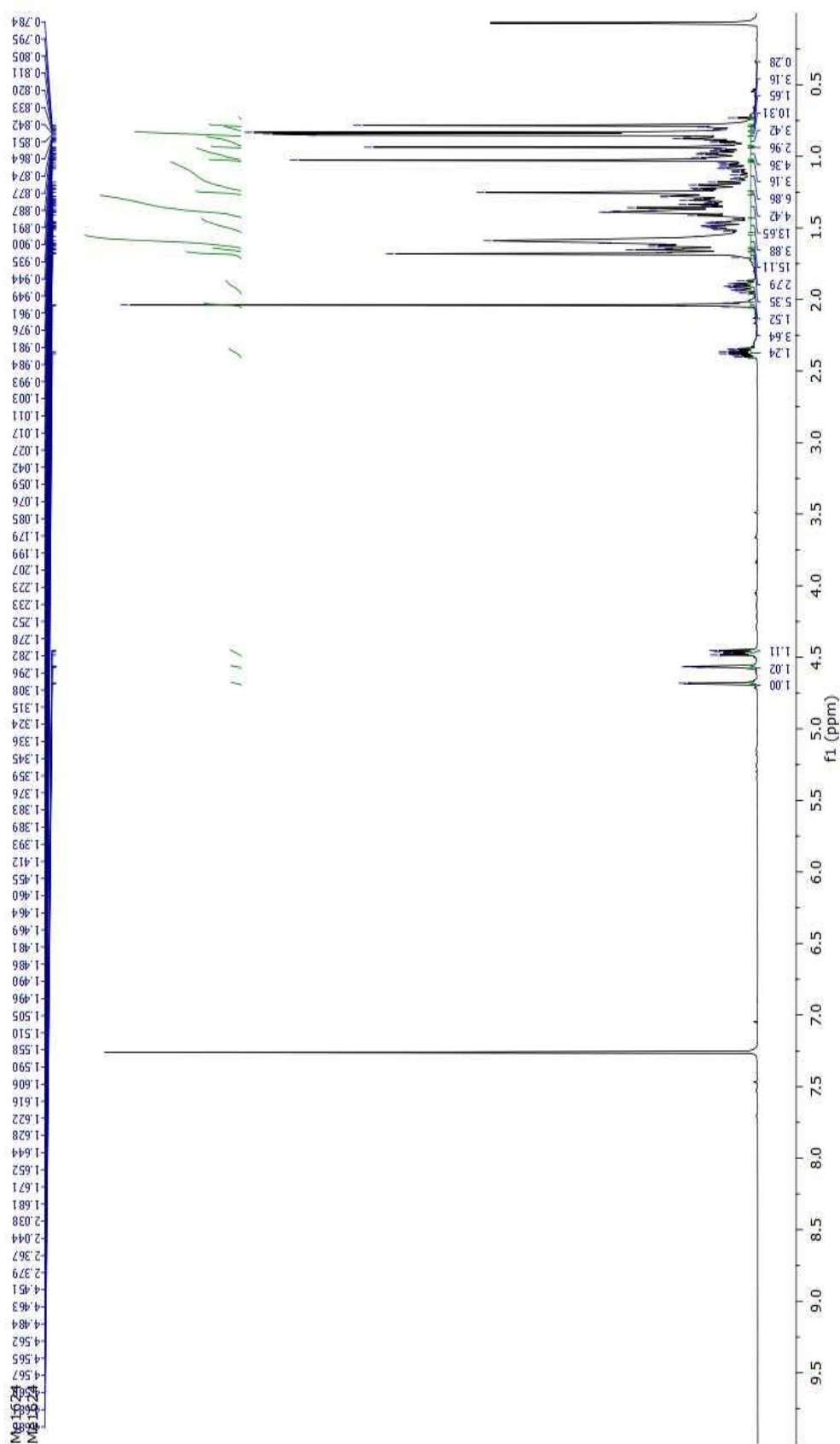


Figure 92 The HR-EI-MS spectrum of taraxerone (VI)



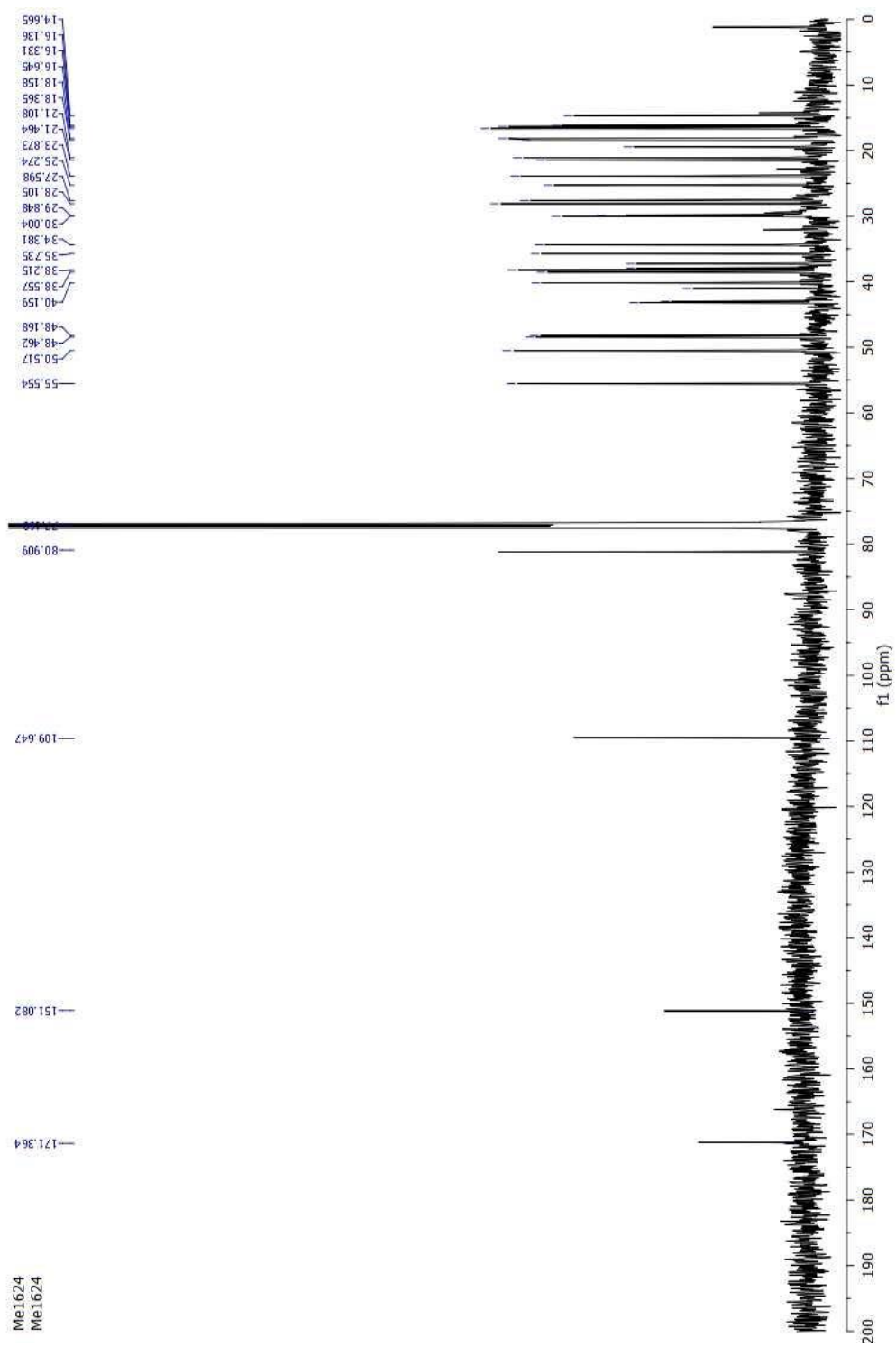


Figure 94 The ^{13}C -NMR spectrum of lupeol acetate (VII)

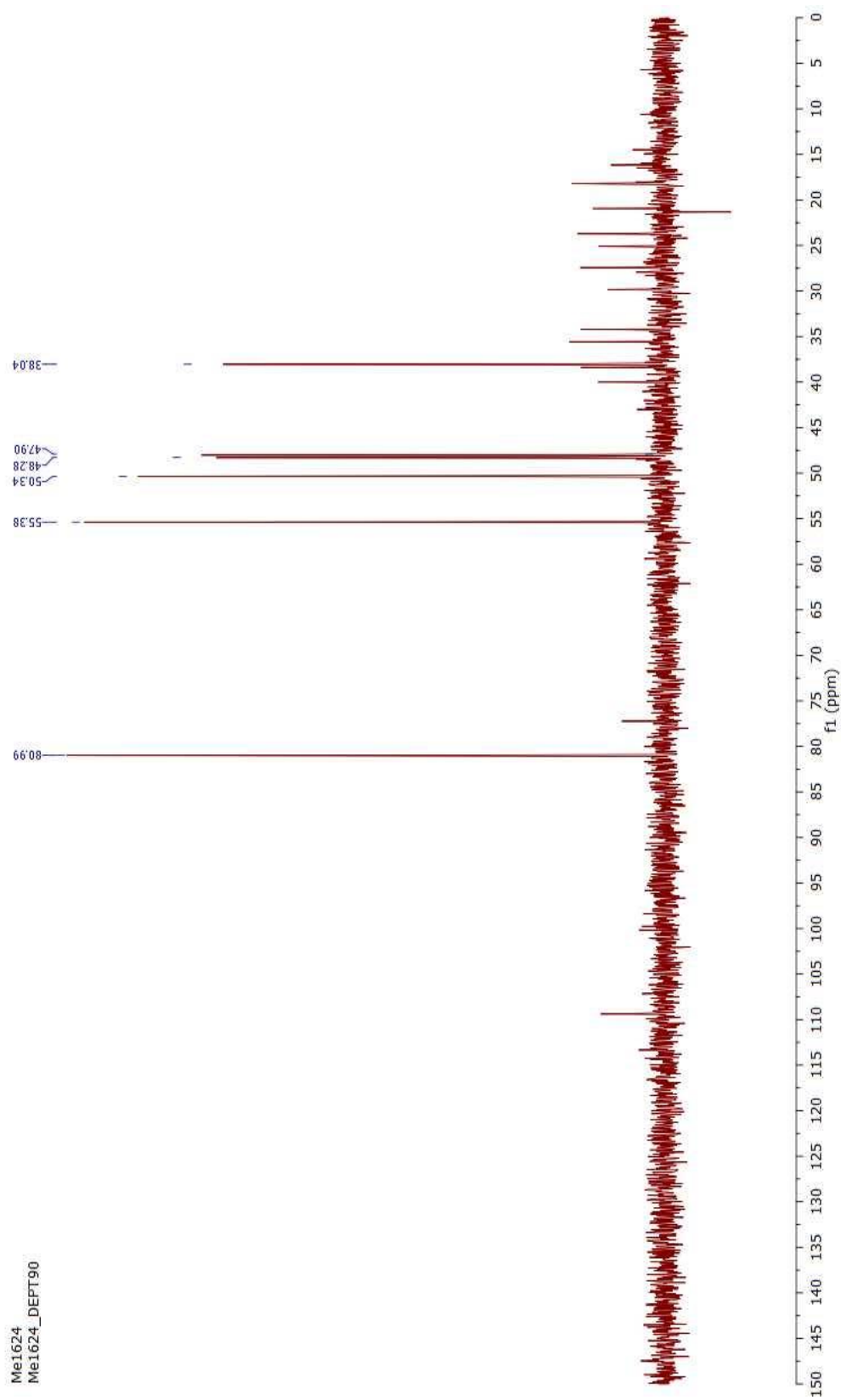


Figure 95 The DEPT90 spectrum of lupeol acetate (VII)

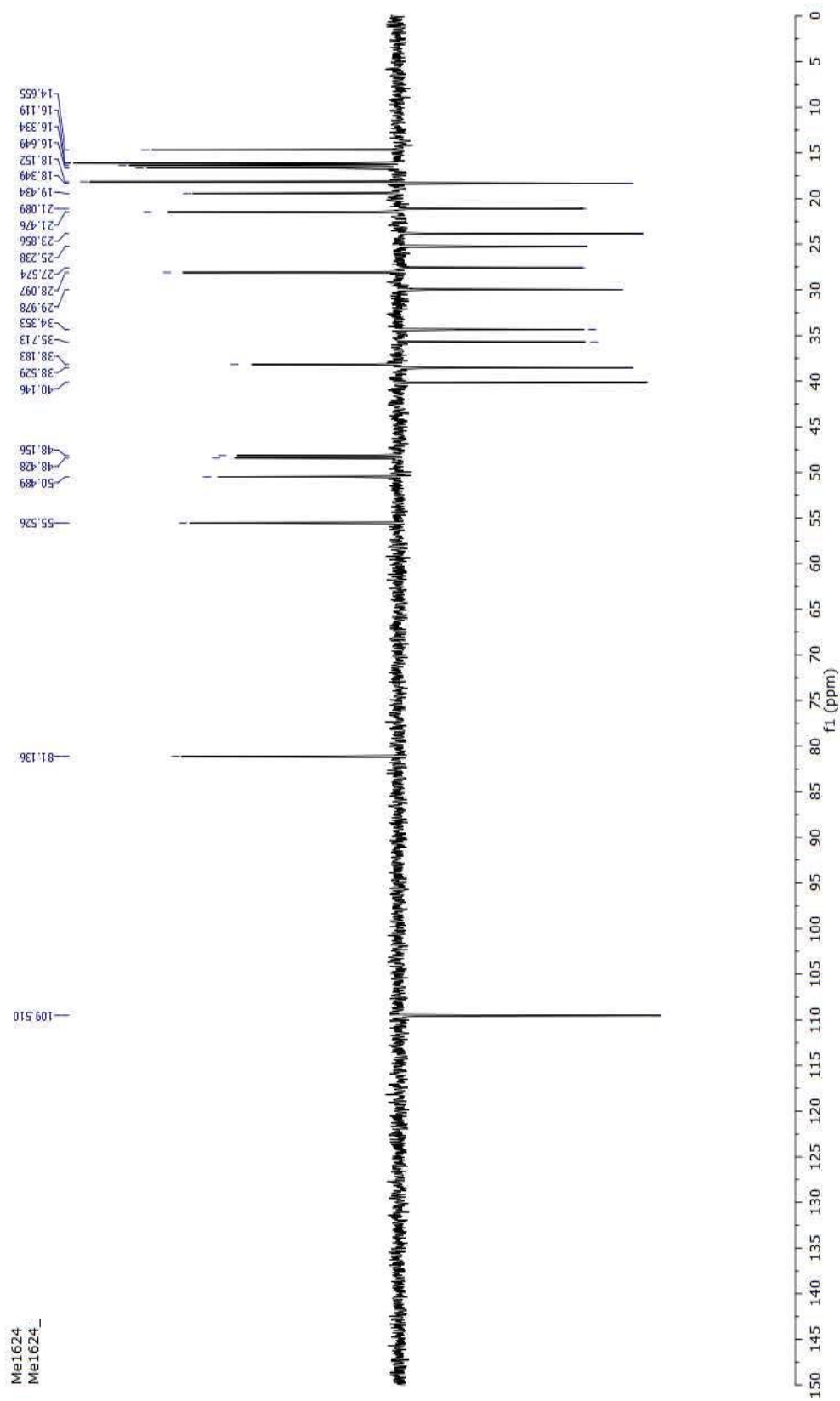


Figure 96 The DEPT135 spectrum of lupeol acetate (VII)

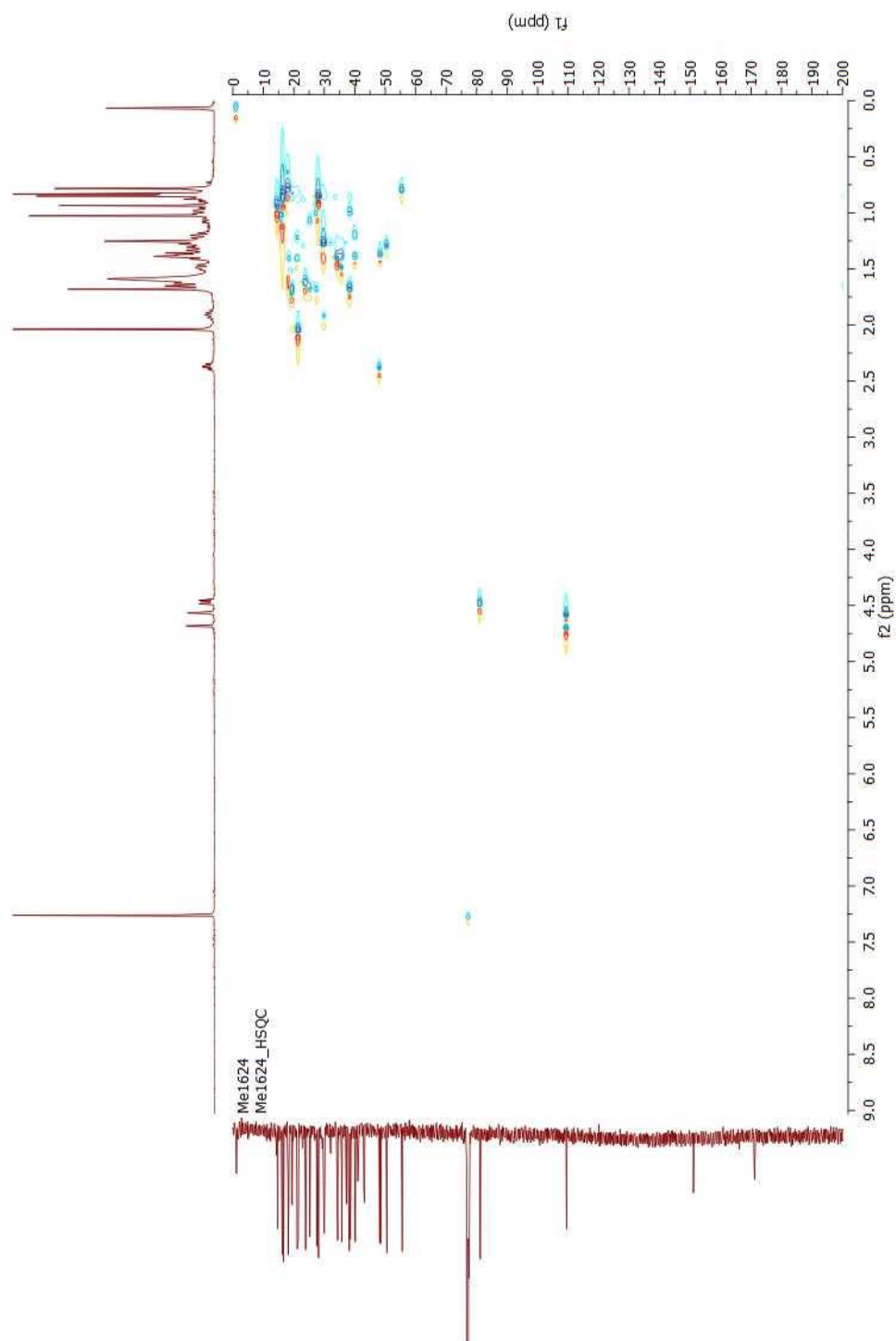


Figure 97 The HSQC spectrum of lupeol acetate (VII)

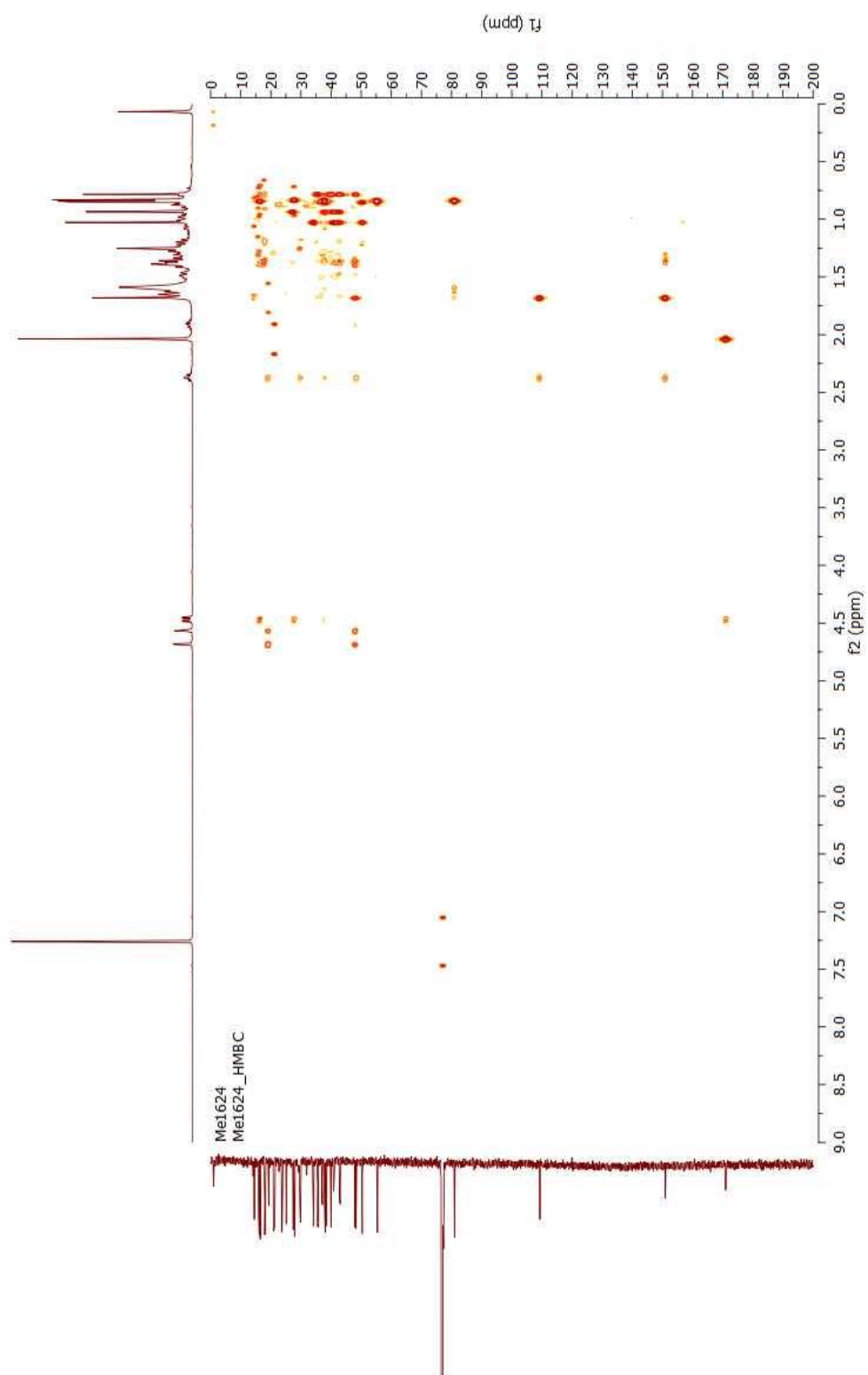


Figure 98 The HMBC spectrum of lupeol acetate (VII)

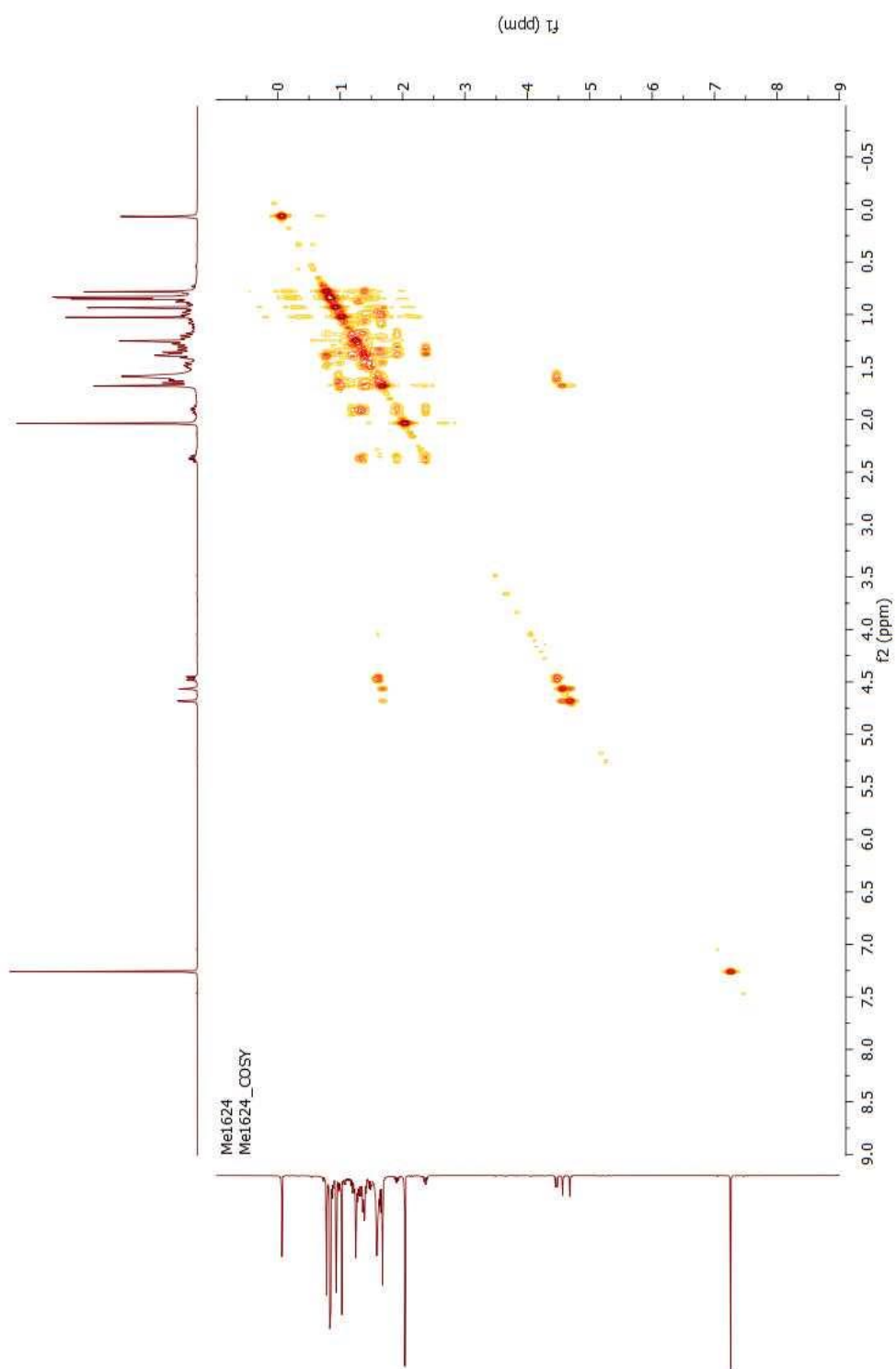


Figure 99 The COSY spectrum of lupeol acetate (VII)

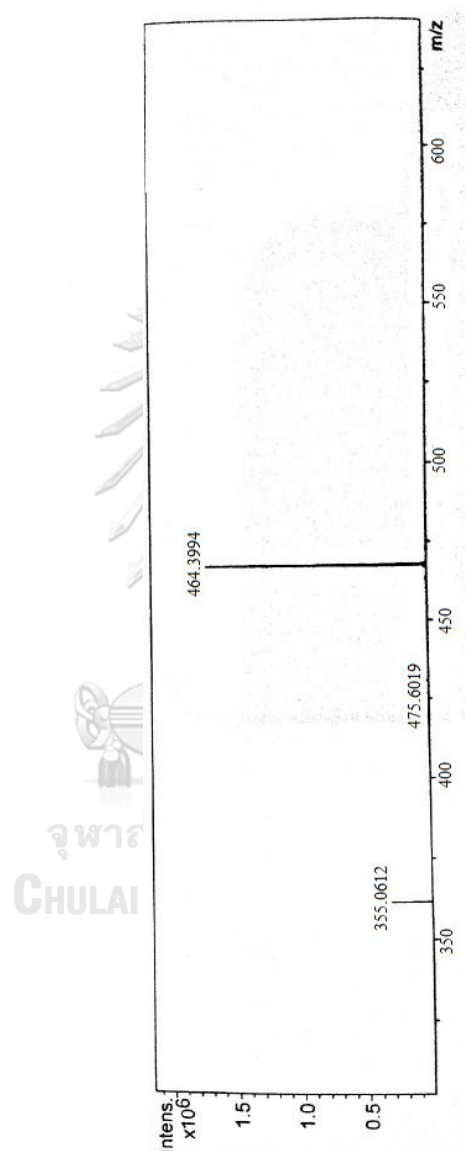


Figure 100 The HR-MS spectrum of lupeol acetate (VII)

VITA

Miss Sutthiduean Chunhakant was born on November 22, 1979 in Pare Province, Thailand. She graduated with a bachelor degree of Science in Chemistry from Department of Chemistry, Phranakorn Rajabhat University, Bangkok, Thailand in 2002. Then, she graduated with master of Science in Biotechnology from Faculty of Science, Chulalongkorn University, Bangkok, Thailand in 2007. After that, she was a lecturer at Department of Chemistry, Phranakorn Rajabhat University, Bangkok, Thailand in 2007. She was admitted doctoral's degree of Program in Biotechnology, Faculty of Science, Chulalongkorn University in 2012. She obtained financial support on her study from Pranakorn Rajabhat University. During the course of study, she obtained financial support on her research from Graduate School Chulalongkorn University. She received poster presentation award at the 9th International Symposium in Science and Technology, Cheng Shiu University, Taiwan in 2014. The title was "Antityrosinase activity of some Thai medicinal plants". She has attended at 10th International Symposium in Science and Technology at Chulalongkorn University, Thailand in 2015 in title "Antityrosinase activity of lupeol acetate from barks of *Manilkara zapota*". She participated the 11st International Symposium in Science and Technology, Kansai University, Japan in 2016 in title "Tyrosinase inhibitory activity of ethyl acetate extract of *Manilkara zapota*".

